Division of Molecular Therapeutics and Formulation
School of Pharmacy

An Investigation into Mechanisms of Non-Ionic Surfactant Effect on Epithelial Cells

Robert Cavanagh, BSc., MSc.

Thesis submitted to the University of Nottingham
for the degree of Doctor of Philosophy

September 2017

Abstract

Amphipathic, non-ionic surfactants are widely used in pharmaceutical and food industries to enhance product features; as pharmaceutical excipients they achieve increased cell membrane permeability and consequently can improve the oral absorption of drugs across the intestinal epithelial barrier. The use of non-ionic surfactants has grown rapidly, and is predicted to increase, however, the mechanism(s) surrounding the induction of surfactant toxicity is not well established and, consequently, the potential risks of surfactant exposure are not well understood.

This work studies the concentration- and time-dependent succession of events that occur during and following exposure of an intestinal epithelial cell model to a 'typical' non-ionic surfactant – Solutol HS15.

The resulted gathered demonstrate that prior to a significant increase in membrane permeability to a model drug (FITC-dextran 4kDa), non-ionic surfactant, at concentrations above its critical micellar concentration (CMC), produced almost immediate redox and mitochondrial effects manifested as an increased NADH pool, increased ROS levels, and hyperpolarisation of the mitochondrial membrane potential. Apoptosis was triggered early in this initial phase, and relied on mitochondrial hyperpolarisation as a crucial step leading to subsequent depolarisation and caspase-3/7 activation. Inhibition of mitochondrial hyperpolarisation prolonged cell

survival, delayed the onset of metabolic reduction by the mitochondrial, and inhibited caspase activation.

The apoptotic cell death pathway appears to be triggered prior to the emergence of substantial membrane damage by the surfactant: loss of plasma membrane integrity, nuclear membrane permeabilisation, and perturbations in calcium homeostasis - indicators of a necrotic process.

It is proposed that the rapid cellular response is triggered *via* rapid surfactant-induced increases in plasma membrane fluidity; a phenomenon akin to the membrane-regulated stress response following membrane fluidisation by heat shock, and consequently cell death events.

Furthermore, work performed on differentiated Caco-2 monolayers, alongside culture models replicating the basement membrane and paracrine signalling, demonstrate surfactant toxicity is reduced. Toxicity *in vivo* is therefore predicted to be less than measured on the standard model.

Acknowledgements

I would like to thank everyone who contributed to this project, knowingly or unknowingly, especially those with the patience to help get me across the finishing line and, a special thanks to my supervisor, Dr. Snow Stolnik, for her enthusiasm, wise counsel and professional advice.

Thanks a lot.

Table of contents

List of Figures

List of tables

Abbreviations

°C	Celsius
µg	Microgram
µl	Microliter
µm	Micrometre
µM	Micromolar
ADI	Acceptable daily intake
AIF	Apoptosis inducing factor
ANOVA	Analysis of variance
ATCC	American tissue culture company
BIBRA	British Industrial Biological Research Association
BSA	Bovine serum albumin
Ca^{2+}	Calcium ion
CDD	Cell death and disease
cm_2	Square centimetres
CMC	Critical micelle concentration
C_nTAB	*n*-Alkyl-N,N,N-trimethylammonium bromides
CO_2	Carbon dioxide
Da	Dalton
DAPI	4',6-diamidino-2-phenylindole
DDPS	N-dodecyl-N,N-dimethylammonium-propanesulfonate
DISC	Death-inducing signaling complex
DNA	Deoxyribonucleic acid
ECM	Extracellular matrix
EDTA	Ethylenediaminetetraacetic acid
EFSA	The European Food Safety Authority
EGF	Epidermal growth factor
EMEM	Eagle's minimal essential medium
FBS	Foetal bovine serum
FCCP	Carbonyl cyanide-p-trifluoromethoxyphenylhydrazone
FD4	FITC-dextran (4 kDa)
FDA	Food and Drug Agency
FITC	Fluorescein isothiocyanate
GLP-1	Glucagon-like peptide 1
GP	General polarisation

HBSS	Hank's buffered saline solution
HEPES	4-(2-hydroxyethyl)-1-piperazineethanesulfonic acid
Ho	Hoechst 33342
HSR	Heat shock response
INT	2-(4-iodophenyl)-3-(4-nitrophenyl)-5-phenyl-2H-tetrazolium chloride
JC-1	1H-Benzimidazolium, 5,6-dichloro-2-[3-(5,6-dichloro-1,3-diethyl-1,3-dihydro-2H-benzimidazol-2-ylidene)-1-propenyl]-1,3-diethyl-, iodide
JECFA	The Joint Food and Drug Organisation/World Health Organisation Expert Committee on Food Additives
L_d	Liquid disordered
LD_{50}	Lethal dose 50%
LDH	Lactose dehydrogenase
L_o	Liquid ordered
LT_{50}	Lethal time 50%
MDCK	Madin Darby canine kidney
mM	Millimolar
MOMP	Mitochondrial outer membrane permeabilisation
MTS	3-(4,5-dimethylthiazol-2-yl)-5-(3-carboxymethoxyphenyl)-2-(4-sulfophenyl)-2H-tetrazolium, inner salt
MTT	3-(4,5-dimethylthiazol-2-yl)-2,5-diphenyltetrazolium bromide
MW	Molecular weight
NAD	Nicotinamide adenine dinucleotide
NADH	Nicotinamide adenine dinucleotide
NADPH	Nicotinamide adenine dinucleotide phosphate
NOAEL	No observable adverse effect level
OECD	The Organisation for Economic Co-operation and Development
PBS	Phosphate buffered saline
PEG	Polyethylene glycol
PC	Polycarbonate

PhRMA	Pharmaceutical Research and Manufacturers of America
PI	Propridium iodide
SDS	Sodium dodecyl sulfate
TEER	Transepithelial electrical resistance
TJ	Tight junctions
TNF	Tumour necrosis factor
v/v	volume *per* volume
w/v	Weight *per* volume
VEGF	Vascular epidermal growth factor
$\Delta\Psi_m$	Mitochondrial membrane potential
Ω	Ohms

1. Chapter One – Introduction

1.1. Background

Surfactants are extensively employed in applications, such as food and pharmaceutical formulations, whereby the consumption of surfactants routinely occurs. Exposure to surfactants, particular non-ionic surfactants, is thus common place and is expected to increase as both the desire for 'designer foods' and the need for novel drug formulations grow.

Animal safety studies have demonstrated that synthetic non-ionic surfactants, such as polysorbates, do have the propensity to elicit abdominal symptoms following repeat doses, and *in vitro* studies demonstrate that non-ionic surfactant toxicity is most likely associated with membrane damage. However, there is a paucity of data regarding the mechanism(s) of toxicity and the conditions of exposure surrounded their induction.

1.2. Surfactant properties – brief overview

Surfactants are a class of amphipathic molecules that contain a hydrophilic segment - which can be zwitterion, ionic, or non-ionic - attached to a non-polar hydrophobic tail that is generally a long chain hydrocarbon residue, but can also be, for example, an oxygenated or halogenated hydrocarbon chain[1,2]. Surfactants are classified as being anionic, non-ionic, cationic, or zwitterionic depending on their polar head groups (Figure 1.1).

The term surfactant originates from *surface active agent*, as these compounds adsorb at interfaces, such as an interface between two liquids, a solid and a liquid, or a liquid and a gas, and reduce interfacial or surface tension.

The hydrophilic-lipophilic balance (HLB) of a surfactant is a measure of the ratio between the strength of the lipophilic and hydrophilic moieties. The HLB concept was proposed in 1949 by Griffin, and can be employed to provide an indication of a surfactant behaviour and its suitability for certain applications[3]

When present in aqueous solutions at concentrations above their critical micelle concentrations (CMC), monomers of surfactants molecules arrange themselves, in equilibrium, into micelle structures (Figure 1.1)[4]. In water, these aggregates arrange themselves such that hydrophobic tails of surfactants form the core and the hydrophilic head groups are positioned facing outwards in contact with the surrounding liquid.

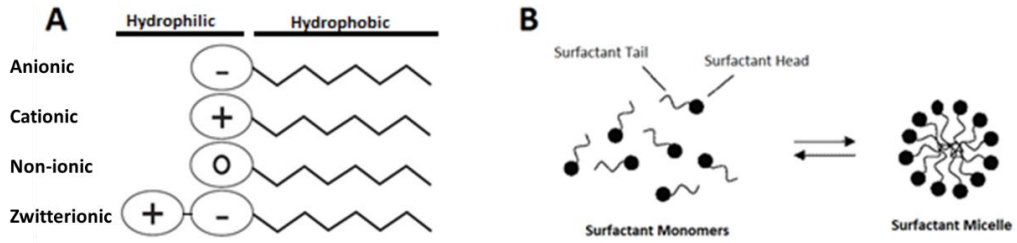

Figure 1.1. (A) Diagram illustrating the different surfactant classes and their polar heads. (B) Schematic of surfactant monomers and their organisation into micelles, in an aqueous environment, with their hydrophilic head facing the external environment and their hydrophobic tails clustered into the centre of the micelle.

1.3. Surfactant applications

Surfactants are employed for a wide range of diverse applications, and may act as wetting agents, foaming agents, emulsifiers and dispersants. It has been estimated that approximately 17.5 million tons of surfactants were used globally in 2014[5]. The highest demand for surfactants is in products for cleaning applications[6]. The surfactant industry is thus dominated by those such as the anionic linear alkylbenzenesulphonates and the non-ionic alcohol ethoxylates, which see predominant usage in laundry detergents[7]. Surfactants are also applied to advantage in many industrial applications such as in the production of petroleum, mineral ores, fuel additives, adhesives, and paints[8]. While the likelihood of an individual's contact with surfactants in cleaning products is high, the incidence of exposure *via* ingestion is low, and generally, the majority of cases are attributed to the accidental ingestion by children under the age of five[9,10].

On the contrary, the general population of all ages frequently ingest surfactants that are used in food and pharmaceutical products and consequently, the associated risk from exposure is greater. The next section will discuss the employment of surfactants in food products.

1.4. Surfactant use in the food industry

Surfactants are utilised in the production of many common food items, in a form of, for instance, food emulsions, dispersions, gels or foams[8]. Table 1.1 presents the main surfactants that are employed in the food industry and their characteristics[11,12].

The use of surfactants in food preparation has been ongoing for centuries, such as the use of naturally occurring surfactants, such as lecithin from egg yolk, in the preparation of mayonnaise[13]. Later, monoglycerides found in seed oils such as rapeseed and olive oil, were introduced in food preparation, and more recently synthetic surfactants, such as the sorbitan-derived Spans and polysorbates (Tweens), have been increasingly employed[11,14].

Many foods are emulsions. The process of emulsification converts two immiscible liquids into an emulsion, or decreases the size of droplets in a pre-established emulsion. This process requires the presence of an emulsifier, such as a surfactant, and energy[12]. Classical examples of water in oil (w/o) emulsions include margarines, butter and other fat-based spreads, while mayonnaise and ice cream are typical examples of oil in water (o/w) emulsions.

In addition to facilitating the formation of an emulsion, surfactants are used as stabilising agents to increase emulsion stability, preventing the immiscible liquids reverting back after processing and as a result can increase product shelf life[12]. This is achieved by lowering the interfacial tension between liquids and generating steric and/or electrostatic hindrance to droplet aggregation[15].

Surfactants are also used widely as foaming agents in the generation of foods such as baked goods, whipping cream, mousses and ice cream[16]. Foams are aerated emulsions, and incorporating gas bubbles into food products can alter textures, microstructure, mouthfeel and lower calorific density[17–19].

Surfactants are also key components in the production of edible coatings, such as those found in confectionery products, to generate an aesthetically pleasing gloss, or on fruits to reduce shrinkage due to water loss[20]. Surfactants are used to allow for proper wetting and adhesion over the surface of the product[21]. Moreover, surfactants such as polysorbate 60, are generally used in chocolate blend coatings to stabilise the coco butter-based emulsion and, also used to increase the palatability of the confection, by generating an emulsion between mouth saliva and fat, which is described to reduce the 'waxy' mouthfeel of some products[22].

The use of surfactants in food products is increasing, as a result of the growing desire to manipulate the contents of food products. For example, there is currently a drive for foods with an increased content in certain oils, such as omega-3, in response to recent national and international reports regarding dietary recommendations[23,24]. Furthermore, increasing the air or water content of foods, using foaming and emulsifying agents, has been suggested in the design of food products that promote products lower caloric density, in order to combat the rising prevalence of global obesity[16,25].

By 2018 it has been estimated that the use of surfactants in food products is to reach 0.9 million tons[26]. The most used surfactants in food are lecithins, mono- and diglycerides of fatty acids, sucrose esters of fatty acids and the sorbitan derivatives,

Spans and polysorbates (Table 1.1)[11,26]. The next section will cover some of these surfactants in more detail and begin to discuss aspects of surfactant safety and levels of exposure levels.

Table 1.1. Classification and characteristics of commonly used surfactants in the food industry

Surfactant	Abbreviation	EU number[27]	Acceptable daily intake[27,28]	HLB[12,29]	Emulsion type	Charge
Lecithin	-	E322	Not limited	<9	w/o and o/w	Zwitterionic to anionic
Mono and diglycerides	-	E471	Not limited	3-6	w/o	Non-ionic
Sucrose esters of fatty acids	-	E473	0-40 mg/kg	7-8	o/w	Non-ionic
Polyglycerol esters of fatty acids	PGE	P475	0-25 mg/kg	6-11	o/w	Non-ionic
Sorbitan monostearate	Span 60	E491	0-25 mg/kg	4.7	w/o	Non-ionic
Sorbitan monolaurate	Span 20	E493	0-25 mg/kg	8.6	o/w	Non-ionic
Sorbitan tristearate	Span 65	E492	0-25 mg/kg	2.1	w/o	Non-ionic
Sorbitan mono-oleate	Span 80	E494	0-25 mg/kg	8.6	o/w	Non-ionic
Polyoxyethylene sorbitan monolaurate	Polysorbate 20 (Tween® 20)	E432	0-25 mg/kg	16.7	o/w	Non-ionic
Polyoxyethylene sorbitan mono-oleate	Polysorbate 80 (Tween® 80)	E433	0-25 mg/kg	15	o/w	Non-ionic
Polyoxyethylene sorbitan monostearate	Polysorbate 60 (Tween® 60)	E435	0-25 mg/kg	14.9	o/w	Non-ionic
Polyoxyethylene sorbitan tristearate	Polysorbate 65 (Tween® 65)	E436	0-25 mg/kg	10.5	o/w	Non-ionic
Sodium stearoyl lactylate	SSL	E481	0-22 mg/kg	11	o/w	Anionic

1.4.1. Lecithin

Lecithins are used widely in the food industry and originate from a variety of sources including egg yolk, sunflower and rapeseed seeds, and soya. Lecithins mainly consist of glycerophospholipids such as phosphatidylcholine (PC), and other phospholipids such as phosphatidylinositol (PI) and phosphatidylethanolamine (PE)[30]. The HLB values of commercial lecithins commonly range between 2 and 7, rarely exceeding 9, and are used in the formation of o/w emulsions and less commonly w/o emulsions[31,32]. Emulsions stabilised by lecithins alone are not very stable and are typically used in combination with other surfactants[31]. The main advantages of lecithins are that they are perceived as being natural product by consumers and are considered non-toxic by authorities, such as those discussed in the next section (1.4) [12]. Following oral administration, consumed lecithins are hydrolysed by phospholipases to liberate choline in the intestines. Choline is well absorbed from the intestinal tract, found predominately as free choline in plasma, and is a precursor for the neurotransmitter acetylcholine. It is estimated that average daily oral intake for lecithins from regular diet is 4 to 71 mg/kg body weight *per* day across all population age groups[33].

1.4.2. Mono- and diglycerides

Mono- and diglycerides are naturally present in various seed oils[34], however their concentration is low and production on an industrial scale is achieved through a glycolysis reaction between glycerol and triglycerides[35].

These surfactants have been assessed as non-toxic by international and European safety committees (discussed in section 1.4), and their use in food products is not limited. Commercially available mono- and diglycerides typically contain 45-55% monoglycerides, 38-45% diglycerides, 8-12% triglycerides and an estimated 1-7% of free glycerol[36,37]. These non-ionic emulsifiers are hydrophobic in nature, are assigned low HLB values between 3 and 6, and typically used to stabilise w/o emulsions[29].

Monoglycerides are commonly used as texturising agents in the food industry, as *per* their ability to, when in contact with water, form mesomorhic phases and dispersions, and are commonly used in formulations such as ice creams[38]. The use of these substances is allowed at a concentration up to 5 g/l in powdered and liquid formulations intended for infants and young children from birth and, no more than 5 g/kg *per* day is advised for intake[39]. As of June 2017, the European Food Safety Authority (EFSA) is requesting further safety information for the re-evaluation of mono- and diglycerides toxicity[40]; much of the toxicity testing for these substances was performed half a century ago using experimental designs now considered limited by regulatory authorities[40].

1.4.3. Sucrose esters of fatty acids

Sugar esters made from a sugar and fatty acids represent a broad range of compounds. The sugar can be sucrose or a polyol, such as xylitol or sorbitan, however the European Food Safety Agency has only authorised the use of sucrose esters of fatty acids and sucroglycerides in food formulations[41]. These compounds consist of a mixture of mono-, di- and tri-esters of

sucrose with fatty acids. The degree of esterification and chain length of the esterified fatty acid (C6-C18) influences the lipophilic character of these surfactants and, as such, these sucrose esters cover a wide range of HLB values (1 to 18), thus conferring them with potential use in various applications[29]. These surfactants are also reported as having good aroma and taste profiles; advantageous properties in the food industry[42]. Mono- and di-esters of sucrose esters of fatty acids are extensively hydrolysed into their constituent fatty acids and sucrose in the gastrointestinal tract prior to absorption, and consequently are considered relatively safe by food safety authorities[43].

Of note however, are reports that the mean dietary intake of mono- and di-esters for children ages 5-12 is estimated at being at 51.6 mg/kg *per* day, a value higher that the safety margin (acceptable daily intake; defined in section 1.6) value (Table 1.1)[43]. The major contributor for this exposure is believed to come from the consumption of fruits, where sucrose esters of fatty acids see common use as glazing agents to prevent water loss[43].

1.4.4. Sorbitan esters and Polysorbates

Sorbitan esters (Spans) are derived from the esterification of dehydrated sorbitol with fatty acids[44], and can produce molecules of varying esterification and HLB value (Table 1.1). Sorbitan monolaurate, for example exhibits a HLB value of 8.6 and sorbitan monostearate a HLB value of 4.7, stabilising o/w and w/o emulsions, respectively[29]. Sorbitan esters can generate polyoxyethylene derivatives, known as polysorbates (or Tweens®), through reaction with ethylene oxide[44].

Polysorbates are non-ionic, water soluble surfactants that exhibit a range of surface activity, HLB value and emulsifying properties (Table 1.1). In the gastrointestinal tract, polysorbates are hydrolysed to oxyethylene sorbitans and fatty acids following hydrolysis of the ester bond between the fatty acid and polyoxyethylene[45]. The fatty acids released from polysorbates are absorbed, metabolised and extracted in the same manner as dietary fatty acids, however, small amounts of polyoxyethylene sorbitans are absorbed[45].

In addition to their use in the food industry, Spans and, particularly polysorbates, are used in pharmaceuticals, cosmetics, fungicides and pesticides, with the annual demand for these compounds in 2012 estimated at 10,000 tons[46]. It is estimated that the mean exposure to these surfactants from use as food additives ranges from 9.6 mg/kg *per* day in children, to 0.3 mg/kg *per* day in adults and the elderly[45]. However, the prediction of exposures from assessment scenarios varies greatly due to the high variability of use levels among different food brands, and mean exposure from 'brand-loyal' assessments can range as high as 18.1 mg/kg *per* day in children and 57.5 mg/kg *per* day in adults[45]. The safety of polysorbates was re-evaluated by the European Food Safety Agency in 2015 and maintained their authorisation as use as food additives in the European Union[47], however, there has been discussion among regulatory and scientific committees regarding the lowering of the ADI from a limit of 25 to 10 mg/kg *per* day[45,48,49].

Polysorbates, also see common usage in the pharmaceutical industry, and this aspect of their application will be discussed in section 1.5.

1.5. Surfactant use in the pharmaceutical industry

In addition to their use in food products, surfactants have important applications in the pharmaceutical industry. Surfactants play different roles depending on the type of pharmaceutical formulation; for example, in liquid preparation surfactants are used to stabilise or solubilise drugs, in topical formulations to improve textural characteristics and physical stabilities, and in manufacture of solid dosage forms, as agents to alter the flow properties and wetting of granulates and powders[78]. Moreover, surfactants are increasing being employed in drug delivery systems as absorption enhancers to increase the bioavailability of drugs in convenient administration forms, such as oral formulations[79].

One important property of surfactants is the formation of micelles in aqueous solutions (Figure 1.1), which have particular significance in drug formulations because of their ability to increase the solubility of substances that are poorly soluble in water[80–83]. It was estimated in 2015 that 40% of market approved drugs and nearly 90% of drug molecules in the discovery pipeline are poorly soluble[84].

Surfactant micelles are known to have anisotropic water distribution within their structure[85]; water concentration decreases from the surface towards the centre, with the micelle core environment being very hydrophobic. The separation of polar bulk aqueous phase from an interior of hydrocarbon chains establishes an interfacial region[86], in which molecules can partition into[87]. Drugs can be solubilised at a number of possible loci in micelles, such as the absorption of (i) hydrophilic drugs on the surface of the micelle, (ii) intermediately soluble drugs in the palisade layer, between the

hydrophobic chains, and (iii) completely insoluble hydrophobic drugs in the micelle core[88–90].

A multitude of non-ionic surfactants are utilised in commercially available solubilised oral formulations including Cremophors, Polysorbates, Solutol HS15 and Spans[83]. Polysorbate 20, for example, is used as a solubilising agent in over the counter products such as children's Benadryl and Sudafed[83]. Cremophor EL is employed as a component of Gengraf® cyclosporine microemulsion and, Norvir® oral solution and soft gelatin capsule formulations of ritonavir[83].

In addition to use as drug solubilisers, surfactants are also being used as absorption enhancers. The need for absorption enhancing technology has grown considerably due to the demand for non-invasive methods for the delivery of small molecules and biologics, the latter including protein, peptide or nucleic-based therapeutics. A report by the Pharmaceutical Research and Manufacturers of America (PhRMA) states in 2013 there were 907 biologics in development, targeting over 100 different diseases[91].

However, despite considerable interest in biologic therapeutics a large challenge is faced in the development of non-invasive delivery systems for this drug category. This is due to their physiochemical properties, including short plasma half-life, large molecular size, immunogenicity, susceptibly to enzymatic degradation, and the tendency to undergo denaturation and aggregation[92–94]. Furthermore, biologics are typically developed to target long term conditions, due to their ability to function as replacement therapy to exploit mechanisms that traditional small molecular drugs cannot[95,96]. Accordingly, chronic dose regimes are generally required to address these

conditions, however patient compliance to long term parental drug administration can be poor[97]. On the other hand, oral administration is non-invasive and generally demonstrates higher levels of patient compliance[98].

There are however, various physiological barriers that limit the oral absorption and consequently bioavailability of biologics, such as enzyme digestion, intestinal flora, gastrointestinal pH (pH 1-8) and the intestinal epithelium barrier function[99]. The effectiveness of these biological barriers as restrictions to drug delivery is highlighted by insulin, for example, which has an oral bioavailability of approximately 1%[100]. As a result, the development of oral formulations for biologics is not viable unless a system which can increase their oral absorption is designed, and to address this, surfactants are being investigated due to their ability to improve permeability across the intestinal epithelium.

1.5.1. Mechanisms of epithelial transport

Depending primarily on their physiochemical properties, compounds traverse the intestinal epithelium in different manners. Active mechanisms use cellular energy sources, such as adenosine triphosphate (ATP) and, transmembrane proteins or lipids, to facilitate the transport of molecules through the bilayers of epithelial plasma membranes. Other pathways can involve molecules diffusing across epithelial layers by travelling through the intracellular space in between cells, or by readily diffusing through lipid bilayers and into, and out of the cell in an apical to basal direction. The transport across epithelial cells can be divided into two categories; paracellular and transcellular transport (Figure 1.2).

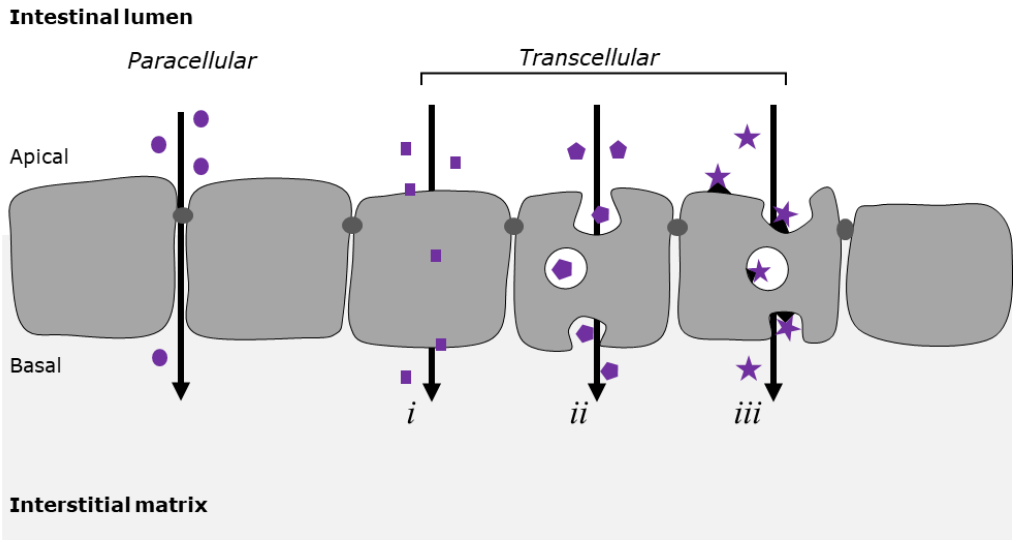

Figure 1.2. Schematic diagram of paracellular and transcellular pathways across epithelium. The transcellular transport can be achieved by (i) passive diffusion, or (ii) transcytotic mechanism, which may be (iii) receptor-mediated.

1.5.2. Paracellular transport

The paracellular route involves the translocation across the epithelium *via* the paracellular space between cells and, is employed in the selective transport of small hydrophilic compounds (Figure 1.2)[101].

The permeability of the paracellular route is not only dependent on the physiochemical properties of the permeating molecule but also on epithelium morphology[102]. As discussed in section 6.1, epithelial cells are held to adjacent cells by three distinct cell-cell protein junctions; the tight junction, the adherens junction and desmosomes. Tight junctions are the most apical junctional complexes and gate solute flux in a size- and charge-dependent manner[103,104]. The paracellular route is easier for cations to permeate across than neutral compounds, and

anions are the least permeable to this pathway[101,105]. Tight junctions are therefore important components in governing permeability across epithelial layers and enable the permeation of small solutes, such as extracellular ions but restrict the transport of macromolecules[106].

1.5.3. Transcellular transport

The transcellular pathway of passive diffusion typically involves the diffusion of molecules through the apical and basolateral membranes of cells (Figure 1.2). However, due to the hydrophobic environment of the phospholipid bilayer, passive diffusion of hydrophilic, charged or zwitterion molecules is severely restricted. On the other hand, the high affinity of lipophilic molecules for the lipid bilayer makes them ideal for utilising this pathway, however molecules that are very lipophilic can become entrapped in the lipid membrane rather than diffusing across it[107].

In addition to unfavourable lipophilicity, the transport of macromolecules may be limited by the ability of their hydrocarbon backbone to form hydrogen bonds with water molecules[108]. Indeed, in order to exploit passive transcellular transport these hydrogen bonds must first be severed, an energy-dependent process, before the molecule is able to transverse the bilayer[109,110].

1.5.4. Surfactant absorption enhancers

Surfactants, including those listed in Table 1.1, are being increasingly employed as intestinal absorption enhancers, i.e. to increase drug transport across the intestinal epithelia layer[111–116]. Polysorbate 80, for example, which is used in the

production of ice cream[117], has also been successfully employed to increase the oral bioavailability of digoxin in rats by approximately 2-fold[118].

In addition to their use in the pharmaceutical industry, non-ionic surfactants such Triton X-100 and polysorbate 20, have been used extensively in biological experiments for their ability to permeabilise cells and extract proteins from their membranes[139–141]. It is unsurprising therefore, that mechanistically, the majority of surfactants have been associated with mediating their cellular effects *via* their influence on plasma membranes, and have been attributed to increase transcellular transport *via* their direct effect on cell plasma membranes (Figure 1.3)[116,119–124]. The effects of surfactant on cellular membranes are discussed further in Chapter 3, however, in general, the incorporation of surfactants into the lipid bilayer of the membrane, directed by the amphipathic nature of surfactants, has been reported to increase transcellular permeability by altering membrane fluidity and tension (Figure 1.3)[124–126].

For example, Petersen et al. investigated the non-ionic alkylglycoside surfactants tetradecylmaltoside and dodecylmaltoside and observed increased transport across Caco-2 intestinal epithelial monolayers in conditions that altered membrane barrier function[113]. Tetradecylmaltoside has been reported to increase the permeability of insulin across nasal epithelial *in vivo* in rats[127]. Furthermore, insulin permeability has also been observed to be enhanced across Caco-2 monolayers with dodecylmaltoside[128] and octylglucoside[129]. Similarly, a study by Dimitrijevic et al. demonstrated that permeability of metformin across Caco-2 cells was increased by polysorbate 20, 60 and 85, and Solulan

C24 and 16, and in exposure conditions associated with surfactant-induced membrane disruption[119]. Furthermore, cremophor EL, a non-ionic surfactant derived from castor oil, is also reported to enhance drug permeability across epithelial cells[111,130].

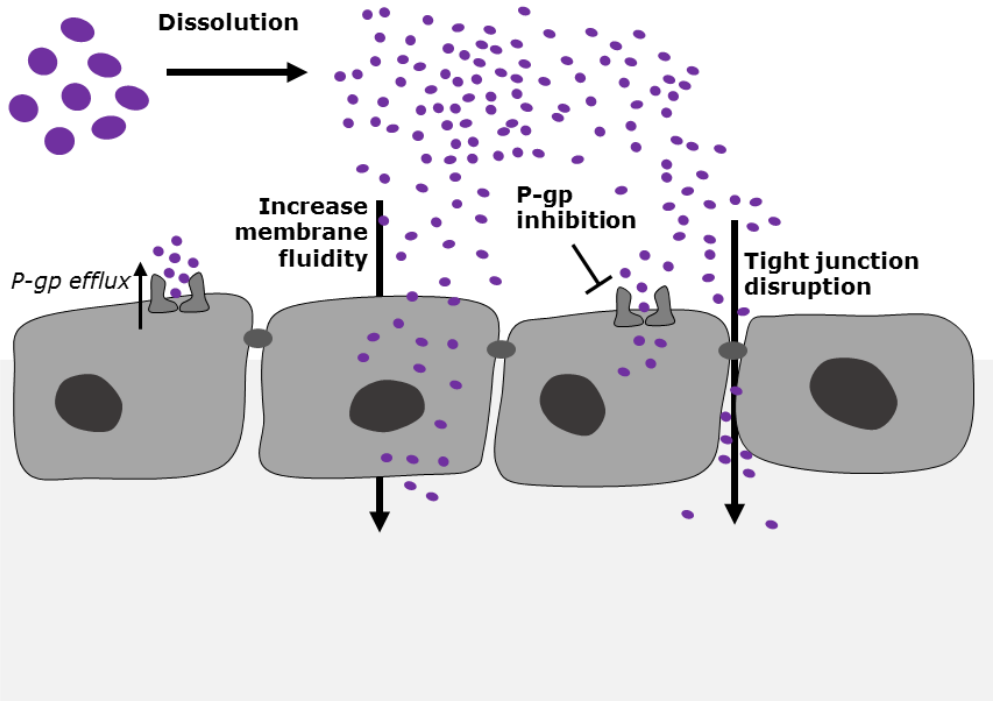

Figure 1.3. Suggested non-ionic surfactant mechanisms of enhancing compound permeability across the epithelial cell layer. Surfactants increase both the dissolution of drug molecules as solubilising agents, and alter plasma membrane fluidity in a manner that enhances delivery of agents. Some surfactants are also associated with inhibiting efflux pumps such as P-glycoprotein (P-gp), and others are reported to alter the gating function of tight junctions. The effects of surfactant on membrane fluidity and efflux pump function are discussed in detail in section 3.1.

Non-ionic surfactants demonstrate an ability to augment paracellular transport (Figure 1.3), however this is generally reported to occur concomitantly with their plasma membrane disrupting effects [116,119,131,132]. It has therefore been suggested that this effect is secondary to, and a result of, membrane

perturbation and consequent effects on the cytoskeleton and junctional complexes[116,123,133]. For example, alkylglycoside surfactants increased mannitol transport along the paracellular pathway, however this is attributed to their asymmetric insertion into the lipid bilayer of cell membranes, consequently disrupting the integrity of tight junctions and therefore their barrier function[123,133].

Furthermore, inhibition of cellular efflux pumps has been reported as an effect of surfactant influence on plasma membranes, and has been attributed to increasing compound transport across the epithelium (Figure 1.3)[115,134–136].

In addition to non-ionic surfactants, the permeability enhancing effect of anionic surfactants has been investigated. For example, the classical anionic surfactant, sodium dodecyl sulphate (SDS) has been observed to increase the transport of mannitol, vasopressin and polyethylene glycol across intestinal epithelia *in vitro*[137]. Other anionic surfactants, such as the anionic bile salt surfactants sodium cholate and sodium taurocholate have also demonstrated an ability to enhance permeability across epithelial cells[131]. It is believed that anionic surfactants increase the transport along both the paracellular and transcellular routes by disrupting the plasma membrane and altering the morphology of tight junctions[131,138].

1.6. Toxicity testing

Toxicity testing, also referred to as safety testing, is carried out to ascertain whether a substance poses a health threat.The government of the United Kingdom of Great Britain (UK) requires that all new chemical compounds be tested *in vivo*, in order to identify toxic and safe levels, and minimise the hazard to health prior to use[50,51].

The Joint Food and Agriculture Organisation of the United Nations (FAO)/World Health Organisation (WHO) Expert Committee on Food Additives (JECFA) is an international expert scientific committee that evaluates the safety of food additives[52]. Furthermore, a European agency, the European Food Safety Authority (EFSA), is another authority on food safety that operates to provide scientific advice to aid European policies and legislation[53]. Together these organisations establish and update safety parameters, such as the acceptable daily intake (ADI) of food additives. The ADI level was introduced by JECFA to provide "an adequate margin of safety to reduce to a minimum any hazards to health in all groups of consumers"[54]. ADI values are used by legislators for the assessing the approval of food additives, and regulating their lawfully allowed limits in products.

Due to their prominent use in the food industry, surfactant toxicity has been well studied over the last fifty years. This section will cover the common toxicity studies that are performed and discuss key points.

1.6.1. Acute toxicity

Acute toxicity is generally defined as the adverse effect(s) that occur immediately or a short time after a single exposure to a substance[55]. An adverse effect is defined as "any effect that results in functional impairment and/or biochemical lesions that may affect the performance of the whole organism or that reduce the organ's ability to respond to an additional challenge"[56]. Therefore, a substance that is orally absorbed during a given time and generates adverse effects with little delay is classified as orally and acutely toxic.

Acute toxicity testing aims to determine possible targets of organ toxicity and it enables substances to be ranked for classification purposes and hazard assessment[55]. Animals are administered a single dose with the test substance and are closely observed during the first 24 hours and then daily for 14 days[55,57].

None of the surfactants classes, synthetic or natural, used in food products (Table 1.1) are labelled as harmful or above (LD_{50} >500 mg/kg), or considered acutely orally toxic[28,45,48,58,59]. For example, lecithin purified from soya (phosphatidylcholine content 75-98%) was orally administered to mice and rats at concentrations up to 16 g/kg with no mortalities[60,61] and, no acute oral toxicity was reported in rats dosed with polysorbates (20, 40, 60, 65, 80) at concentrations of 39 g/kg[62]. Similarly, a case report published in 1955 described how the accidental administration of 19 g/kg of polysorbate 80 for two successive days to a 4 month old infant, was followed by no ill effects aside from diarrhoea[63].

1.6.2. Subacute and subchronic toxicity testing

Subacute and subchronic safety studies, also known as repeat dose studies, are employed to discover the effects repeated exposure to a substance has on an organism and, are important to industries such as the food industry as they allow the determination of threshold doses. The no observed adverse effect level (NOAEL) is a common parameter obtained *via* the study of a series of doses, and is used to determine the ADI level of exposure; to do so, the NOAEL is divided by a safety factor to set the ADI[11]. It is generally accepted that the longer the study, the more accurate and precise the NOAEL

determination[64,65], however, food components are not typically required to undergo long-term studies for regulatory authorisation, consequently, long-term surfactant toxicity is not as well studied[11,24].

Surfactants demonstrate differing levels of oral subchronic toxicity. Lecithins for example do not demonstrate any signs of subchronic toxicity[66,67]. However, a multitude of studies demonstrate that polysorbates demonstrate toxicity upon repeat exposure[45,58,68–72]. Diarrhoea appears to be a commonly observed adverse effect at polysorbate concentrations ≥5% in the diet (~3.7 g/kg *per* day[49])[58,68–72], and is suggested as a result of damage to the brush boarder membrane of the small intestine[68].

1.6.3. Chronic toxicity testing

Chronic toxicity is a result of the progressive or persistent deterioration of cell function or organ systems that result from the long-term exposure to a chemical. Chronic toxicity studies are therefore performed to provide information on the possible hazards likely to arise from repeated exposure over a considerable portion of the lifespan of the species used[73].

Studies from the 1950s report that 2.5 g/kg *per* day of polysorbate 60, 65 or 80 for 24 months increased occurrences of diarrhoea in rats, however no alterations in body weight or survival were observed[74–77]; thus, demonstrating similar observations to those made in subchronic studies.

1.7. In vitro toxicity

The plasma membrane is a key structure of the cell, and performs a vital function in protecting and compartmentalising intracellular contents from extracellular conditions, and a multitude of other functions such as those linked to signalling and metabolism[142–144]; indeed a substantial number of cellular processes are associated with this membrane[145]. Hence, unsurprisingly, perturbations to the plasma membrane, which may increase compound permeability, are also associated with toxic effects. Consequently, many surfactants are limited in their application as permeability enhancers due to reports of cytotoxicity[119,124,137,146].

1.7.1. Ionic surfactants

Surfactants with charged head groups are generally more potent at inducing cytotoxicity than their non-ionic counterparts, inciting toxic effects at concentrations below their CMC values, and thus are less useful for use as absorption enhancers[131,146,147].

Epithelial cell exposure to SDS at concentrations below its CMC, for example, is associated with permeabilising the nuclear membrane, inducing the structural separation of tight junctions and generating gross abnormalities in cytoskeletal organisation[137].

Cationic surfactants, induce toxicity at concentrations far below their CMC[148,149]; a study by Inácio et al. determined that, after 60 minutes of cell exposure, cationic surfactants of the n-Alkyl-N,N,N-trimethylammonium bromides (C_nTAB) series have LD_{50} values >10-fold lower than their CMC[148]. In comparison, the

authors report an LD_{50} value for SDS at approximately 1.5-fold lower than its CMC, the LD_{50} value for the zwitterionic surfactant N-dodecyl-N,N-dimethylammonium-propanesulfonate (DDPS) being approximately at its CMC, and the non-ionic Triton X-100 as having an LD_{50} value approximately at its CMC[148].

Accordingly, cationic surfactants are considered the most toxic surfactant class and are predominately used in bactericidal applications[148–152]. Cationic surfactants, such as the quaternary ammonium compounds, are the only surfactant group that are known to induce toxicity at concentrations that do not concomitantly induce plasma membrane damage, and they do so by perturbing mitochondrial respiration in a manner that promotes apoptosis[148,153]. Moreover, at concentrations closer to its CMC the cationic C_{10}TAB surfactant has been observed to induce necrosis *via* total inhibition of mitochondrial phosphorylation and consequently abolishing cellular energy charge[148]. Cationic surfactants have also been reported to translocate across plasma and nuclear membranes, and interact with nucleic acids[152,154].

1.7.2. Non-ionic surfactants

The cytotoxicity of non-ionic surfactants has been generally described as damage to plasma membrane and the alterations of cellular morphology[113,119,124,137,146]. Non-ionic surfactants induce their cytotoxic and permeability enhancing effects at concentrations in solution that are generally at, or above their CMC[115,119,147]. Therefore, non-ionic surfactants have been suggested to act predominantly on the plasma membrane and their effects associated with micelle-dependent destabilisation

and/or damage[149,155]. Indeed, due to a correlation between increased membrane permeability and cytotoxicity, in the form of intracellular contents leakage and decreased cellular viability, it has been suggested that non-ionic surfactant toxicity may be intrinsic to their mechanism of permeability enhancing action[119,124,156].

The permeability enhancing effect of alkylglycoside surfactants, for example, is attributed to their ability to intercalate into lipid bilayers[127], however this mechanism has also been associated with their toxicity *in vitro*[124] and *in vivo*[127]*. In vitro* alkyglycosides have been observed to damage epithelial plasma membrane integrity, resulting in the loss of intracellular contents, and decrease in cellular viability[124]. Moreover, *in vivo* damage to the epithelial surface morphology, including the shortening of the epithelial villi, has been observed[127]*.*

Polysorbate surfactants (20, 60 and 80) have been observed to damage the integrity of the plasma membrane[119,131,157,158], decrease cell viability[119] and are reported to do so at concentrations associated with increasing solute permeability[131,157]. Sucrose esters of fatty acids have also been reported to induce epithelial plasma membrane leakage, loss of viability and alter cytoskeletal organisation in conditions that increase drug permeability[157].

The relationship between surfactant structure and their ability to influence the cell membranes has been investigated[159–163], and it is believed that the lower the HLB value of a surfactant the greater the effect on the membrane[164]. For example, shortening the alkyl chain length of surfactant tail regions was demonstrated by Ross et al. to alter and promote biocompatibility[164]. This observation was further by Vllasaliu et

al. who demonstrated that as alklgycoside surfactant hydrophobic chain length was increased, surfactant-induced membrane permeability and cytotoxicity were increased[124].

Studies that are performed to illustrate surfactant effect on the cell plasma membrane and on permeability of the epithelial layer only provide limited insight into surfactant toxicity, and detailed surfactant cytotoxicity information is lacking from the literature. The main reasons for this are the limited exposure conditions investigated and the types of parameters assessed.

Studies investigating the ability of surfactants to enhance epithelial permeability, commonly use only one or two cytotoxicity assays; lactose dehydrogenase (LDH) release or the MTT(3-(4,5-Dimethylthiazol-2-yl)-2,5-Diphenyltetrazolium Bromide) or MTS (3-(4,5-dimethylthiazol-2-yl)- 5-(3-carboxymethonyphenol)-2-(4-sulfophenyl)-2H-tetrazolium, inner salt) reduction assay[116,119,124,131,157]. These assays are performed to provide evidence of plasma membrane damage by measuring the leakage of an intracellular enzyme (LDH) and 'viability' / 'metabolic activity' of cells *via* the reduction of formazan salts, such as the MTT and MTS[165]. These assays are discussed in further detail in Chapters 3 and 4, respectively.

While useful, the evaluation of these measures alone, however, does not enable toxicity/cell death mechanisms to be determined and, only provides an indication of non-toxic concentration ranges. Consequently, information in the literature is limited on the cell response to non-ionic surfactant exposure and the mode of cell death induced.

For example, cremophor EL, was observed to decrease cell viability[119], and damage the plasma membrane intregity[166]. It has been suggested that cremophor EL induces cell death by

abolishing cellular calcium ion homeostasis and allowing uncontrolled ion influx[167]. As will be discussed in Chapter 5, increases in intracellular Ca^{2+} are linked to both necrosis and apoptosis[168–171], and cremophor EL was observed to induce parameters associated with both[167]. Studies on polysorbate 20[172] and 80[173] have reported apoptosis as the mechanism of cell death.

In addition to few studies focussing on deciphering cellular responses associated with cell death, the study of surfactant cytotoxicity is also limited by the lack of standardisation of exposure times and the constraint of only measuring parameters following a single time point. For example, cytotoxicity is generally analysed at one set time point, such as following exposures of 1[157], 2[124,131,174], 4[119,175,176] or 24 hours[177]. Using only one exposure period limits the analysis of cytotoxic progression, and prevents mechanisms being observed to unfold. Furthermore, the lack of standardisation with exposure times hinders comparison among surfactants, and also with other substances.

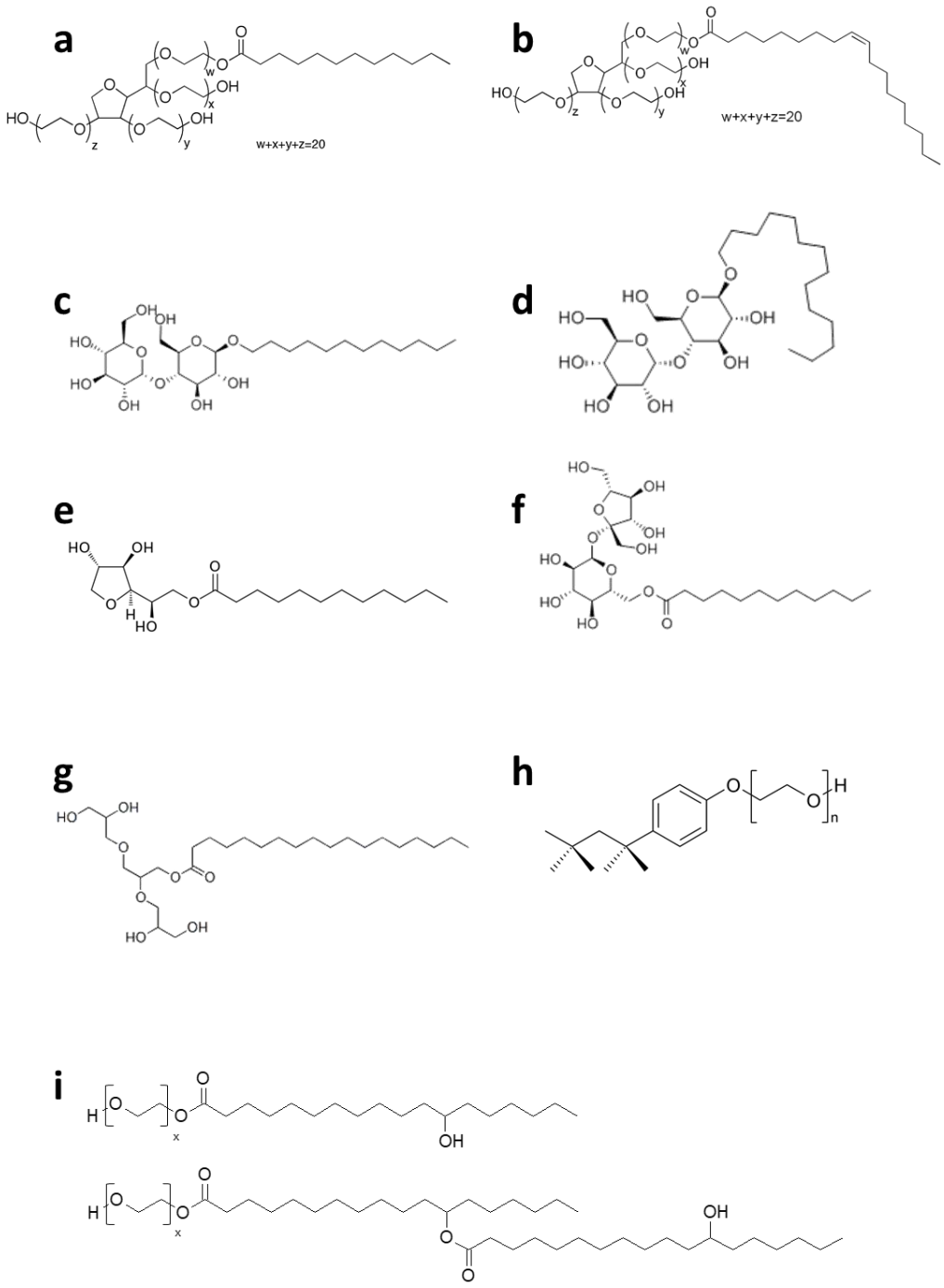

Figure 1.4. Chemical structures of various non-ionic surfactants discussed. Polysorbate (a) 20 and (b) 80, (c) dodecylmaltoside, (d) tetradecylmaltoside, (e) sorbitan monolaurate (Span 20), (f) sucrose monolaurate, (g) triglycerol monostearte, (h) Triton X-100 and (i) Solutol HS15 (a mixture of polyglycol mono- and di-esters of 12 hydroxystearic acid).

1.8. Solutol HS15

For the purpose of studying surfactant effect on intestinal epithelia cells, Solutol HS15 has been chosen as a model surfactant. Solutol HS15 (macrogol 15 hydroxystearate), also known as Kolliphor HS15, is a non-ionic, fatty acid surfactant consisting of a mixture of poly-glycol mono- and di-esters of 12-hydroxystearate[134].

Solutol HS15 is water soluble, it has a HLB value between 14-16 and a CMC which is calculated to lie between 0.06-0.1 mM[116]. Solutol HS15 is used in the formulation and stabilisation of drug delivery systems, such as emulsions[178,179] and nanoemulsions[180–183], and for poorly soluble drugs such as dipyridamole[179] and Coenzyme Q[183]. By improving aqueous solubility, formulations containing Solutol HS15 can increase the bioavailability of drugs, such as cyclosporine, which has demonstrated increased oral bioavailability in such formulations in rats[184].

Solutol HS15 is also employed as an absorption enhancer and, similar to other non-ionic surfactants, is believed to function in this manner *via* its effects on plasma membranes [115,116,136,185,186]. However, as with other non-ionic surfactants, Solutol HS15 induced permeability enhancement is often associated with cytotoxicity[115,116].

A recent study by Shubber et al., demonstrated that Solutol HS15 increased the permeability of insulin and human growth hormone across airway (Calu-3 and A549) and intestinal (Caco-2) epithelial cell lines[116]. Permeability enhancement was observed over 180 minutes and achieved with solutions of Solutol HS15 ≥0.5 mM, however following 180 minutes exposure, these concentrations were associated with damage

to plasma membrane integrity and cellular metabolic activity, as determined by LDH release and MTS assays, respectively[116].

Similarly, Brayden et al. observed increased permeability of solutes across Caco-2 epithelial cells with solutions of 1 mM Solutol HS15 over 120 minutes, however, this concentration was also associated with increasing LDH release following exposures of 60 minutes[115]. Furthermore, the authors report similar results with *ex vivo* experiments on rat ileum and colonic mucosae; observing permeability increases with solutes over 120 minutes, however at Solutol HS15 concentrations that generated increased LDH release following this exposure[115].

1.9. Project aims

The aim of this project is to perform a detailed study on the cellular effects of the model non-ionic surfactant Solutol HS15, in order to observe the conditions surrounding the induction of cellular toxicity (i.e. exposure time and concentration). Solutol HS15 has been selected as a model due its increasingly common usage in various scenarios in the pharmaceutical industry, similarity in use and effect to other non-ionic surfactants, and its regulatory status; including approval by the FDA, inclusion in the European Pharmacopedia and listed by the IID (international insurers department).

The Caco-2 cell line is the most widely used *in vitro* model of intestinal epithelia and displays many of the functional and morphological properties of the *in vivo* intestinal epithelial barrier. The current study employs this cell line to provide data pertaining to the potential oral toxicity of non-ionic surfactants. The resultant information is considered paramount to enabling the safe application of these substances.

From previous studies on Solutol HS15 and non-ionic surfactants it is hypothesised that Solutol HS15 will present with cytotoxic effects at concentrations above its CMC and following exposures including and in excess of 4 hours. These effects will likely include damage to the integrity of the plasma membrane and decline in metabolic activity, however it is unclear what mechanism of cell death will be most prominent.

This project is approached with a focus on exposure time; investigating surfactant effects typically following 5, 10, 20, 60, 120, 180 and 240 minutes, thus enabling the observation of cellular events unfolding over time. Together with the assessment of membrane, mitochondrial and cell death

associated effects this study sets out to decipher the potential mechanism(s) of non-ionic surfactant toxicity on intestinal epithelia and, the influence of *in vitro* culture conditions on toxicity assessment.

1.10. References

1. Goddard, E. D. *Surfactants and interfacial phenomena*. *Colloids and Surfaces* **40,** (1989).
2. Som, I., Bhatia, K. & Yasir, M. Status of surfactants as penetration enhancers in transdermal drug delivery. *Journal of Pharmacy and Bioallied Sciences* **4,** 2 (2012).
3. Griffin, W. C. Classification of surface-active agents by‘ HLB’. *J. Soc. Cosmet. Chem.* **1,** 311–326 (1949).
4. Blankschtein, D., Thurston, G. M. & Benedek, G. B. Phenomenological theory of equilibrium thermodynamic properties and phase separation of micellar solutions. *J. Chem. Phys.* **85,** 7268–7288 (1986).
5. Allied Analytics LLP. World Surfactants Market - Opportunities and Forecast, 2014 - 2020. *Research and Markets* (2016). Available at: https://www.researchandmarkets.com/research/3bjwd5/world_surfactants. (Accessed: 6th September 2017)
6. Ceresana. *Market Study: Surfactants (2nd edition)*. (2015).
7. Kosswig, K. in *Ullmann’s Encyclopedia of Industrial Chemistry* (Wiley-VCH, 2005).
8. Schramm, L. L., Stasiuk, E. N. & Marangoni, D. G. Surfactants and their applications. *Annu. Rep. Prog. Chem., Sect. C Phys. Chem.* **99,** 3–48 (2003).
9. Bronstein, A. C. *et al.* 2010 Annual Report of the American Association of Poison Control Centers’ National Poison Data System (NPDS): 28th Annual Report. *Clin. Toxicol.* **49,** 910–941 (2011).
10. States, U. & June, M. Health hazards associated with laundry detergent pods - United States, May-June 2012. *MMWR. Morb. Mortal. Wkly. Rep.* **61,** 825–9 (2012).
11. Kralova, I. & Sjöblom, J. Surfactants Used in Food Industry: A Review. *J. Dispers. Sci. Technol.* **30,** 1363–1383 (2009).
12. McClements, D. J. Food Emulsions Principles, Practices, and Techniques Second Edition. *Food Emuls. Princ. Pract. Tech.* (2005). doi:10.1093/acprof:oso/9780195383607.003.0002
13. McGee, H. *On Food and Cooking: The Science and Lore of the Kitchen*. *Environment International* **13,** (2007).

14. Girish Solanki. *Surfactants in the Food Industry*. (2001).

15. Aveyard, R., Binks, B. P. & Mead, J. Interfacial Tension Minima in Oil-Water-Surfactant Systems Effects of Alkane Chain Length and Presence of n-Alkanols in Systems containing Aerosol OT. *J. Chem. Soc. Faraday Trans. 1* **82,** 1755–1770 (1986).

16. Aguilera, J. M. Why food micro structure? *Journal of Food Engineering* **67,** 3–11 (2005).

17. Campbell, G. M. & Mougeot, E. Creation and characterisation of aerated food products. *Trends in Food Science and Technology* **10,** 283–296 (1999).

18. Zúñiga, R. N. & Aguilera, J. M. Aerated food gels: fabrication and potential applications. *Trends Food Sci. Technol.* **19,** 176–187 (2008).

19. Dickinson, E. Stabilising emulsion-based colloidal structures with mixed food ingredients. *Journal of the Science of Food and Agriculture* **93,** 710–721 (2013).

20. Baldwin, E. in *Handbook of Food Preservation* (ed. Rahman, M. S.) 477–508 (CRC Press, 2007).

21. Trezza, T. A. & Krochta, J. M. The gloss of edible coatings as affected by surfactants, lipids, relative humidity, and time. *Food Sci* **65,** 658–662 (2000).

22. DZIEZAK, J. EMULSIFIERS - THE INTERFACIAL KEY TO EMULSION STABILITY. *Food Technol.* **42,** 172 (1988).

23. Taneja, A. & Singh, H. Challenges for the Delivery of Long-Chain n-3 Fatty Acids in Functional Foods. *Annu. Rev. Food Sci. Technol.* **3,** 105–123 (2012).

24. European Food Safety Authority. Scientific opinion on dietary reference values for fats, including saturated fatty acids, polyunsaturated fatty acids, monounsaturated fatty acids, trans fatty acids, and cholesterol. *EFSA J.* **8,** 1461 (2010).

25. WHO. *Obesity: Preventing and managing the global epidemic - Technical Report Series 894*. *Technical Report Series 894* (2000).

26. Market Research. *Food Emulsifiers Market by Type (Mono-, Di-Glycerides, Lecithin, Sorbitan Esters, Stearoyl Lactylates, and Polyglycerol Esters), Application (Bakery, Confectionery, Convenience, Dairy, and Meat), and Source (Plant and Animal) - Global Forecast to 2022*. (2016).

27. Efema. EFEMA index of food emulsifiers European Food Emulsifier Manufacturers ' Association. 1–146 (2009).

28. JECFA. Evaluation of Certain Food Additives and Contaminants. Sixty-First Report of the Joint FAO/WHO Expert Committee on Food Additives. *WHO Tech. Rep. Ser. 922; WHO Geneva* 127–132 (2004).

29. Cottrell, T. & Van Peij, J. *Emulsifiers in Food Technology*. *Emulsifiers in Food Technology: Second Edition* (2014). doi:10.1002/9781118921265.ch4

30. Smith, J. in *Food additives data book* (eds. Smith, Hong-Shum & Lily) 334 (2011).

31. Bueschelberger, H.-G., Tirok, S., Stoffels, I. & Schoeppe, A. *Lecithins*. *Emulsifiers in Food Technology: Second Edition* (2015). doi:10.1002/9781118921265.ch2

32. Cottrell, T. & Van Peij, J. *Emulsifiers in Food Technology*. *Emulsifiers in Food Technology: Second Edition* (2014). doi:10.1002/9781118921265.ch4

33. Mortensen, A. *et al.* Re-evaluation of lecithins (E 322) as a food additive. *EFSA J.* **15,** 1–47 (2017).

34. Flickinger, B. D. & Matsuo, N. Nutritional characteristics of DAG oil. in *Lipids* **38,** 129–132 (2003).

35. Sonntag, N. O. V. Glycerolysis of fats and methyl esters — Status, review and critique. *J. Am. Oil Chem. Soc.* **59,** 795A–802A (1982).

36. Garti, N. What can nature offer from an emulsifier point of view: Trends and progress? in *Colloids and Surfaces A: Physicochemical and Engineering Aspects* **152,** 125–146 (1999).

37. Moonen and Bas. in *Emulsifiers in Food Technology* (ed. Whitehurst) 40–58 (Oxford: Blackwell, 2004).

38. Goff, H. D. Colloidal aspects of ice cream - A review. *International Dairy Journal* **7,** 363–373 (1997).

39. SCF. Opinion on Certain Additives for Use in Foods for Infants and Young Children in Good Health and in Foods for Special Medical Purposes for Infants and Young Children (expressed on 21 March 1997 and amended on 13 June 1997). in *Minutes of the 107th Meeting of the Scientific Commitee for Food (SCF)* (1997).

40. Boon, P. *et al.* Scientific Panel on Food Additives and Nutrient Sources added to Food (ANS) Minutes of the 29 th meeting of the Working Group on the re-evaluation of food additives other than gums and colours. (2017).

41. European Food Safety Authority. Scientific opinion on dietary reference values for fats, including saturated fatty acids, polyunsaturated fatty acids, monounsaturated fatty acids, trans fatty acids, and cholesterol. *EFSA J.* **8,** 1461 (2010).

42. Cooper, N. and. in *Emulsifiers in Food Technology in Food Technology* (ed. Whitehurst) 131–161 (Blackwell, 2004).

43. European Food Safety Authority. Scientific Opinion on the safety of sucrose esters of fatty acids prepared from vinyl esters of fatty acids and on the extension of use of sucrose esters of fatty acids in flavourings 1. *Eur. Food Saf. Auth.* **8,** 36 (2010).

44. Márquez-Alvarez, C., Sastre, E. & Pérez-Pariente, J. Solid Catalysts for the Synthesis of Fatty Esters of Glycerol, Polyglycerols and Sorbitol from Renewable Resources. *Top. Catal.* **27,** 105–117 (2004).

45. EFSA. Scientific Opinion on the re-evaluation of polyoxyethylene sorbitan monolaurate (E 432), polyoxyethylene sorbitan monooleate

(E 433), polyoxyethylene sorbitan monopalmitate (E 434), polyoxyethylene sorbitan monostearate (E 435) and polyoxyethylene sorbita. *EFSA J.* **13,** 4152 (2015).

46. Kobayashi, H. & Fukuoka, A. Synthesis and utilisation of sugar compounds derived from lignocellulosic biomass. *Green Chem.* **15,** 1740 (2013).

47. EFSA. Scientific Opinion on the re-evaluation of polyoxyethylene sorbitan monolaurate (E 432), polyoxyethylene sorbitan monooleate (E 433), polyoxyethylene sorbitan monopalmitate (E 434), polyoxyethylene sorbitan monostearate (E 435) and polyoxyethylene sorbita. *EFSA J.* **13,** 4152 (2015).

48. JECFA. Toxicological evaluation of some food additives including anticaking agents, antimicrobials, antioxidants, emulsifiers and thickening agents. *WHO Food Addit. Ser. No 5* (1974).

49. BIBRA (British Industrial Biological Research Association). *A short-term (13 week) study in rats with polyoxyethyLene (20) sorbitan monostearate*. (1981).

50. Government of the United Kingdom. Registration, Evaluation, Authorisation & restriction of CHemicals (REACH).

51. Government of the United Kingdom. Chemical safety research.

52. JECFA. The Joint Food and Agriculture Organisation of the United Nations (FAO)/World Health Organisation (WHO) Expert Committee on Food Additives. Available at: http://www.fao.org/food/food-safety-quality/scientific-advice/jecfa/en/.

53. EFSA. European Food Safety Authority.

54. FAO/WHO. *General principles governing the use of food additives. First report of the Joint FAO/WHO Expert Committee on Food Additives*. (1957).

55. OECD. Test No. 423: Acute Oral toxicity - Acute Toxic Class Method. *Oecd Guidel. Test. Chem.* 1–14 (2002). doi:10.1787/9789264071001-en

56. Rhodes C, Thomas M, A. J. in *General and Applied Toxicology* (eds. Ballantyne, B., Marrs, T. & Turner, P.) 49–87 (Stockton Press, 1993).

57. IPCS. *Principles and Methods for the Assessment of Neurotoxicity Associated with Exposure to Chemicals*. (1986).

58. Eagle and Poling. The oral toxicity and pathology of polyoxyethylene derivatives in rats and hamsters. *J. Food Sci.* **21,** 347–361 (1956).

59. Varma, R. K. *et al.* Polysorbate 80: a pharmacological study. *Arzneimittelforschung.* **35,** 804–808 (1985).

60. FDRL. Approximate LD50 of FDA 71-88 (Lecithin) in mice; FOI request. (1972).

61. FDRL. *Approximate LD50 of FDA 71-88 (Lecithin) in rats; FOI request*. (1973).

62. Joint FAO/WHO expert Committee on Food Additives. Toxicological evaluation of some food additives including anticaking agents, antimicrobials, antioxidants, emulsifiers and thickening agent. *World Heal. Organ. Tech. Rep. Ser.* (1973).

63. Chusid, E., Diamond, J. & York, N. E. W. Accidental massive overdose of monitan in an infant. *J. Pediatr.* 1–2 (1955).

64. FDA. *Guidance for Industry and Other Stakeholders Toxicological Principles for the Safety Assessment of Food Ingredients*. *U.S Department of Heath & Human Services* **3,** (2007).

65. Benson, B. *et al. A review of the reference dose and reference concentration process*. (2002). doi:EPA/630/P-02/002F

66. Gaunt, I. F., Butterworth, K. R., Grasso, P. & Ginocchio, A. V. Long-term toxicity study of emulsifier YN in the mouse. *Food Cosmet. Toxicol.* **15,** 1–5 (1977).

67. Honda, K. *et al.* Toxicity studies of Asahi Kasei PI, purified phosphatidylinositol from soy lecithin. *J. Toxicol. Sci.* **34,** 265–280 (2009).

68. Kimura & Yoshida. Toxicity of detergent feeding and effect of the concurrent feeding of dietary fiber in rats. *Nutr. Rep. Int.* **26,** 271–279 (1982).

69. Nakata & Kimura. Mechanism involved in the ameliorating effect of dietary fiber on the toxicity of a non-ionic surface-active agent and amaranth added to the diet for rats. *Biosci. Biotechnol. Biochem.* **58,** 998–1001 (1994).

70. Harris, Sherman & Jetter. Nutritional and pathological effects of sorbitan monolaurate, polyoxyethylene sorbitan monolaurate, polyoxyethylene monolaurate, and polyoxyethylene monostearate when fed to rats. *Arch. Biochem. Biophys.* **34,** 259–265 (1951).

71. Brush, McCoy, Rosenthal, Stauber & Allison. The addition of non-ionic surface-active agents of the polyoxyethylene type to the diet of the hamster, the mouse and the dog. Journal of Nutrition. *J. Nutr.* **62,** 601–619 (1957).

72. Ershoff & Marshall. Protective effects of dietary fiber in rats fed toxic doses of sodium cyclamate and polyoxyethylene sorbitan monostearate (Tween 60). *J. Food Sci.* **40,** 357–361 (1975).

73. OECD. Test No. 452: Chronic Toxicity Studies. *OECD Guidel. Test. Chem.* 1–16 (2009). doi:http://dx.doi.org/10.1787/9789264071209-en

74. Oser, B. . & Oser, B. . Nutritional studies on rats on diets containing high levels of partial ester emulsifiers. I. General plan and procedures; growth and food utilization. Journal of Nutrition. *J. Nutr.* **60,** 367–390 (1956).

75. Oser, B. . & Oser, M. Nutritional studies on rats on diets containing high levels of partial ester emulsifiers. II. Reproduction and lactation. *J. Nutr.* **60,** 489–505 (1956).

76. Oser, B. L. & Oser, M. Nutritional studies on rats on diets containing high levels of partial ester emulsifiers. III. Clinical and metabolic observations. *J. Nutr.* **61,** 149–166 (1957).

77. Oser, B. . & Oser, M. Nutritional studies on rats on diets containing high levels of partial ester emulsifiers. III. Clinical and metabolic observations. *J. Nutr.* **61,** 235–252 (1957).

78. Corrigan OI & Healy AM. in *Encyclopedia of pharmaceutical technology* (ed. Swarbrick, J.) (Marcel Dekker, 2002).

79. Aungst, B. J. Absorption Enhancers: Applications and Advances. *The AAPS Journal* **14,** 10–18 (2012).

80. Mall, S., Buckton, G. & Rawlins, D. A. Dissolution behaviour of sulphonamides into sodium dodecyl sulfate micelles: A thermodynamic approach. *J. Pharm. Sci.* **85,** 75–78 (1996).

81. Kim, S., Shi, Y., Kim, J. Y., Park, K. & Cheng, J.-X. Overcoming the barriers in micellar drug delivery: loading efficiency, in vivo stability, and micelle-cell interaction. *Expert Opin. Drug Deliv.* **7,** 49–62 (2010).

82. Narang, A. S., Delmarre, D. & Gao, D. Stable drug encapsulation in micelles and microemulsions. *International Journal of Pharmaceutics* **345,** 9–25 (2007).

83. Strickley, R. G. Solubilizing Excipients in Oral and Injectable Formulations. *Pharmaceutical Research* **21,** 201–230 (2004).

84. Kalepu, S., Nekkanti, V. & Pharmaceutica Sinica, A. B. Insoluble drug delivery strategies: review of recent advances and business prospects. *Acta Pharm. Sin. B* **5,** 442–453 (2016).

85. Rangel-Yagui, C. de O., Pessoa, A. & Tavares, L. C. Micellar solubilization of drugs. *Journal of Pharmacy and Pharmaceutical Sciences* **8,** 147–163 (2005).

86. Tanford, C. & Wiley, J. The hydrophobic effect: Formation of micelles and biological membranes. *J. Chem. Educ.* 232 (1980). doi:10.1021/ed058pA246.1

87. De Oliveira, A. G. & Chaimovich, H. Effect of Detergents and Other Amphiphiles on the Stability of Pharmaceutical Drugs. *Journal of Pharmacy and Pharmacology* **45,** 850–861 (1993).

88. Gref, R. *et al.* Biodegradable long-circulating polymeric nanospheres. *Science (80-.).* **263,** 1600–1603 (1994).

89. Torchilin, V. P. Structure and design of polymeric surfactant-based drug delivery systems. *Journal of Controlled Release* **73,** 137–172 (2001).

90. Tehrani-Bagha, A. R. & Holmberg, K. Solubilization of hydrophobic dyes in surfactant solutions. *Materials* **6,** 580–608 (2013).

91. PhRMA. *Biologics*. *Medicines in development* (2014). doi:10.1089/apc.1989.3.4

92. Saffran, M., Pansky, B., Budd, G. C. & Williams, F. E. Insulin and the

gastrointestinal tract. in *Journal of Controlled Release* **46,** 89–98 (1997).

93. Saffran, M. *et al.* A new approach to the oral administration of insulin and other peptide drugs. *Science* **233,** 1081–4 (1986).

94. Fix, J. A. Oral controlled release technology for peptides: Status and future prospects. *Pharmaceutical Research* **13,** 1760–1764 (1996).

95. Veiseh, O., Tang, B. C., Whitehead, K. A., Anderson, D. G. & Langer, R. Managing diabetes with nanomedicine: challenges and opportunities. *Nat. Rev. Drug Discov.* **14,** 45–57 (2014).

96. Carter, P. J. Introduction to current and future protein therapeutics: A protein engineering perspective. *Experimental Cell Research* **317,** 1261–1269 (2011).

97. Glasgow, R. E., McCaul, K. D. & Schafer, L. C. Barriers to regimen adherence among persons with insulin-dependent diabetes. *J. Behav. Med.* **9,** 65–77 (1986).

98. García-Pérez, L.-E., Álvarez, M., Dilla, T., Gil-Guillén, V. & Orozco-Beltrán, D. Adherence to Therapies in Patients with Type 2 Diabetes. *Diabetes Ther.* **4,** 175–194 (2013).

99. Mahato, R. I., Narang, A. S., Thoma, L. & Miller, D. D. Emerging trends in oral delivery of peptide and protein drugs. *Crit. Rev. Ther. Drug Carrier Syst.* **20,** 153–214 (2003).

100. Perakslis, E., Tuesca, A. & Lowman, A. Complexation hydrogels for oral protein delivery: an in vitro assessment of the insulin transport-enhancing effects following dissolution in simulated digestive fluids. *J. Biomater. Sci. Polym. Ed.* **18,** 1475–90 (2007).

101. Adson, A. *et al.* Passive diffusion of weak organic electrolytes across Caco-2 cell monolayers: uncoupling the contributions of hydrodynamic, transcellular, and paracellular barriers. *J. Pharm. Sci.* **84,** 1197–204 (1995).

102. Anderson, J. . & Van Itallie, C. . Physiology and Function of the Tight Junction. *Cold Spring Harb. Perspect. Biol.* **1,** a002584 (2009).

103. Linnankoski, J. & Ma, J. Paracellular Porosity and Pore Size of the Human Intestinal Epithelium in Tissue and Cell Culture Models. **99,** 2166–2175 (2010).

104. Tamura, A. *et al.* Loss of claudin-15, but not claudin-2, causes Na+ deficiency and glucose malabsorption in mouse small intestine. *Gastroenterology* **140,** 913–23 (2011).

105. Nagahara, N., Tavelin, S. & Artursson, P. Contribution of the paracellular route to the pH-dependent epithelial permeability to cationic drugs. *J. Pharm. Sci.* **93,** 2872–2984 (2004).

106. Madara, J. . Regulation of the movement of solutes across tight junctions. *Annu. Rev. Physiol.* **60,** 143–159 (1998).

107. Catnach, S. M., Fairclough, P. D. & Hammond, S. M. Intestinal absorption of peptide drugs: advances in our understanding and clinical implications. *Gut* **35,** 441–444 (1994).

108. Burton, P. S., Conradi, R. A., Ho, N. F. H., Hilgers, A. R. & Borchardt, R. T. How structural features influence the biomembrane permeability of peptides. *J. Pharm. Sci.* **85,** 1336–1340 (1996).

109. Conradi, R. A., Hilgers, A. R., Ho, N. F. H. & Burton, P. S. The influence of peptide structure on transport across Caco-2 cells. *Pharm. Res.* **8,** 1453–1460 (1991).

110. Barford, N. M., Krog, N., Larsen, G. & Buchheim, W. Effects of Emulsifiers on Protein-Fat Interaction in Ice Cream Mix during Ageing I: Quantitative Analyses. *Lipid / Fett* **93,** 24–29 (1991).

111. Katneni, K., Charman, S. A. & Porter, C. J. H. Impact of Cremophor-EL and polysorbate-80 on digoxin permeability across rat jejunum: Delineation of thermodynamic and transporter related events using the reciprocal permeability approach. *J. Pharm. Sci.* **96,** 280–293 (2007).

112. Jha, S. K. *et al. In Vitro* Intestinal Permeability Studies and Pharmacokinetic Evaluation of Famotidine Microemulsion for Oral Delivery. *Int. Sch. Res. Not.* **2014,** 1–7 (2014).

113. Petersen, S. B. *et al.* Evaluation of alkylmaltosides as intestinal permeation enhancers: Comparison between rat intestinal mucosal sheets and Caco-2 monolayers. *Eur. J. Pharm. Sci.* **47,** 701–712 (2012).

114. Maher, S. *et al.* Evaluation of intestinal absorption enhancement and local mucosal toxicity of two promoters. I. Studies in isolated rat and human colonic mucosae. *Eur. J. Pharm. Sci.* **38,** 291–300 (2009).

115. Brayden, D. J., Bzik, V. a, Lewis, a L. & Illum, L. CriticalSorb™ promotes permeation of flux markers across isolated rat intestinal mucosae and Caco-2 monolayers. *Pharm. Res.* **29,** 2543–54 (2012).

116. Shubber, S. *et al.* Mechanism of Mucosal Permeability Enhancement of CriticalSorb® (Solutol® HS15) Investigated In Vitro in Cell Cultures. *Pharm. Res.* **32,** 516–527 (2014).

117. Barford, N. M., Krog, N., Larsen, G. & Buchheim, W. Effects of Emulsifiers on Protein-Fat Interaction in Ice Cream Mix during Ageing I: Quantitative Analyses. *Lipid / Fett* **93,** 24–29 (1991).

118. Zhang, H., Yao, M., Morrison, R. A. & Chong, S. Commonly used surfactant, Tween 80, improves absorption of P-glycoprotein substrate, digoxin, in rats. *Arch. Pharm. Res.* **26,** 768–772 (2003).

119. Dimitrijevic, D., Shaw, A. J. & Florence, A. T. Effects of some non-ionic surfactants on transepithelial permeability in Caco-2 cells. *J. Pharm. Pharmacol.* **52,** 157–162 (2000).

120. Kiss, L. *et al.* Kinetic analysis of the toxicity of pharmaceutical excipients cremophor EL and RH40 on endothelial and epithelial cells. *J. Pharm. Sci.* **102,** 1173–1181 (2013).

121. Ahsan, F., Arnold, J., Meezan, E. & Pillion, D. J. Enhanced bioavailability of calcitonin formulated with alkylglycosides following nasal and ocular administration in rats. *Pharm. Res.* **18,** 1742–1746 (2001).

122. Arnold, J., Ahsan, F., Meezan, E. & Pillion, D. J. Nasal administration of low molecular weight heparin. *J. Pharm. Sci.* **91,** 1707–1714 (2002).

123. Arnold, J. ., Ahsan, F., Meezen, E. & Pillion, D. . Correlation of tetradecylmaltoside induced increases in nasal peptide drug delivery with morphological changes in nasal epithelial cells. *J. Pharm. Sci.* **93,** 2205–2213 (2004).

124. Vllasaliu, D. *et al.* Epithelial toxicity of alkylglycoside surfactants. *J. Pharm. Sci.* **102,** 114–125 (2013).

125. Shinichiro, H., Takatsuka, Y. & Hiroyuki, M. Mechanisms for the enhancement of the nasal absorption of insulin by surfactants. *Int. J. Pharm.* **9,** 173–184 (1981).

126. Liu, D. Z., Lecluyse, E. L. & Thakker, D. R. Dodecylphosphocholine-mediated enhancement of paracellular permeability and cytotoxicity in Caco-2 cell monolayers. *J. Pharm. Sci.* **88,** 1161–1168 (1999).

127. Arnold, J. J., Ahsan, F., Meezan, E. & Pillion, D. J. Correlation of tetradecylmaltoside induced increases in nasal peptide drug delivery with morphological changes in nasal epithelial cells. *J. Pharm. Sci.* **93,** 2205–2213 (2004).

128. Tirumalasetty, P. P. & Eley, J. G. Evaluation of dodecylmaltoside as a permeability enhancer for insulin using human carcinoma cells. *J. Pharm. Sci.* **94,** 246–255 (2005).

129. Tirumalasetty, P. P. & Eley, J. G. Permeability enhancing effects of the alkylglycoside, octylglucoside, on insulin permeation across epithelial membrane in vitro. *J. Pharm. Pharm. Sci.* **9,** 32–39 (2006).

130. Nerurkar, M. M., Burton, P. S. & Borchardt, R. T. The use of surfactants to enhance the permeability of peptides through caco-2 cells by inhibition of an apically polarized efflux system. *Pharm. Res.* **13,** 528–534 (1996).

131. Lin, H. *et al.* Enhancing effect of surfactants on fexofenadine??HCl transport across the human nasal epithelial cell monolayer. *Int. J. Pharm.* **330,** 23–31 (2007).

132. Deli, M. . Potential use of tight junction modulators to reversibly open membranous barriers and improve drug delivery. *Biochim. Biophys. Acta* **1788,** 892–910 (2009).

133. Ahsan, F. *et al.* Effects of the permeability enhancers, tetradecylmaltoside and dimethyl-beta-cyclodextrin, on insulin movement across human bronchial epithelial cells (16HBE14o-). *Eur. J. Pharm. Sci.* **20,** 27–34 (2003).

134. Coon, J. S., Knudson, W., Clodfelter, K., Lu, B. & Weinstein, R. S. Solutol HS 15, nontoxic polyoxyethylene esters of 12-hydroxystearic acid, reverses multidrug resistance. *Cancer Res.* **51,** 897–902 (1991).

135. Koga, K., Ohyashiki, T., Murakami, M. & Kawashima, S. Modification of ceftibuten transport by the addition of non-ionic surfactants. *Eur. J. Pharm. Biopharm.* **49,** 17–25 (2000).

136. Alani, A., Rao, D. & Seidel, R. The effect of novel surfactants and solutol® HS 15 on paclitaxel aqueous solubility and permeability across a Caco-2 monolayer. *J. Pharm. Sci.* **99,** 3473–3485 (2010).

137. Anderberg, E. K. & Artursson, P. Epithelial transport of drugs in cell culture. VIII: Effects of sodium dodecyl sulfate on cell membrane and tight junction permeability in human intestinal epithelial (Caco-2) cells. *J. Pharm. Sci.* **82,** 392–398 (1993).

138. Anderberg, E. K., Nyström, C. & Artursson, P. Epithelial transport of drugs in cell culture. VII: Effects of pharmaceutical surfactant excipients and bile acids on transepithelial permeability in monolayers of human intestinal epithelial (Caco-2) cells. *J. Pharm. Sci.* **81,** 879–887 (1992).

139. Mattei, B., Lira, R. B., Perez, K. R. & Riske, K. A. Membrane permeabilization induced by Triton X-100: The role of membrane phase state and edge tension. *Chem. Phys. Lipids* **202,** 28–37 (2017).

140. Schnell, U., Dijk, F., Sjollema, K. A. & Giepmans, B. N. G. Immunolabeling artifacts and the need for live-cell imaging. *Nat. Methods* **9,** 152–158 (2012).

141. Sot, J., Collado, M. I., Arrondo, J. L. R., Alonso, A. & Goñ, F. M. Triton X-100-resistant bilayers: Effect of lipid composition and relevance to the raft phenomenon. *Langmuir* **18,** 2828–2835 (2002).

142. Laude, A. J. & Prior, I. A. Plasma membrane microdomains: organization, function and trafficking. *Mol. Membr. Biol.* **21,** 193–205 (2004).

143. Simons, K. & Ikonen, E. Functional rafts in cell membranes. *Nature* **387,** 569–572 (1997).

144. Alenghat, F. J. & Golan, D. E. Membrane protein dynamics and functional implications in mammalian cells. *Curr. Top. Membr.* **72,** 89–120 (2013).

145. Bernardino de la Serna, J., Schütz, G. J., Eggeling, C. & Cebecauer, M. There Is No Simple Model of the Plasma Membrane Organization. *Front. Cell Dev. Biol.* **4,** (2016).

146. Anderberg, E. K., Nystrom, C. & Artursson, P. Epithelial transport of drugs in cell culture. VII: Effects of pharmaceutical surfactant excipients and bile acids on transepithelial permeability in monolayers of human intestinal epithelial (Caco-2) cells. *J. Pharm. Sci.* **81,** 879–887 (1992).

147. Inácio, Â. S. *et al.* In vitro surfactant structure-toxicity relationships: Implications for surfactant use in sexually transmitted infection prophylaxis and contraception. *PLoS One* **6,** (2011).

148. Inácio, Â. S. *et al.* Mitochondrial dysfunction is the focus of quaternary ammonium surfactant toxicity to mammalian epithelial cells. *Antimicrob. Agents Chemother.* **57,** 2631–2639 (2013).

149. Inácio, Â. S. *et al.* In vitro surfactant structure-toxicity relationships: Implications for surfactant use in sexually transmitted infection prophylaxis and contraception. *PLoS One* **6,** (2011).

150. Nałęcz-Jawecki, G., Grabińska-Sota, E. & Narkiewicz, P. The toxicity of cationic surfactants in four bioassays. *Ecotoxicol. Environ. Saf.* **54,** 87–91 (2003).

151. Reeve, P. J. & Fallowfield, H. J. The toxicity of cationic surfactant HDTMA-Br, desorbed from surfactant modified zeolite, towards faecal indicator and environmental microorganisms. *J. Hazard. Mater.* **339,** 208–215 (2017).

152. Patrzykat, A., Friedrich, C. L., Zhang, L., Mendoza, V. & Hancock, R. E. Sublethal concentrations of pleurocidin-derived antimicrobial peptides inhibit macromolecular synthesis in Escherichia coli. *Antimicrob Agents Chemother* **46,** 605–614 (2002).

153. Vieira, O. V. *et al.* Surfactants as microbicides and contraceptive agents: A systematic In Vitro study. *PLoS One* **3,** (2008).

154. Husale, S., Grange, W., Karle, M., B??rgi, S. & Hegner, M. Interaction of cationic surfactants with DNA: A single-molecule study. *Nucleic Acids Res.* **36,** 1443–1449 (2008).

155. Aranzazu Partearroyo, M., Ostolaza, H., Goni, F. M. & Barbera-Guillem, E. Surfactant-induced cell toxicity and cell lysis. A study using B16 melanoma cells. *Biochem. Pharmacol.* **40,** 1323–1328 (1990).

156. Whitehead, K. & Mitragotri, S. Mechanistic analysis of chemical permeation enhancers for oral drug delivery. *Pharm. Res.* **25,** 1412–9 (2008).

157. Kiss, L. *et al.* Sucrose Esters Increase Drug Penetration, But Do Not Inhibit P-Glycoprotein in Caco-2 Intestinal Epithelial Cells. *J. Pharm. Sci.* **103,** 3107–3119 (2014).

158. Arechabala, B., Coiffard, C., Rivalland, P., Coiffard, L. J. M. & De Roeck-Holtzhauer, Y. Comparison of cytotoxicity of various surfactants tested on normal human fibroblast cultures using the neutral red test, MTT assay and LDH release. *J. Appl. Toxicol.* **19,** 163–165 (1999).

159. Xia, W. J. & Onyuksel, H. Mechanistic studies on surfactant-induced membrane permeability enhancement. *Pharm. Res.* **17,** 612–618 (2000).

160. Nawaz, S. *et al.* Interactions of PEO–PPO–PEO block copolymers with lipid membranes: a computational and experimental study linking membrane lysis with polymer structure. *Soft Matter* **8,** 6744 (2012).

161. Swenson, E. S., Milisen, W. B. & Curatolo, W. Intestinal permeability enhancement: Structure-activity and structure-toxicity relationships for nonylphenoxypolyoxyethylene surfactant permeability enhancers. *Pharm. Res.* **11,** 1501–1504 (1994).

162. Lo, Y. L. Relationships between the hydrophilic-lipophilic balance values of pharmaceutical excipients and their multidrug resistance modulating effect in Caco-2 cells and rat intestines. *J. Control. Release* **90,** 37–48 (2003).

163. Redhead, M. *et al.* Relationship between the affinity of PEO-PPO-PEO

block copolymers for biological membranes and their cellular effects. *Pharm. Res.* **29,** 1908–1918 (2012).

164. Ross, B. P. *et al.* Micellar aggregation and membrane partitioning of bile salts, fatty acids, sodium dodecyl sulfate, and sugar-conjugated fatty acids: correlation with hemolytic potency and implications for drug delivery. *Mol. Pharm.* **1,** 233–45 (2004).

165. Berridge, M. V., Herst, P. M. & Tan, A. S. Tetrazolium dyes as tools in cell biology: New insights into their cellular reduction. *Biotechnology Annual Review* **11,** 127–152 (2005).

166. Hamid, K. A., Katsumi, H., Sakane, T. & Yamamoto, A. The effects of common solubilizing agents on the intestinal membrane barrier functions and membrane toxicity in rats. *Int. J. Pharm.* **379,** 100–108 (2009).

167. Yamaguchi, J. Y. *et al.* Cremophor EL, a non-ionic surfactant, promotes Ca2+-dependent process of cell death in rat thymocytes. *Toxicology* **211,** 179–186 (2005).

168. Kanduc, D. *et al.* Cell death: apoptosis versus necrosis (review). *International journal of oncology* **21,** 165–170 (2002).

169. Majno, G. & Joris, I. Apoptosis, oncosis, and necrosis. An overview of cell death. *Am. J. Pathol.* **146,** 3–15 (1995).

170. Trump, B. F., Berezesky, I. K., Chang, S. H. & Phelps, P. C. The pathways of cell death: oncosis, apoptosis, and necrosis. *Toxicol. Pathol.* **25,** 82–88 (1997).

171. Kroemer, G. *et al.* Classification of cell death: recommendations of the Nomenclature Committee on Cell Death 2009. *Cell Death Differ* **16,** 3–11 (2009).

172. Eskandani, M., Hamishehkar, H. & Ezzati Nazhad Dolatabadi, J. Cyto/Genotoxicity study of polyoxyethylene (20) sorbitan monolaurate (tween 20). *DNA Cell Biol.* **32,** 498–503 (2013).

173. Yang, Y. W., Wu, C. A. & Morrow, W. J. W. Cell death induced by vaccine adjuvants containing surfactants. *Vaccine* **22,** 1524–1536 (2004).

174. Levine, S. L., Han, Z., Liu, J., Farmer, D. R. & Papadopoulos, V. Disrupting mitochondrial function with surfactants inhibits MA-10 Leydig cell steroidogenesis. *Cell Biol. Toxicol.* **23,** 385–400 (2007).

175. Alvi, M. M. & Chatterjee, P. A prospective analysis of co-processed non-ionic surfactants in enhancing permeability of a model hydrophilic drug. *AAPS PharmSciTech* **15,** 339–53 (2014).

176. Gupta, V., Hwang, B. H., Doshi, N. & Mitragotri, S. A permeation enhancer for increasing transport of therapeutic macromolecules across the intestine. *J. Control. Release* **172,** 541–549 (2013).

177. Yang, Y. W., Wu, C. a. & Morrow, W. J. W. Cell death induced by vaccine adjuvants containing surfactants. *Vaccine* **22,** 1524–1536 (2004).

178. Gan, L., Gan, Y., Zhu, C., Zhang, X. & Zhu, J. Novel microemulsion in

situ electrolyte-triggered gelling system for ophthalmic delivery of lipophilic cyclosporine A: In vitro and in vivo results. *Int. J. Pharm.* **365,** 143–149 (2009).

179. Guo, F. *et al.* Self-microemulsifying drug delivery system for improved oral bioavailability of dipyridamole: Preparation and evaluation. *Arch. Pharm. Res.* **34,** 1113–1123 (2011).

180. Vonarbourg, A. *et al.* The encapsulation of DNA molecules within biomimetic lipid nanocapsules. *Biomaterials* **30,** 3197–3204 (2009).

181. Huynh, N. T., Passirani, C., Saulnier, P. & Benoit, J. P. Lipid nanocapsules: A new platform for nanomedicine. *International Journal of Pharmaceutics* **379,** 201–209 (2009).

182. Mao, C., Wan, J., Chen, H., Xu, H. & Yang, X. Emulsifiers' composition modulates venous irritation of the nanoemulsions as a lipophilic and venous irritant drug delivery system. *AAPS PharmSciTech* **10,** 1058–1064 (2009).

183. Nepal, P. R., Han, H. K. & Choi, H. K. Preparation and in vitro-in vivo evaluation of Witepsol?? H35 based self-nanoemulsifying drug delivery systems (SNEDDS) of coenzyme Q10. *Eur. J. Pharm. Sci.* **39,** 224–232 (2010).

184. Bravo González, R. C., Huwyler, J., Walter, I., Mountfield, R. & Bittner, B. Improved oral bioavailability of cyclosporin A in male Wistar rats: Comparison of a Solutol HS 15 containing self-dispersing formulation and a microsuspension. *Int. J. Pharm.* **245,** 143–151 (2002).

185. Lewis, A. L., Jordan, F. & Illum, L. CriticalSorb(TM): Enabling systemic delivery of macromolecules via the nasal route. *Drug Deliv. Transl. Res.* **3,** 26–32 (2013).

186. Illum, L., Jordan, F. & Lewis, A. L. CriticalSorb: a novel efficient nasal delivery system for human growth hormone based on Solutol HS15. *J. Control. Release* **162,** 194–200 (2012).

2. Chapter Two – Materials and general methods

2.1. Materials

2.1.1. Cells, culture media and components

Caco-2 human epithelial colorectal adenocarcinoma cells were obtained from the American Type Culture Collection (ATCC) and were used between passages 25-55. NIH/3T3 mouse embryonic fibroblast cells were also purchased from the ATCC and used at passages 15-20. Eagle's minimum essential medium (EMEM), Hank's balanced salt solution (HBSS) with sodium bicarbonate and without phenol red, antibiotic/antimycotic solution (containing penicillin, streptomycin and amphotericin), foetal bovine serum (FBS), L-glutamine and 0.25% trypsin/EDTA (with phenol red) solution were all purchased from Sigma Aldrich (UK). Phosphate buffered saline (PBS) tablets were obtained from Oxoid (UK). 4-(2-hydroxyethyl)-1-piperazineethanesulfonic acid (HEPES) was from Biochrom (UK). Industrial methylated spirit (IMS), which was used as an aseptic disinfectant, was purchased from Fisher Chemical (UK).

2.1.2. Plasticware and glassware

Cell culture flasks (75 cm^2 and 25 cm^2, canted neck with vented caps), 96-well polystyrene microplates (clear and black) and sterile pipettes were purchased from Corning Life Sciences (NL). Millicell-96 permeable polycarbonate membrane, cell culture inserts with plate (0.4 µM pore size; 0.11 cm^2 cell growth area; 96 well plate) were purchased from Merck Millipore (USA). Haemocytometer (improved Neubauer) was

purchased from Scientific Laboratory Supplies (SLS; UK). Sterile universals and bijoux tubes were purchased from Sterilin, and sterile centrifuge tubes (15 and 50 ml volume), microcentrifuge tubes (0.5 and 2.5 ml volume) were from Greiner (USA). Sterile cryovials (1 ml volume) were obtained from NUNC (DK). The freezing container ('Mr Frosty™'), capable of delivering a rate of cooling of -1ºC/min, was supplied from Nalgene® Labware (USA).

2.1.3. Assay reagents and dyes

The MTS reagent (known commercially as 'CellTiter 96 Aqueous One Solution Cell Proliferation Assay') and the CellTox™ Green Cytotoxicity Assay were purchased from Promega (US). CellEvent™ Caspase-3/7 Green ReadyProbes™ Reagent, Hoechst 33342, laurdan (6-Dodecanoyl-2-Dimethylaminoaphthalene), CM-H2DCFDA (general oxidative stress indicator), PrestoBlue® Cell Viability Reagent, MitoTracker Red CMXRos and propridium iodide were all obtained from Thermo Fisher Scientific (USA). Flourescein isothiocyanate (FITC)-dextran (average molecular weight 4 kDa) (FD-4), and the LDH detection kit (TOX7; *In Vitro* Toxicology Assay Kit) were acquired from Sigma Aldrich. The JC-1 (iodide salt) (5,5',6,6'-Tetrachloro-1,1',3,3'-tetraethylbenzimidazolylcarbocyanine, iodide) was purchased from Biotium. Dimethyl sulphoxide (DMSO) was used as a general dissolvent and acquired from Sigma Aldrich (UK).

2.1.4. Cell treatments

Solutol HS15 (also known as Kolliphor HS15 and Macrogol (15)-hydroxystearate) was supplied from BASF (UK). Triton X-100, valinomycin, staurosporine (from *Strepomyces sp.*) and carbonyl cyanide 4-(trifluoromethoxy) phenylhydrazone (FCCP) were all obtained from Sigma Aldrich (UK). Ethanol was purchased from Fisher Chemical (UK).

2.2. Methods

2.2.1. Routine maintenance and culture of cells

The growth media used for routine cell culture was EMEM supplemented with 10% (v/v) FBS, 0.10 mg/ml streptomycin, 100 units/ml penicillin, 0.25 µg/ml amphotericin and 2 mM L-glutamine – herein referred to as complete EMEM. Both Caco-2 and NIH/3T3 cells were cultured in 75 cm^2 flasks at 5% CO2, 95% relative humidity and at 37°C until confluence (approximately 75-90 % flask coverage by cells).

Cells were fed every other day by aspirating old media from cell flasks and replacing with 15 ml of fresh, pre-warmed (37°C) media. Once confluent, as determined by optical microscopy, cells were passaged. This involved aspirating the culture media from cell flasks and subsequently washing the cells with 5 ml, pre-warmed (37°C) PBS by gently swirling. Washing with PBS is an important, required step to ensure no traces of cell media remained in the flask; the presence of FBS could potential inhibit the action of trypsin/EDTA. Following the wash step, PBS was removed by aspiration and replaced with 2.5 ml, pre-warmed (37°C) 0.25 % trypsin/EDTA solution, after which the flask was gently rocked ensuring good coverage over the cells

before being transferred to the 37°C incubator. The flask was removed from the incubator at regular intervals to enable observation, using an optical microscope, for cell detachment from the culture flask and returned if not ready, otherwise following cell detachment 5 ml of pre-warmed (37°C) culture media was added to dilute the cell-trypsin/EDTA suspension and deactivate the trypsin. The cell suspension was then transferred from the flask into a sterile 15 ml centrifuge tube and underwent centrifugation at 250g for 5 minutes. The supernatant containing trypsin was then aspirated off and the cell pellet re-suspended in 6 ml pre-warmed (37°C) culture media. Fractions of this cell suspension, required to achieve the desired split ration, were then transferred into flasks containing 15 ml of pre-warmed (37°C) culture media. Caco-2 cells were regularly split at ratios of 1:3 and 1:6, and NIH/3T3 cells split at 1:6.

2.2.2. Frozen storage of cells

Cell stocks were cryopreserved to maintain the passage range and thus help minimise phenotype variance associated with time in culture. Complete EMEM containing 10% (v/v) sterile DMSO was used as the cryopreservant for Caco-2 and NIH/3T3 cells.

Once the desired cells had been cultured to confluence in a 75 cm^2 culture flask, undergone the trypsinisation process and pelleted using centrifugation, as describe above (section 2.2.1), the supernatant was removed and the cell pellet was re-suspended in 1 ml cryopreservant. The resulting cell solution was added to a sterile cryovial (clearly labelled with cell type, passage number and date) and placed into the Mr Frosty

freezing container. This container was then stored in a -80ºC freezer for at least 12 hours to allow for a gradual, controlled decrease in temperature. The cryovials containing cells were then removed from the Mr Frosty container and either stored in the -80ºC freezer for short term storage (< 4 weeks), or transferred into a liquid nitrogen cell storage tank for long term storage.

2.2.3. Cell revival

Upon requiring use of frozen cell stocks, cryovials were removed from the liquid nitrogen storage tank or -80ºC freezers and thawed in a 37ºC water bath by gently immersion for approximately 1-2 minutes. Once thawed the cell suspension (1 ml) was pipetted into a fresh, sterile 15 ml centrifuge tube containing 9 ml of complete EMEM pre-warmed to 37ºC. The resulting solution was then centrifuged at 250g for 5 minutes. The DMSO-containing supernatant was then removed by aspiration and the cell pellet re-suspended in 3 ml of complete EMEM.

Depending on the length of storage depreciation of viable cell number may be encountered, and this may have an influence on subsequent cell proliferation; cell grow is sensitive to seeding densities and cells will struggle to grow to confluence (or survive) if the cells *per* cm^2 is too low on the surface of the culture vessel. To overcome this, once revived cells are re-suspended the cell solution is subjected to a cell count and then seeded in an appropriate flask; if the number of viable cells was < $1x10^6$, the revived cells were seeded into a 25 cm^2 flask, and above this amount seeded into a 75 cm^2 flask. *A confluent 75*

cm^2 flask of Caco-2 cells will typically yield approximately $6x10^6$ cells.

Once cells were revived they were cultured for a least one additional passage prior to their use in experiments. This was to ensure that the cell population had acclimated; allowing the cells time to re-establish their normal cell cycle and protein expression.

2.2.4. Cell seeding

Caco-2 cells were regularly seeded on 96 well plates, both clear and black for absorbance and fluorescent based assays, respectively. Cells were seeded at a density of $1x10^4$ cells *per* well (approximately $3.1x10^4$ cells *per* cm^2), a commonly used density[2,3]. Caco-2 cells were cultured in 150 µl complete EMEM *per* well, in 96 well plates for 48 hours in 5% CO2, 95% relative humidity and at 37°C. To minimise the variance caused by temperature and evaporation affecting wells on the outside edge of the plate (*i.e.,* the 'edge effect'), when possible cells were not seeded on the outer wells and instead 150 µl complete EMEM (without cells) was added *per* well.

2.2.5. Preparation of Solutol HS15

Solutol HS15 was regularly used at concentrations of 0.01, 0.1, 1, 10, 20 and 50 mM. These were prepared by serial dilutions in 1% HEPES:HBSS from a stock solution of 100 mM Solutol HS15 diluted in 1% HEPES:HBSS and were prepared fresh for every experiment. Stock solutions were prepared by weighing out solid Solutol HS15, which at room temperature is a waxy

paste, into a sterile 50 ml centrifuge tube. This is then incubated in a 37ºC water bath for 10 minutes to melt the Solutol HS15 (melting point approximately 30ºC). The appropriate volume of 1% HEPES:HBSS is then added to the liquid Solutol HS15 to create the stock solution. This solution is then vortexed for 30 seconds to ensure homogeneity, and then allowed to stand for at least 30 minutes to settle the foam and bubble formation prior to dilution for preparation of treatment doses. Fresh stock solutions were prepared at least every 2 weeks. Solutol HS15 was stored at room temperature.

The diluent for all cell treatments was 1% (v/v) HEPES:HBSS. This was prepared by diluting 0.5 ml HEPES in 49.5 ml HBSS in a 50 ml centrifuge tube. This buffer was made fresh at least every 2 weeks and stored at 4ºC.

2.2.6. Treatment of cells

The dosing cells with treatments were kept as consistent as possible to minimise any differences between assay techniques and thus enable comparison between assay results.

Following the culture of cells in 96 well plates, growth media was removed, and cells were washed twice with PBS to remove any excess. Wells were then treated by the addition of 150 µl *per* well of 1% HEPES:HBSS or 0.01, 0.1, 1, 10, 20 or 50 mM Solutol HS15 (applied in 1% HEPES:HBSS). It was necessary to test the effect of the vehicle, alternatively called the negative control (1% HEPES:HBSS) to account for any cellular effect induced by its application rather than Solutol HS15 or other treatment of interest; this 'noise' was then normalised out of the resulting data.

In addition to the vehicle control, a positive control was often used and the compounds which performed this task varied depending on the assay. Positive controls were used to demonstrate the induction of a known response for comparison to the response induced by Solutol HS15. Compounds that were used in this manner were diluted in 1% HEPES:HBSS to enable consistent normalisation and comparison. All treatments that were added to cells were pre-warmed to 37ºC prior to their application, unless otherwise stated.

2.2.7. Statistical analysis

Statistical tests were performed using GraphPad Prism software version 7. Values of $P<0.05$ were considered statistically significant. Lethal dose 50% (LD_{50}) and lethal time 50% (LT_{50}) were calculated using non-linear regression equations performed by GraphPad Prism software.

2.3. References

1. Strober, W. Trypan Blue Exclusion Test of Cell Viability. *Curr. Protoc. Immunol.* **111,** A3.B. 1-A3.B.3. (2015).

2. Vllasaliu, D. *et al.* Epithelial toxicity of alkylglycoside surfactants. *J. Pharm. Sci.* **102,** 114–125 (2013).

3. Shubber, S. *et al.* Mechanism of Mucosal Permeability Enhancement of CriticalSorb® (Solutol® HS15) Investigated In Vitro in Cell Cultures. *Pharm. Res.* **32,** 516–527 (2014).

3. Chapter Three – Membrane effects on intestinal epithelia

Summary

This chapter aimed to study the effect of model non-ionic surfactant, Solutol HS15, on Caco-2 intestinal epithelial cell membranes. Plasma membrane permeability was monitored by measuring internalisation of external permeant FITC-dextran 4kDa, leakage of intracellular lactose dehydrogenase enzyme, and intracellular Ca^{2+} flux. The hydration, i.e. fluidity, of the plasma membrane was assessed using the phase-sensitive Laurdan membrane dye, and nuclear membrane permeability was evaluated using a plasma and nuclear membrane-impermeable DNA-binding dye.

Laurdan general polarisation results demonstrate that upon application, surfactant induces concentration-dependent plasma membrane fluidisation within one minute, and in a manner, that does not alter membrane permeability to tested permeants. Following the initial increase in membrane fluidity, the fluidity remains remarkably stable for between 1 and 30 minutes time point. A subsequent increase in membrane fluidity is again noted after this time point, and is associated with an increase in membrane permeability and loss of membrane integrity, as judged from Ca^{2+} and leakage of lactose dehydrogenase.

3.1. Introduction

Surfactants and other amphipathic molecules, have a tendency to accumulate in lipid bilayered membranes, such as the cellular plasma membrane, whereby their hydrophobic hydrocarbon tails localise in the hydrophobic 'core' of the bilayer and their hydrophilic head groups positioned towards the aqueous interface of the membrane. The work in this chapter investigates the effects of model non-ionic surfactant Solutol HS15 on membranes, and begins with a discussion on the composition and function of the plasma membrane.

3.1.1. The cellular plasma membrane

The seminar paper by Singer and Nicolson in 1972 put forth the 'fluid mosaic model' of the plasma membrane[1], separating it from more rigid cell structures such as the cytoskeleton, and highlighted the relative mobility of the membrane as one of the most significant features. Membrane fluidity allows cells to it to act in dynamic manners, for example, membranes can re-orientate to adopt different conformations for cellular motility[2], or when performing endocytotic or exocytotic mechanisms[3].

The cellular plasma membrane is a heterogenous structure, made up of a complex mixture of sterols, proteins and phospholipids[1]. Proteins account for approximately half of the total mass of the plasma membrane[4], and are categorised as peripheral or integral membrane proteins depending on if they are anchored to the lipid bilayer *via* lipid moieties or transmembrane domains, respectively. Additionally, some proteins associate with the membrane *via* a variety of protein-

glycan or protein-protein interactions, and others by electrostatic interactions with lipid headgroups[5].

The major structural lipids in the membrane of eukaryotes are glycerophospholipids such as phosphatidylcholine (PC), phosphatidylserine (PS), phosphatidylinositol (PI), phosphatidylethanolamine (PE) and phosphatidic acid (PA). The hydrophobic backbone of these lipids is a diacylgycerol containing saturated or *cis*-unsaturated fatty acyl chains of varying lengths. PC accounts for >50% of all the phospholipids in eukaryotic membranes. Another class of structural lipids are the sphingolipids. The hydrophobic portion of these lipids are ceramide. In mammalians cells the major sphingolipids are sphingomyelin (SM) and the glycosphingolipids (GSLs). Sphingolipids are able to pack more tightly together than PC molecules of the same chain length because they have saturated or *trans*-unsaturated fatty acyl chains that form taller, narrower structures. The variation in aliphatic chain and headgroup allows the existence of thousands of distinct species of lipid in any mammalian cell[6].

In mammalian cell membranes, sterols such as cholesterol are the major non-polar lipid components. Cholesterol plays an essential role in regulating membrane fluidity and stability by increasing the ordering of phospholipid acyl chains[7,8], and has been shown to preferential mix with sphingolipids in membranes, due to the sphingolipid headgroup shielding the non-polar sterol from the external aqueous environment[9,10].

The plasma membrane bilayer is asymmetric in nature, with the inner and outer leaflets differing in both lipid and protein composition[11]. The lipid asymmetry of the bilayer is maintained

by lipid translocating proteins, such as flippases[12], and has important functional consequences. For example, the exposure of PS on the cell surface acts as a signal for phagocytosis during apoptosis[13], and as signal for bloody coagulation by acting as a scaffold for blood clotting factors on activated platelets[14].

The molecular complexity of the plasma membrane has most likely evolved to serve as a selective barrier and organisation platform for cell signalling[15].

Following the proposal of the fluid mosaic model, it was identified that cell plasma membranes could be separated into distinct fractions, detergent-labile and detergent resistant[16], setting off the idea that distinct membrane subcompartments could be present. Since then, it has been observed that cell plasma membranes are laterally heterogenous at the submicrometre scale (Figure 3.5)[17–19]. The lipid raft hypothesis has emerged to explain this inhomogeneity; it is put forward that in the plane of the membrane, the interactions between specific lipids drives the generation of functionally significant, relatively ordered membrane portions that recruit and cluster proteins[20]. The lipid raft concept has been supported by observations coming from biomimetic model membranes, which demonstrate that certain lipids preferentially interact with one another and engage in the formation of large scale lateral domains as a result of liquid-liquid phase seperation[21] – the coexistence of two phases with distinct compositions and physical properties. Membrane segments enriched in saturated lipid species, such as sphingolipids, and cholesterol are packed together tightly and form relatively viscous, ordered phases[22], termed the liquid ordered (L_o) phase. Membrane regions comprising of mainly unsaturated lipids, such as

glycerophospolipids, form more fluid phases[23,24], termed the liquid disordered (L_d) phase.

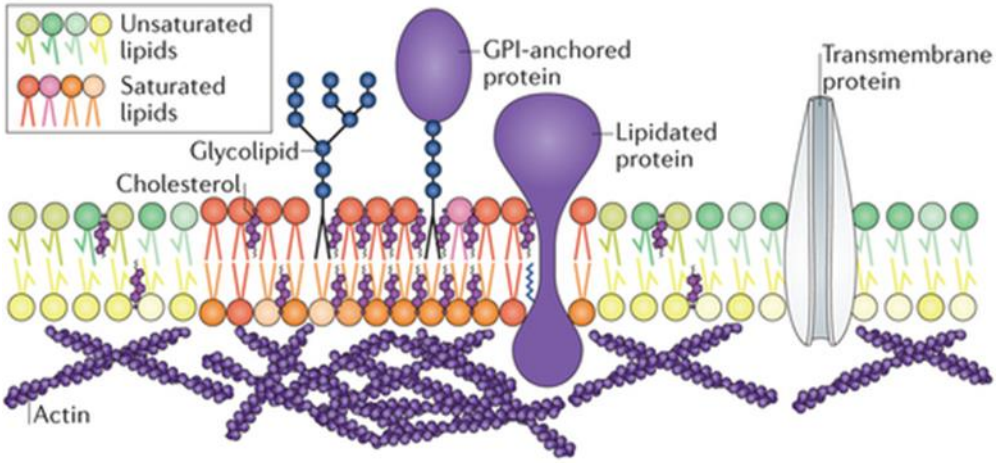

Figure 3.5. Overview of plasma membrane lateral heterogenicity. Lipid raft regions are typically small, highly dynamic and transient regions of the plasma membrane that are enriched in cholesterol, saturated phospholipids, sphingolipids, glycolipids, glycosylphosphatidylinositol (GPI)-anchored proteins and lipidated proteins. The composition of lipid raft domains confers this region with increased lipid packing and order and decreased fluidity. Figure modified from Sezgin et al.[25]

The L_o phase is regarded to be the model for lipid rafts because of their tight molecular packing and the enrichment of saturated lipids and sterol. Glycosylphosphatidylinositol (GPI)-anchored proteins, and lapidated proteins which are proteins attached to saturated acyl chains (such as palmitoyl moiety), are enriched in L_o membrane environments composed of cholesterol and sphingolipids (Figure 3.5)[17,26,27]. Furthermore, GPI-anchored proteins are able to regulate membrane function and structure by transbilayer interactions with membrane adjacent actin filaments[28]. Thus, the enrichment of these components in these lipid raft domains confers them with distinct physiological functions. Indeed, interactions with the distinct biophysical environment of rafts, *i.e.* phospholipid composition, increased

phase order and decreased fluidity, has been shown to alter the conformation of raft-associated proteins and thus change their activity[29,30].

Lipid rafts have been associated with various cell functions, such as cell signalling. For example, signalling can be regulated by the repositioned of proteins into and out of lipid rafts, for example, CD45 localised in rafts antagonises IL-2 production, however when excluded from rafts it promotes IL-2 production[31]. Also, lipid rafts can be used to spatial coordinate the interaction of proteins of signalling complexes to regulate their activation, such as that achieved by proximal CD4/TCR signalling through the colocalisation of Lck and Fyn proteins[32]. Moreover, another example of spatial coordinated regulation, which has relevance for later discuss in this thesis, is the clustering of growth factor tyrosine kinases in lipid raft regions. This occurs during the membrane phase reorganisation that is induced by heat stress, and consequently activates the heat shock response[33].

The disruption of lipid rafts by methyl-β-cyclodextrin, a cyclic oligosaccharide that sequesters cholesterol from membranes, was shown to disrupt T-cell activation by affecting the localisation and phosphorylation of Lck, LAT and ZAP-70[34].

Lipid raft are also associated with budding and vesicle formation which can occur *via* the clustering rafts (Figure 3.6). Lipid rafts usually form in a minority dispersed within continuous non-raft regions[35,36]. Lipid raft clustering can be induced by the oligomerisation of raft components[37]. The processes of cluster is believed to play an important role in cell sorting to recruit certain protein and exclude others as only proteins that have an affinity for L_o domains are recruited[38]. The enlargement of

the L_o membrane region, as the lipid raft cluster grows, results in the increase in line tension at phase boundaries. The energic cost of line tension is reduce by the minority phase (*i.e.* the raft cluster) budding out from the majority phase (non-raft membrane region). Opposing the line tension induced budding is the energy that is required to bend the membrane, however when a critical size of the growing membrane domain is reached budding becomes energetically favourable[39–41]. This mechanism is known as domain-induced budding and lipid asymmetry between membrane leaflets is thought to play a role controlling this process[42], as is regulation by proteins such as dynamin[43]

Lipid raft domains are also associated with the expression of a specialised type of region known as caveolae[44,45]. These highly abundant membrane features are described as ~50-100 nm membrane invaginations[46]. Sphingolipids and GPI-anchored proteins are enriched in caveola[47], and the density of packing of lipids found here are higher than other plasma membrane sections[48]. As with the lipid raft budding, it is believed that sphingolipids, cholesterol, and the generation of line tension are essential in the assemble and budding processes of caveolae[38].

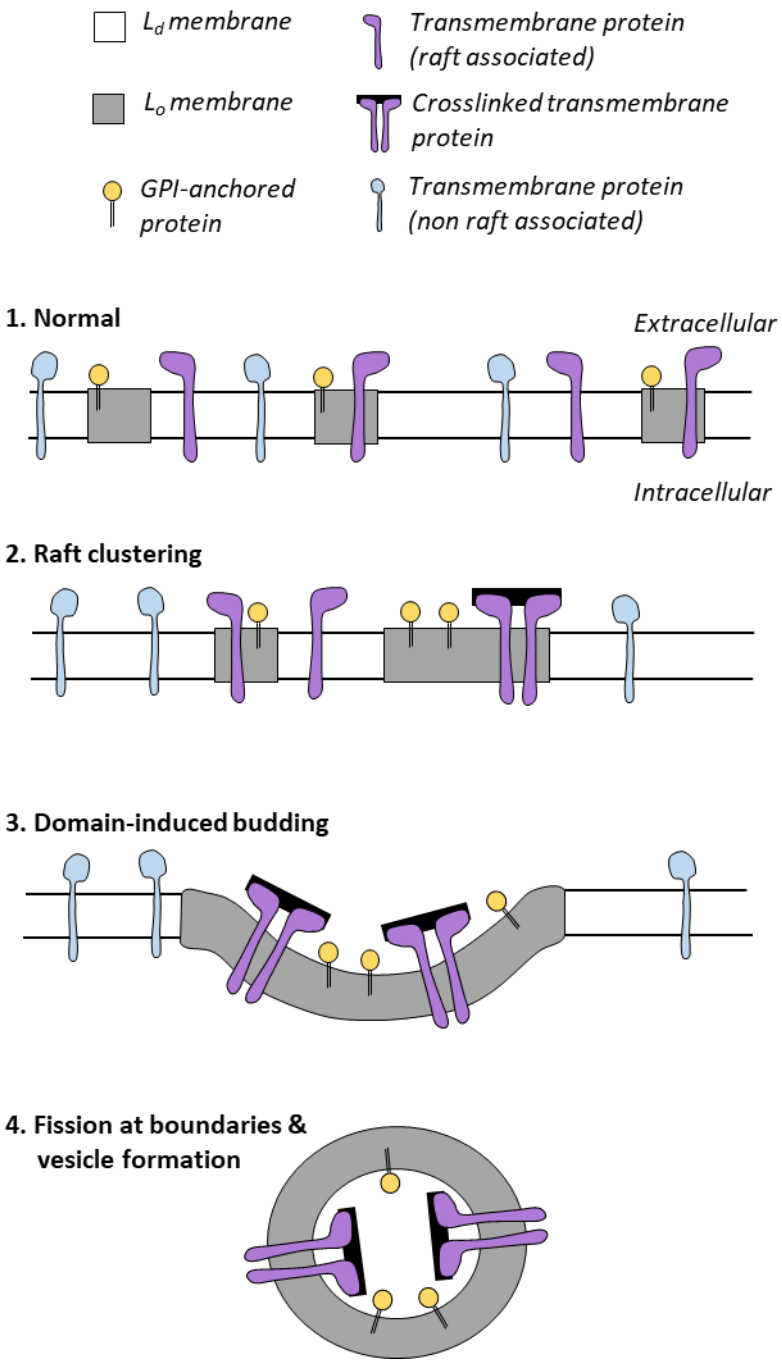

Figure 3.6. Raft clustering and domain-induced budding. Before clustering, membrane proteins associated with raft regions (L_o domains) to various extents. GPI-anchored proteins (yellow) resides exclusively in rafts, a transmembrane protein (purple) is found in both raft and non-raft regions, and another transmembrane protein (blue) is excluded from rafts. (1) Upon clustering, the raft-associated GPI-anchored proteins are partitioned into clustered rafts, and the semi raft-associated transmembrane protein is driven into clustered rafts by crosslinking. (2) The clustered raft region grows until a critical size is reached and the membrane beings to bud. (3) A vesicle containing raft components buds off from the plasma membrane by fission at the domain boundaries.

Caveola are rich in caveolin proteins[49,50], which associate and bind to cholesterol in membranes[45]. Knock out studies reveal that these proteins are essential in the formation of caveola[51,52]. Similarly depleting cholesterol from the membrane with filipin and nystalin disrupts the structure of caveola[44]. Functionally, caveolae have been shown to participate in the endocytosis and transcytosis of both small and large molecules[53]. Furthermore, they are implicated in calcium signalling and a range of other signalling events[54–56]. A multitude of receptor proteins have been demonstrated to localise in caveolae, including the muscarinic acetylcholine receptor, β-adrenergic receptor[57], adenylate cyclase[58] and the IP_3 receptor[59].

3.1.2. Surfactant effects on membranes

Studies that have employed model membranes have demonstrated that non-ionic surfactants, such as octyl glucoside and Solutol HS15, are able to partition into lipid bilayers, decrease lipid order and increase fluidity and permeability of membranes[60–62]. Indeed, by acting in this manner surfactant amphipathicity is believed to confer these molecules with their ability to function as permeability enhancers[63–65]. The non-ionic alkylglycoside surfactant, Tetradecyl-β-D-maltoside, for example has been suggested to increase transport of macromolecules across epithelial cells by partitioning into cellular plasma membranes, increasing line tension and membrane fluidity[66]. Similarly, another alkylcoside, Dodecyl-β-D-maltoside, is attributed to increasing epithelial transport of smaller molecules (fluorescently tagged dextran, 4 kDa) by also fluidising membranes[67].

Furthermore, non-ionic surfactants have been indicated in inducing lateral and transbilayer inhomogeneities in the plasma membrane that can drive endocytosis by lipidic forces[68]. To this end, Hilgemann and Fine, suggest that non-ionic surfactants expand and reorganise the outer leaflet of the plasma membrane in a manner that promotes coalesce and internalisation of L_d domains by expanding L_d membrane regions[68] – similar to raft domain induced budding.

A multitude of non-ionic surfactants, including polysorbates, Spans, Cremphors (EL and RH40), Solutol HS15 and Pluronic block copolymers, have also been attributed with disrupting membrane transporters[69–72]. Many studies on surfactant-induced membrane transporter inhibition have focused on the lipid raft associated efflux transporter, P-glycoprotein[73–77]. This transported is highly expressed in the gastrointestinal tract and is associated with multidrug resistance and reducing the oral absorption of drugs. Thus, its inhibition is a target for increasing drug oral bioavailability. However, polysorbates and other non-ionic surfactants have also been associated with inhibiting influx transporter system too, such as the human intestinal peptide transporter (hPepT-1) and monocarboxylic acid transporter (MCT)[70,74,78–80]. These systems enhance drug absorption thus their inhibition is undesirable for absorption enhancing formulations. In addition to transporters, surfactants such as Cemophor EL, have also shown inhibition of kinases such as protein kinase C[81]. This kinase is translocated to the membrane upon activation and is believed to play important roles in a multitude of signal transduction cascades[82,83]. It is believed that surfactants induce these effects on proteins by altering membrane fluidity, thereby influencing the conformation of membrane bound proteins[84,85].

Therefore, as discussed, the cellular plasma membrane plays critical roles; as an interface and barrier defining cell shape and contents, and also as a signalling platform. Disruptions to the lipid bilayer can have wide ranging effects and severely perturb cellular functions and viability.

Therefore, initial work set out to investigate the non-ionic surfactant effects, using Solutol HS15, on several plasma membrane parameters. These include assessing membrane permeability to cell-impermeable solute (FITC-dextran, wt 4000; FD-4), plasma membrane integrity, ion homeostasis, and membrane fluidity. Furthermore, the permeability of the nuclear envelope following exposure was evaluated to investigate the propensity of Solutol HS15 exposure to affect intracellular membranes.

Results demonstrate that Solutol HS15 increases the permeability of the plasma membrane to the model drug FD-4, however this was only achieved in conditions that severely perturbed the plasma membrane integrity. Solutol HS15 increased the fluidity of the plasma membrane almost immediately upon application (>60 seconds). Enhancement of plasma membrane permeability (FD-4 uptake) was achieved approximately an hour after initial application. This event kinetically coincided with disruptions in Ca^{2+} homeostasis and loss of intracellular contents indicating the loss of plasma membrane barrier function. Permeabilisation of the nuclear membranes was observed subsequent to the plasma membrane at 120 minutes of exposure, in conditions that perturb the plasma membrane.

3.2. Methodology

3.2.1. Plasma membrane integrity

Lactose dehydrogenase (LDH) is a cytosolic protein that has a molecular weight of 140 kDa[86]. The plasma membrane surrounding the cell functions acts as a physiological barrier when integrity is maintained. The presence of LDH in the extracellular milieu therefore indicates that it has been released from cells with damaged plasma membrane. The activity of the released LDH is then detected by a colourmetric assay on the principle of converting iodinitrotetrazolium (INT) to a coloured formazan. In the first step, released LDH in samples reduce NAD^+ to $NADH/H^+$ through the reduction of lactate to pyruvate. A diaphorase then catalyses the transfer of H/H^+ from $NADH/H^+$ to INT, reducing it to a formazan dye. An increase in plasma membrane damaged cells results in increased LDH activity in supernatant samples, which correlates to the amount of produced formazan. The amount of dye produced is therefore proportional to the number of damaged cells.

The LDH detection kit is comprised of three solutions (substrate, cofactor preparation and dye solution) which are stored at -20ºC until use. On the day of assaying, these solutions are thawed at 37ºC in a water bath. To prepare the LDH detection solution, equal amounts of the three solutions are combined. The resulting detection solution is light sensitive and protected from light by use of aluminium foil on all containers and plates.

Caco-2 cells (passages 30-40) were cultured in 96 well plates (clear) and treated in manners described in section 2.2.4 and 2.2.6, respectively. 1% (v/v) Triton X-100 applied in 1%

HEPES:HBSS was employed as the positive control to induce rapid cell lysis – this concentration of TX was used as it was determined to induce total LDH release within 5 minutes; total lysis was confirmed by comparing to LDH release when Triton X-100 exposure was increased to 60 minute (Figure 3.7). Following the exposure to treatments, 75 µl supernatant samples were taken per well and transferred to a fresh clear 96 well plate. *Nota bene,* samples for LDH detection are taken directly from the treatment solution in wells as washing treatments off would remove released LDH from the samples.

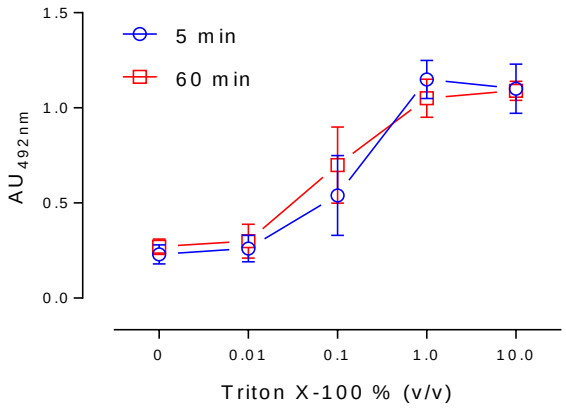

Figure 3.7. Dose response of Triton X-100 LDH release signal. Solution absorbance was measured at 492nm following exposure for either 5 or 60 minutes. TX was diluted and applied in 1% HEPES:HBSS. Data represents mean ± S.D from three independent experiments. AU, absorption units.

To test for LDH, 150 µl of LDH detection solution was added to each 75 µl sample, and incubated for 25 minutes at room temperature. Following incubation with detection solution absorbance of the samples was measured at 492 nm. Relative LDH release was calculated by setting the absorbance for the

vehicle control (1% HEPES:HBSS) as 0%, and the lysis control (1 % Triton X-100) set at 100% (
Equation 1).

$$Relative\ LDH\ release = \left(\frac{x - Negative\ control}{Positive\ control - negative\ control}\right) \times 100$$

Equation 1. Calculation of relative LDH release. Values used represent absorbance at 492 nm. X = sample absorbance.

3.2.2. Cellular internalisation of FITC-Dextran

To assess the permeability of the plasma membrane to cell impermeable solutes, FITC-Dextran (4 kDa) (FD-4) was employed as a model permeant. Internalisation of this probe has been previously used as a maker for plasma membrane permeability[87,88]. Cellular influx of higher molecular weight FITC-Dextrans (e.g. 70 kDa) is used in the detection and quantification of macropinocytosis[89–91]. Thus, increased internalisation of FD-4 may also reflect increased enhanced activation of cellular endocytotic mechanisms. Therefore, in addition to FD-4 internalisation, a series of other markers were used for evaluating plasma membrane permeability.

Caco-2 cells (passages 40-45) were cultured in 96 well plates (black) as described in sections 2.2.4. Following the culture period, cells were washed with PBS (three times) and then exposed to Solutol HS15 solutions (0.01-50 mM) containing 200 µg/ml FD-4. This was achieved by preparing Solutol HS15 and FD-4 solutions at 2X concentration, mixing in equal parts (1:1) and then adding 150 µl of the resulting solutions *per* well. FD-4 was prepared in 1% HEPES:HBSS. Solutol HS15:FD-4

solutions were applied for 5 - 240 minutes, and were compared (fold-change) to solutions that contained FD-4 and the vehicle (1% HEPES:HBSS) only.

Following exposure, treatment solutions were removed and the cells washed three times with PBS, to remove excess FD-4 solution. 50 µl PBS was added *per* well and fluorescent intensity measured following excitation at 490 nm and detection of emission at 525 nm. Intensity values were then normalised to the negative control (200 µg/ml FD-4 applied in 1% HEPES:HBSS) to enable evaluation of Solutol HS15 effect on Caco-2 internalisation of the FD-4 probe.

3.2.3. Calcium imagining

Intracellular Ca^{2+} was monitored by epifluorescent microscopy with the Ca^{2+} fluophore, FLUO-4 AM[92]. Caco-2 cells were seeded on 15 mm borosilicate coverslips inside 12 well plates at a density of $1.2x10^5$ cells *per* well and cultured for 48 hours in complete EMEM (1 ml/well). Cells were then washed with 1% HEPES:HBSS and coverslips loaded onto a slide chamber. To this set up, 1 ml of 1 µM FLUO-4 (applied in HBSS) was added for 30 minutes at 22°C in the dark. Following dye incubation chambers were loaded on the viewing platform, dye removed and replaced with 1% HEPES:HBSS.

Experiments were then performed by perifusing 1% HEPES:HBSS, 50 mM Solutol HS15 or 1% (v/v) Triton X-100 over cells at 32°C. Cells were imaged on an inverted Axiovert 135T*V* microscope and were continually illuminated at 490 nm with an infrared blocking filter KG5 (XF83 Omega) in the excitation light path to prolong cell viability. Cell fluorescence

at >510 nm was captured under 20 x magnification at 1 Hz with a Coosnap HQ2 camera (Photometrics, UK) with 4x4 bin size and 513 gaining using Imaging Workbench (Ver 6, Indec).

For each visual field studied, up to 15 regions of interest (ROI) were drawn around single cells and cell clusters. These were corrected for background fluorescence by subtraction, and fluorescence intensity traces generated as a function over time. Image analysis was performed with custom scripts written in Labtalk (OriginLab Corporation, MA USA).

3.2.4. Laurdan polarisation

To assess the effect of Solutol HS15 on the fluidity of Caco-2 plasma membranes the Laurdan probe was employed. This probe incorporates into membranes and is sensitive to water content. In this manner, Laurdan's fluorescence spectra is responsive to the physical state of the surrounding environment; it has an emission maximum of 440 nm when in L_o membrane regions (containing less water) and 490 nm when in L_d regions (containing more water). This shift in the spectral emission between membrane order states is employed to calculate the general polarisation (GP); a relative value representing a quantitative measure of lipid packing and membrane fluidity[93,94].

$$Generalised\ polarisation\ (GP) = \frac{(I_{440} - I_{490})}{(I_{440} + I_{490})}$$

Equation 2. Calculation of generalised polarisation (GP) of Laurdan. Where I_{440} and I_{490} represent the fluorescent intensities emitted at 440 nm and 490 nm, respectively, following excitation at 390 nm.

Stock solutions of Laurdan were prepared by dissolving Laurdan in DMSO to a concentration of 1 mg/ml Laurdan:DMSO. The resulting solution was sonicated at 37 kHz for 5 minutes to ensure dissolution. Stock solutions were stored at 4°C protected from light. Working solutions were prepared at a concentration of 2 µM by dilution of the stock in 1% HEPES:HBSS (final DMSO concentration of $7x10^{-4}$ % (v/v)), followed by vortexing to ensure homogeneity.

Laurdan polarisation was measured using two experimental designs; (i) the first method involved first preloading Laurdan into cells and then applying surfactant[95], and (ii) the second method involved treating with surfactant first and then incubation with Laurdan[62].

Caco-2 cells (passages 40-45) were used for Laurdan experiments and were culture in 96 well plates (black) as described in section 2.2.4.

(i) *Laurdan preloaded method* was performed by incubating cells with 200 µl 2 µM Laurdan working solution *per* well for 30 minutes in an incubator at 37°C with 5% CO_2. Following this, Laurdan solutions were removed by gentle aspiration, cells washed twice with PBS and 150 µl 1% HEPES:HBSS buffer returned to each well.

Fluorescent intensities were measured every 1 minute for 4 minutes (T_{-4}, T_{-3}, T_{-2} and T_{-1min}) to establish baseline levels of GP. Buffer was then removed from wells, by gently pipetting off, and 150 µl of treatment solutions (as listed below) added. Fluorescent intensities were then gathered every minute for at least 40 minutes. Laurdan GP was evaluated following a range of treatments, including; 1% HEPES:HBSS, Solutol HS15 (0.01, 0.1, 1 and 10 mM), 1% (v/v) Triton X-100, all applied at 37ºC

in 1% HEPES:HBSS buffer. Experiments were performed at 37°C by setting the internal temperature of the plate reader as such.

The background fluorescence of each treatment was measured and subtracted from the experimental intensities measured to account for the different degrees of auto-fluorescence from the distinct treatments and their concentrations. ΔGP *per* minute values between 1-30 and 30-40 minutes were calculated by linear regression analysis using Graphpad prism software and taking the gradient of the line of Laurdan GP versus time (minute) plot.

(ii) *Surfactant pre-treatment method* was performed in an end point manner to measure Laurdan GP, and involved treating cells with 1% HEPES:HBSS or 10 mM Solutol HS15 for 1, 30 and 180 minutes. Solutions were then removed and cells incubated with 200 µl 2 µM Laurdan working solution *per* well for 30 minutes in an incubator at 37°C with 5% CO_2. Following this, Laurdan solutions were removed, cells washed twice with PBS and fluorescent intensities read in 150 µl 1% HEPES:HBSS.

3.2.5. Nuclear membrane permeability

In addition to plasma membrane parameters the effect of Solutol HS15 on the permeability of the nuclear membranes was investigated using the CellTox™ Green Cytotoxicity Assay (CellTox green); an assay which uses a cell-impermeable asymmetric cyanine DNA-binding dye that relies on presence of both a permeabilised plasma and nuclear envelope for generation of a response.

This response can develop in two main manners. (i) Leakage of DNA from the nucleus, into the cytoplasm and subsequently extracellular milieu, followed by DNA binding to the CellTox green dye in these locations. Or (ii) diffusion of the CellTox green dye through permeabilised membranes into the cytoplasm and subsequently the nuclei, followed by dye binding to nuclear DNA. Nevertheless, an increased response indicates the increased permeability of the plasma and nuclear membranes to the CellTox green dye.

Total signal generated by the CellTox green dye binding to DNA was assessed by measuring fluorescence intensity (spectrophotometrically on plate reader) and by imaging on a fluorescent microscope. The CellTox green assay was performed on Caco-2 cells (passage 35-45) cultured in 96 well plates (black plates for plate reader studies and clear for microscopy) as described in section 2.2.5. Cells were treated in the manner described in section 2.2.7. In addition to Solutol HS15 and the vehicle control (1% HEPES:HBSS), cells were treated with 1% TX (applied in 1% HEPES:HBSS) as a positive control to permeabilise all cell membranes[96].

The CellTox green assay kit consists of a CellTox green dye and a CellTox green buffer, both of which are stored at -20ºC, until

use. On the day of assaying, the kit components are thawed at 37ºC in a water bath. To prepare the staining solution of the CellTox green assay, CellTox green dye is diluted 1:500 in the CellTox green buffer. 150 µl of the resulting solution (0.002% (v/v) CellTox dye:CellTox buffer) is then added to each well following treatment (*Nota Bene, treatments are not removed*). Plates containing the test samples are then shielded from light with use of aluminium foil and incubated for 15 minutes in an incubator at 37ºC with 5% CO_2.

Fluorescent intensity of the resulting solution was then measured following excitation at 495 nm and detecting emission at 520 nm. Relative CellTox green signal was calculated by setting the fluorescence intensity for the untreated cell control (1 % HEPES:HBSS) as 0 %, and the positive control (1 % Triton X-100) as 100 % (Equation 3).

$$Relative\ CTG\ signal = \left(\frac{x - Negative\ control}{Positive\ control - negative\ control}\right) \times 100$$

Equation 3. Calculation of relative CellTox green (CTG) signal. All values used represent fluorescence signal following excitation at 495 nm and detection of emission at 520 nm. X = sample fluorescent signal.

Assessment of CellTox green signal by fluorescent imaging was performed on an EVOS microscope at a magnification of 20X using a bright field filter and a GFP filter (excitation 470/22 nm; emission 510/42 nm). For microscopic analysis, treatment periods were limited to 120, 180 and 240 minutes.

3.3. Results

3.3.1. Plasma membrane integrity

Figure 3.8 illustrates that Solutol HS15 induced LDH release from Caco-2 cells in a concentration- and time-dependent manner following exposures ≥60 minutes.

Following exposure of 5, 10 and 20 minutes, no detectable release of LDH was induced (Figure 3.8a,b and c). LDH release occurs initially at Solutol HS15 concentrations ≥1 mM following exposures of 60 minutes (Figure 3.8d), and the magnitude of release increases at 120 minutes with these concentrations (Figure 3.8e). After 180 minutes of exposure, LDH release continues to increase, and is also noted at 0.1 mM Solutol HS15 (Figure 3.8f). After 240 minutes, total release (~100%) of cellular LDH content is observed for Solutol HS15 ≥10 mM (Figure 3.8g).

LD_{50} values for LDH release (Figure 3.8h) demonstrate that as exposure time is increased surfactant potency to induce membrane damage is increased, and that a significant increase ($P<0.001$) in potency of approximately 28-fold is experienced between 180 and 240 minutes.

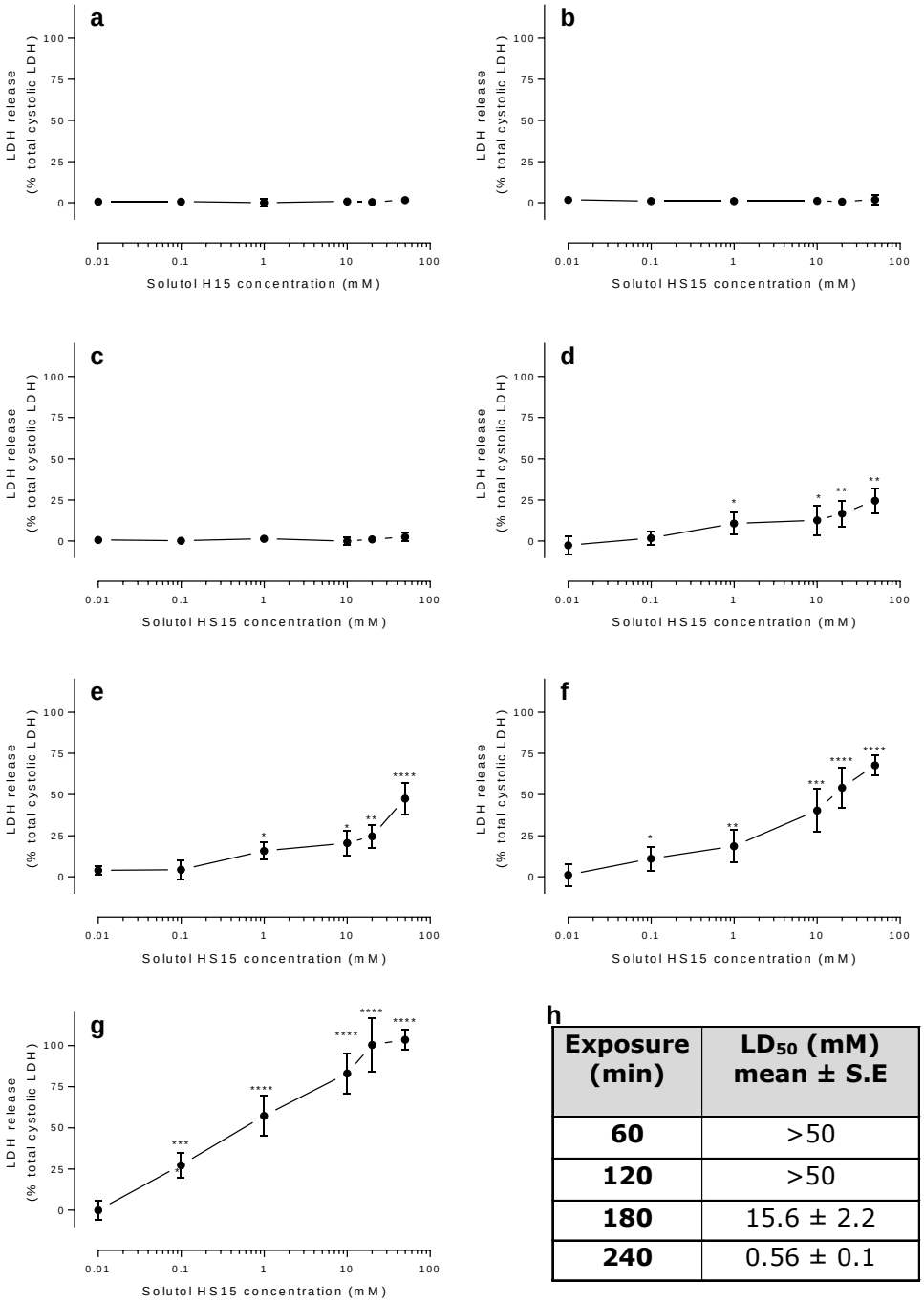

h

Exposure (min)	LD_{50} (mM) mean ± S.E
60	>50
120	>50
180	15.6 ± 2.2
240	0.56 ± 0.1

Figure 3.8. Effect of Solutol HS15 on Caco-2 plasma membrane integrity assessed by LDH assay. Cells were exposed for (a) 5, (b) 10, (c) 20, (d) 60, (e) 120, (f) 180 and (g) 240 minutes. Calculated LD_{50} values are displayed in (h). Data are presented as relative values (%) following normalisation to vehicle (0% LDH release) and 1% Triton X-100 (100% LDH release). Data presented as mean ± S.D and represent triplicates from three independent experiments.

3.3.2. Cellular internalisation of FD-4

To assess the ability of Solutol HS15 to increase the plasma membrane permeability to permeants, cellular internalisation of FD-4 was measured. As discussed in section 3.2.2, this measurement could also be detecting endocytotic mechanisms, such as macropinocytosis. However, values are calculated relative to the control therefore changes represent variations from baseline levels of endocytosis in cells not exposed to surfactant. FD-4 internalisation is displayed in Figure 3.9 and demonstrates that Solutol HS15 had a time- and concentration-dependent effect on this parameter.

Initially after 5 minutes of exposure it appears that Solutol HS15 at concentrations ≥10 mM induces a significant decrease in FD-4 uptake; with 10, 20 and 50 mM resulting in uptakes 0.7, 0.5 and 0.5-fold that of relevant control cells not exposed to the surfactant, respectively (Figure 3.9a). Examining internalisation after 10 minutes revealed that this effect remained significant but had however diminished in magnitude; concentrations ≥10 mM now generate uptakes approximately 0.8-fold baseline values (Figure 3.9b). Following 20 minutes of exposure, levels of FD-4 cellular internalisation return to values corresponding to control cells (Figure 3.9c).

Significant increases in FD-4 cellular internalisation in response to Solutol HS15 application are generated following exposures ≥60 minutes at concentrations ≥20 mM, and *initially* increase with time; at 60 minutes a maximal response of 1.3-fold increase is noted (50 mM), at 120 minutes ≥10 mM induce significant increases, the maximal noted is a 1.5-fold increase (50 mM), and ≥1 mM induce significant increases at 180

minutes, with a 2.3-fold increase in uptake achieved by 50 mM (Figure 3.9d,e and f).

However, at 240 minutes FD-4 internalisation was observed to then decrease with Solutol HS15 concentrations ≥10 mM and a maximal increase of 1.7-fold was achieved by 1 mM (Figure 3.9g).

In summary, ≥50% (1.5-fold) increases in FD-4 internalisation were achieved at conditions of 120 minutes exposure to ≥50 mM Solutol HS15, at 180 minutes to ≥20 mM Solutol HS15 and 240 minutes to 1 mM Solutol HS15.

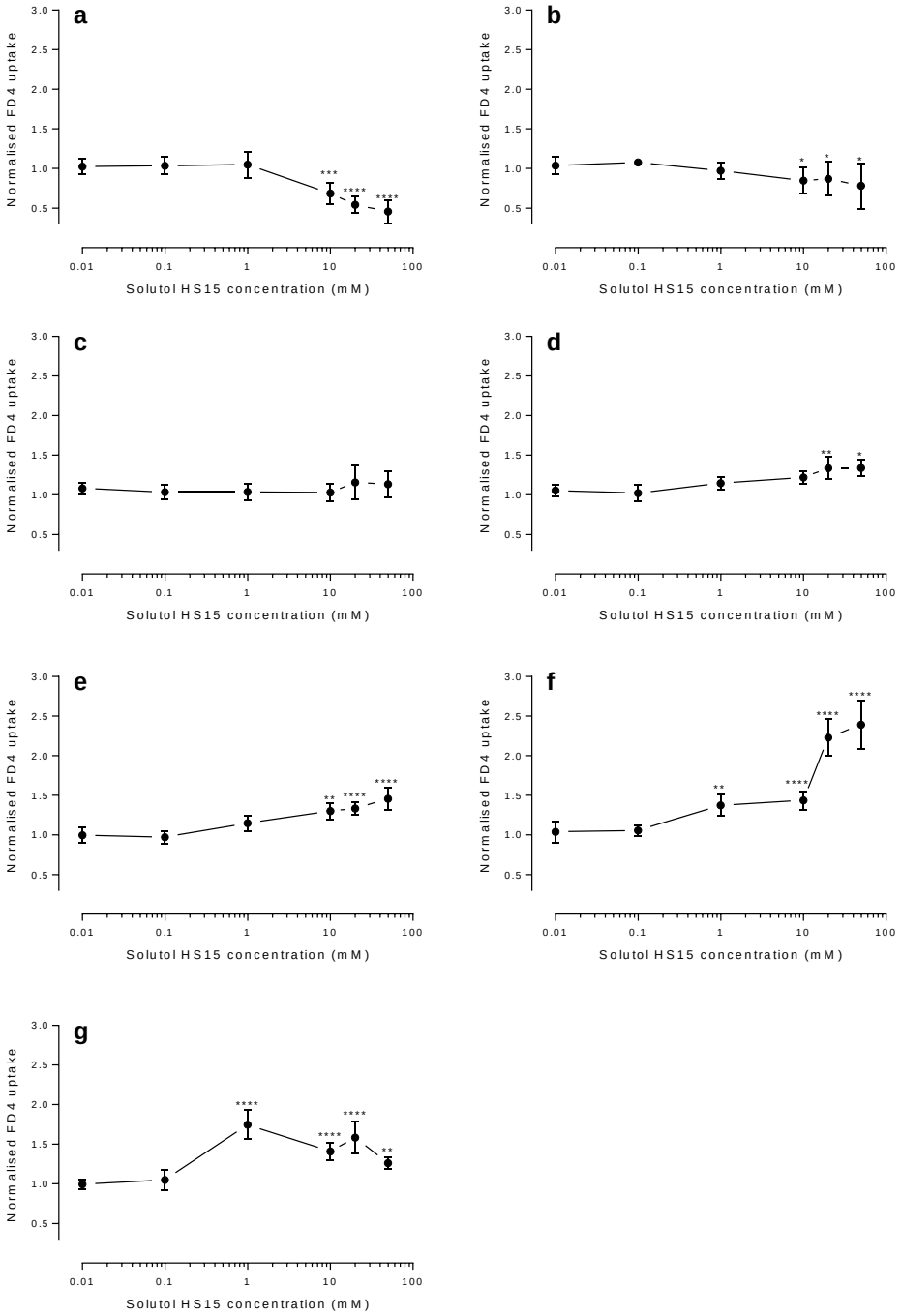

Figure 3.9. FD-4 cellular internalisation on exposure to Solutol HS15. Cells were exposed for (a) 5, (b) 10, (c) 20, (d) 60, (e) 120, (f) 180 and (g) 240 minutes. Uptake is normalised to that elicited by the vehicle control. Data are presented as mean ± S.D and represent triplicates from three independent experiments.

3.3.3. Calcium imagining

Perifusion of 50 mM Solutol HS15 produced an increase in Fluo-4 fluorescence, indicative of increased intracellular Ca^{2+} (Figure 3.10a). Three distinct types of Ca^{2+} response were observed: a sustained elevation (Figure 3.10a, red profile; 11 cells), a transient increase with either a return to baseline (Figure 3.10a, green profile; 12 cells) or lysis of the cell and dye loss (Figure 3.10a, blue profile; 8 cells) similar to that seen with TX (Figure 3.10a). Perifusion of Triton X-100 resulted in a 'spike' - rapid increase, followed by decrease in Ca^{2+} levels.

Cells were first perifused with the vehicle control (1% HEPES:HBSS) for 5 minutes to establish basal levels. An initial increase in fluorescence is observed upon the application of Solutol HS15 (black arrow; at ~5 minutes time point) and is due to a focus artefact resulting from the differing optical properties of the solutions.

Upon perifusion, Solutol HS15 (black arrow) did not result in immediate responses; the time to onset of the responses were independent of their type (as described above), with a mean ± S.D of 40.2 ± 37.6 minutes (Figure 3.10b).

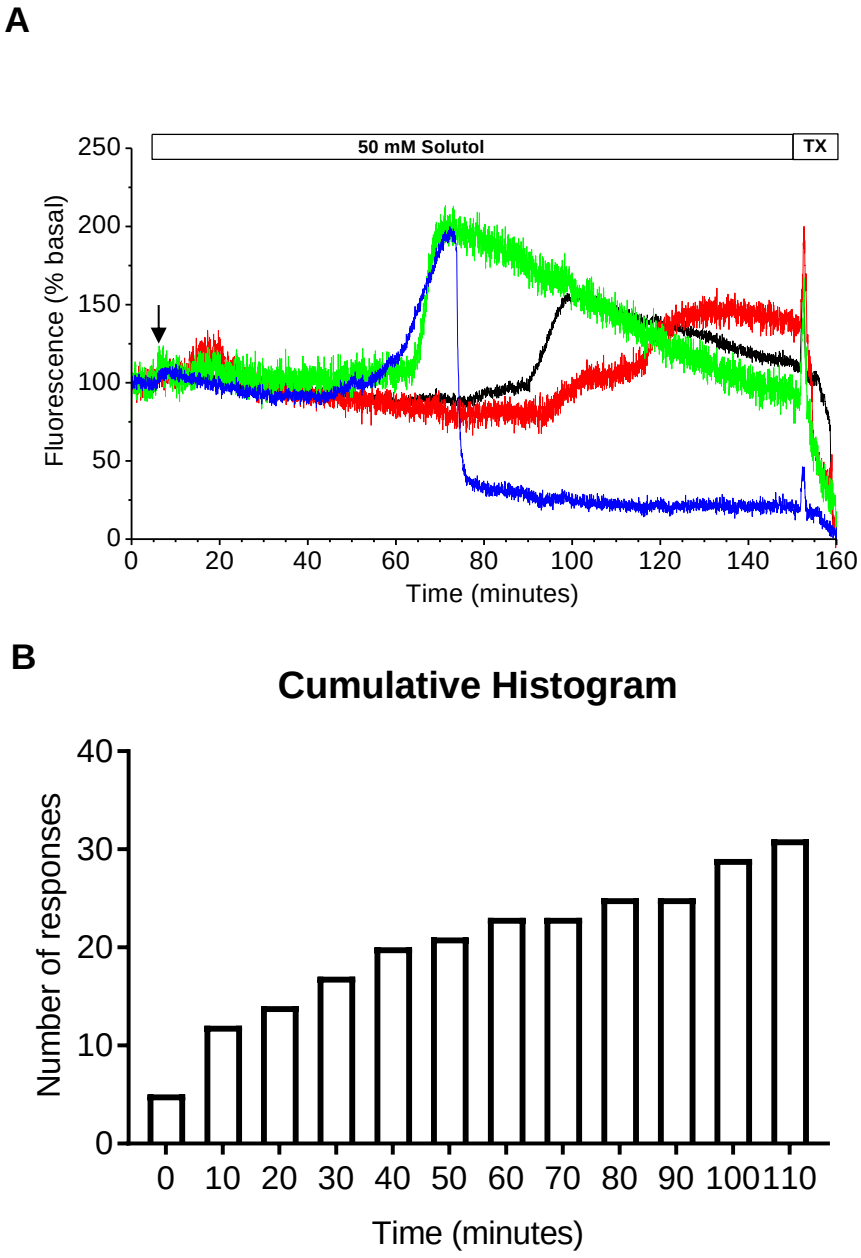

Figure 3.10. Intracellular Ca^{2+} flux induced by 50 mM in Caco-2 cells. (a) Representative records of the types of resposnes in intracellular Ca^{2+} seen on perifusion with 50 mM Solutol HS15. Ca^{2+} levels were assessed by Fluo-4 fluorescence and are normalised to that measured under basal conditions (1% HEPES:HBSS perfusion). (b) Cumulative histogram for the time of onset of intracellular Ca^{2+} changes seen in cell populations.

3.3.4. Laurdan polarisation

To investigate non-ionic surfactant effect on plasma membrane fluidity, the hydration of this membrane was measured using Laurdan general polarisation (GP) following exposure to model surfactant Solutol HS15 (Figure 3.11).

Caco-2 cells in 1% HEPES:HBSS buffer, prior to treatments (-4 to 0 minutes), have baseline GP values of approximately 0.19 ± 0.04, similar to values previously observed in the literature for this cell line[97].

Addition of surfactant resulted in a concentration-dependent decline in GP measured that was evident after the first minute of exposure (Figure 3.11b). Significant decreases in GP measured at one minute of exposure were exhibited by ≥0.1 mM Solutol HS15 solutions (Figure 3.11b). Following the initial decline (0-1 minute), GP values were maintained for at least 30 minutes; ≤1 mM Solutol HS15 display rates in ΔGP over 1-40 minutes of exposure that do not significantly differ from the buffer control (Figure 3.11c), however 10 mM Solutol HS15 demonstrated a significant decay in GP that was evident over 1-40 minutes but most prominent between 30-40 minutes (Figure 3.11c).

Treating Caco-2 cells with 1% (v/v) Triton X-100 solution resulted in a significant initial decline in GP value (0-1 minutes) compared to the vehicle control; this initial drop in GP was larger in magnitude than with Solutol HS15, but did not significantly differ ($P>0.05$) from that induced by 10 mM Solutol HS15 (Figure 3.11b). However, unlike Solutol HS15, Triton X-100 induced a steady and significant decay in GP value between 1-40 minutes of -1.2×10^{-3} ΔGP/min (Figure 3.11c).

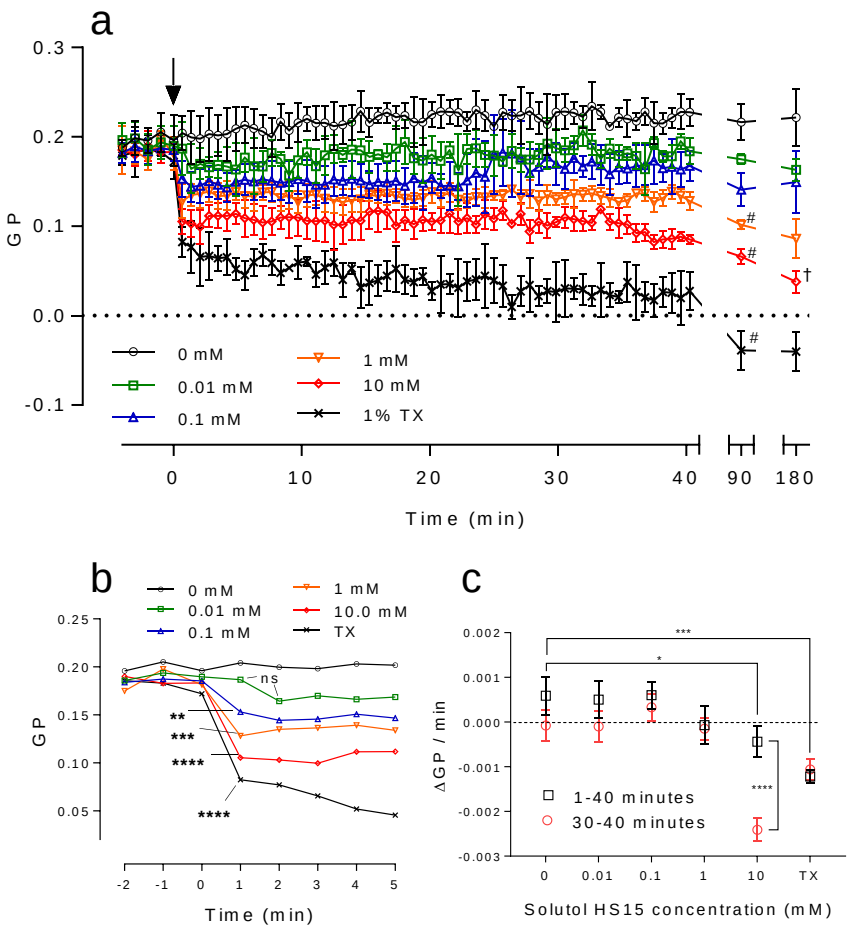

Figure 3.11 Laurdan generalised polarisation (GP) of Caco-2 cells. (a) GP fluctuations measured versus time upon of treatments including the vehicle control (0 mM; 1% HEPES:HBSS; H:H), Solutol HS15 solutions at concentrations of 0.01-10.0 mM and 1% Triton X-100 solution (TX). # signifies significant difference ($P<0.05$) between GP values measured at 1 and 90 minutes and † signifies significance ($P<0.05$) between 90 and 180 minutes. For clarity (b) displays GP values between -2 and 5 minutes and highlights significant decreases in GP observed between 0 and 1 minute. (c) Rate of Laurdan GP change *per* minute (ΔGP/min) for data gathered between 1-40 and between 30-40 minutes time points. Data were gathered using the Laurdan pre-loaded method as described in section 3.2.4, and are presented as mean ± S.D and represents triplicates from 3 independent experiments. *, $P<0.05$; **, $P<0.01$; ***, $P<0.001$; ****, $P<1x10^{-4}$)

Determining GP values at 90 minutes of exposure revealed that ≥1 mM Solutol HS15 resulted in significant declines in GP levels compared to those induced following 1 minute of exposure (Figure 3.11a), thus an additional reduction in GP values has occurred. This was also present with Triton X-100 treatment. GP values then declined significantly further at 180 minutes with 10 mM Solutol HS15 (Figure 3.11a).

Figure 3.12 illustrates that no significant difference in measured Laurdan GP values following surfactant treatment at various time points was observed between the two different experiment methods described in section 3.2.4; Laurdan 'pre-loaded' and surfactant 'pre-treated' protocols.

Thus, Laurdan data revealed that Solutol HS15 at concentrations ≥0.1 mM is capable of increasing membrane fluidity after one minute of exposure in a statistically significant manner. Furthermore, GP values remained relatively unchanged between 1-40 minutes during exposure to ≤1 mM Solutol HS15, and 1-30 minutes for 10 mM Solutol HS15. Exposure of ≥90 minutes was associated with subsequent GP reductions with solutions of Solutol HS15 ≥1 mM.

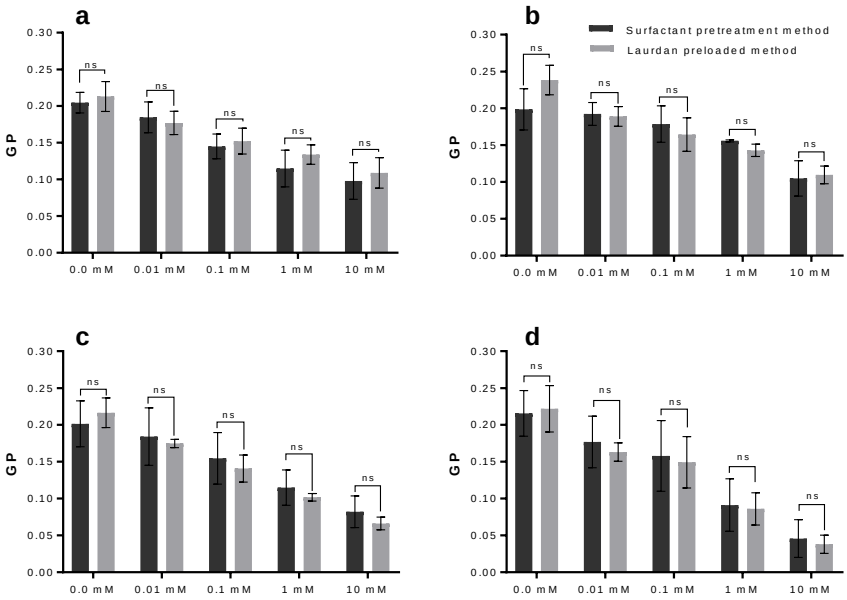

Figure 3.12. Laurdan GP performed on Caco-2 cells using two experimental methods. Cells were exposed to surfactant solutions for (a) 1, (b) 30, (c) 90 and (d) 180 minutes. The two methods are described in Section 3.2.4. Statistical significance was assessed using one-way ANOVA. ns, no significant difference.

3.3.5. Nuclear membrane permeability

3.3.6. Assessment of CellTox green fluorescent intensity

As illustrated in Figure 3.13, increases in nuclear membrane permeability were not induced following 5, 10 and 20 minutes exposure to Solutol HS15 solutions at all tested concentrations. It can be noted that the surfactant applied at concentrations of 10, 20 and 50 mM for 60 minutes elicited increases in nuclear permeability, of 5.3 ± 7.0, 8.7 ± 6.6, and 8.8 ± 5.7 %, respectively, relative to the untreated control, however, these responses did not significantly differ from that of the control ($P>0.05$).

Pronounced increases in nuclear membrane permeability were observed in a concentration and time-dependent manner following exposures ≥120 minutes to surfactant solutions of concentrations ≥10 mM. Maximal increases of approximately 18.9 ± 4.3 %, 26.3 ± 7.5 % and 44.4 ± 4.7 % in nuclear membrane permeability were noted following exposures of 120, 180 and 240 minutes, respectively to 50 mM Solutol HS15 (Figure 3.13e,f and g).

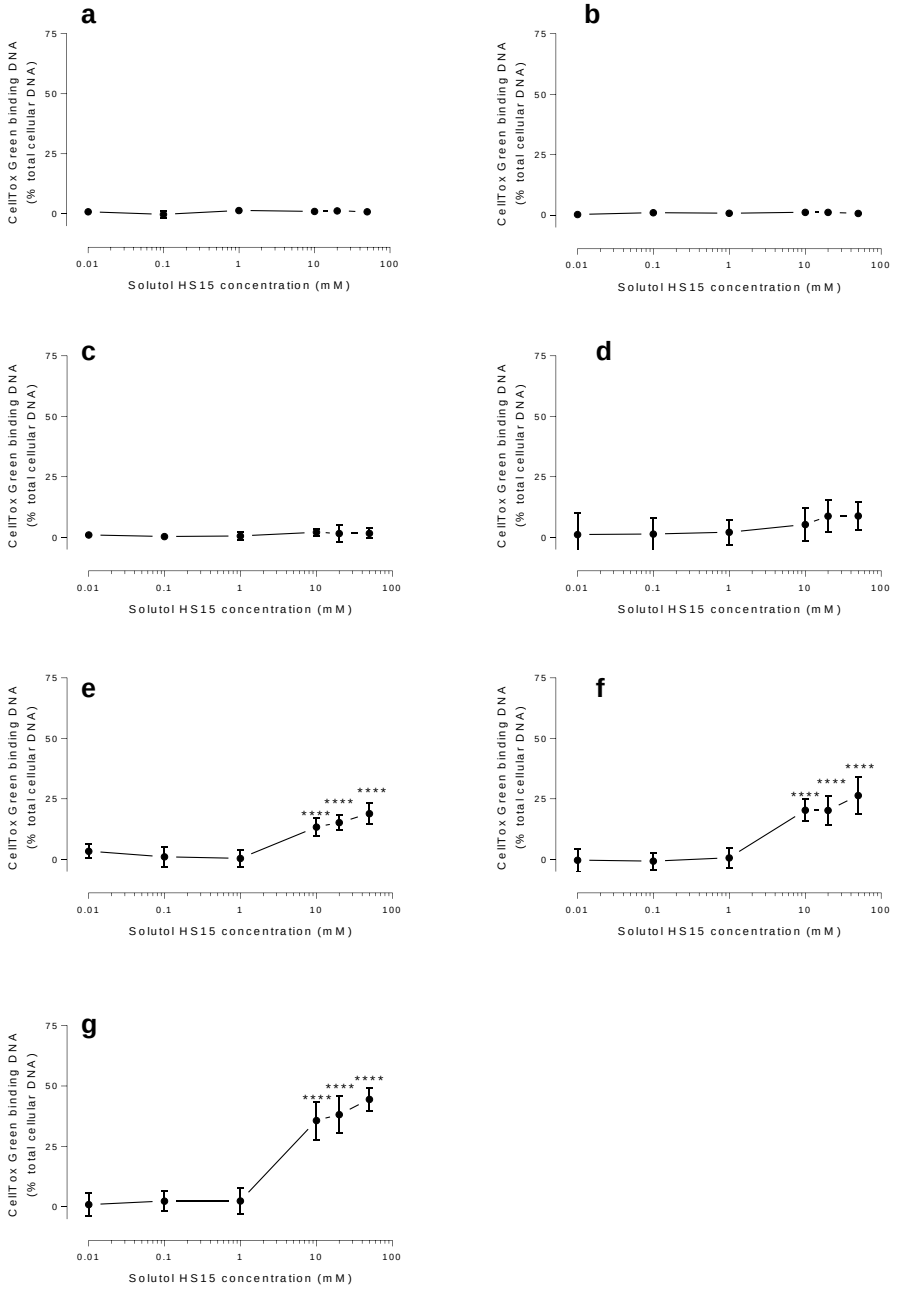

Figure 3.13. Effect of Solutol HS15 on Caco-2 nuclear membrane permeability. Cells were exposed to surfactant solutions for (a) 5, (b) 10, (c) 20, (d) 60, (e) 120, (f) 180 and (g) 240 minutes. Nuclear membrane permeability was assessed using the CellTox green probe. Data are presented as relative values (%) following normalisation to vehicle (0% dye binding DNA) and 1% Triton X-100 (100% dye binding DNA). Data are presented as mean ± S.D and represents triplicates from three independent experiments.

3.3.7. Visualisation of CellTox green fluorescence

CellTox green staining of Caco-2 cells was visualised by fluorescence imaging following exposure for 240 minutes to 0.1 and 1 mM Solutol HS15 solutions (Figure 3.14), and to 10 mM Solutol HS15 for exposures of 120, 180 and 240 minutes (Figure 3.15).

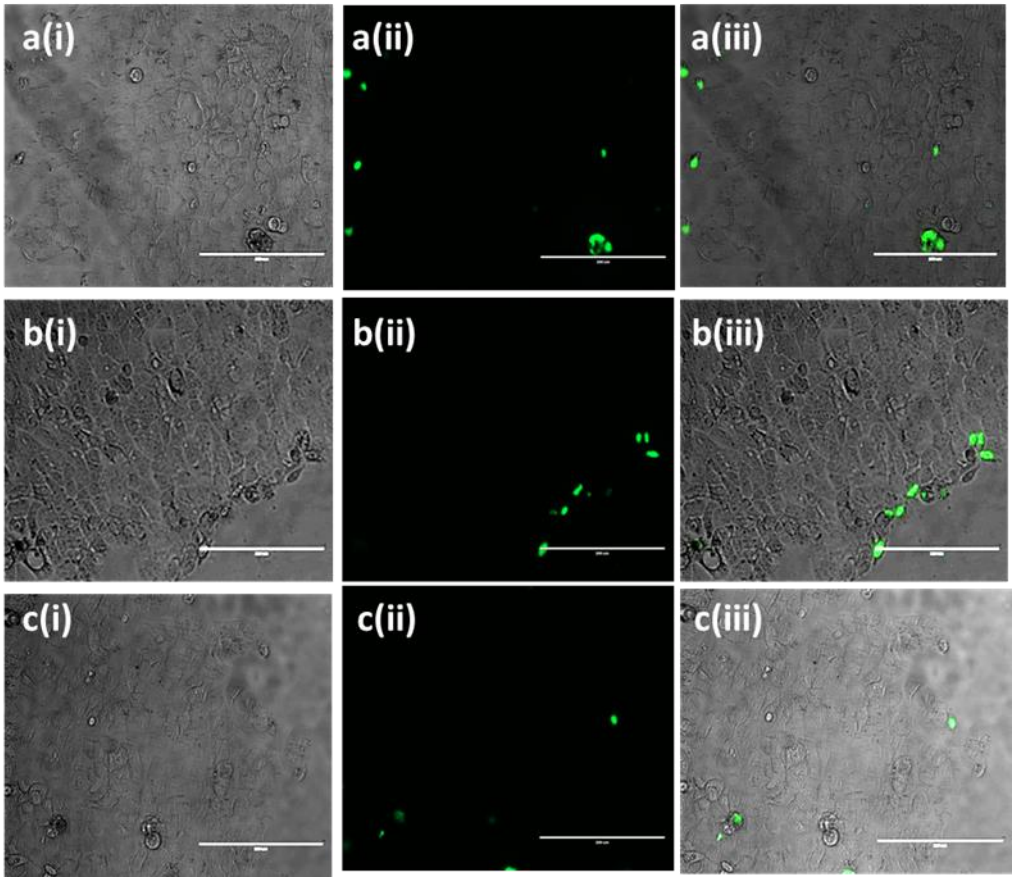

Figure 3.14. Fluorescent imaging of Caco-2 cells staining with CellTox green dye. (a) 1% HEPES:HBSS, (b) 0.1 mM and (c) 1 mM Solutol HS15 solution following 240 minute exposure. Caco-2 cells were imaged using EVOS microscope on (i) bright field and (ii) GFP filter at excitation 470/22nm, emission 510/42nm (wavelength/bandwidth) for CellTox green, and (iii) merged by ImageJ software. Magnification 20X; scale bar = 200µm.

It is possible to observe in Figure 3.14 that cells exposed to 0.1 and 1 mM Solutol HS15 for 240 minutes have low levels of CellTox green staining of nuclei, and that this level of staining was similar to that induced by the negative control (1% HEPES:HBSS buffer).

Exposure of Caco-2 cells to 10 mM Solutol HS15 was observed to induce positive staining, indicated by the presence of green nuclei (Figure 3.15), supporting data from spectroscopic measurements (Figure 3.13); exposure ≥120 minutes to ≥10 mM Solutol HS15 induce increased nuclear membrane permeability. From the bright field images, it is possible to observe that cells treated with 10 mM Solutol HS15 for 120 minutes appear more intact and defined than those exposed for 180 or 240 minutes; substantial 'rounding up' of cells is exhibited at 240 minutes (Figure 3.13a,b and c).

Imaging of CellTox green staining revealed that were morphological differences between cells treated with Triton X-100 (Figure 3.15d) and Solutol HS15 (Figure 3.15a, b and c). The stained nuclei of cells treated with Solutol HS15 appear well defined, while TX treated cells have nuclear staining that is 'fuzzy' and poorly defined (Figure 3.15). Inspecting the merged images (Figure 3.15ciii and diii) one can see that morphologically, there appears little left of Triton X-100 treated cells aside from their nuclei (i.e., no presence of cell outline in bright field image). Therefore, in addition to the plasma membrane, the nuclear envelope of cells treated with Triton X-100 may thus be more damaged than Solutol HS15 treated cells.

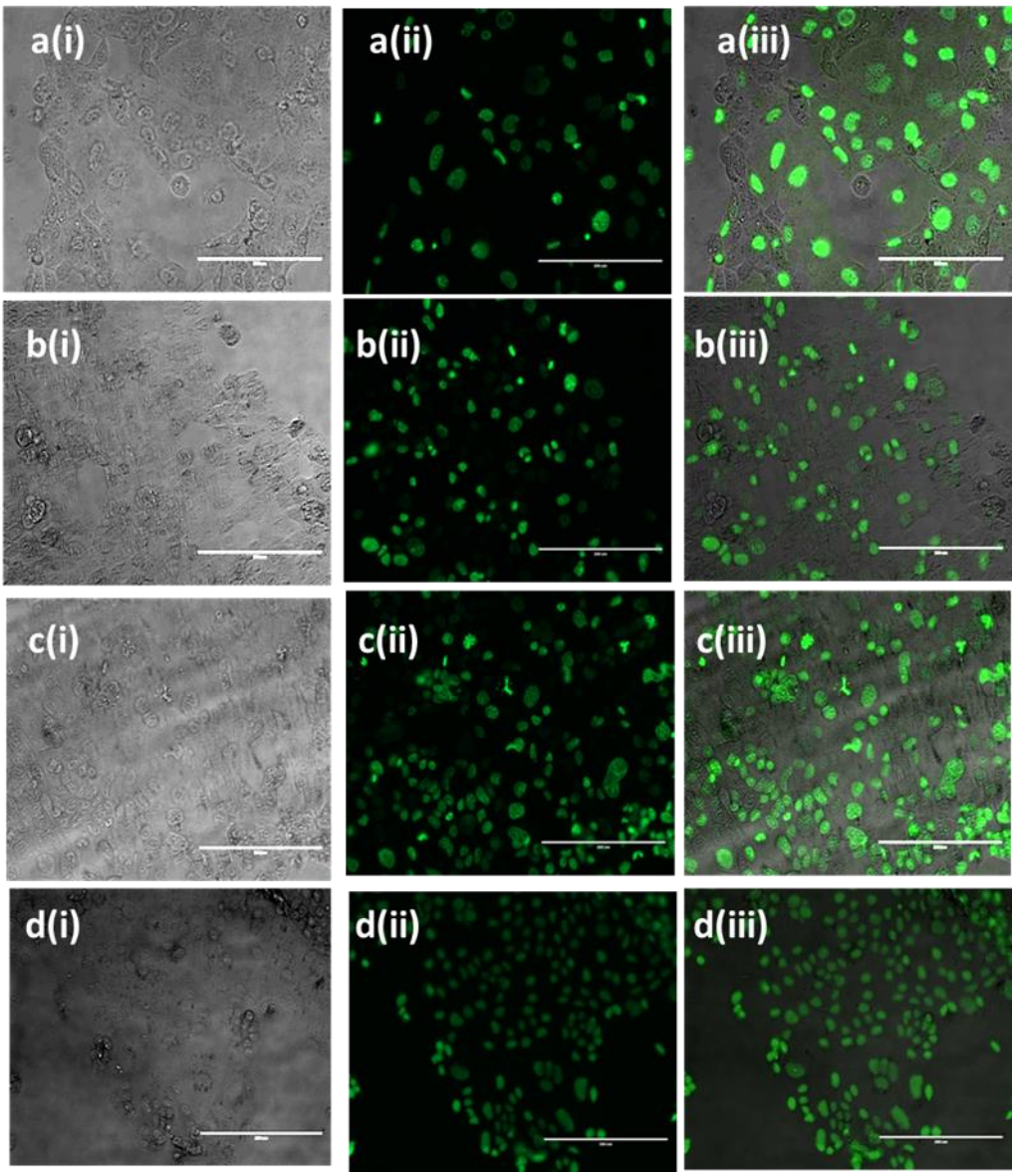

Figure 3.15. Fluorescent imaging of CellTox green dye staining following treatment of Caco-2 cells with 10 mM Solutol HS15 for (a) 120, (b) 180 and (c) 240 minutes, and (d) 1% Triton X-100 for 240 minutes. Caco-2 cells were imaged using EVOS microscope on (i) bright field and (ii) GFP (Excitation 470/22nm; Emission 510/42nm; [wavelength/bandwidth]) filters, and (iii) merged with ImageJ software. Magnification 20X; scale bar = 200μm.

3.4. Discussion

3.4.1. Rapid plasma membrane fluidisation

The first observed effect on Caco-2 cells exposure to Solutol HS15, occurring within 0-1 minute, was an increase in the plasma membrane fluidity (Figure 3.11). Measured at the 5 minutes time point, no significant release of intracellular LDH enzyme was observed (Figure 3.8). During the same time period (0-5 minutes) disruptions in calcium homeostasis were not observed (Figure 3.10). Unexpectedly, after 5 minutes of exposure, a significant reduction in cellular permeability to the external permeant FD-4 was observed at high Solutol HS15 concentrations (≥10 mM) (Figure 3.9). This would hence indicate that the initial event occurring on cells exposure to the surfactant is its incorporation into the plasma membrane.

Laurdan is often used in the study of non-ionic surfactant solubilisation of liposomes and determination of partition co-efficient[98–100], however there is lack of data on cell membranes following short surfactant exposures to allow for comparisons. Other studies in the literature have measured Laurdan GP fluorescence over time, however to study membrane fluidisation following treatment with alcohols, such as benzyl alcohol and heptanol. They reported rapid reductions (0-1 minute) in GP values following application to these compounds[95,101] and, this is believed to occur due to lipid disordered of membranes because of the compounds intercalation[102].

In support of our observation of the rapid Solutol HS15 surfactant incorporation into the plasma membrane are measurements of cell membrane conductance made by Fine et

al.[103]. They suggest that non-ionic surfactant insertion into cell plasma membranes is rapid (<10 seconds); the increased membrane conductance was observed with the non-ionic surfactants, Triton X-100 and NP-40, and was suggested to indicate an increase in membrane area as a result of surfactant molecule insertion[103].

Treatment of Caco-2 cells with Solutol HS15 solutions below the CMC (0.01 mM) did not result in any detectable response that differed from the control at all the time periods tested. Thus, in agreement with previous work, the membrane effects of Solutol HS15 appear to be dependent on the presence of surfactant micelles[72,104]. The authors suggest that the presence of micelles in the surrounding solution acts as a reservoir to supply surfactant monomers to participate in membrane interactions[74,105–107]. It is hence possible to conclude that Solutol HS15 induced increases in Caco-2 cell membrane fluidity is a consequence of the incorporation of the surfactant monomers/molecules into the plasma membrane[84], which in turn, alters the packing efficiency of lipids. The concentration dependent reduction in GP values suggests that the membrane is not 'saturated' with surfactant monomers, as increasing the concentration of Solutol HS15 increased the level of fluidisation.

As exposure occurs on the extracellular side of the membrane, the insertion of surfactant monomers would be expected to, at least initially, occur into the outer leaflet of the membrane bilayer. If the surfactant molecules do not translocate to the inner membrane, their insertion will expand the bilayer asymmetrically by increasing the area of the outer leaflet and result in positive curvature[108], a process described as membrane budding[106]. If the bilayer is unable to bend and assume curvature, it develops curvature stress, resulting in

strain disordering and thinning of the hydrophobic core of the membrane[109]. After a threshold level, this stress may induce rupture of the bilayer[108].

In the present study, the initial fluidisation of Caco-2 cell plasma membrane on exposure to Solutol HS15 did not correspond to an increased calcium ion flux or cellular leakage of LDH (during 5-20 minutes exposure), suggesting that the overall membrane barrier integrity is maintained despite surfactant incorporation into the plasma membrane. This would indicate that the level of plasma membrane fluidisation, and possibly membrane perturbation, may not be sufficient to result in increased membrane permeability. In fact, the observed reduction in FD-4 internalisation in this early time period could be a consequence of outer leaflet 'crowding' by the incorporated surfactant molecules, consequently bilayer asymmetry and budding, which in turn is hindering diffusion across the membrane and/or endocytotic mechanisms and transport. It is also possible that, while the outer lipid layer has been fluidised, the inner layer may not be immediately affected[108,110], and remains impermeable to FD-4.

Interestingly, unlike treatment with Triton X-100, the fluidisation of cell membranes treated with Solutol HS15 remained unchanged between 1-30 minutes after the initial event (0-1 minute), suggesting that there may be resistance to further surfactant incorporation. The reason for this remains unclear but, as will be discussed in Chapter Four and Five, may be a consequence of the induction of cellular responses.

The fluidisation of the plasma membrane induced by the model surfactant will likely reflect a re-organisation of the membrane domains; expanding L_d regions and in turn coalescing L_o

region[103,111]. Moreover, non-ionic surfactants are cholesterol phobic[112], and thus promote the segregation of cholesterol into L_o domains. This coalescing of L_o membrane domains may in turn result in the clustering of lipid raft associated proteins and trigger and/or disrupt cellular signalling, such as those discussed in section 2.1.

3.4.2. Changes in plasma membrane permeability

Exposing Caco-2 cells to Solutol HS15 solutions ≥1 mM for ≥60 minutes was associated with increased permeability of the plasma membrane.

Increased internalisation of the external FD-4 probe was observed in response to ≥20 mM solutions of surfactant following 60 minutes, and most prominent following 180 minutes to solutions ≥1 mM (Figure 3.9), supporting the concept that Solutol HS15 and similar compounds could function as absorption enhancers[72], as discussed in Chapter 1. However, the conditions required to do so also induce the leakage of intracellular components (LDH release), suggesting damage to the barrier function of the plasma membrane (Figure 3.8); for example, to achieve a 50% increase in FD-4 internalisation required conditions that, at the least, also induced ~40% loss of intracellular LDH. This correlation between permeability enhancing effects and cellular damage has been noted with other non-ionic surfactants, such as polysorbates and Solulans[113].

Furthermore, at 240 minutes of exposure a decrease in FD-4 internalisation, relative to 180 minutes, is observed with ≥10 mM Solutol HS15 (Figure 3.9). These conditions also generated

≥80% loss of LDH (Figure 3.8). Therefore, the decrease in intracellular FD-4 is likely a result of surfactant inducing cellular lysis, evident from LDH release (Figure 3.8), and cellular death (observed using MTS reduction assay, Chapter 4, Figure 4.4); any FD-4 that has been internalised is subsequently released, as the cells can no longer withhold intracellular material.

Significant LDH release was observed with surfactant concentrations that were associated with additional membrane fluidisation at ≥90 minutes of exposure (Figure 3.11); ≥1 mM Solutol HS15 generated significant release of LDH when applied to cells for ≥60 minutes, and cells exposed to ≥1 mM Solutol HS15 for 90 minutes had GP values that were significantly lower than those measured after one minute. Therefore, the increase in plasma membrane permeability may be associated with the additional fluidisation of the membrane that is noted at 90 minutes. As discussed in section 3.1, this mechanism of mediating permeability by membrane fluidisation is suggested to occur with other non-ionic surfactants[66,67].

The reason for this additional fluidisation effect at later time points (Figure 3.11) remains unclear. It could be possible that both leaflets of the lipid bilayer are becoming fluidised by the surfactant molecules continued incorporation over time and a consequence of surfactant presence in both (as opposed to only the outer leaflet at one minute). For this to occur, Solutol HS15 molecules would have to diffuse or cross by a flip-flop mechanism. In model membranes, some surfactants, such as Triton X-100 and $C_{12}EO_7$, were observed to equilibrate with both bilayer leaflets within a matter of milliseconds to tens of seconds[114,115]. However, non-ionic surfactants with larger hydrophilic headgroups, such as Solutol HS15, may take hours or days to 'cross' i.e. become incorporated into both leaflets of

the membrane bilayer, as shown with the alkylmaltosides[108,110]. Hence, the initial increase in membrane fluidity may be due to outer leaflet incorporation and the secondary phase of fluidisation a result of surfactant incorporation into the inner leaflet at later time points.

As suggested above, Solutol HS15 insertion into the plasma membrane may have been hindered or inhibited between 1 and 30 minutes of exposure by cellular mechanisms that promote membrane stabilisation against shock. For example, components of the heat shock response, such as the HSP17 protein, are known to bind to the membrane and act as stabilising factors by influencing membrane microviscosity[116,117]. When the cessation of such a response occurs, it may re-enable Solutol HS15 incorporation into the membrane, and this may be reflected in the 'additional' membrane fluidisation observed at 90 minutes. The resumed insertion of surfactant into the outer leaflet may result in increased curvature stress of the monolayer and ultimately, once a threshold is overcome, membrane rupturing or the formation of toroidal pores to relieve the line tension[118,119]. In this manner, the plasma membrane could become permeabilised.

The average onset of intracellular Ca^{2+} influx occurs at approximately 40 minutes for Caco-2 cells exposed to 50 mM Solutol HS15 solution (Figure 3.10). This corresponds to an increase in the rate of membrane fluidisation (ΔGP/min) observed in similar conditions (30-40 minutes of exposure with 10 mM Solutol HS15) (Figure 3.11c), supporting the concept that further fluidisation occurring after the initial effect within the first minute, is responsible for increased cell membrane permeability.

Ca^{2+} is a highly versatile intracellular signal that is responsible for a wide range of physiological responses[120,121]. Calcium exists as a gradient across the plasma membrane, and low intracellular levels are maintained with respect to the extracellular milieu, by a magnitude of approximately 13,000-fold[122]. The uncontrolled influx of Ca^{2+} intracellularly, can therefore be a signal of membrane damage and can trigger membrane repair mechanisms, such as membrane patching[123–125]. Moreover, elevated cytosolic Ca^{2+} concentrations can induce actin remodelling, which in turn have been shown to influence plasma membrane permeability[126]. Therefore, influx of calcium intracellularly could further propagate surfactant induced membrane effects *via* disruptions to the underlying cytoskeleton. Elevated levels of intracellular Ca^{2+} can also regulate stress responses, where it can function as an initiator and effector of both pro-survival and pro-death cellular responses[122,127]. While not measuring intracellular levels Ca^{2+} *per se*, as in this work, Yamaguchi et al. were able to provide evidence that Ca^{2+}-dependent cell death was associated with the cellular toxicity of the non-ionic surfactant Cremophor EL by observing a positive correlation between levels of cell death and levels of Ca^{2+} in extracellular solutions[128]. Mechanisms of cell death induced by Solutol HS15 are discussed further in Chapter 5.

Interestingly, heterogenous Ca^{2+} responses were observed by cells. This might be due to the Caco-2 cell line being heterogeneous, i.e. containing subpopulations of cells with different biochemical, morphological and electrophysiological characteristics[129,130]. Therefore, further work would benefit from utilising a different cell line(s) to investigate if the Ca^{2+} responses to Solutol HS15 are truly heterogenous or due to the

Caco-2 cell line. Application of Triton X-100 induced a rapid spike in Ca^{2+} levels (Figure 3.10), this is likely a result of cellular lysis. When applied at concentrations above its CMC, such as used here, Triton X-100 is known to permeabilise membranes rapidly [131,132]; this is further highlighted by data in Figure 3.7 demonstrating Triton X-100 induces, at applied concentration (1%), total leakage of LDH after 5 minutes of exposure on cells.

3.4.3. Nuclear membrane permeabilisation

Exposure of Caco-2 cells to ≥10 mM Solutol HS15 for ≥120 minutes generated nuclear membrane permeability (Figure 3.13); these conditions were also associated with increased internalisation of FD-4, LDH release and flux Ca^{2+}. It is noted however that Solutol HS15 increased permeability of the nuclear probes requires longer cell exposures to the surfactant and higher surfactant concentrations than plasma membrane permeants.

For example, LDH release was observed at 60 minutes exposure however an increase in nuclear permeability was not at any of the tested surfactant concentrations. Furthermore, increased nuclear permeability was not induced by concentrations of ≤1 mM, at exposure times up to 240 minutes, despite the LD_{50} for LDH release at this time point being calculated as 0.56±0.1 mM.

The inner membrane of the nuclear envelope is lined with proteins that connect to a meshwork of lamin filaments, known as the nuclear lamina which confer mechanical strength to the nucleus[133,134]. The multitude of membrane-lamin proteins have indeed been implicated in making the nuclear envelope

much stiffer and more resilient than the plasma membrane to mechanical strain[133]. These reasons taken together with its intracellular location may explain why the nuclear membrane was found less susceptible to perturbation. To the best of our knowledge, no other study in the literature has investigated non-ionic surfactant plasma membrane *versus* nuclear membrane permeability effects to enable a comparison for our observation.

The cell nucleus is surrounded by two bilayered lipid membranes that separate nuclear contents from the cytoplasm. The nuclear membranes are highly regulated and contain a multitude of proteins that have been implicated in vital cellular functions. These include nuclear pore complexes that mediate the bidirectional exchange of RNA and proteins between the nucleus and the cytoplasm[135]; inner nuclear membrane proteins that play diverse and vital roles in DNA metabolism and gene expression[136,137]; and outer nuclear membrane proteins that bind to the cytoskeleton, positioning the nucleus within the cell[138]. Thus, in addition to shielding genomic material from cytoplasmic constituents, the nuclear membrane and its components are associated with carrying out cellular functions[139]. Permeabilisation of this membrane can result in DNA damage[140,141], and promotion of cell death[142,143].

There are two possible mechanisms for Solutol HS15 induced increased nuclear membrane permeability: (i) by the promotion and activation of apoptotic death, and/or (ii) Solutol HS15 incorporation into the nuclear membranes in a similar manner to the plasma membrane.

(i) Indirect mechanism to increase nuclear membrane permeability

During late apoptosis, nuclear DNA is fragmented, the nuclear membrane becomes permeabilised and the nucleus breaks into numerous distinct bodies (apoptotic bodies)[144,145]. The induction of programmed cell death could therefore account for the nuclear permeabilisation observed. Mechanisms of cell death are investigated further in Chapter 5 and suggest, however, that the permeability increase of the nuclear membrane is occurring independently of pro-apoptotic mechanisms. Hence, this points to direct Solutol HS15 induced nuclear membrane permeabilisation.

(ii) Direct mechanism to increase nuclear membrane permeability

For Solutol HS15 to directly interact with, and incorporate into nuclear membranes, the surfactant must first gain intracellular access. This could possibly occur *via* cellular internalisation of the plasma membrane segments that contain incorporated surfactant.

Idone et al. reported a mechanism of injury-induced endocytosis (triggered in a Ca^{2+}-dependent manner) which involve internalisation of damaged plasma membrane 'portions' in order to remove pores caused by bacterial toxins or lesions caused by mechanical tears[146,147]. These endocytic vesicles are then sorted into lysosomes for degradation[148]. It may be possible that following delivery to lysosomes, accumulation of surfactant in this organelles membrane induces lysis. For

example, Triton X-100 exposure is demonstrated to lyse lysosomes, resulting in the release of lysosomal contents[149].

A possible way for surfactant molecules to escape the endosomal-lysosomal system may be by hijacking nucleocytoplasmic shuttling mechanisms[150,151]. The vesicles utilised in these intracellular transport mechanisms are derived from the endosomal membrane, thus surfactant molecules incorporated in this membrane could potentially be present in the vesicles formed, and in this manner surfactant molecules could be transported to the nucleus.

Studies have also revealed that plasma membrane injury resulting from pore-forming toxins or mechanical force can trigger caveolae internalisation[152]. Sphingomyelinase, a hydrolase that breaks down sphingomyelin into ceramide, has been observed to induce caveolin-mediated endocytosis of damage plasma membrane[147,152,153]. The presence of ceramide in the membrane is suggested to create membrane curvature and facilitate caveolin recruitment and membrane curvature[154]. The trafficking routes of internalised caveolae and their cargo remains unclear, however, sorting to cavesosomes, endosomal-like compartments has been decscribed[50,155]. From here, caveolae cargo has been reported to travel to distinct organelles such as the endoplasmic reticulum[156], or the Golgi complex[157].

As mentioned in section 3.1, non-ionic surfactant incorporation into the plasma membrane has been described to induce membrane internalisation driven by lipodic forces[103,111]. However the fractions of the membrane that are endocytosed are suggested to be predominately L_o regions and bind surfactant less efficiently than membrane remaining at the

surface[111], and consequently may possibly not facilitate surfactant entry intracellularly. This issue could also limit transport of surfactant intracellularly *via* caveolae endocytosis, owning to the fact caveolae themselves are highly ordered lipid raft regions of the membrane (as discussed in section 3.1).

Shuttling of plasma membrane-derived vesicles to the nucleus has been reported for mechanisms such as the internalisation of epidermal growth factor receptor (EGFR)[158,159]. The presence of surfactant in these endocytosed vesicles could result in direct transport to the nucleus without first being sorted to the endosomes or lysosomes, as is the case for internalisation of damage membrane segments[149]. This could increase the rate of nuclear membrane perturbation by surfactant.

Alternatively, a much less subtle and less complex mechanism of cell entry could be mediated *via* the loss of plasma membrane integrity; the absence of lipid bilayer in places may allow access through the cytoplasm and to the nuclear membrane.

As discussed above, the nuclear membrane was more resistant to surfactant induced perturbation than the plasma membrane. Loss of plasma membrane integrity alone does not appear to lead to increased nuclear membrane permeability, but instead this effect appears mediated by high Solutol HS15 concentrations. One explanation for this could be the requirement of excessive levels of surfactant to account for entrapment in the plasma membrane. Once the cell membrane is permeabilised, there must remain further, free surfactant to interact with the nuclear membrane. Taken together this suggests that with high surfactant concentrations (≥10 mM

Solutol HS15), the plasma membrane may be saturated with surfactant, and that the mechanism of surfactant entry may indeed be *via* membrane perforations (pores, lesions, ruptures etc).

3.5. Conclusions

Exposure of Caco-2 intestinal epithelial cells to model surfactant, Solutol HS15 results in plasma membrane and nuclear membrane perturbation in a concentration- and exposure time dependent manner.

The insertion of Solutol HS15 into cellular plasma membranes appears to occur within the first minute of exposure, as indicated by membrane fluidisation. Remarkably, the plasma membrane remains intact and resistant to increases in permeability initially. Interestingly, following the initial drop, levels of plasma membrane fluidisation remain relatively unchanged between 1 to 40 minutes in response to surfactant exposure. However, 'additional' fluidisation to the plasma membrane is observed after 40 minutes, and is associated with disruption to calcium homeostasis, increases in plasma membrane permeability to external FD-4 probe and the leakage of the intracellular LDH enzyme. It is thus suggested that this 'secondary' fluidisation of the plasma membrane mediates increases in membrane permeability, and possible indicates surfactant incorporation into the inner leaflet of the membrane bilayer. Alterations in nuclear permeability were more resistant than the plasma membrane; they were observed to occur later during surfactant exposure than plasma membrane effects, and with higher surfactant concentrations, suggesting a non-specific, subsequent membrane effect.

3.6. References

1. Singer, S. J. & Nicolson, G. L. The fluid mosaic model of the structure of cell membranes. *Science* **175,** 720–31 (1972).

2. Keren, K. Cell motility: The integrating role of the plasma membrane. *Eur. Biophys. J.* **40,** 1013–1027 (2011).

3. McMahon, H. T. & Gallop, J. L. Membrane curvature and mechanisms of dynamic cell membrane remodelling. *Nature* **438,** 590–596 (2005).

4. Dupuy, A. D. & Engelman, D. M. Protein area occupancy at the center of the red blood cell membrane. *Proc. Natl. Acad. Sci.* **105,** 2848–2852 (2008).

5. McLaughlin, S. & Murray, D. Plasma membrane phosphoinositide organization by protein electrostatics. *Nature* **438,** 605–611 (2005).

6. Sud, M. *et al.* LMSD: LIPID MAPS structure database. *Nucleic Acids Res.* **35,** (2007).

7. Róg, T., Pasenkiewicz-Gierula, M., Vattulainen, I. & Karttunen, M. Ordering effects of cholesterol and its analogues. *Biochimica et Biophysica Acta - Biomembranes* **1788,** 97–121 (2009).

8. Redondo-Morata, L., Giannotti, M. I. & Sanz, F. Influence of cholesterol on the phase transition of lipid bilayers: A temperature-controlled force spectroscopy study. *Langmuir* **28,** 12851–12860 (2012).

9. Huang, J. & Feigenson, G. W. A Microscopic Interaction Model of Maximum Solubility of Cholesterol in Lipid Bilayers. *Biophys. J.* **76,** 2142–2157 (1999).

10. Ali, M. R., Cheng, K. H. & Huang, J. Ceramide drives cholesterol out of the ordered lipid bilayer phase into the crystal phase in 1-palmitoyl-2-oleoyl-sn-glycero-3-phosphocholine/cholesterol/ ceramide ternary mixtures. *Biochemistry* **45,** 12629–12638 (2006).

11. van Meer, G., Voelker, D. R. & Feigenson, G. W. Membrane lipids: where they are and how they behave. *Nat. Rev. Mol. Cell Biol.* **9,** 112–124 (2008).

12. Canagarajah, B. J., Hummer, G., Prinz, W. A. & Hurley, J. H. Dynamics of Cholesterol Exchange in the Oxysterol Binding Protein Family. *J. Mol. Biol.* **378,** 737–748 (2008).

13. Fadok, V. A. *et al.* Exposure of phosphatidylserine on the surface of apoptotic lymphocytes triggers specific recognition and removal by macrophages. *J. Immunol.* **148,** 2207–16 (1992).

14. Nagata, S., Suzuki, J., Segawa, K. & Fujii, T. Exposure of phosphatidylserine on the cell surface. *Cell Death Differ.* **23,** 952–961 (2016).

15. Cebecauer, M., Spitaler, M., Sergé, A. & Magee, A. I. Signalling complexes and clusters: functional advantages and methodological hurdles. *J. Cell Sci.* **123,** 309–20 (2010).

16. Yu, J., Fischman, D. A. & Steck, T. L. Selective solubilization of proteins and phospholipids from red blood cell membranes by nonionic detergents. *J. Supramol. Struct.* **1,** 233–248 (1973).

17. Brown, D. A. & Rose, J. K. Sorting of GPI-anchored proteins to glycolipid-enriched membrane subdomains during transport to the apical cell surface. *Cell* **68,** 533–544 (1992).

18. Varma, R. & Mayor, S. GPI-anchored proteins are organized in submicron domains at the cell surface. *Nature* **394,** 798–801 (1998).

19. Brown, D. A. & London, E. Structure and origin of ordered lipid domains in biological membranes. *Journal of Membrane Biology* **164,** 103–114 (1998).

20. Simons, K. & Ikonen, E. Functional rafts in cell membranes. *Nature* **387,** 569–572 (1997).

21. Simons, K. & Vaz, W. L. C. Model systems, lipid rafts, and cell membranes. *Annu. Rev. Biophys. Biomol. Struct.* **33,** 269–295 (2004).

22. Hjort Ipsen, J., Karlström, G., Mourtisen, O. G., Wennerström, H. & Zuckermann, M. J. Phase equilibria in the phosphatidylcholine-cholesterol system. *BBA - Biomembr.* **905,** 162–172 (1987).

23. Kaiser, H.-J. *et al.* Order of lipid phases in model and plasma membranes. *Proc. Natl. Acad. Sci.* **106,** 16645–16650 (2009).

24. Veatch, S. L. & Keller, S. L. Separation of Liquid Phases in Giant Vesicles of Ternary Mixtures of Phospholipids and Cholesterol. *Biophys. J.* **85,** 3074–3083 (2003).

25. Sezgin, E. *et al.* Elucidating membrane structure and protein behavior using giant plasma membrane vesicles. *Nat. Protoc.* **7,** 1042–1051 (2012).

26. Bagatolli, L. A., Parasassi, T. & Gratton, E. Giant phospholipid vesicles: Comparison among the whole lipid sample characteristics using different preparation methods - A two photon fluorescence microscopy study. *Chem. Phys. Lipids* **105,** 135–147 (2000).

27. Levental, I., Grzybek, M. & Simons, K. Greasing their way: Lipid modifications determine protein association with membrane rafts. *Biochemistry* **49,** 6305–6316 (2010).

28. Raghupathy, R. *et al.* Transbilayer lipid interactions mediate nanoclustering of lipid-anchored proteins. *Cell* **161,** 581–594 (2015).

29. Lingwood, D. *et al.* Cholesterol modulates glycolipid conformation and receptor activity. *Nat. Chem. Biol.* **7,** 260–262 (2011).

30. Laganowsky, A. *et al.* Membrane proteins bind lipids selectively to modulate their structure and function. *Nature* **510,** 172–5 (2014).

31. Zhang, M. *et al.* CD45 signals outside of lipid rafts to promote ERK activation, synaptic raft clustering, and IL-2 production. *J. Immunol.* **174,** 1479–1490 (2005).

32. Filipp, D., Leung, B. L., Zhang, J., Veillette, A. & Julius, M. Enrichment

of lck in lipid rafts regulates colocalized fyn activation and the initiation of proximal signals through TCR alpha beta. *J. Immunol.* **172,** 4266–4274 (2004).

33. Vigh, L. *et al.* The significance of lipid composition for membrane activity: New concepts and ways of assessing function. *Progress in Lipid Research* **44,** 303–344 (2005).

34. Zhang, W., Trible, R. P. & Samelson, L. E. LAT palmitoylation: Its essential role in membrane microdomain targeting and tyrosine phosphorylation during T cell activation. *Immunity* **9,** 239–46 (1998).

35. Prior, I. A., Muncke, C., Parton, R. G. & Hancock, J. F. Direct visualization of ras proteins in spatially distinct cell surface microdomains. *J. Cell Biol.* **160,** 165–170 (2003).

36. Simons, K. & Toomre, D. Lipid rafts and signal transduction. *Nat Rev Mol Cell Biol* **1,** 31–39 (2000).

37. Harder, T. & Engelhardt, K. R. Membrane domains in lymphocytes - From lipid rafts to protein scaffolds. *Traffic* **5,** 265–275 (2004).

38. Schuck, S. Polarized sorting in epithelial cells: raft clustering and the biogenesis of the apical membrane. *J. Cell Sci.* **117,** 5955–5964 (2004).

39. Baumgart, T., Hess, S. T. & Webb, W. W. Imaging coexisting fluid domains in biomembrane models coupling curvature and line tension. *Nature* **425,** 821–824 (2003).

40. Lipowsky, R. Domains and rafts in membranes - Hidden dimensions of selforganization. in *Journal of Biological Physics* **28,** 195–210 (2002).

41. Lipowsky, R. Domain-induced budding of fluid membranes. *Biophys. J.* **64,** 1133–1138 (1993).

42. Huttner, W. B. & Zimmerberg, J. Implications of lipid microdomains for membrane curvature, budding and fission: Commentary. *Current Opinion in Cell Biology* **13,** 478–484 (2001).

43. Kreitzer, G., Marmorstein, A., Okamoto, P., Vallee, R. & Rodriguez-Boulan, E. Kinesin and dynamin are required for post-Golgi transport of a plasma-membrane protein. *Nat. Cell Biol.* **2,** 125–127 (2000).

44. Rothberg, K. G. *et al.* Caveolin, a protein component of caveolae membrane coats. *Cell* **68,** 673–682 (1992).

45. Murata, M. *et al.* VIP21/caveolin is a cholesterol-binding protein (membrane microdomains/intracellular transport/membrane reconstitution). *Cell Biol.* **92,** 10339–10343 (1995).

46. Severs, N. J. Caveolae: static inpocketings of the plasma membrane, dynamic vesicles or plain artifact? *J Cell Sci* **90 (Pt 3),** 341–348 (1988).

47. Anderson, R. G. W. Plasmalemmal caveolae and GPI-anchored membrane proteins. *Curr. Opin. Cell Biol.* **5,** 647–652 (1993).

48. Örtegren, U. *et al.* Lipids and glycosphingolipids in caveolae and

surrounding plasma membrane of primary rat adipocytes. *Eur. J. Biochem.* **271,** 2028–2036 (2004).

49. Way, M. & Parton, R. G. M-caveolin, a muscle-specific caveolin-related protein. *FEBS Lett.* **378,** 108–112 (1996).

50. Parton, R. G. & Simons, K. The multiple faces of caveolae. *Nat. Rev. Mol. Cell Biol.* **8,** 185–94 (2007).

51. Drab, M. Loss of Caveolae, Vascular Dysfunction, and Pulmonary Defects in Caveolin-1 Gene-Disrupted Mice. *Science (80-.).* **293,** 2449–2452 (2001).

52. Galbiati, F. *et al.* Caveolin-3 Null Mice Show a Loss of Caveolae, Changes in the Microdomain Distribution of the Dystrophin-Glycoprotein Complex, and T-tubule Abnormalities. *J. Biol. Chem.* **276,** 21425–21433 (2001).

53. Travis, J. Cell biologists explore `Tiny Caves'. *Science (80-.).* **262,** 1208–1209 (1993).

54. Lisanti, M. P. *et al.* Caveolae, transmembrane signalling and cellular transformation. *Mol. Membr. Biol.* **12,** 121–124 (1995).

55. Kurzchalia, T. V. & Parton, R. G. Membrane microdomains and caveolae. *Current Opinion in Cell Biology* **11,** 424–431 (1999).

56. Williams, T. M. & Lisanti, M. P. Caveolin-1 in oncogenic transformation, cancer, and metastasis. *Am. J. Physiol. Cell Physiol.* **288,** C494-506 (2005).

57. STROSBERG, A. D. Structure/function relationship of proteins belonging to the family of receptors coupled to GTP-binding proteins. *European Journal of Biochemistry* **196,** 1–10 (1991).

58. Wagner, R. C., Kreinert, P., Barrnett, R. J. & Bitenskyt, M. W. Biochemical Characterization and Cytochemical Localization of a. **69,** 3175–3179 (1972).

59. Fujimoto, T., Nakade, S., Miyawaki, A., Mikoshiba, K. & Ogawa, K. Localization of inositol 1,4,5-trisphosphate receptor-like protein in plasmalemmal caveolae. *J. Cell Biol.* **119,** 1507–1513 (1992).

60. Wenk, M. R., Alt, T., Seelig, A. & Seelig, J. Octyl-beta-D-glucopyranoside partitioning into lipid bilayers: thermodynamics of binding and structural changes of the bilayer. *Biophys. J.* **72,** 1719–1731 (1997).

61. Almog, S. *et al.* States of Aggregation and Phase Transformations in Mixtures of Phosphatidylcholine and Octyl Glucoside. *Biochemistry* **29,** 4582–4592 (1990).

62. Shubber, S. The evaluation of Solutol HS15 as a mucosal absorption enhancer. (University of Nottingham, 2015).

63. Shinichiro, H., Takatsuka, Y. & Hiroyuki, M. Mechanisms for the enhancement of the nasal absorption of insulin by surfactants. *Int. J. Pharm.* **9,** 173–184 (1981).

64. Liu, D. Z., Lecluyse, E. L. & Thakker, D. R. Dodecylphosphocholine-

mediated enhancement of paracellular permeability and cytotoxicity in Caco-2 cell monolayers. *J. Pharm. Sci.* **88,** 1161–1168 (1999).

65. Vllasaliu, D. *et al.* Epithelial toxicity of alkylglycoside surfactants. *J. Pharm. Sci.* **102,** 114–125 (2013).

66. Ahsan, F. *et al.* Effects of the permeability enhancers, tetradecylmaltoside and dimethyl-beta-cyclodextrin, on insulin movement across human bronchial epithelial cells (16HBE14o-). *Eur. J. Pharm. Sci.* **20,** 27–34 (2003).

67. Petersen, S. B. *et al.* Evaluation of alkylmaltosides as intestinal permeation enhancers: Comparison between rat intestinal mucosal sheets and Caco-2 monolayers. *Eur. J. Pharm. Sci.* **47,** 701–712 (2012).

68. Lariccia, V. *et al.* Massive calcium-activated endocytosis without involvement of classical endocytic proteins. *J. Gen. Physiol.* **137,** 111–132 (2011).

69. Rege, B. D., Yu Lawrence, X., Hussain, A. S. & Polli, J. E. Effect of common excipients on Caco-2 transport of low-permeability drugs. *J. Pharm. Sci.* **90,** 1776–1786 (2001).

70. Koga, K., Ohyashiki, T., Murakami, M. & Kawashima, S. Modification of ceftibuten transport by the addition of non-ionic surfactants. *Eur. J. Pharm. Biopharm.* **49,** 17–25 (2000).

71. Nerurkar, M. M., Burton, P. S. & Borchardt, R. T. The use of surfactants to enhance the permeability of peptides through caco-2 cells by inhibition of an apically polarized efflux system. *Pharm. Res.* **13,** 528–534 (1996).

72. Shubber, S. *et al.* Mechanism of Mucosal Permeability Enhancement of CriticalSorb® (Solutol® HS15) Investigated In Vitro in Cell Cultures. *Pharm. Res.* **32,** 516–527 (2014).

73. Lavie, Y., Fiucci, G. & Liscovitch, M. Up-regulation of caveolae and caveolar constituents in multidrug- resistant cancer cells. *J. Biol. Chem.* **273,** 32380–32383 (1998).

74. Rege, B. D., Kao, J. P. Y. & Polli, J. E. Effects of nonionic surfactants on membrane transporters in Caco-2 cell monolayers. *Eur. J. Pharm. Sci.* **16,** 237–246 (2002).

75. Hanke, U. *et al.* Commonly used nonionic surfactants interact differently with the human efflux transporters ABCB1 (p-glycoprotein) and ABCC2 (MRP2). *Eur. J. Pharm. Biopharm.* **76,** 260–268 (2010).

76. Zhang, H., Yao, M., Morrison, R. A. & Chong, S. Commonly used surfactant, Tween 80, improves absorption of P-glycoprotein substrate, digoxin, in rats. *Arch. Pharm. Res.* **26,** 768–772 (2003).

77. Bogman, K., Erne-Brand, F., Alsenz, J. & Drewe, J. The role of surfactants in the reversal of active transport mediated by multidrug resistance proteins. *J. Pharm. Sci.* **92,** 1250–1261 (2003).

78. Koga, K., Murakami, M. & Kawashima, S. Effects of fatty acid sucrose esters on ceftibuten transport by rat intestinal brush-border

membrane vesicles. *Biol. Pharm. Bull.* **21,** 747–51 (1998).

79. Koga, K., Murakami, M. & Kawashima, S. Modification of ceftibuten transport by changes in lipid fluidity caused by fatty acid glycerol esters. *Biol. Pharm. Bull.* **22,** 103–6 (1999).

80. Koga, K., Murakami, M. & Kawashima, S. Effects of fatty acid glycerol esters on intestinal absorptive and secretory transport of ceftibuten. *Biol.Pharm.Bull.* **22,** 402–406 (1999).

81. Zhao, F. K., Chuang, L. F., Israel, M. & Chuang, R. Y. Cremophor EL, a widely used parenteral vehicle, is a potent inhibitor of protein kinase C. *Biochem. Biophys. Res. Commun.* **159,** 1359–1367 (1989).

82. Ali, E. S. *et al.* The glucagon-like peptide-1 analogue exendin-4 reverses impaired intracellular Ca2 + signalling in steatotic hepatocytes. *Biochim. Biophys. Acta - Mol. Cell Res.* **1863,** 2135–2146 (2016).

83. Spitaler, M. & Cantrell, D. a. Protein kinase C and beyond. *Nat. Immunol.* **2,** 24 (2004).

84. Dudeja, P. K., Anderson, K. M., Harris, J. S., Buckingham, L. & Coon, J. S. Reversal of multidrug resistance phenotype by surfactants: relationship to membrane lipid fluidity. *Arch Biochem Biophys.* **319,** 309–15 (1995).

85. Woodcock, D. M. *et al.* Reversal of multidrug resistance by surfactants. *Br J Cancer* **66,** 62–8 (1992).

86. Javed, M. H., Azimuddin, S. M., Hussain, A. N., Ahmed, A. & Ishaq, M. Purification and characterization of lactate dehydrogenase from Varanus liver. *Exp. Mol. Med.* **29,** 25–30 (1997).

87. Vaslin, A., Puyal, J., Borsello, T. & Clarke, P. G. H. Excitotoxicity-related endocytosis in cortical neurons. *J. Neurochem.* **102,** 789–800 (2007).

88. Navone, S. E. *et al.* Isolation and expansion of human and mouse brain microvascular endothelial cells. *Nat. Protoc.* **8,** 1680–1693 (2013).

89. Commisso, C., Flinn, R. J. & Bar-Sagi, D. Determining the macropinocytic index of cells through a quantitative image-based assay. *Nat. Protoc.* **9,** 182–192 (2014).

90. Falcone, S. *et al.* Macropinocytosis: regulated coordination of endocytic and exocytic membrane traffic events. *J. Cell Sci.* **119,** 4758–4769 (2006).

91. Nakase, I. *et al.* Cell-surface accumulation of flock house virus-derived peptide leads to efficient internalization via macropinocytosis. *Mol. Ther.* **17,** 1868–1876 (2009).

92. Bentley, D. C., Pulbutr, P., Chan, S. & Smith, P. A. Etiology of the membrane potential of rat white fat adipocytes. *AJP Endocrinol. Metab.* **307,** E161–E175 (2014).

93. Parasassi, T., De Stasio, G., Ravagnan, G., Rusch, R. M. & Gratton, E. Quantitation of lipid phases in phospholipid vesicles by the

generalized polarization of Laurdan fluorescence. *Biophys. J.* **60,** 179–189 (1991).

94. Sanchez, S. A., Tricerri, M. A., Gunther, G. & Gratton, E. Laurdan Generalized Polarization: from cuvette to microscope. *Mod. Res. Educ. Top. Microsc.* **2,** 1007–1014 (2007).

95. Scheinpflug, K. *et al.* Antimicrobial peptide cWFW kills by combining lipid phase separation with autolysis. *Sci. Rep.* **7,** 44332 (2017).

96. Mark C. Willingham. in *Methods in molecular biology (Clifton, N.J.)* 153–164 (2009).

97. Verstraeten, S. V., Jaggers, G. K., Fraga, C. G. & Oteiza, P. I. Procyanidins can interact with Caco-2 cell membrane lipid rafts: Involvement of cholesterol. *Biochim. Biophys. Acta - Biomembr.* **1828,** 2646–2653 (2013).

98. Becerra, N., De La Nuez, L. R., Zanocco, A. L., Lemp, E. & Günther, G. Solubilization of dodac small unilamellar vesicles by sucrose esters: A fluorescence study. *Colloids Surfaces A Physicochem. Eng. Asp.* **272,** 2–7 (2006).

99. Paternostre, M. *et al.* Partition coefficient of a surfactant between aggregates and solution: application to the micelle-vesicle transition of egg phosphatidylcholine and octyl beta-D-glucopyranoside. *Biophys. J.* **69,** 2476–2488 (1995).

100. Heerklotz, H., Binder, H. & Lantzsch, G. Determination of the partition coefficients of the nonionic detergent C12E7 between lipid-detergent mixed membranes and water by means of Laurdan fluorescence spectroscopy. *J. Fluoresc.* **4,** 349–352 (1994).

101. Balogh, G. *et al.* The hyperfluidization of mammalian cell membranes acts as a signal to initiate the heat shock protein response. *FEBS J.* **272,** 6077–6086 (2005).

102. Shigapova, N. *et al.* Membrane fluidization triggers membrane remodeling which affects the thermotolerance in Escherichia coli. *Biochem. Biophys. Res. Commun.* **328,** 1216–1223 (2005).

103. Fine, M. *et al.* Massive endocytosis driven by lipidic forces originating in the outer plasmalemmal monolayer: a new approach to membrane recycling and lipid domains. *J. Gen. Physiol.* **137,** 137–154 (2011).

104. Brayden, D. J., Bzik, V. a, Lewis, a L. & Illum, L. CriticalSorb™ promotes permeation of flux markers across isolated rat intestinal mucosae and Caco-2 monolayers. *Pharm. Res.* **29,** 2543–54 (2012).

105. Preté, P. S. C. *et al.* Multiple stages of detergent-erythrocyte membrane interaction-A spin label study. *Biochim. Biophys. Acta - Biomembr.* **1808,** 164–170 (2011).

106. Lichtenberg, D., Ahyayauch, H. & Goñi, F. M. The mechanism of detergent solubilization of lipid bilayers. *Biophys. J.* **105,** 289–299 (2013).

107. Som, I., Bhatia, K. & Yasir, M. Status of surfactants as penetration enhancers in transdermal drug delivery. *Journal of Pharmacy and*

Bioallied Sciences **4,** 2 (2012).

108. Heerklotz, H. Membrane stress and permeabilization induced by asymmetric incorporation of compounds. *Biophys. J.* **81,** 184–195 (2001).

109. Lafleur, M. *et al.* Correlation between lipid plane curvature and lipid chain order. *Biophys. J.* **70,** 2747–2757 (1996).

110. Kragh-Hansen, U., le Maire, M. & Møller, J. V. The Mechanism of Detergent Solubilization of Liposomes and Protein-Containing Membranes. *Biophys. J.* **75,** 2932–2946 (1998).

111. Hilgemann, D. W. & Fine, M. Mechanistic analysis of massive endocytosis in relation to functionally defined surface membrane domains. *J. Gen. Physiol.* **137,** 155–72 (2011).

112. Heerklotz, H. Interactions of surfactants with lipid membranes. *Q. Rev. Biophys.* **41,** 205 (2008).

113. Dimitrijevic, D., Shaw, A. J. & Florence, A. T. Effects of some non-ionic surfactants on transepithelial permeability in Caco-2 cells. *J. Pharm. Pharmacol.* **52,** 157–162 (2000).

114. Heerklotz, H. H., Binder, H. & Epand, R. M. A 'release' protocol for isothermal titration calorimetry. *Biophysj* **76,** 2606–2613 (1999).

115. Heerklotz, H., Szadkowska, H., Anderson, T. & Seelig, J. The sensitivity of lipid domains to small perturbations demonstrated by the effect of triton. *J. Mol. Biol.* **329,** 793–799 (2003).

116. Tsvetkova, N. M. *et al.* Small heat-shock proteins regulate membrane lipid polymorphism. *Proc Natl Acad Sci U S A* **99,** 13504–13509 (2002).

117. Horváth, I., Multhoff, G., Sonnleitner, A. & Vígh, L. Membrane-associated stress proteins: More than simply chaperones. *Biochimica et Biophysica Acta - Biomembranes* **1778,** 1653–1664 (2008).

118. Karatekin, E., Sandre, O. & Brochard-Wyart, F. Transient pores in vesicles. *Polym. Int.* **52,** 486–493 (2003).

119. Groot, R. D. & Rabone, K. L. Mesoscopic simulation of cell membrane damage, morphology change and rupture by nonionic surfactants. *Biophys. J.* **81,** 725–736 (2001).

120. Berridge, M. J., Bootman, M. D. & Roderick, H. L. Calcium signalling: dynamics, homeostasis and remodelling. *Nat. Rev. Mol. Cell Biol.* **4,** 517–29 (2003).

121. Carafoli, E., Santella, L., Branca, D. & Brini, M. Generation, control, and processing of cellular calcium signals. *Crit Rev Biochem Mol Biol* **36,** 107–260 (2001).

122. Orrenius, S., Zhivotovsky, B. & Nicotera, P. Regulation of cell death: the calcium-apoptosis link. *Nat. Rev. Mol. Cell Biol.* **4,** 552–565 (2003).

123. Steinhardt, R. A., Bi, G. & Alderton, J. M. Cell membrane resealing by a vesicular mechanism similar to neurotransmitter release. *Science*

263, 390–3 (1994).

124. Cheng, X., Zhang, X., Yu, L. & Xu, H. Calcium signaling in membrane repair. *Seminars in Cell and Developmental Biology* **45,** 24–31 (2015).

125. Terasaki, M., Miyake, K. & McNeil, P. L. Large plasma membrane disruptions are rapidly resealed by Ca2+- dependent vesicle-vesicle fusion events. *J. Cell Biol.* **139,** 63–74 (1997).

126. Xu, S. *et al.* Palmitate induces ER calcium depletion and apoptosis in mouse podocytes subsequent to mitochondrial oxidative stress. *Cell Death Dis* **6,** e1976 (2015).

127. Harr, M. W. & Distelhorst, C. W. Apoptosis and autophagy: decoding calcium signals that mediate life or death. *Cold Spring Harbor perspectives in biology* **2,** (2010).

128. Yamaguchi, J. Y. *et al.* Cremophor EL, a non-ionic surfactant, promotes Ca2+-dependent process of cell death in rat thymocytes. *Toxicology* **211,** 179–186 (2005).

129. Sambuy, Y. *et al.* The Caco-2 cell line as a model of the intestinal barrier: Influence of cell and culture-related factors on Caco-2 cell functional characteristics. *Cell Biol. Toxicol.* **21,** 1–26 (2005).

130. Woodcook, S., Williamson, I., Hassan, I. & Mackay, M. Isolation and characterisation of clones from the Caco-2 cell line displaying increased taurocholic acid transport. *J. Cell Sci.* **98 (Pt 3),** 323–32 (1991).

131. Morandat, S. & El Kirat, K. Membrane resistance to triton X-100 explored by real-time atomic force microscopy. *Langmuir* **22,** 5786–5791 (2006).

132. Nyholm, T. & Slotte, J. P. Comparison of Triton X-100 penetration into phosphatidylcholine and sphingomyelin mono- and bilayers. *Langmuir* **17,** 4724–4730 (2001).

133. Dahl, K. N., Kahn, S. M., Wilson, K. L. & Discher, D. E. The nuclear envelope lamina network has elasticity and a compressibility limit suggestive of a molecular shock absorber. *J. Cell Sci.* **117,** 4779–4786 (2004).

134. Lammerding, J. *et al.* Lamin A / C deficiency causes Tema Grupo defective nuclear mechanics and mechanotransduction. *J. Clin. Invest.* **113,** 370–378 (2004).

135. Beck, M., Lucić, V., Förster, F., Baumeister, W. & Medalia, O. Snapshots of nuclear pore complexes in action captured by cryo-electron tomography. *Nature* **449,** 611–615 (2007).

136. Heessen, S. & Fornerod, M. The inner nuclear envelope as a transcription factor resting place. *EMBO Rep.* **8,** 914–919 (2007).

137. Reddy, K. L., Zullo, J. M., Bertolino, E. & Singh, H. Transcriptional repression mediated by repositioning of genes to the nuclear lamina. *Nature* **452,** 243–7 (2008).

138. Fridkin, A., Penkner, A., Jantsch, V. & Gruenbaum, Y. SUN-domain

and KASH-domain proteins during development, meiosis and disease. *Cellular and Molecular Life Sciences* **66,** 1518–1533 (2009).

139. Burke, B. & Stewart, C. L. Functional architecture of the cell's nucleus in development, aging, and disease. *Curr. Top. Dev. Biol.* **109,** 1–52 (2014).

140. Hatch, E. M., Fischer, A. H., Deerinck, T. J. & Hetzer, M. W. Catastrophic Nuclear Envelope Collapse in Cancer Cell Micronuclei. *Cell* **154,** (2013).

141. Hatch, E. M. & Hetzer, M. W. Nuclear envelope rupture is induced by actin-based nucleus confinement. *J. Cell Biol.* **215,** (2016).

142. Denais, C. M. *et al.* Nuclear envelope rupture and repair during cancer cell migration. *Science (80-.).* **352,** 353–358 (2016).

143. Grandinetti, G., Smith, A. E. & Reineke, T. M. Membrane and nuclear permeabilization by polymeric pdna vehicles: Efficient method for gene delivery or mechanism of cytotoxicity? *Mol. Pharm.* **9,** 523–538 (2012).

144. Nagata, S. Apoptotic DNA fragmentation. *Exp. Cell Res.* **256,** 12–8 (2000).

145. Collins, J. A., Schandl, C. A., Young, K. K., Vesely, J. & Willingham, M. C. Major DNA Fragmentation Is a Late Event in Apoptosis. *J. Histochem. Cytochem.* **45,** 923–934 (1997).

146. Idone, V. *et al.* Repair of injured plasma membrane by rapid Ca2+ dependent endocytosis. *J. Cell Biol.* **180,** 905–914 (2008).

147. Tam, C. *et al.* Exocytosis of acid sphingomyelinase by wounded cells promotes endocytosis and plasma membrane repair. *J. Cell Biol.* **189,** 1027–1038 (2010).

148. Corrotte, M., Fernandes, M. C., Tam, C. & Andrews, N. W. Toxin Pores Endocytosed During Plasma Membrane Repair Traffic into the Lumen of MVBs for Degradation. *Traffic* **13,** 483–494 (2012).

149. Kågedal, K. *et al.* Lysosomal membrane permeabilization during apoptosis--involvement of Bax? *Int. J. Exp. Pathol.* **86,** 309–21 (2005).

150. Benmerah, A. Endocytosis: Signaling from endocytic membranes to the nucleus. *Current Biology* **14,** (2004).

151. Giri, D. K. *et al.* Endosomal transport of ErbB-2: mechanism for nuclear entry of the cell surface receptor. *Mol. Cell. Biol.* **25,** 11005–11018 (2005).

152. Corrotte, M. *et al.* Caveolae internalization repairs wounded cells and muscle fibers. *Elife* **2013,** (2013).

153. Xu, M. *et al.* Requirement of translocated lysosomal V1 H+-ATPase for activation of membrane acid sphingomyelinase and raft clustering in coronary endothelial cells. *Mol. Biol. Cell* **23,** 1546–1557 (2012).

154. Andrews, N. W., Almeida, P. E. & Corrotte, M. Damage control: Cellular mechanisms of plasma membrane repair. *Trends in Cell*

Biology **24,** 734–742 (2014).

155. Nichols, B. J. A distinct class of endosome mediates clathrin-independent endocytosis to the Golgi complex. *Nat. Cell Biol.* **4,** 374–8 (2002).

156. Pelkmans, L., Kartenbeck, J. & Helenius, a. Caveolar endocytosis of simian virus 40 reveals a new two-step vesicular-transport pathway to the ER. *Nat. Cell Biol.* **3,** 473–483 (2001).

157. Richards, A. A., Stang, E., Pepperkok, R. & Parton, R. G. Inhibitors of COP-mediated Transport and Cholera Toxin Action Inhibit Simian Virus 40 Infection. *Mol. Biol. Cell* **13,** 1750–1764 (2002).

158. David, M. *et al.* STAT activation by epidermal growth factor (EGF) and amphiregulin: Requirement for the EGF receptor kinase but not for tyrosine phosphorylation sites or JAK1. *J. Biol. Chem.* **271,** 9185–9188 (1996).

159. Lin, S. Y. *et al.* Nuclear localization of EGF receptor and its potential new role as a transcription factor. *Nat. Cell Biol.* **3,** 802–808 (2001).

4. Chapter Four – Mitochondria associated effects on intestinal epithelia

Summary

This chapter investigates how Solutol HS15 affects Caco-2 mitochondrial-associated parameters including metabolic activity, evaluated using cellular reduction of MTS and PrestoBlue salts, mitochondrial membrane potential, using JC-1 and MitoTracker dyes, and levels of intracellular reactive oxygen species (ROS) by employing a H2DCFDA derived probe.

Results illustrate that upon application of surfactant, Caco-2 cells present a range of time-dependent mitochondrial effects. Within 5-20 minutes of exposure, a metabolic burst, mitochondrial membrane hyperpolarisation, and oxidative stress are detected. These parameters then return to baseline levels between 20-60 minutes, followed later, after 60 minutes of exposure, by the progressive decline in mitochondrial processes, including mitochondrial membrane potential depolarisation and loss of metabolic activity.

Together, the succession of events unfolding suggest a co-ordinated cellular response when exposed to ≥10 mM Solutol HS15; beginning with what is likely redox signalling accompanied by a survival response and succeeded by effects associated with cytotoxicity and cell death.

4.1. Introduction

The work in this chapter sets out to investigate the biological effects of Solutol HS15, specifically the metabolic effects on cells in culture.

The metabolism of a cell is a complex network of interconnected chemical reactions that enable both the breakdown and synthesis of molecules. These metabolic pathways are in delicate balance, they require a tight control on calcium ion homeostasis[1], and many of them are dependent on an array of transmembrane processes[2,3]. Thus, recognising that Solutol HS15 is capable of inducing plasma and nuclear membrane perturbations (Figures 3.5 and 3.10, respectively), one must evaluate if, and which, intracellular processes may be affected as a consequence.

Without doubt, the most important intracellular process is the synthesis of bioenergetic molecules, such as adenosine triphosphate (ATP) molecules – the main chemical energy source for a multitude of cellular processes and activities. The majority of processes/reactions occurring within cells are energetically unfavourable and may only be achieved by the expenditure of energy. The generation, and utilisation of metabolic energy is therefore fundamental for cell function and survival, and any disruption to these processes will be catastrophic[4–6].

The main source of cellular energy is derived from the breakdown of glucose and other carbohydrates in a series of controlled oxidative reactions. These reactions use reduced coenzymes, such as nicotinamide adenine dinucleotide (NADH) to generate chemical energy in the form of ATP. There are three fundamental sets of metabolic reactions that act in succession

to achieve this. These are glycolysis (occurring in the cytosol), the Krebs cycle (occurring in the matrix of mitochondria) and oxidative phosphorylation (the electron transfer chain occurring across the inner mitochondria membrane). The majority of energy production thus occurs in mitochondria, with an estimated 95% of ATP production generated here[7].

Activity of these bioenergetic processes can be evaluated experimentally by measuring various parameters. For example glycolysis can be assessed by measuring glucose consumption[8] and the Krebs cycle *via* production of NADH molecules[9]. Oxidative phosphorylation can be assessed either directly by measuring ATP synthesis or, indirectly by monitoring the mitochondrial membrane potential ($\Delta\Psi_m$).

The $\Delta\Psi_m$ is maintained by cells actively undertaking oxidative phosphorylation (OXPHOS). OXPHOS is initiated by the oxidation of NADH (or flavin adenine dinucleotide; $FADH_2$) from the Krebs cycle at complex I and is followed by a succession of redox reactions that transfer electrons from donors to acceptors (Figure 4.). These redox reactions occur in a series of complexes (complex I-IV) and are coupled to the efflux of protons across this membrane. These complexes are collectively known as the electron transport chain (ETC), they are located within the inner mitochondrial membrane, and are responsible for driving the electrochemical gradient that is the $\Delta\Psi_m$. The cell then couples influx of protons *via* this gradient to the production of ATP through the ion motor known as ATP synthase (Figure 4.).

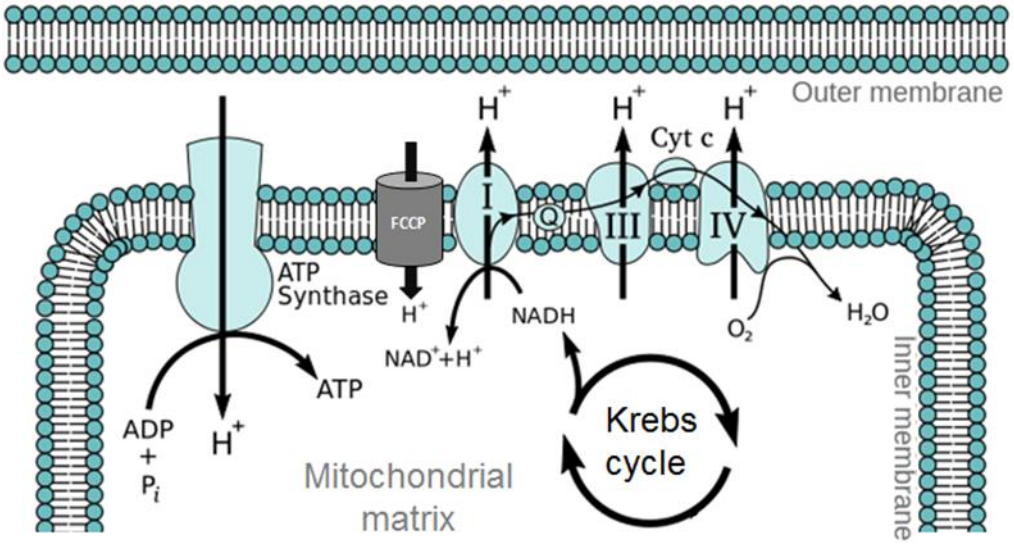

Figure 4.1. Schematic diagram of mitochondrial electron transport chain. NADH generated from the Krebs cycle is oxidised providing energy for ATP synthase. FCCP is shown to illustrate its ability to act as a protonophore across inner membrane of the mitochondrion. Complexes I, III and IV, are labelled as I, II and IV; Cyto C, Cytochrome C; Q, coenzyme Q (ubiquinone). Image modified from[10].

Damage to components of these mitochondrial processes normally leads to impaired function and can ultimately induce cell death[11,12]. Indeed, much of what is known about mitochondrial function arises from studying mitochondrial toxins, such as uncoupling agents and ionophores[13]. These compounds are typically small, amphipathic and increase the ionic permeability of phospholipid bilayers.

Uncoupling agents, such as carbonyl cyanide-4-phenylhydrazone (FCCP), abolish the linkage, or coupling, of the ETC with ADP phosphorylation (ATP production)[14]. FCCP does so by incorporating into the inner mitochondrial membrane and acting as a protonophore, allowing the influx of protons (H^+) and dissipating the proton gradient responsible for $\Delta\Psi_m$ (Figure 4.)[15]. Such action abolishes ATP generation *via* the ATP synthase pump which relies on the presence of a maintained $\Delta\Psi_m$.

Valinomycin, on the other hand, is an example of an ionphore that catalyses the movement of potassium ions across phospholipid bilayers. Valinomycin does not act as a pore, but rather a mobile carrier[16], diffusing backwards and forwards across membranes, such as the inner mitochondrial membrane, and in so doing destroys any established electrochemical gradient.

Additionally, other compounds are capable of inhibiting the function of ETC complexes. These respiratory chain inhibitors, as they are known, bind to components of the ETC and block their abilities to perform redox reactions[11]. This prevents the flow of electrons and in turn abolishes maintenance of the $\Delta\Psi_m$. Cyanide is a classical example, and binds to cytochrome c oxidase (complex IV) of the ETC[17]. Doing so prevents electrons being released to oxygen molecules, and consequently shuts down the ETC.

Other mechanisms of mitochondrial toxicity include the inhibition of ADP phosphorylation, thus directly preventing ATP generation. Oligomycin is the classical example; it inhibits ATP synthase by blocking the Fo subunit which acts as the proton channel[18].

In addition to cytotoxic compounds directly damaging mitochondrial components, mitochondrial (and cell) damage can be caused indirectly by excessive levels of reactive oxygen species (ROS). ROS are a collection of chemically reactive molecules that have roles in cell signalling and homeostasis[19]. These molecules are O_2-derived free radicals such as hydroxyl radicals (HO●), superoxide anions ($O_2^{\bullet-}$), alkoyl (RO●) and peroxyl (RO_2●), and the non-radical hydrogen peroxide species (H_2O_2)[20].

There are a variety of sources of ROS generation, both endogenous and exogenous. The main source of intracellular ROS generation is as a byproduct of normal metabolism (OXPHOS) occurring in mitochondria. It is estimated that 1-2% of total O_2 consumed in mitochondria is involved in the production of ROS, predominately *via* complex I (NADH ubiquinone oxidoreductase) and complex III[21,22]. Additionally, plasma membrane bound enzymes such as NADPH oxidase (NOX) transfer electrons across biological membranes and are examples of non-mitochondria ROS sources[23].

Further to physiological roles in signalling, generation of excessive ROS can result in response to stressors such as disease, radiation damage and exposure to toxicants[24–26]. This can lead to local oxidative stress and cell damage if cellular anti-oxidant defence mechanisms are overwhelmed[27]. ROS induced damage occurs as a consequence of substantial modification of intracellular targets such as lipids, DNA and proteins – all of which can impact cell survival. In fact, cytotoxic ROS levels have been observed to induce diverse cell death pathways including apoptosis[28], autophagy[29] and even necrosis[30].

The work in this chapter investigates the metabolic effects induced by Solutol HS15 and their kinetics by studying a range of mitochondrial-associated parameters *versus* time including metabolic activity (reductive activity of NADH-dependent enzymes), the assessment of $\Delta\Psi_m$, and oxidative stress (general ROS levels).

4.2. Methodology

4.2.1. Assessment of Metabolic activity

As described above in section 4.1 generation of cellular energy involves a complex series of redox reactions. Measuring the reductive environment of cells provides an indirect measure of these activities. There are a variety of cell-based assays that are used to determine metabolic activity in this manner and they include tetrazolium reduction and resazurin reduction.

Tetrazolium salts such as MTT, MTS and WST-1 are reduced by NAHD-mediated processes to a formazan salt; this produces a colourmetric change from pale yellow to a dark blue/purple which can be assessed. Although various metabolites and cofactors (such as glutathione and succinate) are potential electron donors driving these reduction reactions, NADH and NADPH are the most efficient[31]. Thus, cellular reduction of tetrazolium salts is related to the intracellular concentration of NAD(P)H. When applied with an intermediate electron acceptor (IEA), such as PMS (found in the MTS reagent), the MTS salt can be reduced in the absence of enzymes by NAD(P)H, albeit at a slower rate than enzymatically[32]. It is believed that MTT and MTS are able to enter into cells and are reduced intracellularly by NADH-dependent enzymes[33]. Mitochondrial[34], as well as endoplastic reticulum[34,35] and cytosolic-associated[34,36] oxidoreductases are most commonly associated with reducing tetrazolium dyes. However, various other cellular oxidases, dehydrogenases and peroxidases have demonstrated some capability to perform these reductions[33].

Assays such as AlamarBlue and PrestoBlue are based on resazurin salts, which transform from blue in colour to highly fluorescent, pink resorufin. These salts are cell permeable and

are reduced in the cytoplasm by NADH-dependent enzymes[37]. Resazurin dyes do not appear to be reduced in the mitochondrial, but instead in the cell cytoplasm, and to some extent in nuclei[37]. Diaphorases such as, dihydrolipoamine-dehydrogenase[38] and quionone oxidoreductase[39] have been identified as the enzymes most likely responsible for resazurin reduction[40], however others including NADH dehydrogenase could also utilise resazurins as acceptors of electrons.

4.2.1.1. MTS reduction assay

The MTS reagent (CellTiter 96® AQueous One Solution Cell Proliferation Assay) was stored at - 20ºC until required. The entire bottle of stock was thawed in a water bath at 37ºC –*this reagent does not suffer from issues arising from repeated freeze-thawing*[41]. Since MTS is light sensitive, all MTS containing solutions were protected from light by the use of aluminium foil on all containers and plates.

To prepare a working solution of MTS, the MTS stock was diluted in complete EMEM (without antibiotics) to a concentration of 17% (v/v) MTS:EMEM. The resulting solution was then vortexed to ensure homogeneity and warmed to 37ºC in a water bath prior to application. Antibiotics were excluded to minimise the potential of additional cytotoxicity relating to drug-drug interactions (e.g. the effect of penicillin/streptomycin on Solutol-treated cells).

The MTS assay was performed on cells culture in 96 well plates (clear) and treated with Solutol in manners described in section 2.2.4 and section 2.2.6, respectively. Triton X-100 (1%) applied in 1% HEPES:HBSS was used as the positive control to

induce total abolishment of metabolic activity *via* rapid cell permeabilisation (*c.f* section 3.2.1; Figure 3.1).

Once the exposure period had elapsed, cell treatments were gently aspirated off cells and the wells were then washed twice with PBS to remove any excess. Wells were then replaced with 120 µl 17% (v/v) MTS:EMEM, and incubated for a total of 120 minutes in an incubator at 37°C with 5% CO_2. Following incubation with the MTS solution absorbance of the wells was read immediately at 492 nm. Relative metabolic activity was then determine with regard to the vehicle control (1% HEPES:HBSS) taken as 100%. Cells treated with the positive control (1% Triton X-100) were set to 0% relative metabolic activity (Equation 4).

$$Relative\ Metabolic\ Activity = \left(\frac{x - Positive\ control}{Negative\ control - Positive\ control}\right) \times 100$$

Equation 4 Calculation of relative metabolic activity. Values used represent absorbance at 492 nm for the MTS assay and for the PrestoBlue assay fluorescence signal following excitation at 530 nm and emission at 590 nm. X = sample absorbance/fluorescent signal value.

4.2.1.2. PrestoBlue reduction assay

PrestoBlue (PrestoBlue® Cell Viability Reagent) stock was stored at 4ºC until use and protected from light. PrestoBlue working solutions were made up on the day of assaying and prepared by diluting the stock solution in complete EMEM (without antibiotics) to create a 10% (v/v) PrestoBlue:EMEM solution. The working solution was then vortexed to ensure homogeneity and warmed to 37ºC in a water bath prior to application.

Caco-2 cells were cultured in 96 well plates (black) and dosed with treatments as described in sections 2.2.4 and 2.2.6, respectively. As with the MTS assay 1% TX was used as the positive control. Following cell dosing, treatments were removed by gentle aspiration and the cells washed twice with PBS. One hundred microliters of 10% (v/v) PrestoBlue:EMEM solution was then applied to each well for 30 minutes at 37°C with 5 % CO_2 in an incubator. Once incubated with the PrestoBlue solution fluorescent intensity of wells was measured by excitation at 530 nm and detecting emission at 590 nm. Relative metabolic activity was then calculated in the same manner as the MTS assay using Equation 4.

4.2.2. Assessment of Mitochondrial membrane potential

The mitochondrial membrane potential ($\Delta\Psi_m$) is a major determinant and indicator of mitochondrial function as (discussed above in section 4.1). Various techniques are available for measuring this vital parameter, such as the relatively new click chemistry combined with LC-MS/MS approach[42], however fluorescent dyes are the most well established and commonly used methods. These dyes are typically lipophilic cationic compounds that diffuse across membranes in a Nernstain fashion, thereby accumulating into the mitochondrial membrane matrix in a manner that is inversely proportional to $\Delta\Psi_m$; a more negative (*i.e.,* more polarised) $\Delta\Psi_m$ will result in higher dye accumulation[43,44].

To examine the effect of Solutol HS15 of Caco-2 ($\Delta\Psi_m$) two fluorescent indicators were employed; the ratiometric cationic carbocyanine dye JC-1 and MitoTracker® Red CMXRos dye.

4.2.2.1. JC-1 assay

The JC-1 dye readily permeates across the cell plasma membrane and it then accumulates in the electronegative interior of the mitochondrial. When present in the mitochondria JC-1 molecules form aggregates (J-aggregates) (Figure 4.2b), emitting fluorescence at a red wavelength ($\lambda_{EM\text{-}595nm}$), distinct from the dye present in the cytoplasm which remains in monomer (J-monomer) form emitting fluorescence at green wavelength ($\lambda_{EM\text{-}530nm}$) (Figure 4.2a). Mitochondrial depolarisation is consequently indicated by a decrease in the J-aggegrate:monomer intensity ratio, thus representing an arbitrary value for $\Delta\Psi_m$.

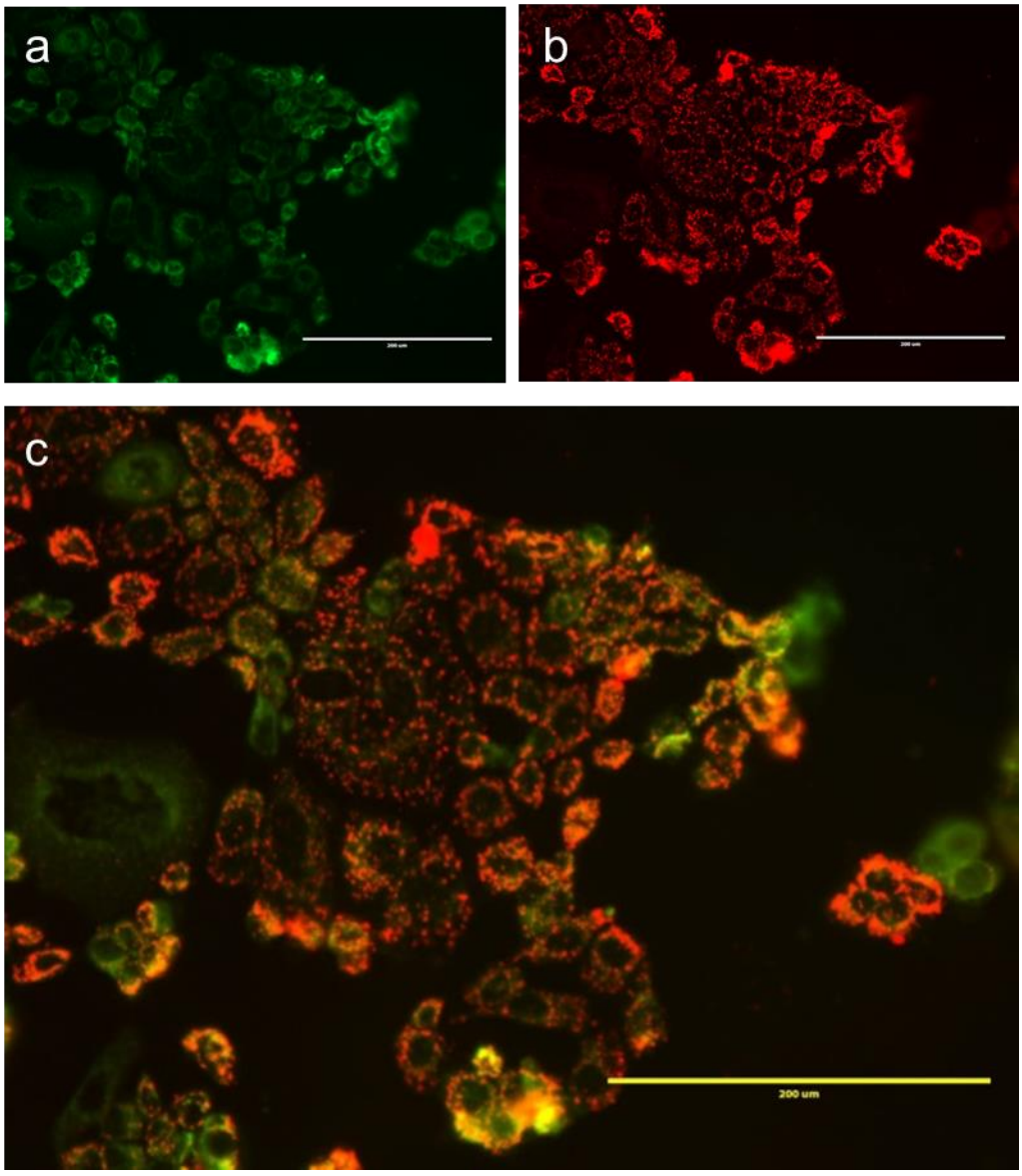

Figure 4.2 Staining of Caco-2 cells with 5 µg/ml JC-1 probe. (a) J-monomer signal imaged on GFP filter (Excitation 470/22nm; Emission 510/42nm), (b) J-aggregate signal imaged on RFP filer (Excitation 531/40nm; Emission 593/40nm) and (c) merged signals (using ImageJ software). Cells were imaged on EVOS microscope; Scale bar = 200 µm.

Stock solutions of the JC-1 probe were prepared by dissolving 5 mg JC-1 iodide salt (5,5′,6,6′-Tetrachloro-1,1′,3,3′-tetraethylbenzimidazolylcarbocyanine, iodide) in 5 ml DMSO. The resulting solution was vortexed for 1 minute followed by 10 minutes of ultrasonication at 37 kHz to ensure dissolution and homogeneity. This 5 ml solution of 1 mg/ml JC-1:DMSO was

then separated into stock aliquots of 25 µl in 0.5 ml micro centrifuge tubes and stored at -20ºC until use. JC-1 staining solution was made up on the day of assaying, and was prepared by diluting 25 µl of JC-1 stock solution in 5 ml complete EMEM (without antibiotics) (1:200 dilution). The final staining solution at working concentration is thus 5 µg/ml JC-1:EMEM containing 0.5 % DMSO; a volume of 5 ml is sufficient to stain a full 96 well plate of Caco-2 cells. The staining solution was then vortexed for 3 minutes, allowed to stand for 2 minutes at room temperature and then vortexed again for another 3 minutes to ensure a homogenous solution. The solution was then warmed to 37ºC in a water bath prior to application on cells. The JC-1 probe is light sensitive; therefore, all JC-1 solids and solutions were protected from light by use of aluminium foil on containers and plates.

The JC-1 assay was carried out on Caco-2 cells grown in 96 well plates (black) as described in section 2.2.4. Assessment of $\Delta\Psi_m$ by the JC-1 probe was achieved by measuring the fluorescent intensity of JC-1 (*i.e.* spectrophotometrically) and by obtaining fluorescent images (*i.e.* fluorescent microscopy). Treatment of cells was carried out as described in section 2.2.6. In addition to Solutol HS15 and the vehicle control (1% HEPES:HBSS), valinomycin was used as a positive control for this assay. Valinomycin was employed as a known depolarising agent of $\Delta\Psi_m$[45], and demonstrated this capability when applied ≥5 min at a concentration of 1 µM (Figure 4.3).

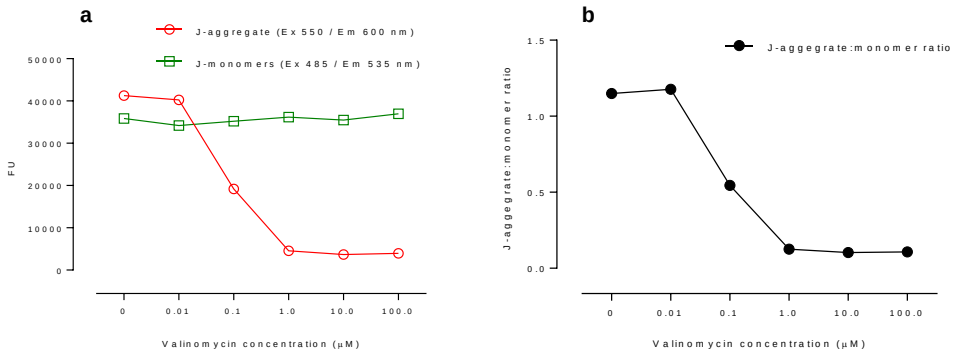

Figure 4.3 Optimisation of valinomycin concentration for JC-1 assay control. (a) Raw fluorescent signal of J-aggregates and J-monomers and (b) J-aggegrate:monomer intensity ratio. Valinomycin was applied in 1% HEPES:HBSS and for 5 minutes. Data represents values from triplicates of one experiment (n=3, N=1), and demonstrates that 1 µM valinomycin is capable of depolarising Caco-2 $\Delta\Psi_m$.

Following exposure, treatments were gently aspirated off and the wells were then washed twice with pre-warmed PBS. Fifty microliters of 5 µg/ml JC-1 staining solution was then added to wells. Plates were then incubated with staining solution for 15 minutes in an incubator at 37°C with 5 % CO_2. The staining solution was then gently aspirated off followed by two subsequent washes in PBS and then 50 µl PBS returned to each well, at which point the JC-1 staining was ready for analysis either by the assessment of fluorescent intensity or fluorescent imaging.

Fluorescent intensity was then measured for the J-aggregate signal at an excitation of 550 nm and an emission of 600 nm, followed by the J-monomer signal at an excitation of 485 nm and an emission of 535 nm on TECAN plate reader. The J-aggegrate:monomer intensity ratio was then calculated for data analysis and presentation.

Assessment of JC-1 staining by fluorescent imaging was performed on an EVOS fluorescent microscope on RFP filter

(excitation 531/40 nm; emission 593/40 nm) for J-aggregate signal and GFP filter (excitation 470/22 nm; emission 510/42 nm) for J-monomer signal, and at a magnification of 20X. Images were then analysed using ImageJ software which involved quantification signals.

4.2.2.2. MitoTracker assay

The Mitotracker probe (MitoTracker® Red CMXRos) is cell permeable and a derivative of X-rosamine. This probe accumulates in active mitochondria and contains a mildly thiol-reactive chloromethyl moiety that is metabolised in the mitochondria to generate a fluorescent conjugate.

This probe is purchased as pre-packaged 50 µg vials of lyophilised solid which are stored at -20ºC. To prepare a stock solution, vials were heated to room temperature followed by the addition of 38 µl DMSO to a 50 µg vial to create a 1 mM MitoTracker:DMSO solution which was then vortexed for 1 minute followed by 10 minutes of ultrasonication at 37 kHz to ensure dissolution and homogeneity. A fraction of the reconstituted stock solution was used immediately (~ 1.5µl *per* 96 well plate) and any remainder was stored in multiple aliquots of approximately 6 µl at -20ºC for future use. For reasons regarding stability, these aliquots of 1 mM MitoTracker:DMSO were kept for a maximum of 3 weeks. MitoTracker is sensitive to light, therefore all MitoTracker solids and solutions were protected from light by use of aluminium foil on containers and plates.

MitoTracker was used at a working concentration of 300 nM diluted in complete EMEM (without supplements). The resulting solution, 300 nM MitoTracker:EMEM containing 0.03% DMSO,

was vortexed to ensure homogeneity and heated to 37ºC prior to addition to cells.

MitoTracker assessment of $\Delta\Psi_m$ was performed by measuring fluorescent intensity spectrophotometrically and was carried out on Caco-2 cells grown in 96 well plates (black) as described in section 2.2.4. Cells underwent treatment in an identical manner to the JC-1 assay; which involved dosing with Solutol HS15, the vehicle control (1% HEPES:HBSS) and 1 µM valinomycin (applied in 1% HEPES:HBSS) as the positive $\Delta\Psi_m$ depolarising control.

Following exposure, treatments were gently aspirated off and the wells were then washed twice with pre-warmed PBS. Fifty microliters of 300 nM MitoTracker staining solution was then added to wells. Plates were incubated with staining solution for 30 minutes in an incubator at 37°C with 5 % CO_2. The staining solution was gently aspirated off followed by two subsequent washes in PBS and 50 µl PBS returned to each well. Fluorescent intensity of MitoTracker staining was measured at an excitation of 580 nm and an emission of 615 nm.

4.2.3. Assessment of Reactive Oxygen Species

ROS generation was assessed using CM-H2DCFDA, a chloromethyl derivative of the general oxidative stress indicator H2DCFDA. This probe passively diffuses into cells where intracellular esterases cleave its acetate groups and the probes thiol-reactive chloromethyl group reacts with thiols such as glutathione. Once oxidised the probe becomes fluorescent. CM-H2DCFDA is highly sensitive to light and was thus protected from it at all stages of its preparation and application with use of aluminium foil. Furthermore, because of its sensitivity to air,

containers of CM-H2DCFDA were only kept open for very brief moments.

This product was purchased as multiple vials of 50 µg lyophilised solid which are stored at -20ºC. To 50 µg of the probe 8.6 µl DMSO was added to create a 10 mM Stock solution. This solution was then ultrasonicated at 37 kHz for 5 minutes to ensure dissolution. Ten millimolar CM-H2DCFDA stock was diluted to a working concentration of 10 µM by the addition of 8.6 ml HBSS. The resulting staining solution, 10 µM CM-H2DCFDA:HBSS containing 0.1% DMSO, was vortexed and heated to 37°C prior to its addition on cells.

Assessment of ROS using CM-H2DCFDA was performed spectrophotometrically and was carried out on Caco-2 cells grown in 96 well plates (black) as described in section 2.2.4. Treatment of cells was carried out as described in section 2.2.6 and involved dosing cells with Solutol HS15 and the vehicle control. Once exposure had elapsed treatments were removed by gentle aspiration and the cells were washed twice with HBSS followed by the addition of 10 µM CM-H2DCFDA staining solution for 30 minutes in an incubator at 37°C with 5 % CO_2. Following the staining period, the CM-H2DCFDA solution was gently aspirated off, wells were washed with HBSS twice and 50 µl HBSS added back *per* well. Fluorescent intensity was then measured by excitation at 492 nm and an emission of 520 nm.

4.3. Results

4.3.1. Assessment of Metabolic activity

4.3.1.1. Metabolic activity determined by MTS assay

When applied to Caco-2 cells for 5 minutes Solutol HS15 concentrations of 10, 20 and 50 mM generated substantial increases in metabolic activity of approximately 2.1, 2.3 and 2.3 -fold that of baseline metabolic activity, respectively, while concentrations <10 mM elicited no such change (Figure 4.4a). Following 10 minutes exposure no change relative to the baseline was observed at concentrations <10 mM. Meanwhile, metabolic activities induced by 10, 20 and 50 mM remained high but have, however decreased compared to their values at 5 minutes to approximately 1.5, 1.5 and 1.6-fold that of the baseline, respectively (Figure 4.4b). At exposures of 20 and 60 minutes Solutol HS15 did not appear to produce any significant changes in metabolic activity, at all concentrations tested, with the exception of 50 mM at 60 minutes which demonstrated a decrease (Figure 4.4d).

Exposing Caco-2 cells to Solutol HS15 ≥1 mM for ≥120 minutes was associated with a concentration- and time-dependent decline in cells metabolic activity (Figure 4.4e, f and g). Exposure for ≤240 min to 0.01 mM did not induce any significant metabolic damage. Metabolic damage in response to 0.1 mM Solutol was not observed until 240 minutes.

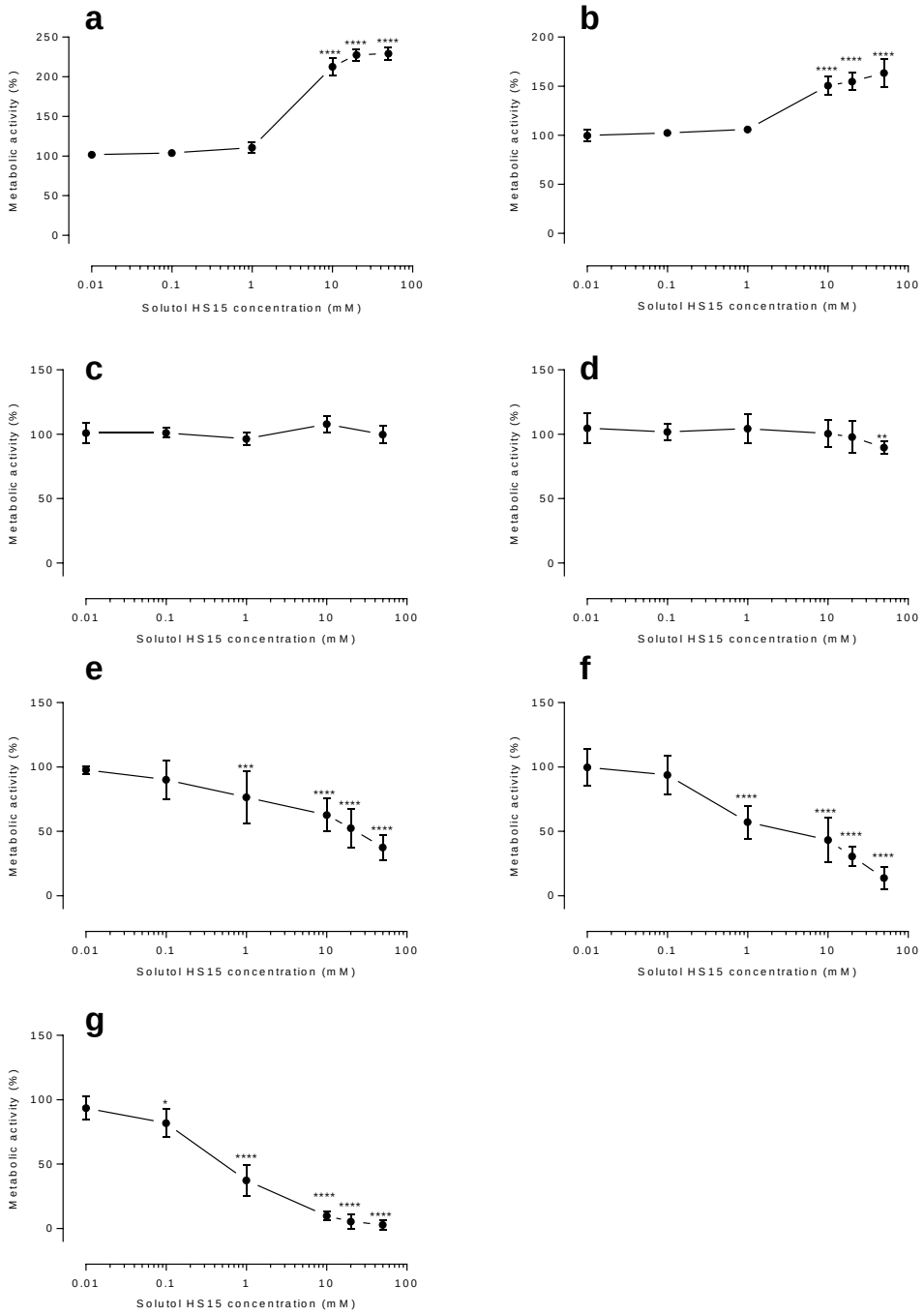

Figure 4.4. Metabolic activity, determined by MTS assay, of Caco-2 cells following Solutol HS15 exposure. Cells were exposed for (a) 5, (b) 10, (c) 20, (d) 60, (e) 120, (f) 180 and (g) 240 minutes. Data are presented as relative values (%) following normalisation to vehicle (100% metabolic activity) and 1% Triton X-100 (0% metabolic activity). Data are presented as mean ± S.D and represents triplicates from three independent experiments. Statistical difference from vehicle control performed by one-way ANOVA followed by Dunnett's multiple comparison post hoc test. *, $P<0.05$; **, $P<0.01$ ***, $P<0.001$; ****, $P<1x10^{-3}$

4.3.1.2. Metabolic activity determined by PrestoBlue assay

To confirm data gathered using the MTS assay the PrestoBlue assay was employed. PrestoBlue is a resazurin-based assay, compared to MTS which is tetrazolium, and it is claimed to offer increased sensitivity[46,47] while requiring a much reduced incubation time (section 4.2.1). Results from the PrestoBlue experiments (Figure 4.5) echo those observed by MTS (Figure 4.4), namely an early increase in metabolic activity (at 5-10 minutes), a 'levelling off' period (20-60 minutes), and ultimately metabolic decline (120-240 minutes).

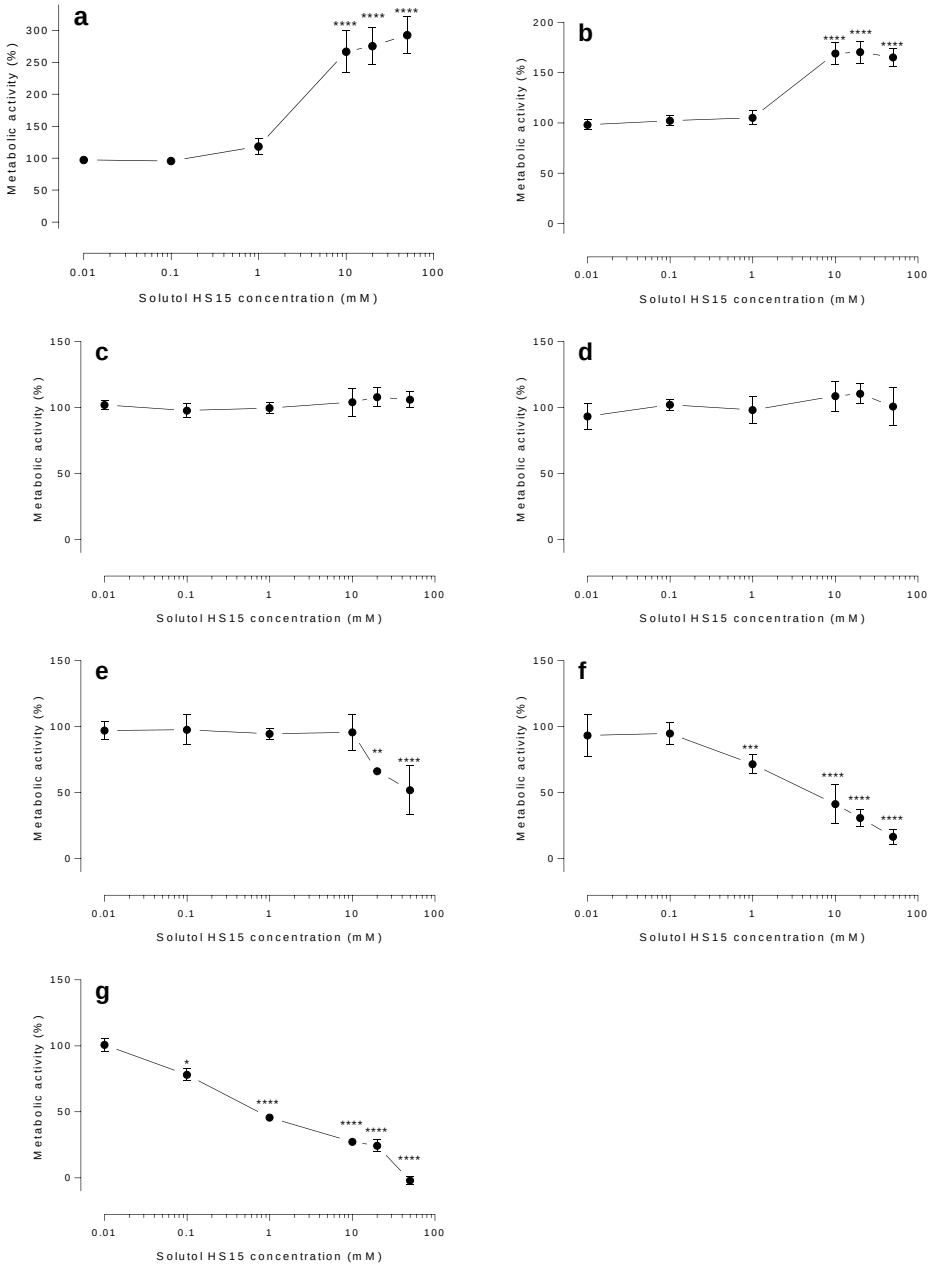

Figure 4.5. Metabolic activity, determined by PrestoBlue assay, of Caco-2 cells following application of Solutol HS15. Cells were exposed for (a) 5, (b) 10, (c) 20, (d) 60, (e) 120, (f) 180 and (g) 240 minutes. Data are presented as relative values (%) following normalisation to vehicle (100% metabolic activity) and 1% Triton X-100 (0% metabolic activity). Data presented as mean ± S.D and represents triplicates from three independent experiments. Statistical difference from vehicle control performed by one-way ANOVA followed by Dunnett's multiple comparison post hoc test. *, $P<0.05$; **, $P<0.01$ ***, $P<0.001$; ****, $P<1x10^{-3}$.

4.3.2. Assessment of Mitochondrial Membrane Potential ($\Delta\Psi_m$)

4.3.2.1. JC-1 assay

4.3.2.1.1. Assessment by fluorescence intensity

Data presented in Figure 4.6 illustrate that Solutol HS15 following 5 minutes exposure and applied at concentrations ≥0.1 mM generated a concentration-dependent increase in $\Delta\Psi_m$, as indicated by the increase in JC-1 J-aggregate:monomer ratio (Figure 4.6a). This increase in $\Delta\Psi_m$ is maintained after 10 minute exposure (Figure 4.6b). At 20 minutes of exposure, $\Delta\Psi_m$ values remain significantly high but have however decreased relative to 10 minutes exposure, at all concentrations with the exception of 0.1 mM which has increased (Figure 4.6c). Exposure for ≥60 minutes elicits a concentration and time-dependent decrease in $\Delta\Psi_m$ relative to the vehicle control at concentrations ≥1 mM (Figure 4.6d). A decrease in $\Delta\Psi_m$ can be observed at concentrations ≥10 mM, ≥1 mM, and ≥0.1 mM, following 60, 120, and 180 minute exposures, respectively (Figure 4.6d,e and f).

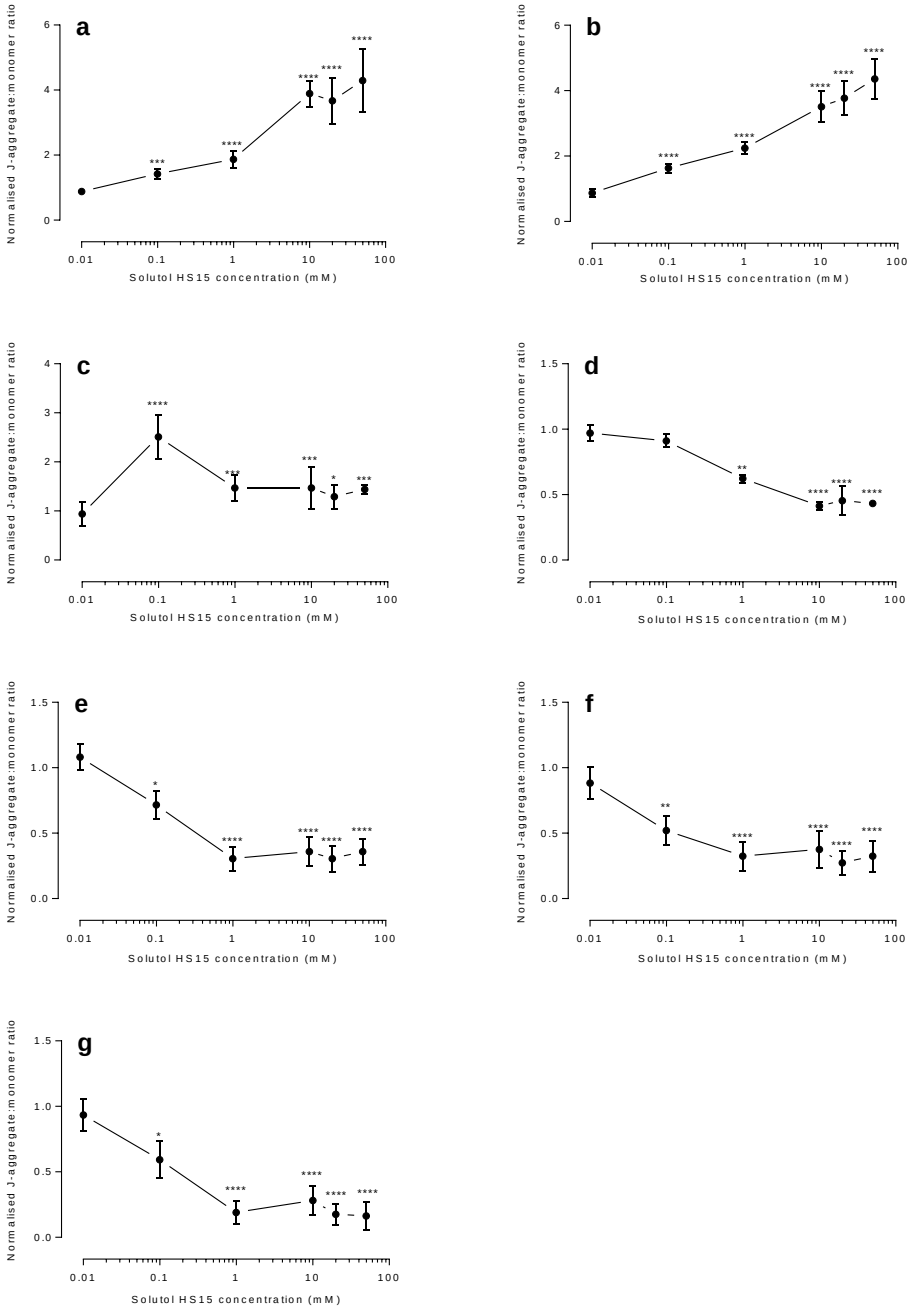

Figure 4.6. Caco-2 mitochondrial membrane potential ($\Delta\Psi_m$), assayed with JC-1 probe, following Solutol HS15 application. Cells were exposed for (a) 5, (b) 10, (c) 20, (d) 60, (e) 120, (f) 180 and (g) 240 minutes. Data presented as relative values (%) following normalisation to vehicle (set to a value of 1) and 1 μM valinomycin (set to value of 0). Data are presented as mean ± S.D and represents triplicates from three independent experiments. Statistical difference from vehicle control performed by one-way ANOVA followed by Dunnett's multiple comparison post hoc test. *, $P<0.05$; **, $P<0.01$ ***, $P<0.001$; ****, $P<1x10^{-3}$

4.3.2.1.2. Assessment by fluorescence images

To support and visualise the JC-1 mitochondrial membrane results measured spectrophotometrically (in above section 4.3.2.1.1), fluorescent microscopy of Caco-2 cells followed by quantification with image analysis software was conducted (Figure 4.7).

Images obtained following JC-1 staining support the spectrophotometrically results made previously; a concentration, and time dependent hyperpolarisation followed by depolarisation of Caco-2 $\Delta\Psi_m$ is evident.

Exposing cells for 5 minutes to 1 and 50 mM Solutol HS15 solutions resulted in approximately 2 and 4-fold increases in JC-1 J-aggregate:monomer ratio, relative to the negative control, respectively (Figure 4.7a). Solutol HS15 applied at 1 and 50 mM for 20 minutes generated JC-1 ratios similar to the negative control (Figure 4.7b). At 60 minutes of exposure both 1 and 50 mM Solutol HS15 solutions have reduced the JC-1 J-aggregate:monomer ratio to approximately 0.7 and 0.5-fold that of the negative control (Figure 4.7c). Furthermore, it can be noted that the hyperpolarising and depolarising effects on the JC-1 J-aggregate:monomer ratio ($\approx\Delta\Psi_m$) are induced by increasing or decreasing the J-aggregate signal which originates from dye located mitochondrially.

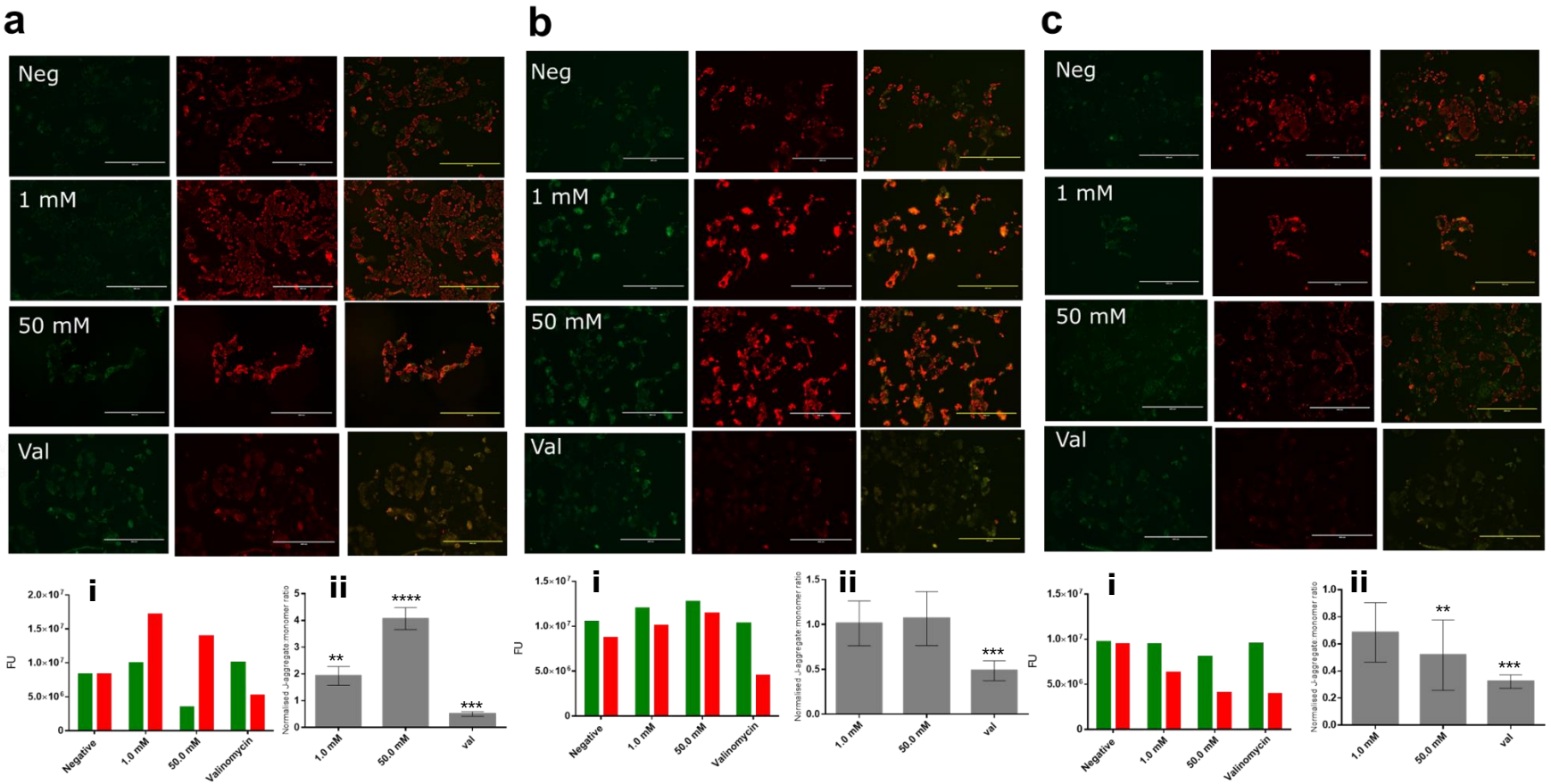
a
b
c
Neg
1 mM
50 mM
Val
i
ii
FU
Normalised J-aggregate monomer ratio
Negative
1.0 mM
50.0 mM
Valinomycin
val
**
****
***

Figure 4.7. Fluorescent micrographs (top) and quantification (bottom) of Caco-2 $\Delta\Psi_m$ stained with JC-1 probe, following Solutol HS15 exposures of (a) 5, (b) 20 and (c) 60, minutes. Images taken on EVOS microscope (scale bar = 400 µm) on GFP filter (right column), RFP filter (middle column) and then overlaid (left column) using ImageJ software. Bar charts underneath images represent intensities of signals (i;left) measuring using ImageJ software of present images (n=1; red bar = J-aggregate signals, green bar = J-monomer), and calculated ratios of normalised J-aggregate:monomer ratio (ii;right) taken from three independent sets of images per treatment (n=3). Data represents mean ± S.D. Neg, negative control (1% HEPES:HBSS); Val, 1 µM valinomycin solution. Statistical difference from negative control performed by one-way ANOVA followed by Dunnett's multiple comparison post hoc test. *, $P<0.05$; **, $P<0.01$ ***, $P<0.001$; ****, $P<1x10^{-3}$

4.3.2.2. MitoTracker assay

In addition to assessment with the JC-1, the MitoTracker probe (MitoTracker® Red CMXRos) was utilised to further support results on Solutol HS15 induced changes in Caco-2 $\Delta\Psi_m$. The MitoTracker compound acts similarly to JC-1 as a probe, however it is not ratiometric (reducing accuracy of processed data) but is well retained following fixing of cell samples, unlike JC-1. Imaging of fixed cells stained with MitoTracker was not undertaken in this work due to time constraints, and instead measuring spectrophotometrically to allow higher throughput analysis.

Results are shown in Figure 4.8. The graph profiles follow similar trends to those observed with the JC-1 dye, namely, early $\Delta\Psi_m$ hyperpolarisation (5-10 minutes exposures) followed by subsequent depolarisation (60-240 minutes).

Solutol HS15 induced $\Delta\Psi_m$ hyperpolarisation was detected with the MitoTracker probe in a concentration-dependent manner at 5 and 10 minutes exposure with concentrations ≥1 and ≥10 mM, respectively (Figure 4.8a and b). A reduction in $\Delta\Psi_m$ to baseline levels at 20 minutes was then observed with most of Solutol HS15 concentrations (the exception being 50 mM, which remains slightly high at approximately 1.5-fold the vehicle control) (Figure 4.8c). Finally, similar to the JC-1 profiles, the MitoTracker probe detects that Solutol HS15 induces concentration and time-dependent depolarisation of $\Delta\Psi_m$ when exposed ≥60 minutes. This depolarisation is initially observed with ≥10 mM Solutol HS15 at 60 minutes (Figure 4.8d), but progresses to 1 mM and 0.1 mM at exposures of 120 and 180 minutes, respectively (Figure 4.8e and f).

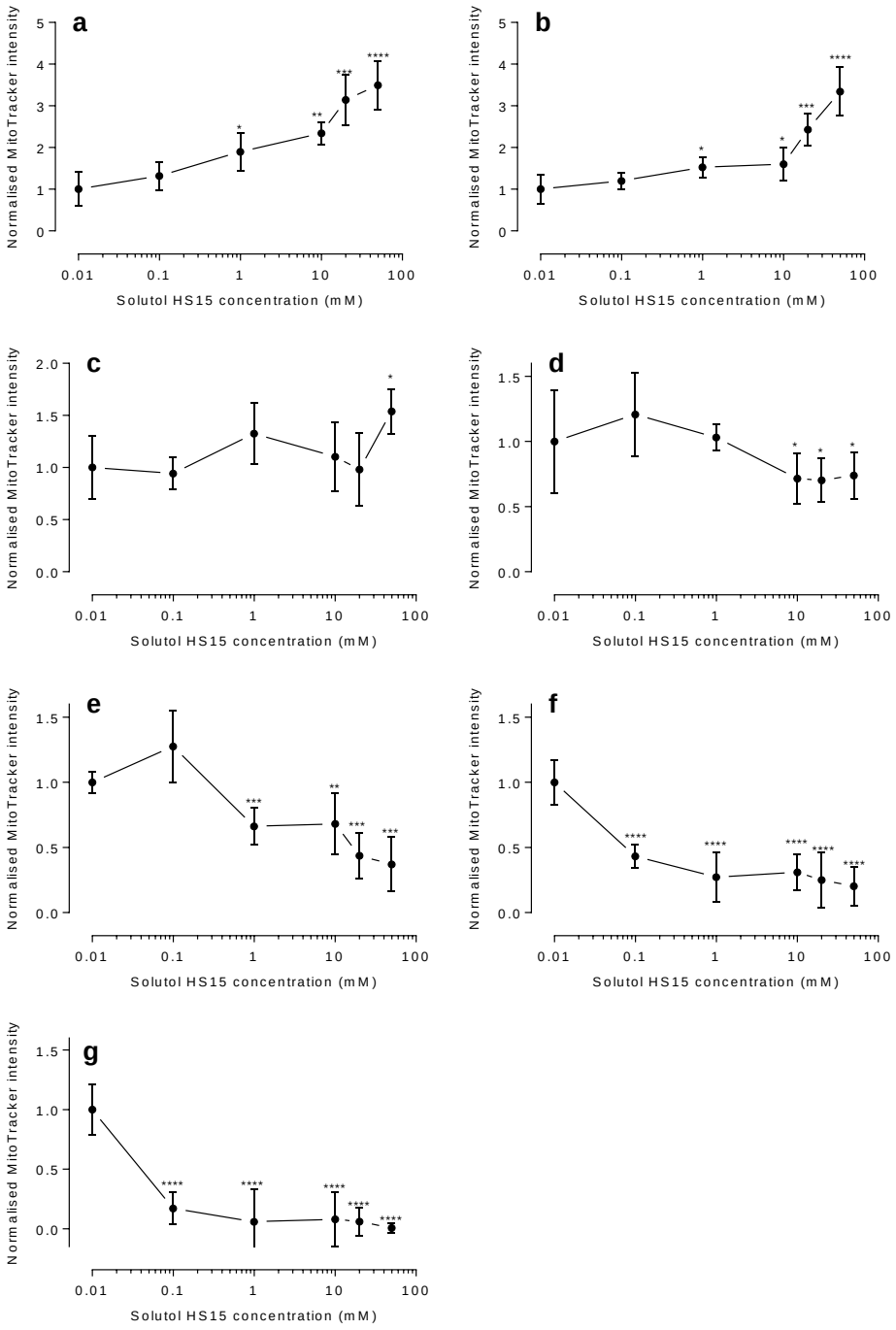

Figure 4.8 MitoTracker probe assessment of Solutol HS15 induced Caco-2 mitochondrial membrane potential ($\Delta\Psi_m$). Cells were exposed for (a) 5, (b) 10, (c) 20, (d) 60, (e) 120, (f) 180 and (g) 240 minutes. Data presented as relative values (%) following normalisation to vehicle (set to a value of 1) and 1.0 μM valinomycin (set to value of 0). Data are presented as mean ± S.D and represents triplicates from three independent experiments. Statistical difference from vehicle control performed by one-ANOVA followed by Dunnett's multiple comparison post hoc test. *, $P<0.05$; **, $P<0.01$ ***, $P<0.001$; ****, $P<1x10^{-3}$

4.3.3. Assessment of Reactive Oxygen Species

ROS generation was assessed using CM-H2DCFDA and results are presented in Figure 4.9. Data demonstrate that Solutol HS15 induced ROS generation is concentration and time dependent. Initially, during exposure of 5-20 minutes, Solutol HS15 at concentrations ≥10 mM generates high levels of ROS, with no effect noted for concentrations ≤1 mM (Figure 4.9a,b and c). ROS levels are highest after the first 5 minutes, with a maximum of 6.5-fold increases being observed with 10 mM Solutol HS15 (Figure 4.9a). Levels then decline slightly at 10 minutes, with 5.8-fold increases induced by 50 mM Solutol HS15 (Figure 4.9b). Following 20 minutes exposures ROS levels decrease further but remain significantly high, with a maximum of 4-fold increases induced by 50 mM Solutol HS15 (Figure 4.9c). In addition, dissimilar to 5 and 10 minutes exposure, at 20 minutes 1 mM Solutol HS15 induced significantly increased level of ROS (approximately 1.8-fold increase) (Figure 4.9c).

Exposing cells to ≥1 mM Solutol HS15 for ≥60 minutes elicited a time and concentration dependent decline in ROS levels, relative to the cells treated with the vehicle control. Following 60 minutes it can be noted ≥ 10 mM Solutol HS15 induces relative ROS levels approximately 0.35-fold that of the control and 1 mM Solutol HS15 induces levels 0.7-fold the control (Figure 4.9d). Similar levels are observed after 120 minutes with Solutol HS15 applied ≥10 mM, however 1 mM induces further reduced levels of approximately 0.5-fold the control (Figure 4.9e). This trend of decreasing ROS levels continues at 180 minutes; 1, 10, 20 and 50 mM Solutol HS15 stimulating levels of approximately 0.4, 0.3, 0.1, and 0.06-fold, respectively (Figure 4.9f). Following the final time point at 240

minutes 1 mM Solutol HS15 has reduced levels to 0.3-fold the control, and with ≥10 mM Solutol HS15 ROS levels are all <0.1-fold the control (Figure 4.9g).

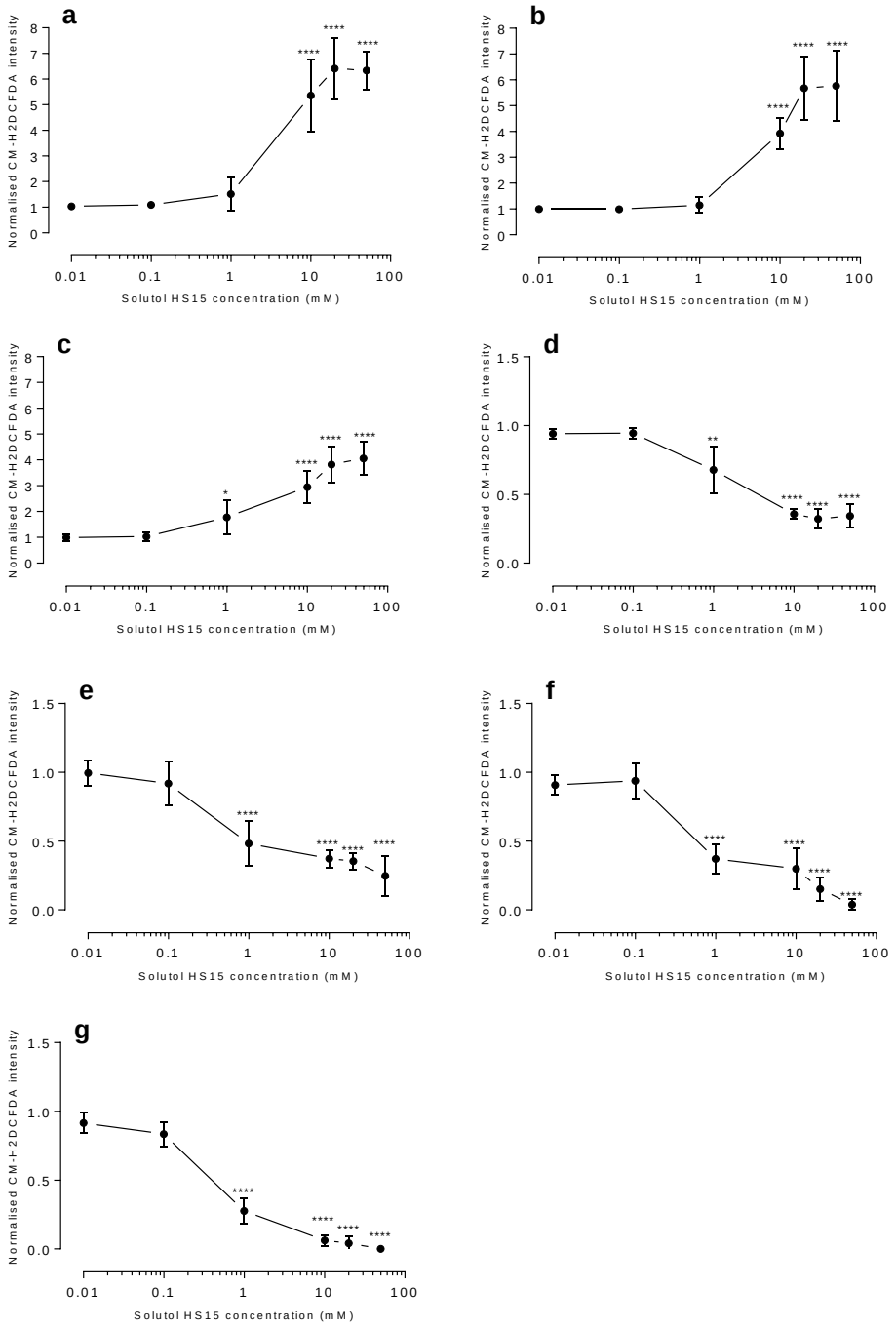

Figure 4.9 Detection of general oxidative stress with use of CM-H2DCDFA probe following Solutol HS15 exposures. Cells were treated for (a) 5, (b) 10, (c) 20, (d) 60, (e) 120, (f) 180 and (g) 240 minutes. Data presented as relative values (%) following normalisation to vehicle (set to a value of 1). Data are as mean ± S.D and represents triplicates from three independent experiments. Statistical difference from vehicle control performed by one-ANOVA followed by Dunnett's multiple comparison post hoc test. *, P<0.05; **, P<0.01 ***, P<0.001; ****, P<1x10^{-3}

4.4. Discussion

Work described in this chapter observed the presence of time-dependent, 'biphasic' mitochondrial responses of Caco-2 cells on exposure to Solutol HS15 solutions, as illustrated in Figure 4.10.

Solutol HS15 concentrations ≥10 mM applied for 5-20 minutes resulted in $\Delta\Psi_m$ hyperpolarisation, an increase in MTS reduction (metabolic activity) and an increase in levels of ROS. Succeeding these events was a 'levelling off' period (20-60 minutes of exposure) whereby responses appeared to return to baseline levels. In response to longer exposures of 60-240 minutes, time-dependent decline in 'cell health' attributes can be witnessed; depolarisation of $\Delta\Psi_m$ and reductions in metabolic activity.

The observation of metabolic attributes representative of cytotoxic effects, which could be associated with cell death, was expected on the longer exposures to the surfactant, however the effects observed on short exposures were surprising; they have not been previously reported in the literature for similar compounds – although it should be mentioned that such brief exposures are not commonly investigated and that typically results are reported for one fixed time point, following 2[48,49], 4[50,51] or 24[52] hours, for example. The observed time, as well as concentration dependency of cell metabolic profiles may reveal further details on the cellular response to Solutol HS15.

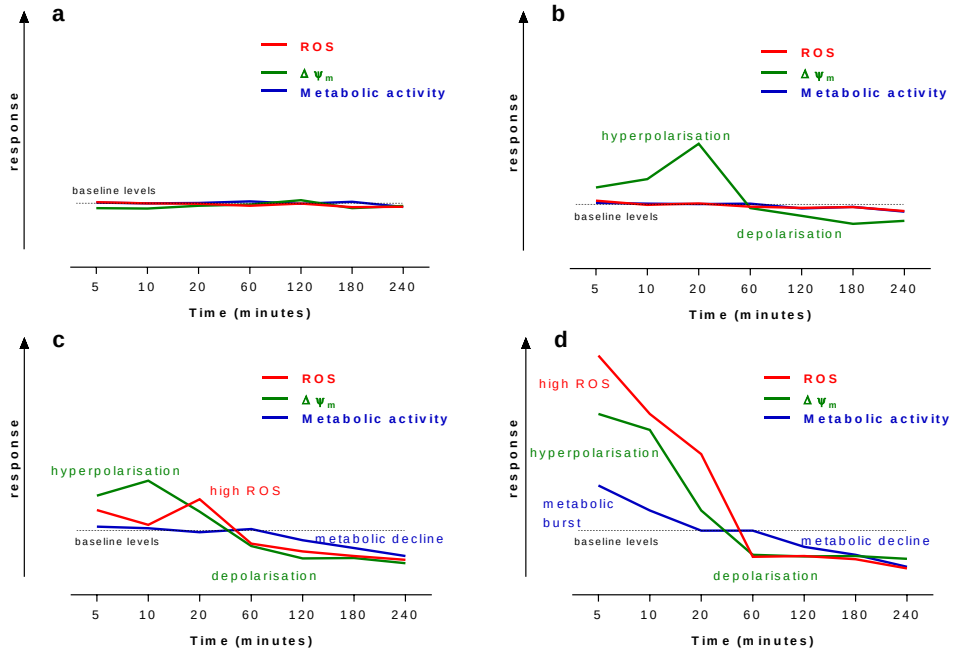

Figure 4.10. The kinetic profiles of the tested metabolic effects in Caco-2 cells exposed to (a) 0.01, (b) 0.1, (c) 1 and (d) 10 mM Solutol HS15. Normalised ROS levels, metabolic activity and mitochondrial membrane potential ($\Delta\Psi_m$) following application of 10 mM Solutol HS15 are displayed together and relative to the baseline levels as fold-increases to aid discussion.

4.4.1. Metabolic burst

As discussed above in section 4.2.1, the basis for the MTS and PrestoBlue assays is the reduction of starting salts driven by NADH-dependent processes. Thus, these assays are indirectly probing for cellular NADH levels. The increase in metabolic activity observed almost immediately (from the first time point assayed; 5 minutes) following exposure to Solutol HS15 therefore could represent a rapid increase in NADH levels.

One explanation for the rapid increase in NADH levels may be the enhancement of glycolysis. Upon activation of survival pathways, one known consequence is the enhancement of glycolysis to fuel the immediate synthesis of proteins involved in mediating the response[53–55].

In addition to being classically associated with bioenergetics, NADH is also involved in cell signalling *via* its redox state and its oxidised counterpart NAD+. This redox system has been shown to modulate various cell functions such as gene transcription[56] and cell death signalling[57,58]. Thus, high levels of NADH could be both driving a survival response and also represent elements of redox signalling mediated by the imbalance in the NADH/NAD+ redox state of the cell.

Mechanistically, at this point in the study, it would not be possible to unequivocally suggest the order of the initial metabolic responses observed. However, as will be investigated and discussed further (Chapter 5), the transient $\Delta\Psi_m$ hyperpolarisation and increased levels of ROS are likely related to the increased cellular NADH levels and the subsequent effect on complex I activity, as discussed below.

4.4.2. $\Delta\Psi_m$ hyperpolarisation

The presence of a hyperpolarised $\Delta\Psi_m$ indicates that the mitochondrial interior (matrix) is markedly more negative than that experienced in physiological conditions. This can result from the components of the electron transport chain (ETC) 'pumping' protons into the intermembrane space at an enhanced rate. One likely suspect for this is complex I (NADH-ubiquinone oxidoreductase). To address the NADH/NAD+ redox imbalance, and return this redox system to homeostasis, NAD+ is regenerated *via* mitochondrial complex I by NADH oxidisation. NADH oversupply could however overwhelm complex I capacity[59], and this is known to result in $\Delta\Psi_m$ hyperpolarisation, as well as increased ROS formation[60]. Hyperpolarisation is reported to effectively shut off

mitochondrial respiration; the very negative mitochondrial potential prevents further proton pumping inhibiting the ability of the ETC to function[61]. ROS generation then increases as incoming electrons can no longer be oxidised and instead interact with molecular O_2[61]. Thus, hyperpolarisation may be a knock-on effect of the heightened NADH levels, and increased ROS production a consequence of hyperpolarisation.

Akin to a feedforward mechanism, cells may then undergo a 'metabolic shift' to glycolysis to compensate for the abolishment of mitochondrial-mediated energy production mediated by hyperpolarisation (further promoting the NADH burst). In addition to this potential link with bioenergetics, hyperpolarisation represents an important mitochondrial signal involved in initiating apoptotic cell death pathways[62,63].

Interestingly, mitochondrial potential was more sensitive to lower concentrations of Solutol HS15 than other parameters; 0.1 mM Solutol HS15, for example induced both hyperpolarisation and depolarisation, albeit to a lesser degree than the higher concentrations. This emphasises how responsive mitochondria are to Solutol HS15 – Laurdan GP data (section 3.3.4, Figure 3.8) demonstrated ≥0.1 mM Solutol HS15 induces significant fluidisation of the plasma membrane; taken together, this could point to a mitochondrial response to fluidisation.

4.4.3. Reactive oxygen species generation

High levels of ROS detected in Caco-2 cells on initial 5-20 minutes exposures to Solutol HS15 at concentrations ≥10 mM coincide with the events discussed above. Literature suggests

that redox signalling (*via* ROS) and oxidative stress can be associated with both $\Delta\Psi_m$ hyperpolarisation, *via* enhanced activity of complex I, and the metabolic burst (as discussed above). High levels of NADH are linked to elevated ROS production *via* mitochondrial α-KGDH, an NADH-dependent enzyme involved in the Krebs cycle[64].

ROS levels decline relative to baseline values at ≥60 minutes exposures. The probable reason for this is the shutdown of mitochondrial-mediated process (maintenance of $\Delta\Psi_m$ and metabolic activity) at these exposure conditions, and as discussed in section 4.1, these are associated with the majority of cellular ROS formation.

4.4.4. $\Delta\Psi_m$ depolarisation

Following what appears to be a 'levelling off' period at 20 minutes, characterised by the return to baseline levels of metabolic activity and $\Delta\Psi_m$, at 60 minutes $\Delta\Psi_m$ depolarisation is evident, while metabolic activity remains at physiological levels. Depolarisation of $\Delta\Psi_m$ represents a loss of the electrochemical gradient across the mitochondrial membranes. Thus, mitochondrial-mediated OXPHOS will no longer be possible, but some degree of metabolic capability *via* glycolysis may be retained (sustaining NADH levels)[65,66].

Dissipation of $\Delta\Psi_m$ is commonly caused by the formation of channels or pores across the inner mitochondrial membrane, such as the permeability transition pore that is activated by pro-apoptotic Bcl-2 family members (*e.g.,* Bid, Bak and Bax)[67]. Reported studies demonstrate that a collapse in $\Delta\Psi_m$ occurs shortly after permeabilisation of the outer mitochondrial

membrane[68], a process often suggested as a 'point of no return' in the succession of event promoting apoptosis[69–71].

4.4.5. Metabolic decline

The detection of the metabolic decline/damage induced by Solutol HS15 in this work is in line with previous studies from our group conducted in similar experimental conditions[72]. Along with damage to the plasma membrane, metabolic damage is a well-established toxic effect of non-ionic surfactants[48,73–76].

Damage to cellular metabolic activity is a classical sign of compound toxicity and, in this system, following Solutol HS15 exposure, could potentially result from; (i) cell-mediated processes (*via* apoptotic mechanisms) and/or (ii) directly mediated Solutol HS15 effects (*via* perturbation/damage of phospholipid bilayer structure).

Regarding (i), it is evident that after 120 minutes exposure Solutol HS15 induces a decline in cellular metabolic activity, which is most likely a consequence of the preceding collapse in $\Delta\Psi_m$ at 60 minutes. Once mitochondrial membranes have been permeabilised (as demonstrated by loss of $\Delta\Psi_m$), cell death is likely imminent and the majority of cellular processes will begin to shut off as the cell undergoes apoptosis.

Considering (ii), and as discussed in Chapter 3, damage to the plasma membrane was detected at approximately the same time point (60 minutes). This damage will generate unfavourable cytoplasmic conditions for metabolic processes for several reason; loss of ion homeostasis, influx of extracellular milieu, efflux of intracellular components, *etc.*

Another possibility is the direct permeabilisation of the mitochondrial membranes by Solutol HS15 at 60 minutes, similar to nuclear membrane permeabilisation at this time point (section 3.3.6, Figure 3.10) suggesting direct permeabilisation of organelles may be possible early during exposure.

Therefore, at this stage it is unclear if metabolic damage revealed by the tests conducted in this chapter is to be associated with direct Solutol HS15 action or, brought about indirectly, *via* pro-apoptotic mechanisms - *Chapter 5 investigates the mechanism of cell death and explores this further.*

4.5. Conclusions

Results from work described in this chapter demonstrate that upon Solutol HS15 exposure at concentrations ≥10 mM Caco-2 cells are showing a succession of metabolic effects; beginning with what is likely redox signalling and an attempted survival response in the first 20 minutes, followed later after 60 minutes exposure, by the shutdown of mitochondrial processes.

The coordination of observed mitochondrial events, preceding the onset of cytotoxicity, could suggest that they may, to some degree, be associated with programmed cell death mechanisms. The next chapter will investigate these connections further.

4.6. References

1. Shepherd, R. M. & Henquin, J. C. The role of metabolism, cytoplasmic Ca2+, and pH-regulating exchangers in glucose-induced rise of cytoplasmic pH in normal mouse pancreatic islets. *Journal of Biological Chemistry* **270,** 7915–7921 (1995).

2. Wright, E. M. & Turk, E. The sodium/glucose cotransport family SLC5. *Pflugers Archiv European Journal of Physiology* **447,** 510–518 (2004).

3. Baker, M. A. & Lawen, A. Plasma Membrane NADH-Oxidoreductase System: A Critical Review of the Structural and Functional Data. *Antioxid. Redox Signal.* **2,** 197–212 (2000).

4. Kushnareva, Y. & Newmeyer, D. D. Bioenergetics and cell death. in *Annals of the New York Academy of Sciences* **1201,** 50–57 (2010).

5. Skulachev, V. P. Bioenergetic aspects of apoptosis, necrosis and mitoptosis. *Apoptosis* **11,** 473–485 (2006).

6. Lartigue, L. *et al.* Caspase-independent mitochondrial cell death results from loss of respiration, not cytotoxic protein release. *Mol. Biol. Cell* **20,** 4871–84 (2009).

7. Bernardi, P., Di Lisa, F., Fogolari, F. & Lippe, G. From ATP to PTP and back: A dual function for The mitochondrial ATP synthase. *Circulation Research* **116,** 1850–1862 (2015).

8. Greiner, E. F., Guppy, M. & Brand, K. Glucose is essential for proliferation and the glycolytic enzyme induction that provokes a transition to glycolytic energy production. *J. Biol. Chem.* **269,** 31484–31490 (1994).

9. Miller, S. L. & Smith magowan, D. The Thermodynamics of the Krebs Cycle and Related Compounds. *J. Phys. Chem. Ref. Data* **19,** 1049–1073 (1990).

10. Fvasconcellos. Electron Transport Chain. *Wikimedia Commons* (2007). Available at: wikipedia.org/wiki/Electron_transport_chain. (Accessed: 11th September 2016)

11. Chen, Y., McMillan-Ward, E., Kong, J., Israels, S. J. & Gibson, S. B. Mitochondrial electron-transport-chain inhibitors of complexes I and II induce autophagic cell death mediated by reactive oxygen species. *J. Cell Sci.* **120,** 4155–4166 (2007).

12. Maharjan, S., Oku, M., Tsuda, M., Hoseki, J. & Sakai, Y. Mitochondrial impairment triggers cytosolic oxidative stress and cell death following proteasome inhibition. *Sci. Rep.* **4,** 5896 (2015).

13. Friedman, J. R. & Nunnari, J. Mitochondrial form and function. *Nature* **505,** 335–343 (2014).

14. Benz, R. & McLaughlin, S. The molecular mechanism of action of the proton ionophore FCCP (carbonylcyanide p-trifluoromethoxyphenylhydrazone). *Biophys. J.* **41,** 381–398 (1983).

15. Stoetzer, O. J. *et al.* Modulation of apoptosis by mitochondrial uncouplers: Apoptosis-delaying features despite intrinsic cytotoxicity.

Biochem. Pharmacol. **63,** 471–483 (2002).

16. Thoma, a. P., Viviani-Nauer, a., Arvanitis, S., Morf, W. E. & Simon, W. Mechanism of neutral carrier mediated ion transport through ion-selective bulk membranes. *Anal. Chem.* **49,** 1567–1572 (1977).

17. Van Buuren, K. J. H., Nicholls, P. & Van Gelder, B. F. Biochemical and biophysical studies on cytochrome aa3. VI. Reaction of cyanide with oxidized and reduced enzyme. *BBA - Bioenerg.* **256,** 258–276 (1972).

18. Kagawa, Y. & Racker, E. Partial resolution of the enzymes catalyzing oxidative phosphorylation. IX. Reconstruction of oligomycin-sensitive adenosine triphosphatase. *J. Biol. Chem.* **241,** 2467–2474 (1966).

19. D'Autréaux, B. & Toledano, M. B. ROS as signalling molecules: mechanisms that generate specificity in ROS homeostasis. *Nat. Rev. Mol. Cell Biol.* **8,** 813–824 (2007).

20. Halliwell, B. & Cross, C. E. Oxygen-derived species: Their relation to human disease and environmental stress. in *Environmental Health Perspectives* **102,** 5–12 (1994).

21. Ames, B. N., Shigenaga, M. K. & Hagen, T. M. Oxidants, antioxidants, and the degenerative diseases of aging. *Proc. Natl. Acad. Sci.* **90,** 7915–7922 (1993).

22. Turrens, J. F. Mitochondrial formation of reactive oxygen species. *J. Physiol.* **552,** 335–344 (2003).

23. Panday, A., Sahoo, M. K., Osorio, D. & Batra, S. NADPH oxidases: an overview from structure to innate immunity-associated pathologies. *Cell. Mol. Immunol.* **12,** 5–23 (2015).

24. Xia, Q., Hwang, H.-M., Ray, P. C. & Yu, H. Mechanisms of nanotoxicity: Generation of reactive oxygen species. *J. Food Drug Anal.* **22,** 64–75 (2014).

25. Murphy, M. P. How mitochondria produce reactive oxygen species. *Biochem. J.* **417,** 1–13 (2009).

26. Mikkelsen, R. B. & Wardman, P. Biological chemistry of reactive oxygen and nitrogen and radiation-induced signal transduction mechanisms. *Oncogene* **22,** 5734–5754 (2003).

27. Finkel, T. & Holbrook, N. J. Oxidants, oxidative stress and the biology of ageing. *Nature* **408,** 239–247 (2000).

28. Ozben, T. Oxidative stress and apoptosis: Impact on cancer therapy. *Journal of Pharmaceutical Sciences* **96,** 2181–2196 (2007).

29. Scherz-Shouval, R. & Elazar, Z. ROS, mitochondria and the regulation of autophagy. *Trends Cell Biol.* **17,** 422–427 (2007).

30. Hampton, M. B. & Orrenius, S. Dual regulation of caspase activity by hydrogen peroxide: Implications for apoptosis. *FEBS Lett.* **414,** 552–556 (1997).

31. Berridge, M., Tan, A., McCoy, K. & Wang, R. The biochemical and cellular basis of cell proliferation assays that use tetrazolium salts. *Biochemica* 4–9 (1996).

32. Dunigan, D. D., Waters, S. B. & Owen, T. C. Aqueous soluble tetrazolium/formazan MTS as an indicator of NADH- and NADPH-dependent dehydrogenase activity. *Biotechniques* **19,** 640–649 (1995).

33. Berridge, M. V., Herst, P. M. & Tan, A. S. Tetrazolium dyes as tools in cell biology: New insights into their cellular reduction. *Biotechnology Annual Review* **11,** 127–152 (2005).

34. Berridge, M. V & Tan, A. S. Characterization of the cellular reduction of 3-(4,5-dimethylthiazol-2-yl)-2,5-diphenyltetrazolium bromide (MTT): subcellular localization, substrate dependence, and involvement of mitochondrial electron transport in MTT reduction. *Arch. Biochem. Biophys.* **303,** 474–482 (1993).

35. Goodwin, C. J., Holt, S. J., Riley, P. A., Downes, S. & Marshall, N. J. Growth Hormone-Responsive DT-Diaphorase-Mediated Bioreduction of Tetrazolium Salts. *Biochem. Biophys. Res. Commun.* **226,** 935–941 (1996).

36. Prochaska, H. J. & Santamaria, A. B. Direct measurement of NAD(P)H:quinone reductase from cells cultured in microtiter wells: A screening assay for anticarcinogenic enzyme inducers. *Anal. Biochem.* **169,** 328–336 (1988).

37. O'Brien, J., Wilson, I., Orton, T. & Pognan, F. Investigation of the Alamar Blue (resazurin) fluorescent dye for the assessment of mammalian cell cytotoxicity. *Eur. J. Biochem.* **267,** 5421–5426 (2000).

38. Matsumoto, K. *et al.* Fluorometric determination of carnitine in serum with immobilized carnitine dehydrogenase and diaphorase. *Clin. Chem.* **36,** 2072–2076 (1990).

39. Belinsky, M. & Jaiswal, A. K. NAD(P)H:Quinone oxidoreductase1 (DT-diaphorase) expression in normal and tumor tissues. *Cancer Metastasis Rev.* **12,** 103–117 (1993).

40. Zalata, A. A., Lammer Tijn, N., Christophe, A. & Comhaire, F. H. The correlates and alleged biochemical background of the resazurin reduction test in semen. *Int. J. Androl.* **21,** 289–294 (1998).

41. Promega Corporation. CellTiter 96 ® AQueous One Solution Cell Proliferation Assay. *Www.Promega.Com/Protocols/* 2014-12–15 (2012).

42. Logan, A. *et al.* Assessing the mitochondrial membrane potential in cells and in vivo using targeted click chemistry and mass spectrometry. *Cell Metab.* **23,** 379–385 (2016).

43. Ehrenberg, B., Montana, V., Wei, M. D., Wuskell, J. P. & Loew, L. M. Membrane potential can be determined in individual cells from the nernstian distribution of cationic dyes. *Biophys. J.* **53,** 785–794 (1988).

44. Lemasters, J. J. & Ramshesh, V. K. Imaging of Mitochondrial Polarization and Depolarization with Cationic Fluorophores. *Methods in Cell Biology* **80,** 283–295 (2007).

45. Perelman, A. *et al.* JC-1: alternative excitation wavelengths facilitate mitochondrial membrane potential cytometry. *Cell Death Dis.* **3,** e430 (2012).

46. Xu, M., McCanna, D. J. & Sivak, J. G. Use of the viability reagent PrestoBlue in comparison with alamarBlue and MTT to assess the viability of human corneal epithelial cells. *J. Pharmacol. Toxicol. Methods* **71,** 1–7 (2015).

47. Boncler, M., Rózalski, M., Krajewska, U., Podswdek, A. & Watala, C. Comparison of PrestoBlue and MTT assays of cellular viability in the assessment of anti-proliferative effects of plant extracts on human endothelial cells. *J. Pharmacol. Toxicol. Methods* **69,** 9–16 (2014).

48. Levine, S. L., Han, Z., Liu, J., Farmer, D. R. & Papadopoulos, V. Disrupting mitochondrial function with surfactants inhibits MA-10 Leydig cell steroidogenesis. *Cell Biol. Toxicol.* **23,** 385–400 (2007).

49. Lin, H. *et al.* Enhancing effect of surfactants on fexofenadine??HCl transport across the human nasal epithelial cell monolayer. *Int. J. Pharm.* **330,** 23–31 (2007).

50. Alvi, M. M. & Chatterjee, P. A prospective analysis of co-processed non-ionic surfactants in enhancing permeability of a model hydrophilic drug. *AAPS PharmSciTech* **15,** 339–53 (2014).

51. Gupta, V., Hwang, B. H., Doshi, N. & Mitragotri, S. A permeation enhancer for increasing transport of therapeutic macromolecules across the intestine. *J. Control. Release* **172,** 541–549 (2013).

52. Yang, Y. W., Wu, C. a. & Morrow, W. J. W. Cell death induced by vaccine adjuvants containing surfactants. *Vaccine* **22,** 1524–1536 (2004).

53. Plesofsky, N., Higgins, L. A., Markowski, T. & Brambl, R. Glucose starvation alters heat shock response, leading to death of wild type cells and survival of MAP kinase signaling mutant. *PLoS One* **11,** 1–31 (2016).

54. Gao, H. *et al.* Global transcriptome analysis of the heat shock response of Shewanella oneidensis. in *Journal of Bacteriology* **186,** 7796–7803 (2004).

55. Wang, L., Schumann, U., Liu, Y., Prokopchuk, O. & Steinacker, J. M. Heat shock protein 70 (Hsp70) inhibits oxidative phosphorylation and compensates ATP balance through enhanced glycolytic activity. *J. Appl. Physiol.* **113,** 1669–1676 (2012).

56. Zhang, Q., Piston, D. W. & Goodman, R. H. Regulation of corepressor function by nuclear {NADH}. *Science (80-.).* **295,** 1895–1897 (2002).

57. Virag, L. & Szabo, C. The therapeutic potential of poly(ADP-ribose) polymerase inhibitors. *Pharmacol Rev* **54,** 375–429 (2002).

58. Sundaresan, N. R., Samant, S. A., Pillai, V. B., Rajamohan, S. B. & Gupta, M. P. SIRT3 Is a Stress-Responsive Deacetylase in Cardiomyocytes That Protects Cells from Stress-Mediated Cell Death by Deacetylation of Ku70. *Mol. Cell. Biol.* **28,** 6384–6401 (2008).

59. He, Q., Wang, M., Petucci, C., Gardell, S. J. & Han, X. Rotenone induces reductive stress and triacylglycerol deposition in C2C12 cells. *Int. J. Biochem. Cell Biol.* **45,** 2749–2755 (2013).

60. Starkov, A. A. & Fiskum, G. Regulation of brain mitochondrial H2O2 production by membrane potential and NAD(P)H redox state. *J. Neurochem.* **86,** 1101–1107 (2003).

61. Michelakis, E. D. Mitochondrial medicine: A new era in medicine opens new windows and brings new challenges. *Circulation* **117,** 2431–2434 (2008).

62. Giovannini, C. *et al.* Mitochondria hyperpolarization is an early event in oxidized low-density lipoprotein-induced apoptosis in Caco-2 intestinal cells. *FEBS Lett.* **523,** 200–206 (2002).

63. Perl, A., Gergely, P., Nagy, G., Koncz, A. & Banki, K. Mitochondrial hyperpolarization: A checkpoint of T-cell life, death and autoimmunity. *Trends in Immunology* **25,** 360–367 (2004).

64. Tretter, L. & dam-Vizi, V. Generation of reactive oxygen species in the reaction catalyzed by alpha-ketoglutarate dehydrogenase. *J. Neurosci.* **24,** 7771–7778 (2004).

65. Rafikov, R. *et al.* Complex I dysfunction underlies the glycolytic switch in pulmonary hypertensive smooth muscle cells. *Redox Biol.* **6,** 278–286 (2015).

66. Jayasena, T. *et al.* Upregulation of glycolytic enzymes, mitochondrial dysfunction and increased cytotoxicity in glial cells treated with Alzheimer's disease plasma. *PLoS One* **10,** (2015).

67. Marzo, I. *et al.* Bax and adenine nucleotide translocator cooperate in the mitochondrial control of apoptosis. *Science (80-.).* **281,** 2027–2031 (1998).

68. Kroemer, G., Galluzzi, L. & Brenner, C. Mitochondrial membrane permeabilization in cell death. *Physiol. Rev.* **87,** 99–163 (2007).

69. Green, D. R. & Kroemer, G. The pathophysiology of mitochondrial cell death. *Science* **305,** 626–629 (2004).

70. Von Ahsen, O., Waterhouse, N., Kuwana, T., Newmeyer, D. & Green, D. The 'harmless' release of cytochrome C. *Cell Death Differ.* **7,** 1192–1199 (2000).

71. Chipuk, J. E., Bouchier-Hayes, L. & Green, D. R. Mitochondrial outer membrane permeabilization during apoptosis: the innocent bystander scenario. *Cell Death Differ.* **13,** 1396–1402 (2006).

72. Shubber, S. *et al.* Mechanism of Mucosal Permeability Enhancement of CriticalSorb® (Solutol® HS15) Investigated In Vitro in Cell Cultures. *Pharm. Res.* **32,** 516–527 (2014).

73. Dimitrijevic, D., Shaw, A. J. & Florence, A. T. Effects of some non-ionic surfactants on transepithelial permeability in Caco-2 cells. *J. Pharm. Pharmacol.* **52,** 157–162 (2000).

74. Warisnoicharoen, W., Lansley, A. B. & Lawrence, M. J. Toxicological evaluation of mixtures of nonionic surfactants, alone and in

combination with oil. *J. Pharm. Sci.* **92,** 859–868 (2003).

75. Aranzazu Partearroyo, M., Ostolaza, H., Goni, F. M. & Barbera-Guillem, E. Surfactant-induced cell toxicity and cell lysis. A study using B16 melanoma cells. *Biochem. Pharmacol.* **40,** 1323–1328 (1990).

76. Vllasaliu, D. *et al.* Epithelial toxicity of alkylglycoside surfactants. *J. Pharm. Sci.* **102,** 114–125 (2013).

5. Chapter Five – Investigation of the mode of cell death

Summary

This chapter aimed to study the mode of cell death associated with Solutol HS15 exposure. Experiments were performed to assess nuclear morphology and activation of effector caspases-3/7, as well as investigate the post-exposure fate of cells following surfactant application, in order to evaluate the reversibility of surfactant effects. Additionally, the connection between cell death and mitochondrial membrane potential was explored using an inhibitor of mitochondrial hyperpolarisation.

Results illustrate that exposure of Caco-2 cells to Solutol HS15 concentrations ≥1 mM induces the irreversible activation of mitochondrial-mediated apoptosis after 10 minutes of application. This cell death is characterised by mitochondrial depolarisation, caspase activation and nuclear fragmentation. Furthermore, this mechanism was shown to use mitochondrial hyperpolarisation as a crucial step in its induction.

5.1. Introduction

The main objective of this chapter is to provide an insight into cellular processes occurring in Caco-2 cells following Solutol HS15 exposure in order to establish the mechanism(s) of toxicity. Data presented in previous chapters indicate that the surfactant concentrations that would enhance drug permeability, also show toxic effects, a correlation observed previously with other non-ionic surfactants[1–3].

Once toxic effects are observed questions arise regarding the surfactant safety; *Are the toxic effects reversible? What kind of cellular death is induced? What is the triggering factor?*

The difference between dead and dying cells can be determined based on morphological features[4]. The editors of Cell Death and Differentiation (CDD) journal suggest a cell *in vitro* to be declared dead when: (i) there is loss of membrane integrity; and/or (ii) total nuclear and cell fragmentation has occurred[4].

As with other surfactants, Solutol HS15 exposure, under specific conditions, results in loss of membrane integrity[3,5–7]; therefore, by the first CDD definition it would appear Solutol HS15 has induced cell death. However, given that typically the primary effect of surfactants is to permeabilise lipid membranes, it may be premature, and perhaps erroneous, to declare Solutol HS15 treated cells dead without further insight. This presented a major issue in this work when assessing cell death induced by surfactant exposure – routinely used cell death assays typically rely on a form of dye/probe exclusion test; the exclusion of cell plasma membrane impermeable indicators, e.g. propridium iodide (PI) or tryphan blue[8,9]. The determination of cell death should therefore be made by

assessing criteria (ii) above, by observing cell/nuclear fragmentation.

Cell death can occur through different mechanisms which are defined by their physiological implication and nature. It is crucial to correctly assess cell death in *in vitro* assessments of a tested compound, as it will have crucial implications in *in vivo* conditions. For example; if the mode of death is immunogenic it will induce inflammation in the surrounding tissue *in vivo*, which can confound the desired response. Customarily, cell programmed cell death, such as apoptosis, has been considered as immunologically silent, whereas necrotic death as capable of inducing an immune response[10,11]. However, recent publications are demonstrating that this is not exclusively the case and immunogenic forms of apoptosis have been reported[4,12–15].

In all eukaryotes, programmed cell death plays pivotal roles in numerous biological processes including development of immunity, sculpting tissues during embryogenesis and destruction of damaged cells[16–18]. Apoptosis is the most studied form of programmed cell death however, this classification also applies to other mechanisms including autophagy and forms of regulated necrosis, such as necroptosis[17,19,20].

In apoptotic death, cells undergo morphological changes that aim to avoid release of cellular components into the extracellular milieu, and thus prevent development of an immunogenic response. This is, in essence, achieved by 'breaking' the cell into multiple vesicles known as apoptotic bodies. To do so, the cell cytoskeleton collapses, cells 'shrink' and condense, the nuclear envelope dismantles and DNA is fragmented.

Studies on apoptotic cell death demonstrate that this mode of cell death is promoted by several different pathways, whereby the major regulators appear to be the Bcl-2 family of proteins, which have both pro- and anti-apoptotic functions[21–23], and the caspase family of proteases[23–27].

Two principle routes that lead to apoptotic cell death are the intrinsic (mitochondrial) and the extrinsic pathways, both of which involve an activation phase which is then followed by an execution phase. Effector caspases are responsible for the proteolytic actions, which mediate the morphological changes associated with apoptosis[26–28], whereas initiator caspases are involved in the activation phase, initiating the apoptotic signal and activating the effectors[26,27,29]. The effector caspases 3 and 7 participate in both intrinsic and extrinsic apoptosis. The initiator caspases are specific however, and dependent upon the apoptotic pathway induced; for example, caspases 8 and 10 are associated with the extrinsic route and caspase 2 and 9 the intrinsic.

The extrinsic route is initiated by extracellular signals or triggers emanating from external ligands binding to death receptors at the cell surface. Examples of death receptor ligands include, tumour necrosis factor-alpha (TNF-α)[30–32], TNF-related apoptosis-inducing ligand (TRAIL)[32,33] and Fas ligand[34,35]. Binding of death ligands to their associated receptors induces the formation of the death-inducing signal complex (DISC) at the cytoplasmic side of the activated receptor, which in turn recruits pro-caspase-8, resulting in its dimerization and activation as caspase-8[36]. Once caspase-8 is activated it in turn cleaves, and thereby activates, the effector caspases 3 and 7, trigging the execution phase of apoptosis.

The intrinsic route of apoptosis relies on signals that initiate from the mitochondria, hence it is also known as mitochondrial apoptosis. This pathway can be triggered by a wide range of cellular stresses, including DNA damage[37], hypoxia[38], cytoskeletal disruption[39] or, heat shock[40]. These stimuli generate changes in the inner mitochondrial membrane which consequently results in membrane permeabilisation, loss of mitochondrial membrane potential ($\Delta\Psi_m$) and the cytoplasmic release of pro-apoptotic proteins from the mitochondrial intermembrane space[41–43]. This ensemble of proteins includes Smac/DIABLO, apoptosis inducing factor (AIF), endonuclease G, Omi/HtrA2, as well as cytochrome C, which upon release binds to the adaptor protein apoptotic protease-activating factor-1 (APAF1) stimulating the formation of the apoptosome[41,44,45]. The apoptosome is a large heptameric complex that recruits and activates pro-caspase-9, which then activates the effector caspases bringing about apoptotic cell death[46].

Necrotic cell death does not follow the apoptotic signal transduction pathways and is morphologically distinct; characterised by swelling of the cell nucleus and other organelles, cellular swelling and early loss of plasma membrane integrity. Even through necrosis is often the result of extensive cellular injury which leads to an 'uncontrolled' mode of cell death, an increasing body of evidence suggests that forms of this death may be more regulated, with various catabolic mechanisms and signalling pathways now being associated with what is known as programmed necrosis[17,19,20,47,48].

The uncoupling of mitochondria, ROS production, mitochondrial overload and cytosolic increases in calcium, are all processes that have been associated with regulating programmed

necrosis[4,48]. However, no signalling mediator or process has been exclusively attributed, thus one should be cautious when identifying cells as undergoing programmed necrosis[4]. A commonly used classification for cells undergoing necrotic death is early plasma membrane damage in the absence of recognised apoptotic markers[47].

Furthermore, another key distinction between apoptotic and necrotic cell death is *bioenergetics* - apoptotic events require energy, and the total loss of cellular energy (bioenergetic crisis) has been suggested to function as a molecular switch between apoptosis and necrosis[49,50].

Evidence in the literature suggests that surfactants are capable of inducing both necrosis and apoptosis, depending on their nature (head group) and concentration. Enomoto and co-workers demonstrated that cationic surfactants, such as benzalkonium chloride induce cell apoptosis at low concentrations (below CMC)[51]. This is supported by work performed on other cationic surfactants, such as quaternary ammonium surfactants, by Inácio et al. who observed the induction of apoptosis at surfactant concentrations below the CMC[52]. Interestingly, this group noted that at concentrations above the CMC, quaternary ammonium surfactants do not induce caspase activation, and furthermore, the inhibition of mitochondrial complex I was observed[52]. Taken together, the authors concluded that quaternary ammonium surfactants induce a necrotic cell death when applied at concentrations above the CMC *via* the disruption to mitochondrial energy generation[52]. This concentration-dependent induction of distinct cell death modes is also observed in an earlier study on non-ionic surfactants[53]; however only a dye exclusion test was used to assess and contrast apoptotic or necrotic death.

Interestingly, anionic and zwitterionic surfactants have only been observed to cause necrosis[51].

A study performed by Eskandani et al. reported that, at concentrations greater than its CMC, polysorbate 20 induces chromatin fragmentation in the nuclei of treated cells, and the authors attributed this to the induction of apoptosis[54]. Furthermore, polysorbate 80 was also observed to result in chromatin fragmentation and chromosomal condensation, in cells treated with surfactant concentrations above the CMC[55]. Yamaguchi et al. report that the non-ionic surfactant, Cemophor EL, induces cell shrinkage, indicative of apoptosis, but does not generate nuclear fragmentation[56]. Moreover, the authors observed increased nuclear permeability to DNA-binding dye, propridium iodide, and demonstrated that Cremophor EL-induced cell death was attenuated by reducing extracellular Ca^{2+} [56]. Taken together, it was concluded by Yamaguchi et al. that Cremophor was most likely inducing necrosis in cells[56]. To the best of our knowledge no further studies have been conducted investigating the mechanism of cell death induced by non-ionic surfactants.

At this point in the present study it is unclear what mode of cell death will cells exposed to Solutol HS15 undergo. The observation of loss of membrane integrity (as described in section 3.3.1) could indicate necrotic death, however the profiles of mitochondrial membrane potential *versus* time and exposure concentration (hyperpolarisation followed by depolarisation, as presented in section 4.3.2) suggest mitochondrial involvement in cell death - which may point to apoptosis. Evidence from other non-ionic surfactants suggests neither apoptosis[54,55] or necrosis[53,56] can be dismissed, and that

both processes may play a part in Solutol HS15 induced cell death[53,56].

To investigate the mode of cell death, detection of effector caspase activation is employed in this work, alongside morphological assessment of cell nuclei. To study the reversibility of Solutol HS15 toxicity, and gain an insight into the kinetics of death induction, metabolic activity and caspase activation are studied post exposure following a 'recovery' period. A likely cell death trigger – rapid plasma membrane fluidisation – is compared to that of Caco-2 cells experiencing heat shock using the Laurdan probe. The association of the mitochondria with cell death is explored by employing an inhibitor of mitochondrial hyperpolarisation. Together these experiments aim to provide an understanding to the sequence of events underlying non-ionic surfactant-mediated cell death.

5.2. Methodology

5.2.1. Hoechst 33342 / Propidium iodide double staining of nuclei

To investigate potential apoptotic features of Caco-2 cells following Solutol HS15 treatment, cell nuclei were co-stained with the DNA binding dyes Hoechst 33342 (Ho) and propidium iodide (PI)[57]. Ho is cell permeable and PI is cell-impermeable; thus, Ho stains all nuclei, giving an indication of cell number and PI stains nuclei of cells with permeabilised plasma *and* nuclear membranes.

Stock solutions of PI and Ho were stored protected from light at 4ºC, and were prepared by dissolving solids in PBS to concentrations of 0.1 and 1 mg/ml, respectively, followed by sonication at 37 kHz for 5 minutes to ensure dissolution. Ho was used at a working concentration of 1 µM (0.6 µg/ml); this was achieved by diluting further in PBS.

Caco-2 cells (passages 45-55) were seeded at a density of $6x10^4$ cells *per* well in clear 24 well plates (Corning) and cultured for 48 hours in complete EMEM culture medium. Wells were washed twice with PBS after the removal of culture medium, followed by the addition of 0.5 ml treatment solution *per* well. Cells were treated with either the negative control (1% HEPE:HBSS), 10 mM Solutol HS15 (applied in 1% HEPES:HBSS), the apoptotic control (10 µM Staurosporine dissolved in 1% HEPES:HBSS containing 0.1% DMSO)[58], or the necrotic control (100% Ethanol)[59] for 240 minutes.

Following exposure, treatments were removed, wells were washed with PBS and dyes sequentially added; initially wells were incubated with 0.5 ml 1 µM Ho for 5 minutes. 10 µl 0.1 mg.ml PI was then added to the dye solution (final PI

concentration is 2 µg/ml). The resulting soluton was incubated for an additional 5 minutes, after which it was removed, the cells washed twice with PBS, and 0.25 ml PBS returned to the wells prior to imaging.

Stained cells were imaged on an inverted EVOS fluorescent microscope. This involved capturing images on the DAPI filter (Excitation 357/44 nm; Emission 447/60nm) for Ho signals and the RFP filter (Excitation 531/40 nm; Emission 593/40 nm) for PI signals. Images were then merged using ImageJ software.

5.2.2. Assessment of Caspase-3/7 activation

Activation of effector caspases 3 and 7 represent conserved events in the execution phases of both intrinsic and extrinsic apoptosis. Effector caspases are activated by cleavage at their DEVD peptide sequence which is mediated by an initiator caspase. CellEvent® Caspase-3/7 Green ReadyProbes™ Reagent (CellEvent) is a cell permeable reagent that contains a nucleic acid-binding dye conjugated to the caspase-3/7 target cleavage sequence (DEVD). The CellEvent reagent is intrinsically non-fluorescent as the DEVD peptide inhibits binding of the dye to DNA. Upon activation of the effector phase of apoptosis, cleavage of DEVD peptide sequences occurs activating caspases-3/7 and the CellEvent probe which then binds nucleic acids to generate bright green fluorescence labelling apoptotic cells. Detection of caspase-3/7 activation was performed on Caco-2 cells (passages 50-55) cultured in 96 well plates (black) and treated as described in section 2.2.4 and 2.2.6, respectively.

In addition to treatment with Solutol HS15 and the 1% HEPES:HBSS, cells were also treated with 0.01-50 µM Staurosporine to test the validity of the assay, and the concentration of the CellEvent probe used (Figure 5.1). Staurosporine is a well-established inducer of apoptosis and effector caspases[60,61].

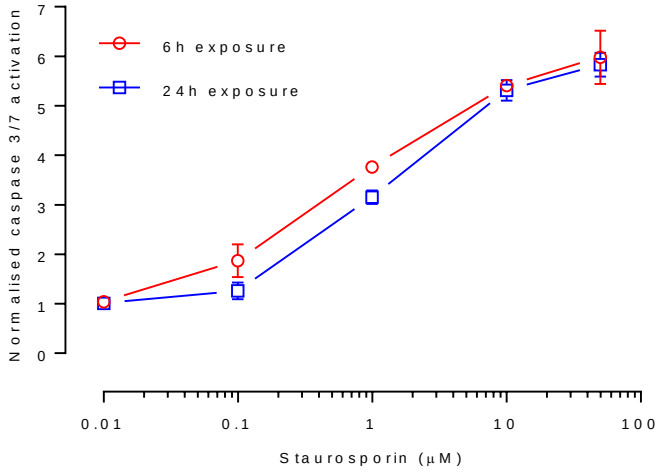

Figure 5.1. Staurosporine dose response curves of Caco-2 caspase-3/7 activation. Cells were exposed for 6 or 24 hours followed by detection with 1% CellEvent probe applied in PBS for 30 minutes. Data is presented as relative values normalised to the vehicle control (1% HEPES:HBSS) set as a value of 1, and is presented as mean ± S.D and represents triplicates from two independent experiments.

CellEvent reagent was acquired as a solution, stored at room temperature, protected from light, and prepared as a 2% (v/v) solution diluted in PBS for application. Following exposure to treatments 150 µl 2% (v/v) CellEvent:PBS solution was added directly to wells for 30 minutes without removing treatment solutions; thus the final CellEvent reagent concentration in wells was 1% (v/v). Preliminary work with staurosporine deemed this concentration of reagent appropriate to detect for the activation of caspases-3/7 (Figure 5.1).

Detection of CellEvent probe cleavage was achieved by measuring the fluorescence of well solutions following excitation at 502 nm and detection of emission at 530 nm.

5.2.3. Post exposure analysis

To study the reversibility of Solutol HS15 induced cytotoxicity metabolic activity (measured by MTS reduction) and activation of caspases-3/7 were evaluated post-exposure. This was achieved by subjecting Caco-2 cells to 'recovery' periods following varying exposure times to 1% HEPES:HBSS, Solutol HS15 or 1% (v/v) Triton X-100 (MTS assay only); this method is illustrated in Figure 5.2.

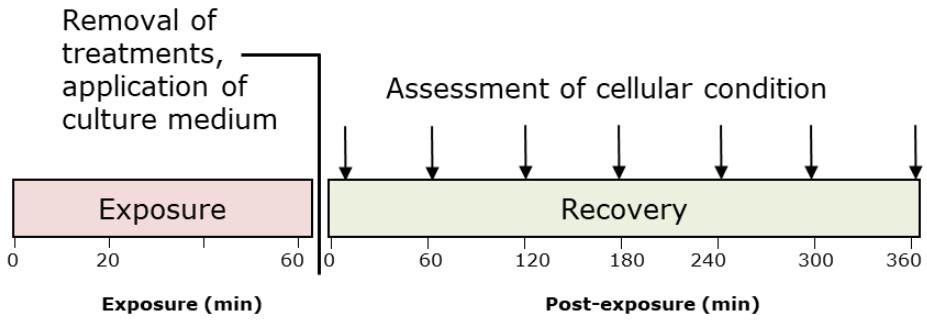

Figure 5.2. Schematic of post-exposure analysis method. Cells were exposed to treatments for 5, 10, 20 and 60 minutes. Treatments were then removed and cells were washed with PBS. Complete EMEM (without antibiotics) was then added to the cells for 60, 120, 180, 240, 300 or 360 minutes prior to measuring MTS reduction or activation of caspases-3/7.

Following recovery cells were washed with PBS and then either 150 µl 17% (v/v) MTS:EMEM or 150 µl 1% (v/v) CellEvent:PBS was added for 120 or 30 minutes, respectively. The former solution detects for MTS reduction (metabolic activity) and was

assessed by measuring resulting solution absorption at 492 nm, and data processed into relative metabolic activity values as described in section 4.2.1.1. The CellEvent:PBS solution probes for the activation of caspases-3/7 and activity was detected, as described above (section 5.2.2).

5.2.4. FCCP inhibition of mitochondrial membrane hyperpolarisation

FCCP is a mitochondrial uncoupler that acts a protonophore in the inner mitochondrial membrane. Results gathered by others in the literature demonstrates that at low concentrations, FCCP exerts an antiapoptotic effect by inhibiting mitochondrial membrane potential hyperpolarisation[62,63]. Thus, FCCP presents itself as a useful tool to investigate the role of mitochondrial hyperpolarisation.

Stock solutions of FCCP were prepared at a concentration of 10 mM by dissolving the FCCP solid in DMSO. The resulting solution was sonicated at 37 kHz to ensure dissolution, aliquoted into microcentrifuge tubes at a volume of 25 µl and stored at -20ºC until use. FCCP was diluted in 1% HEPES:HBSS for the application on cells.

Caco-2 cells (passage 40-55) were subjected to the co-treatment of FCCP and Solutol HS15; this involved preparing FCCP and Solutol HS15 at 2X their desired concentration, mixing in equal parts (1:1) and then adding 150 µl of the resulting solutions *per* well.

The first experiments assessed the effect of FCCP concentration on Caco-2 mitochondrial membrane potential, using the JC-1 assay, to determine a non-toxic range; toxicity was identified

by depolarisation of the potential. This was then followed by investigating the effect of a range of non-toxic FCCP concentrations with 10 mM Solutol HS15 on Caco-2 mitochondrial membrane potential to evaluate if FCCP had the desired effect of inhibiting hyperpolarisation induced by Solutol HS15. These preliminary studies are shown in Figure 5.8 and from these 0.5 μM FCCP was selected as an appropriate concentration.

5.2.5. Laurdan polarisation

Caco-2 cells (passage 40-45) were heat shocked by the application of 1% HEPES:HBSS warmed to 42ºC. To maintain this temperature in the experimental system, the internal temperature of the plate reader (TECAN, Spark 10M) was set to 42ºC.

To assess effect of temperature on plasma membrane fluidity, Laurdan general polarisation (GP) was employed as described in section 3.2.4 using the Laurdan pre-loaded method.

5.3. Results

5.3.1. Mode of cell death

5.3.1.1. Hoechst 33342 / Propridium iodide double staining of nuclei

Figure 5.3 presents fluorescence microscopy obtained images of Hoechst 33342 (Ho) and popridium iodide (PI) double staining of Caco-2 nuclei. It depicts that treatment with 10 mM Solutol HS15 solution for 240 minutes induces positive PI staining of all cells within the imaged population, similar to the necrotic control (ethanol); as indicated by the purple colour of nuclei in the merged images (Ho/PI). Exposure to the negative control (1% HEPES:HBSS) and the apoptotic control (10 μM staurosporine) for 240 minutes did not result in positive double Ho/PI staining; only the blue Ho staining is present in nuclei of merged images (Figure 5.3).

The formation of nuclear fragmentation, a pro-apoptotic feature, is noted in some Solutol HS15, as well as the staurosporine control treated cells (Figure 5.3; inserts i and ii; indicated by white arrows).

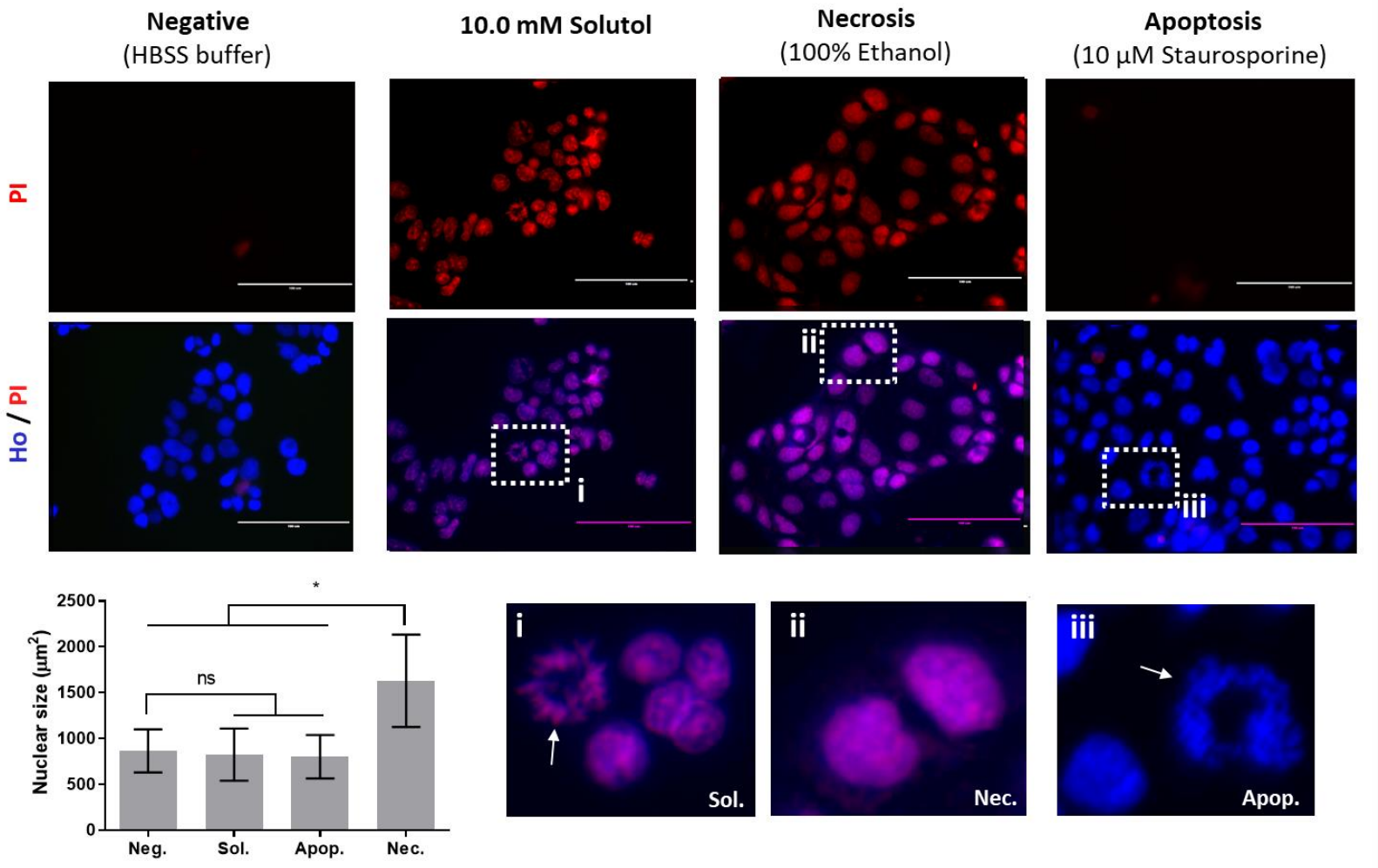
Negative
(HBSS buffer)
10.0 mM Solutol
Necrosis
(100% Ethanol)
Apoptosis
(10 µM Staurosporine)
PI
Ho / PI
i
ii
iii
Nuclear size (µm²)
2500
2000
1500
1000
500
0
ns
*
Neg.
Sol.
Apop.
Nec.
Sol.
Nec.
Apop.

Figure 5.3. Hoechst 33342 and propidium iodide double staining of Caco-2 nuclei. Top row of micrographs show propidium iodide (PI) staining imaged on RFP filter (Excitation 531/40nm; Emission 593/40nm); bottom row shows merged images of PI staining with Hoechst 33342 (Ho) (Ho/PI), Ho stain was imaged on DAPI filter (Excitation 357/44nm; Emission 447/60nm) and images merged using ImageJ software. Images shown are representative of other images gathered (N=3). Cells were exposed to treatments for 240 minutes and imaged on EVOS microscope 40X magnification (scale bar 100 µm). Bar chart illustrates the mean ± S.D of nuclei size (μm^2) of treated cells (Neg, negative control; Sol., 10 mM Solutol; Apop., 10 µM Staurosporine; Nec., 100% Ethanol) measured using ImageJ analysis software and comes from the counting of at least 100 cells per group. Statistical significance measured using one-way ANOVA (ns, not significant; *, $p < 0.05$). Inserts (i,ii and iii) represent enlarged areas highlighted by white dotted boxes from Ho/PI micrographs and used to highlight morphological differences between nuclei of treatments. White arrows are used to single out nuclei with apoptotic features.

Nuclear fragmentation was a feature observed in repeated Solutol HS15 treatment experiments (10.0 mM, 240 minutes); normally absent in the negative control and not observed in the necrotic treatment group. Cells treated with the necrotic control, ethanol, appeared to have swollen nuclei (Figure 5.3; insert ii). Upon further analysis of nuclei size, it is apparent that the nuclei of ethanol-treated cells are significantly larger than the other treatment groups (Figure 5.3; bar chart). Treatment with Solutol HS15, or the apoptotic control, for 240 minutes did not result in significant changes in nuclei size (Figure 5.3; bar chart).

The data in Figure 5.3 supports results from the CellTox green DNA binding assay (section 3.3.6) where Solutol HS15 applied at concentrations ≥10.0 mM induced permeabilisation of the nuclear membrane.

5.3.1.2. Assessment of Caspase-3/7 activation

To further investigate Solutol HS15 induced cell death, caspase-3 and/or 7 activation was assessed by investigating pro-apoptotic peptide cleavage using the CellEvent probe. As discussed above (section 5.1), both caspases 3 and 7 are effector caspases that implement the execution phase of apoptosis and are conserved in both intrinsic and extrinsic forms. Results presented in Figure 5.4 reveal that exposure to Solutol HS15 induces activation of effector caspases in a concentration- and time-dependent manner in Caco-2 cells.

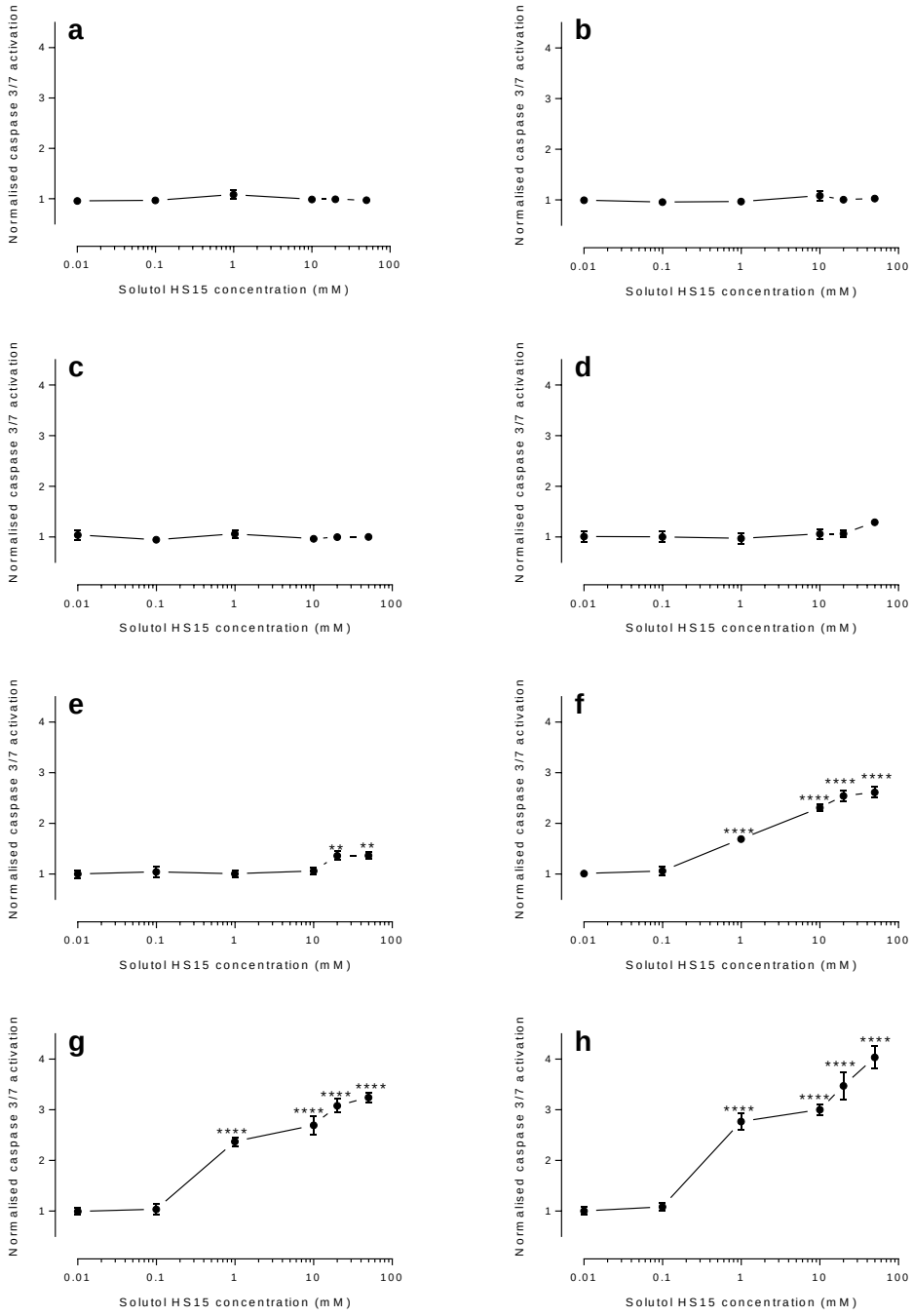

Figure 5.4. Caspase-3/7 activation in Caco-2 cells exposed to Solutol HS15. Cells were exposed for (a) 5, (b) 10, (c) 20, (d) 60, (e) 120, (f) 180, (g) 240, and (h) 360 minutes. Caspase activation was determined using the CellEvent probe. Data are presented normalised to the vehicle control (1% HEPES:HBSS), mean ± S.D and represent triplicates from three independent experiments. Statistical analysis performed by one-way ANOVA and Dunnett's multiple comparison test. *, $P < 0.05$; **, $P < 0.01$; ***, $P < 0.001$; ****, $P < 1x10^{-3}$.

No caspase-3/7 activation was observed for exposures of ≤60 minutes (Figure 5.4a,b and c). When applied for 120 minutes small, but significant increases of 1.35 ± 0.09 fold and 1.36 ± 0.07 fold were observed for 20 and 50 mM Solutol HS15 solutions, respectively (Figure 5.4e). Following 180 minutes, a large increase in caspase activation is exhibited at ≥1 mM Solutol HS15; a maximum fold-increase of 2.61 ± 0.11 induced by 50 mM Solutol HS15 (Figure 5.4f). Caspase-3/7 activation continues to increase in a time-dependent manner in cells treated with ≥1 mM. At 240 and 360 minutes, maximal fold-increases of 3.24 ± 0.10 and 4.14 ± 0.30, respectively are noted (both induced by 50.0 mM Solutol HS15) (Figure 5.4g and h).

5.3.2. Reversibility of cytotoxic effects

To examine the reversibility of Solutol HS15 induced toxic effects, cells were exposed to surfactant and then, allowed a post-exposure period of 'recovery' in growth medium while toxicity parameters were measured at certain time points to assess their trend (as per Figure 5.2 treatment scheme).

Results gathered using this approach are presented and discussed in the following sections.

5.3.2.1. Post exposure MTS reduction

Assessing metabolic activity of Caco-2 cells, by their ability to reduce MTS, revealed that the post-exposure metabolic toxicity is dependent on both the concentration and length of the exposure (Figure 5.6). Exposures to 0.01 mM Solutol HS15 did not result in any changes from basal levels of metabolic activity. Cells treated with 0.1 mM Solutol HS15 for 5 and 10 minutes did not demonstrate any post-exposure toxicity, however, following initial exposures of 20 and 60 minutes, significant decreases in metabolic activity are observed at recover periods ≥300 minutes (Figure 5.6).

Cells exposed to ≥1 mM Solutol HS15 for 10 minutes do not begin to exhibit metabolic damage until 240 minutes post-exposure, and substantial loss of metabolic activity (>80%) was observed 300 minutes post-exposure; a general trend then appears, that as exposure time is increased the time required for the emergence of toxicity is decreased (Figure 5.5). For concentrations ≥1 mM Solutol HS15, and applied for ≥10 minutes exposure, the time for occurrence of post-exposure damage appeared concentration-independent, as was the rate;

i.e., higher concentrations (10 and 50 mM) did not induce a faster rate of decline or an earlier manifestation of toxic effect compared to 1 mM, when measured at post-exposure intervals of 60 minutes (Figure 5.6).

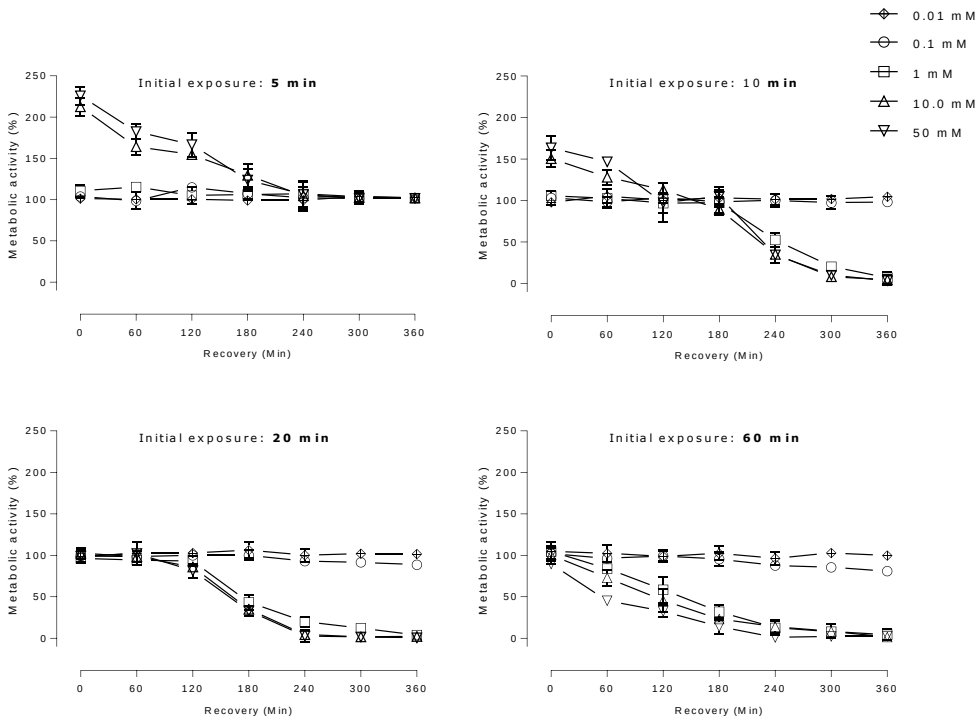

Figure 5.5. Post exposure assessment of metabolic activity. Caco-2 cells were exposed to Solutol HS15 (0.01-50 mM) for 5, 10, 20 and 60 minutes. Metabolic activity was then measured at post exposure time points using the MTS assay. Results are shown as mean ± S.D from three independent experiments.

A trend is apparent in metabolic activity *versus* recovery time profiles; detectable manifestations of the surfactant toxicity occurs for 1, 10 and 50 mM solutions after 240 minutes of recovery following an initial 10 minutes exposure, at 180 minutes recovery following 20 minutes exposure, and at 60 minutes recovery following 60 minutes exposure (Figure 5.5).

As observed previously (section 3.2.1), immediately following a 10 minutes exposure to 10 and 50 mM Solutol HS15 a notable

increase in activity is induced. When Solutol HS15 is removed it appears that these values decrease slightly but still remain notably high 60 minutes post exposure. Metabolic activity returns to, and remain at baseline levels between 120 and 180 minutes post-exposure, however a subsequent decline is observed 240 minutes post-exposure.

Exposing cells to Solutol HS15 for 5 minutes did not appear to induce any post-exposure toxicity with any of the tested concentrations (Figure 5.5). It appears that once Solutol HS15 is removed, the excessively high metabolic activities induced by 10 and 50 mM remain above baseline levels for a considerable time; values decline over time but do not return to the baseline until measured 240 minutes post-exposure.

Analysis of the rates of metabolic decline (Figure 5.6), reveals the following: (i) once initiated, metabolic decline progressed in a linear manner; (ii) rate of decline was concentration-independent for 1, 10 and 50 mM concentrations, as no significant difference was observed between these concentrations when applied for the same initial exposure time; (iii) metabolic decline proceeded at similar rates following exposure of 10 and 20 minutes (~0.65 % *per* minute), however the rate was significantly slower following 60 minute exposures (~ 0.37 % *per* minute).

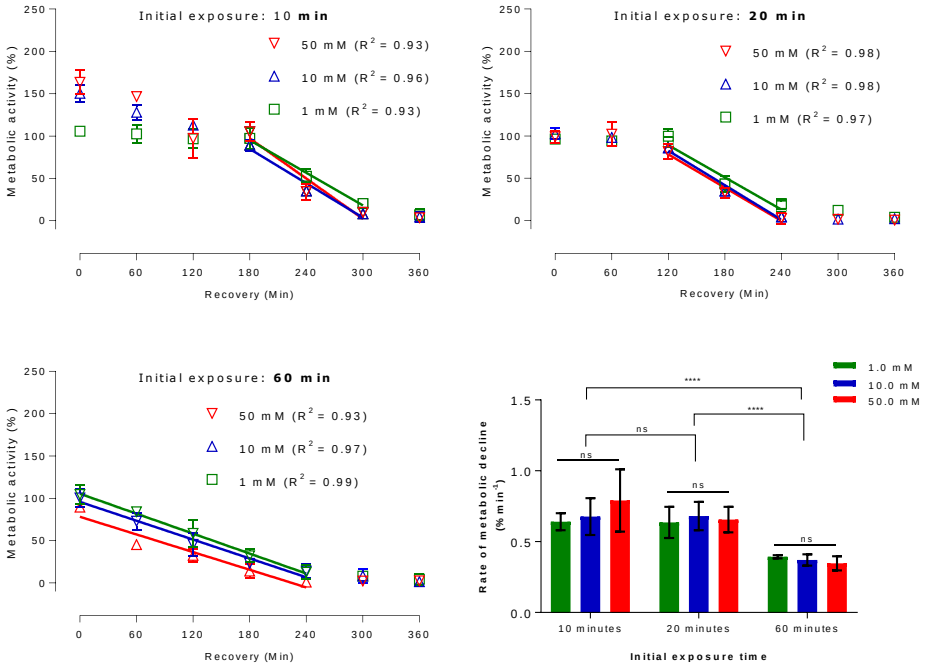

Figure 5.6. Analysis of post-exposure metabolic decline. Data represent linear regression analysis of post exposure metabolic activity values (Figure 5.5). Analysis was performed on linear portions of profiles from the initiation and end of decline (~ 100% to < 20%). Bar chart values represent mean ± standard error. Statistical analysis was performed using two-way ANOVA (ns, not significant; ****, $p < 0.0001$).

5.3.2.2. Post exposure Caspase

Observing that exposure for ≥10 minutes to Solutol HS15 above 0.1 mM induce irreversible toxicity in cells, raises the question whether the activation of cell death pathways under these conditions contributes to this. Measured *immediately* following 5, 10, 20 and 60 minutes exposures, Solutol HS15 does not appear to induce effector caspase activation (Figure 5.4, section 5.2.1.2). However, as observed with post-exposure metabolic damage (section 5.2.2.1), these conditions may still be capable to induce post-exposure caspase activation. Thus, to probe this, activation of caspase-3 or 7 was assessed 360 minutes following cell exposures for 5, 10, 20 and 60 minutes to Solutol HS15 at different concentrations (Figure 5.7).

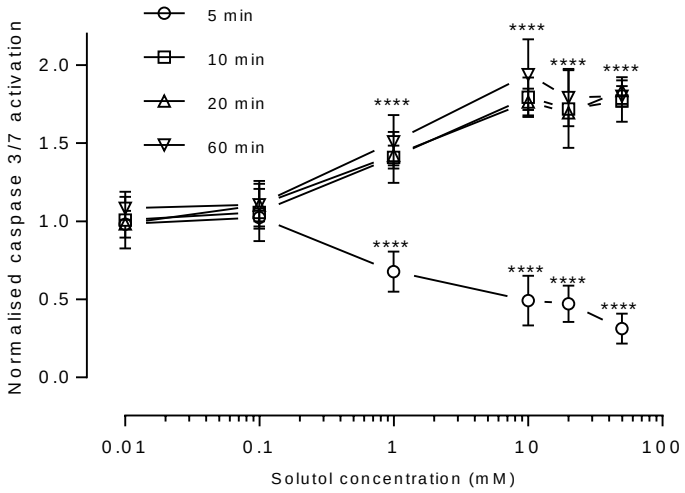

Figure 5.7. Post-exposure detection of caspase-3 or 7 activation. Caco-2 cells were initially exposed to Solutol HS15 concentrations for 5, 10, 20 and 60 minutes and subjected to a 'recovery' period of 360 minutes followed by the assessment of post-exposure caspase activation. Data presented normalised to the vehicle control (1% HEPES:HBSS), as mean ± S.D and represent triplicates from three independent experiments. Statistical analysis performed by one-way ANOVA and Dunnett's multiple comparison test. *, $P < 0.05$; **, $P < 0.01$; ***, $P < 0.001$; ****, $P < 1x10^{-3}$.

When measured 360 minutes post-exposure, analysis revealed that initial treatments of ≥10 minutes with ≥1 mM Solutol HS15 solutions generates caspase-3/7 activation in a concentration-dependent manner (Figure 5.7). Interestingly, when applied for a short period of 5 minutes concentrations of ≥1 mM Solutol HS15 induced an apparent concentration-dependent decrease in caspase-3/7 activation, relative to the vehicle control (1% HEPES:HBSS).

5.3.3. Inhibition of mitochondrial hyperpolarisation with FCCP

Results presented in Figure 5.4 and Figure 5.7 suggest that caspase-dependent cell death may be occurring, and that irreversible initiation of this pathway takes place between 5 to 10 minutes into exposure to Solutol HS15 at concentrations ≥1 mM.

To investigate a connection between mitochondrial membrane potential ($\Delta\Psi_m$) hyperpolarisation and Solutol HS15 induced cell death, a non-cytotoxic dose of the uncoupling agent FCCP was co-administered to Caco-2 cells during exposure to Solutol HS15 to inhibit hyperpolarisation[63]. Data are summarised in Figure 5.8.

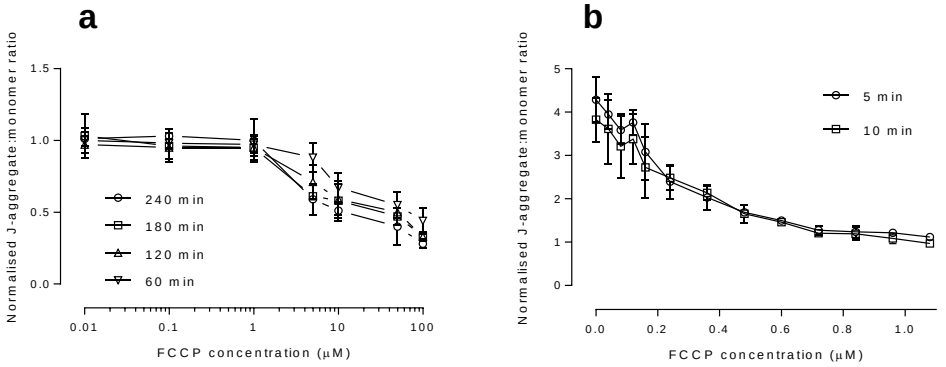

Figure 5.8. Optimisation of nontoxic FCCP inhibitor concentration. Effect of FCCP concentration on (a) basal Caco-2 $\Delta\Psi_m$ and (b) $\Delta\Psi_m$-induced by 50 mM Solutol HS15 exposures of 5 and 10 minutes, as determined by the JC-1 assay. Data are presented as mean ± S.D and represents triplicates from three independent experiments.

FCCP exhibited a depolarising effect on Caco-2 $\Delta\Psi_m$ when applied at concentrations >1.0 µM for 60 minutes or greater (Figure 5.8a). Non-toxic FCCP concentrations (≤1.0 µM) were thus applied to investigate their capacity to inhibit the $\Delta\Psi_m$ hyperpolarisation induced by exposure to 50 mM Solutol HS15 (Figure 5.8b). FCCP had a concentration-dependent effect on inhibiting hyperpolarisation. 0.5 µM FCCP was selected as a concentration capable of reducing Solutol HS15 induced $\Delta\Psi_m$ hyperpolarisation in a non-toxic manner (Figure 5.8).

Following the above optimisation, further experiments assess cytotoxicity parameters, both membrane- and mitochondrial-related, following Caco-2 cell exposure to Solutol HS15 in the presence of 0.5 µM FCCP - in order to ascertain what influence inhibiting $\Delta\Psi_m$ hyperpolarisation has on Solutol HS15 induced cytotoxicity, thus exploring the role of this feature.

5.3.3.1. Effect of FCCP on Solutol HS15 induced mitochondrial membrane potential

As indicated from preliminary results (Figure 5.8b), further work demonstrates that application of FCCP (0.5 μM) alongside Solutol HS15 resulted in significantly reducing the magnitude of $\Delta\Psi_m$ hyperpolarisation following exposures of 5, 10 and 20 minutes to ≥ 0.1 mM Solutol HS15 (Figure 5.9a, b and c).

Moreover, FCCP treatment significantly affected the kinetics of Solutol HS15 induced $\Delta\Psi_m$ depolarisation (Figure 5.9d,e,f and g). Co-treatment with FCCP confers Caco-2 cells the ability to withstand longer exposures of Solutol HS15 prior to depolarisation of $\Delta\Psi_m$; unlike cells exposed to the surfactant alone, FCCP co-treated cells demonstrate no depolarisation at 60 or 120 minutes exposure, and when this effect does occur at 180 and 240 minutes it appears significantly reduced at Solutol HS15 concentrations ≤10 mM and ≤1 mM, respectively (Figure 5.9).

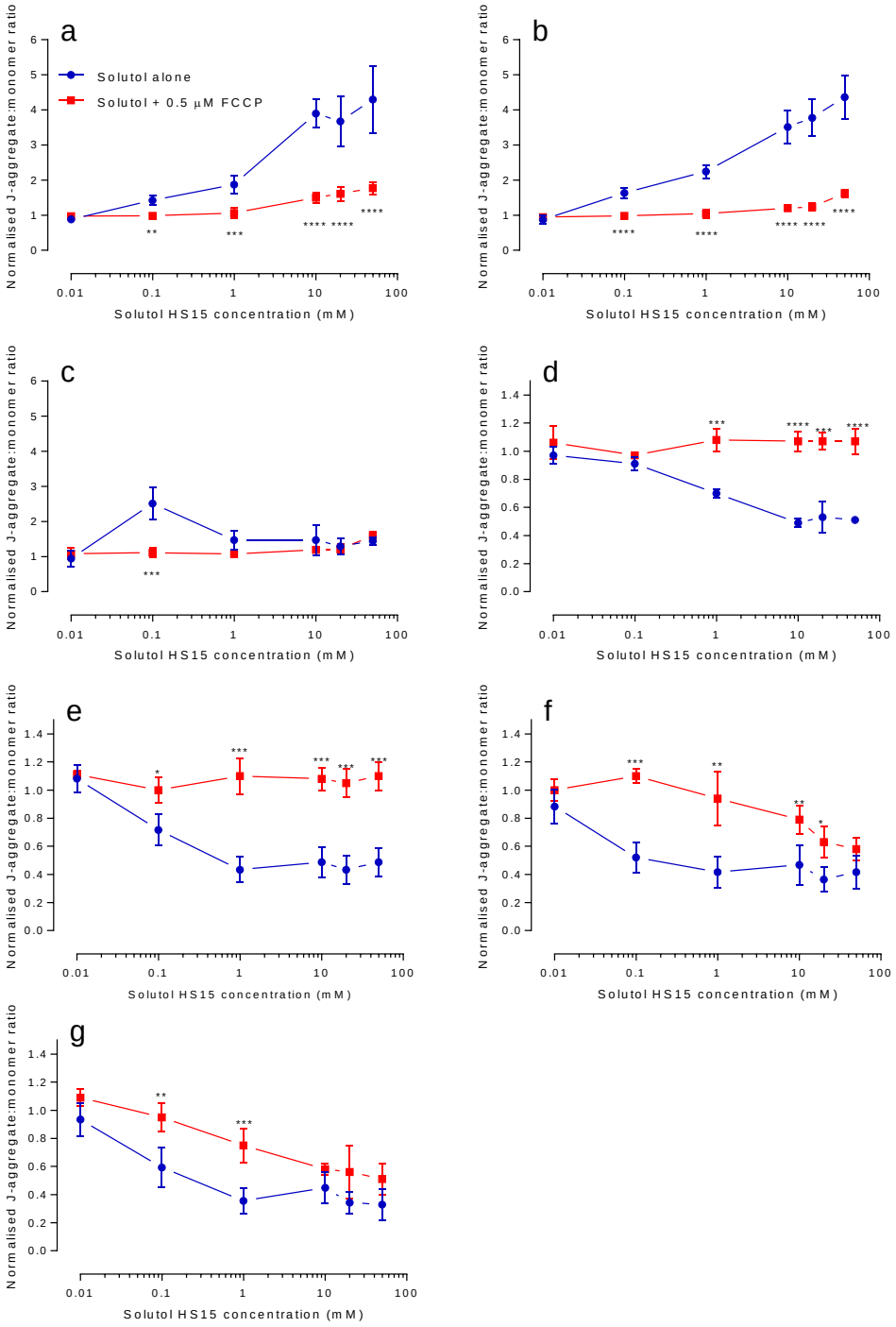

Figure 5.9. Effect of 0.5 µM FCCP treatment on $\Delta\Psi_m$ induced by exposure to Solutol HS15. Caco-2 cells were exposed for (a) 5, (b) 10, (c) 20, (d) 60, (e) 120, (f) 180 and (g) 240 minutes. Data are presented as values normalised to vehicle (set to value of 1) and 1.0 µM valinomycin (set to value of 0). Data are presented as mean ± S.D and represents triplicates from three independent experiments. Statistical analysis performed by one-way ANOVA and Dunnett's multiple comparison test. *, $P < 0.05$; **, $P < 0.01$; ***, $P < 0.001$; ****, $P < 1x10^{-3}$.

5.3.3.2. Effect of FCCP co-treatment on Solutol HS15 induced effector caspase activation

Data presented in Figure 5.10 demonstrate that inhibiting $\Delta\Psi_m$ hyperpolarisation with FCCP (0.5 µM) had a significant effect on the Solutol HS15 induced activation of effector caspases-3/7. It can be observed that co-treatment with FCCP suppresses caspase activation induced by Solutol HS15 exposures of ≥120 minutes.

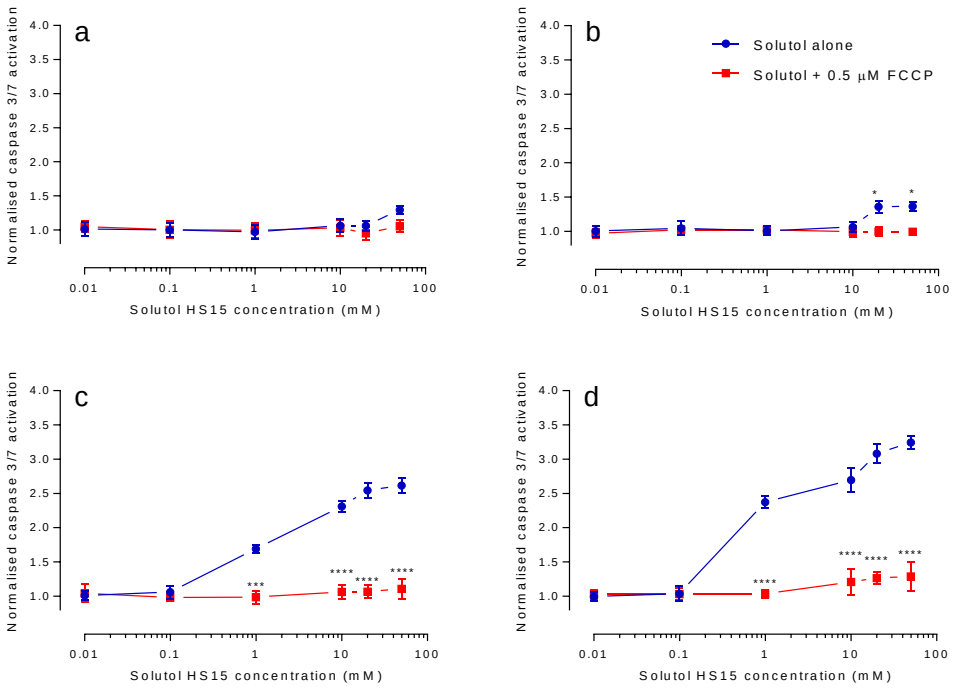

Figure 5.10. Effect of 0.5 µM FCCP on Solutol HS15 induced caspase-3/7 activation. Caco-2 cells were exposed for (a) 60, (b) 120, (d) 180 and (e) 240 minutes and caspase activation measured immediately. Data presented normalised to the vehicle control (1% HEPES:HBSS), mean ± S.D and represent triplicates from three independent experiments. Statistical analysis performed by one-way ANOVA and Dunnett's multiple comparison test. *, $P < 0.05$; **, $P < 0.01$; ***, $P < 0.001$; ****, $P < 1x10^{-3}$.

5.3.3.3. Effect of FCCP co-treatment on Solutol HS15 induced metabolic activity

The effect of FCCP co-treatment with Solutol HS15 on Caco-2 metabolic activity, measured by the MTS reduction assay. Data summarised in Figure 5.11 demonstrate that FCCP treatment produced a significant effect on metabolic activity; it prolongs the metabolic burst observed on short exposures to high surfactant concentrations and reduces the decline in metabolic activity observed on longer exposures to concentrations ≥1 mM (Figure 5.11).

Interestingly, FCCP co-treatment did not alter the initial metabolic burst elicited by higher Solutol HS15 concentrations that is observed following a 5 minute exposure (Figure 5.11a). After a 10 minute exposure, FCCP co-treatment induces metabolic activities significantly higher than cells exposed to Solutol HS15 alone; both treatment group values decrease relative to those observed after 5 minutes however co-treatment with FCCP has significantly reduced this decline and enhanced values remain >2-fold higher than the baseline (Figure 5.11b). FCCP co-treated cells appear to sustain this enhanced level of metabolic activity following 20, 60 and 120 minutes (Figure 5.11d and e). Values then return to baseline levels in cells co-treated with FCCP and ≤20 mM Solutol HS15 after 180 minutes exposure, however treatment with 50 mM Solutol HS15 reduced activity to 80.0 ± 8.7 %; nevertheless, all metabolic activity values are significantly higher than if cells are exposed to Solutol HS15 in the absence of FCCP (Figure 5.11f). Exposures of 240 minutes to FCCP and ≥10.0 mM Solutol HS15 generate metabolic decline; Solutol HS15 concentrations of 1, 10 and 20 mM remain significantly higher than those treated with Solutol HS15 alone, however treatment

with 50 mM Solutol HS15 does differ significantly between the treatment groups (Figure 5.11g).

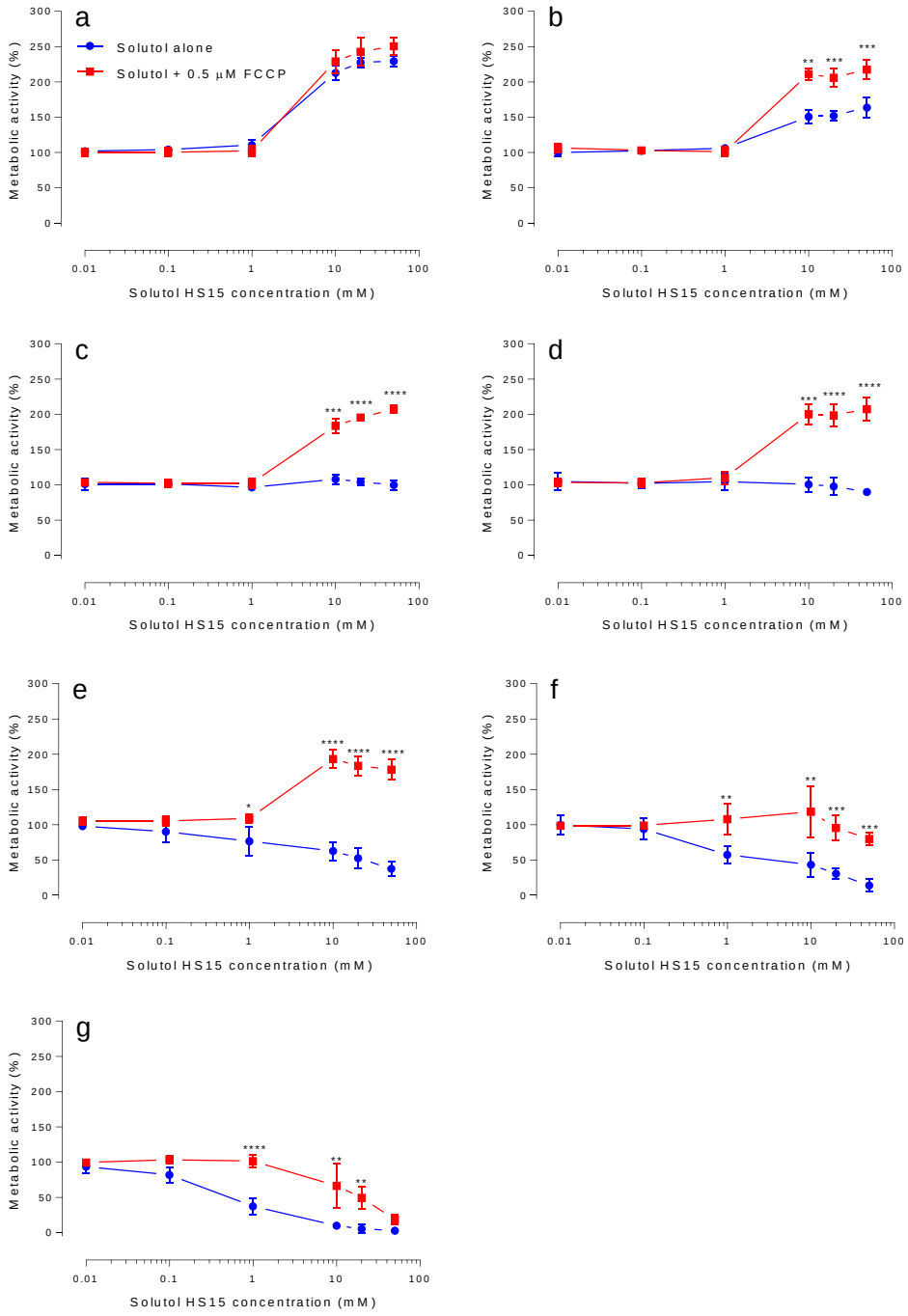

Figure 5.11. Effect of 0.5 µM FCCP on metabolic activity induced by Solutol HS15. Caco-2 cells were exposed for (a) 5, (b) 10, (c) 20, (d) 60, (e) 120, (f) 180 and (g) 240 minutes. Metabolic activity was assessed using the MTS assay. Data is presented as relative values (%) following normalisation to vehicle control (100% metabolic activity) and to 1% Triton X-100 (0% metabolic activity). Data are presented normalised to the vehicle control (1% HEPES:HBSS), mean ± S.D and represents triplicates from three independent experiments. Statistical analysis performed by one-way ANOVA and Dunnett's multiple comparison test. *, $P < 0.05$; **, $P < 0.01$; ***, $P < 0.001$; ****, $P < 1x10^{-3}$.

5.3.3.4. Effect of FCCP co-treatment on Solutol HS15 induced ROS generation

Considering the effect FCCP treatment had on $\Delta\Psi_m$ and cellular reduction capacity (metabolic activity), the effect of FCCP on Solutol HS15 induced oxidative stress was also evaluated. Assessing ROS levels following FCCP co-treatment may provide an insight into which of these mitochondrial processes is most associated with ROS formation.

Figure 5.12 illustrates how ROS levels elicited by Solutol HS15 appear unchanged with FCCP co-treatment, following exposures of 5 and 10 minutes. However, following moderate exposures of 20, 60 and 120 minutes, the FCCP co-treatment induced significant changes to the profiles of ROS generation; instead of a decrease at 20 and 60 minutes, treatment with FCCP has maintained high ROS levels. A subsequent Solutol HS15 concentration-dependent decline to sub-baseline values is noted at 120 minutes (Figure 5.12c,d and e). No significant differences are observed in ROS profiles between the two treatment groups at exposures of 180 and 240 minutes (Figure 5.12f and g).

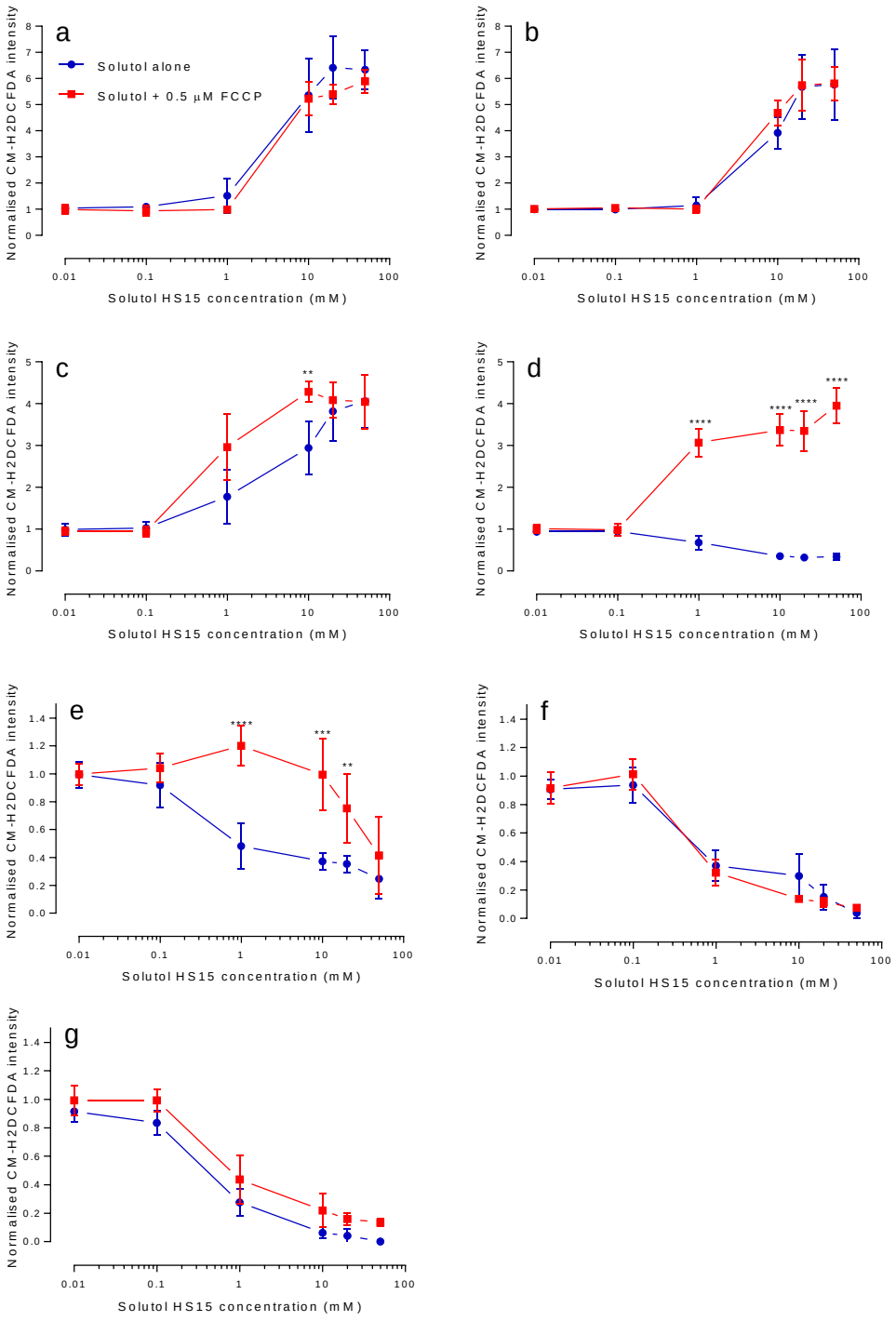

Figure 5.12. Assessment of Solutol HS15 induced ROS levels following co-treatment with 0.5 μM FCCP. Caco-2 cells were exposed for (a) 5, (b) 10, (c) 20, (d) 60, (e) 120, (f) 180 and (g) 240 minutes. ROS levels evaluated with the CM-H2DCDFA probe. Data are presented normalised to the vehicle control (1% HEPES:HBSS), mean ± S.D and represents triplicates from three independent experiments. Statistical analysis performed by one-way ANOVA and Dunnett's multiple comparison test. *, $P < 0.05$; **, $P < 0.01$; ***, $P < 0.001$; ****, $P < 1x10^{-3}$.

5.3.3.5. Effect of FCCP co-treatment on Solutol HS15 induced nuclear membrane permeabilisation

With the knowledge that FCCP treatment inhibited $\Delta\Psi_m$ hyperpolarisation and prevented the activation of effector caspases it was of interest to investigate whether this treatment had an effect on nuclear membrane permeabilisation in response to Solutol HS15 exposure. Doing so would indicate whether nuclear permeabilisation is a process associated with cell death (apoptosis) or the direct action of Solutol HS15.

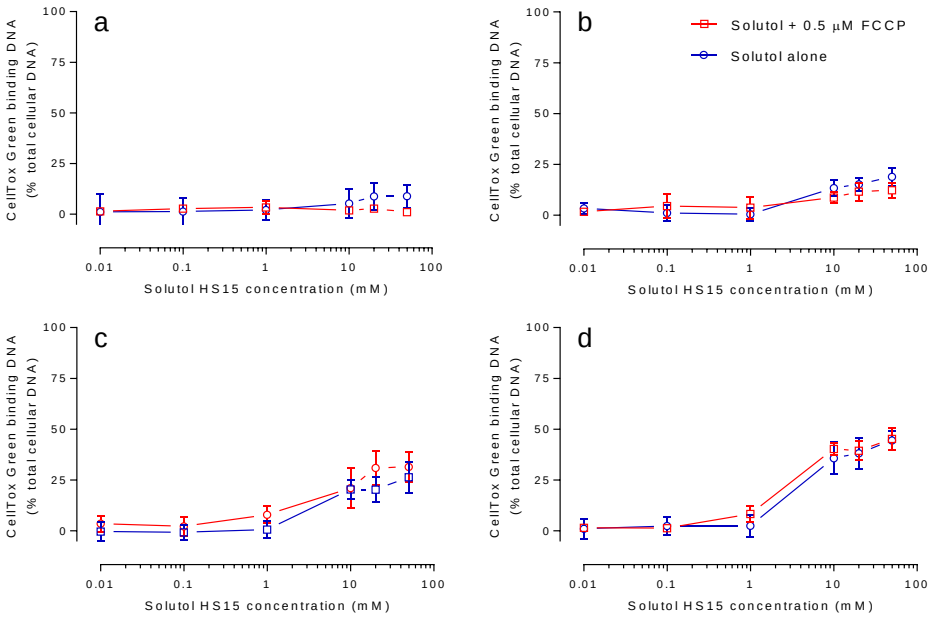

Figure 5.13. Permeabilisation of nuclear membrane induced by Solutol HS15 exposure in the presence and absence of 0.5 µM FCCP. Caco-2 cells were exposed for (a) 5, (b) 10, (c) 20 and (d) 60 minutes. Permeabilisation of nuclear membranes was assessed using the CellTox green dye. Data are presented normalised to the vehicle control (set to value of 0%) and 1% Triton X-100 (set to value of 100%), as mean ± S.D and represents triplicates from three independent experiments. Statistical analysis performed by one-way ANOVA revealed no significant differences between the treatment groups.

Using the CellTox green nuclear DNA binding dye indicates that FCCP co-treatment had no significant effect on the level of permeabilisation Solutol HS15 induces on the nuclear membranes (Figure 5.13).

5.3.3.6. Effect of FCCP co-treatment on Solutol HS15 induced plasma membrane integrity

To further study the influence of $\Delta\Psi_m$ hyperpolarisation on the cellular effects of Solutol HS15, LDH release was studied following co-treatment with FCCP. As shown in Figure 5.14 application of FCCP resulted in significantly reduced Solutol HS15 induced LDH release. This effect was particularly evident at 240 minutes exposure.

In the presence of FCCP, the emergence of LDH release at 60 minutes is absent, resulting in significant differences between co-treatment and Solutol HS15 alone at 20.0 and 50.0 mM (Figure 5.14a). Following 120 minutes exposures, cells co-treated with FCCP produce similar, albeit slightly reduced releases of LDH, however this reduction is significantly different with 50 mM Solutol HS15 (Figure 5.14b). At an exposure of 180 minutes FCCP treatment significantly reduced LDH release induced by Solutol HS15 concentrations of 0.1, 10, 20 and 50 mM (Figure 5.14c). Finally, at 240 minutes FCCP substantially, and significantly reduces LDH release at all Solutol HS15 concentrations ≥ 0.1 mM (Figure 5.14d).

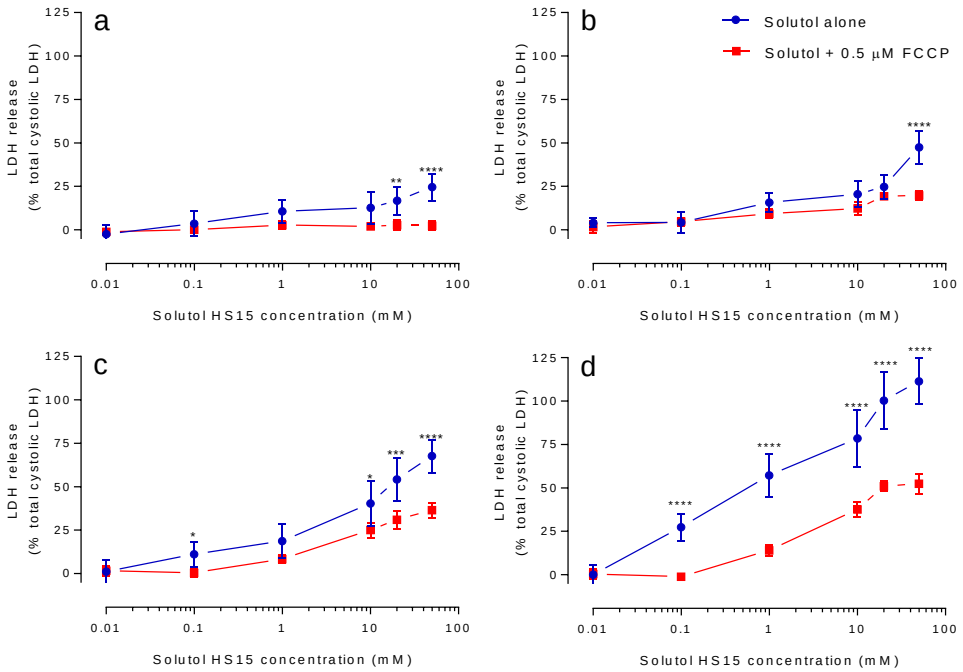

Figure 5.14. Effect of 0.5 µM FCCP on Solutol HS15 induced LDH release. Caco-2 cells were exposed for (a) 5, (b) 10, (c) 20 and (d) 60 minutes. Data are presented normalised to the vehicle control (set to value of 0%) and 1% Triton X-100 (set to value of 100%), as mean ± S.D and represents triplicates from three independent experiments. Statistical analysis performed by one-way ANOVA and Dunnett's multiple comparison test. *, $P < 0.05$; **, $P < 0.01$; ***, $P < 0.001$; ****, $P < 1x10^{-3}$.

5.3.4. Comparison to heat shock induced plasma membrane fluidisation

It is apparent from data presented above in this, and the previous chapter, that the cellular processes that are induced early during Solutol HS15 exposure (0-10 minutes) are not only prominent (e.g. metabolic burst, oxidative stress, $\Delta\Psi_m$ hyperpolarisation), but that they influence cell fate and toxicity profiles at later time points *via* irreversible activation of cell death mechanisms. Thus, deciphering the trigger that initiates these observed cellular effects is paramount in understanding these cellular responses.

Considering the speed of onset of these effects, one factor that requires consideration as the trigger is the Solutol HS15 induced fluidisation of the plasma, that occurs almost immediately (0-1 minute) upon application, as described in section 3.3.5. Fluidisation of the plasma membrane is suspected to be the mechanism of permeability enhancing action for non-ionic surfactants[5,6,64].

A factor that is described in the literature to induce fluidisation of the plasma membrane is heat shock (stress)[65–67], and it has been well established that heat stress can stimulate cell survival and cell death pathways[67–71]. Moreover, work from a group at the Biological Research Centre of the Hungarian Academy of Sciences, have shown that compounds that induce an increase in membrane fluidisation (benzyl alcohol and heptanol) can initiate a similar cellular response to that of heat shock[72]. Thus, the Laurdan probe was employed in the present work to assess if Caco-2 plasma membrane fluidisation induced by a temperature (42ºC), that is reported to induce the heat shock response[73,74], can be compared in its kinetics and magnitude to that of Solutol HS15's effect.

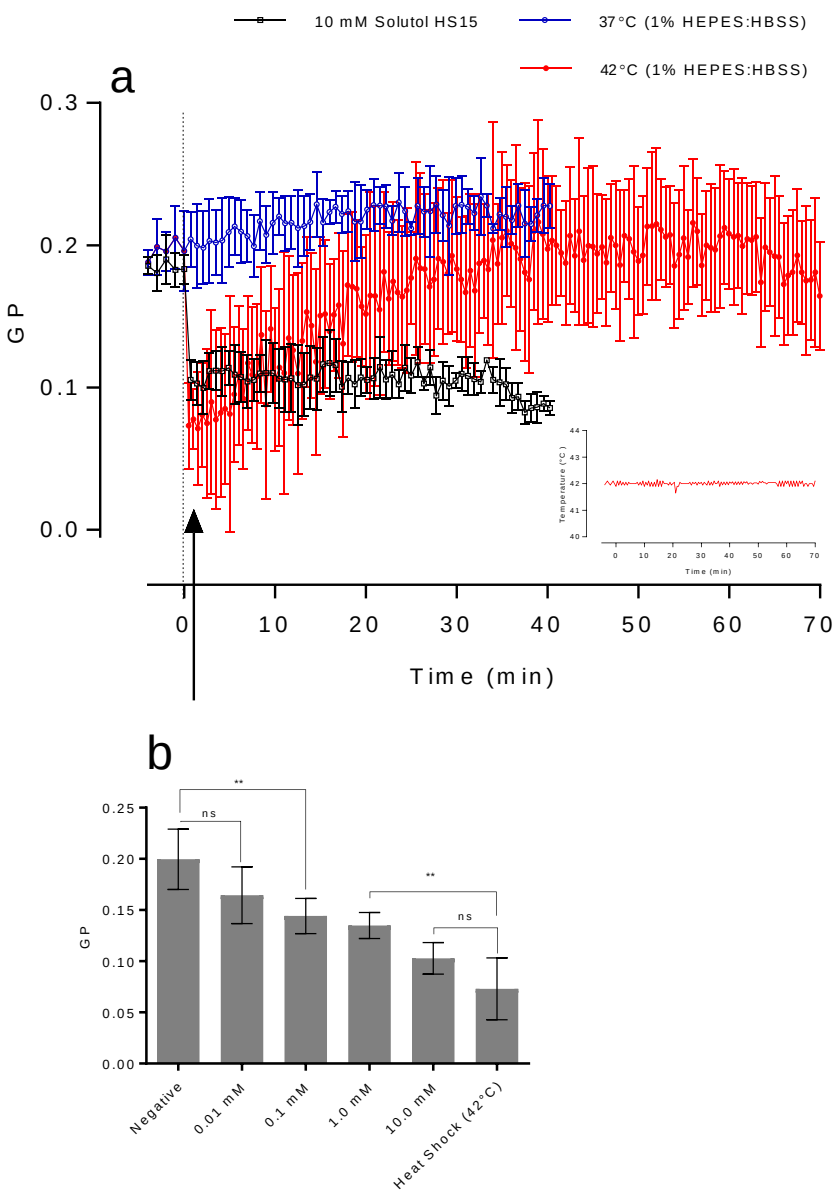

Figure 5.15. Caco-2 heat shock (42°C) effect on Laurdan generalised polarisation (GP). (a) GP fluctuations measured *versus* time following heat shock at 42°C in 1% HEPES:HBSS (dotted line). For reference, Larudan GP profiles of 1% HEPES:HBSS applied at 37°C and 10 mM Solutol HS15 are displayed (original displayed in Figure 3.8). GP values from -4 to 0 minutes represent baseline values. Values represent mean ± S.D of triplicates from three independent experiments. Insert displays average (mean) temperature of system (TECAN plate reader interior) measured throughout repeats. (b) Bar chart comparing GP values of Solutol HS15 and heat shock treatments 1 minute into exposure.Statistical analysis performed by one-way ANOVA and Dunnett's multiple comparison test. ns, not significant; **, P<0.01

Exposure to buffer heated to heated to 42°C (1% HEPES:HBSS) resulted in the rapid fluidisation of Caco-2 plasma membrane, as indicated by the sharp drop in Laurdan GP values (Figure 5.15). Following this initial drop GP values gradually increased over time and returned to their original GP level at approximately 40 minutes (Figure 5.15a). This apparent recovery of GP was unexpected at this temperature[73,74]. It is possible that 42°C induces non-lethal, reversible membrane effects in Caco-2 cells. Thus, it would be of interest to study the consequence of temperatures > 42°C. It should be noted that the temperature of the system remained constant at 42°C throughout exposure (Figure 5.15a insert), hence the GP value profile is not reflecting the system's cooling down to physiological temperature. It is apparent that GP values from heat treated cells had high levels of variation (standard deviation); the reason for this is unclear, but may be related to temperature differentials across the 96 well plates (temperature measurement was made by an internal sensor in the plate reader and thus did not represent individual wells).

Importantly, heat treatment induced similar effects to Caco-2 Laurdan GP values as Solutol HS15 treatment; both Solutol HS15 and heat treatment induce cell membrane fluidisation within 1 minute (Figure 5.15b). Furthermore, heat shock and Solutol HS15 exposure GP values are within a comparable range at high surfactant concentrations (no observed significant difference). However, while capable of reducing GP values, the effect of 1 mM Solutol HS15 was deemed significantly different to that induced by heat treatment (Figure 5.15b).

5.4. Discussion

5.4.1. Apoptosis versus necrosis

In literature, a common assay for the assessment of apoptosis in a cell population is annexin V / PI staining measured by means of flow cytometry[4,10,11]. This assay was initially performed during the study, but suffered however, from limited cell numbers and high levels of cell fragmentation during the detection with flow cytometry (data not shown). It is speculated that the processes that are involved in this assay - trypsinisation, multiple wash steps and high pressure associated with flow - acted detrimentally on the fragile, surfactant-treated cells. Therefore, to overcome this problem, alterative, less-invasive measures of apoptosis were performed.

The experimental data summarised in this chapter demonstrate that Solutol HS15 is likely inducing cell death in a caspase-dependent manner (Figure 5.4 and Figure 5.7). Furthermore, cells presenting apoptotic bodies (nuclear fragmentation) are noted among the cell population (Figure 5.3).

Thus, taken together with lack of bioenergetic crisis (*but rather the opposite – metabolic burst*) it would appear that exposure to Solutol HS15 at concentrations ≥1 mM (~10-fold the CMC) for >5 minutes, is inducing cell death characterised by the hallmarks of apoptosis.

The early loss of cell membrane integrity (section 3.3.1, Figure 3.8), prior to activation of effector caspases (Figure 5.4), suggests however that immunogenic consequences may also be induced, despite the apoptotic nature of the cell death. This, necrotic-like characteristic may be a result of a direct action of

the surfactant on the cell membrane rather than a necrotic process.

Solutol HS15 did not induce nuclear swelling under the exposure conditions that resulted in permeabilisation of cellular membranes (absence of swelling, Figure 5.3; plasma membrane permeabilisation, Figures 3.8 and 3.9; permeabilisation of nuclear membrane, Figure 3.13). Taken alongside the observation of caspase activation, these assessments indicate that necrosis is probably not occurring in this case. Thus, permeabilisation of the nuclear and plasma membranes is most likely a consequence of the direct action of Solutol HS15 rather than associated with a necrotic mechanism of cell death.

Cell and organelle swelling, known as oncosis is well-established in non-apoptotic cell death[4,75]. Oncosis is believed to be induced by selective membrane damage and energy depletion, which result in the leakage of water and ions[76]. Disruption to energy homeostasis is described to be an important event that leads to oncosis and necrosis, as opposed to apoptosis[49,50,77]. Without sufficient ATP levels, the plasma membrane Na^+/K^+-ATPase pump will cease to function. This in turn will result in hypotonic shock **-** increased intracellular levels of sodium and chloride ions, water influx and swelling of the cytoplasm and nucleus[78,79]. Measurements on cell volume were not performed here, however the absence of nuclear swelling suggests the lack of cellular swelling. Therefore, it would appear that cells exposed to Solutol HS15 are not experiencing oncosis.

Apoptosis is associated with cell and nuclear shrinkage[80], however this was not observed in neither Solutol HS15, nor

Staurosporine treated cells; for the latter, shrinkage was an expected outcome[81]. The reason for this may lie in the chosen time scale of the experiment; typically this parameter is measured following 24 hours of cell exposure to staurosporine[81,82], thus it is likely that in the 4 hour experiment conducted in this study, there was not sufficient time for the development of this process.

5.4.2. Reversibility of cell injury

Examining the reversibility of Solutol HS15 exposure effects, revealed that exposures ≥10 minutes induce subsequent effector caspase activation and toxicity (Figure 5.7 and Figure 5.5, respectively). Taken together, the data suggest that the apoptotic cell pathway is being activated after this short exposure time. Post-exposure cell parameters were only assessed over a relatively short time period of 6 hours following treatment. It would thus be of further interest to investigate time points such as 12 and 24 hours post treatment, to determine if the observed effects are truly irreversible, or if a degree of cellular recovery is possible.

The toxicity observed post-exposure indicates that this early initiation of a cell death is contributing to the toxic cell condition (*i.e.,* metabolic decline) observed later during Solutol HS15 exposure.

Alternatively, there is a possibility that post exposure toxicity results from surfactant remaining in the test system. Removing the treatment solution and washing cells will unlikely remove all the surfactant, as a portion will almost certainly remain incorporated in the plasma membrane, which may then go on

to generate further effects. This does not however explain the dependency on exposure time (5 vs 10 minute) on post-exposure effects; previous results indicate that Solutol HS15 rapidly fluidises the cell membrane (within 60 seconds), the magnitude then remains steady over the next 40 minutes. Therefore, the level of surfactant incorporation is likely consistent between 5 and 10 minutes of exposure. Further assessment is required (such as evaluating the amount of incorporated surfactant) however it would appear that time, rather than degree of incorporation, is triggering the cell death cascade. Similarly, if level of incorporation was directly inducing activation of cell death one would expect the kinetics of induction to be concentration-dependent, *i.e.,* higher level of fluidisation equating to more surfactant incorporation, resulting in faster induction of death, which is not the case. Thus, it would appear that the cell death cascade is kinetically activated by processes which are time dependent.

Moreover, the rate of cell death associated toxicity appeared to be dependent on exposure time rather than Solutol HS15 concentration *per se*; once the threshold of 1 mM Solutol HS15 is passed, exposing cells for ≥ 10 minutes triggers the death pathway, increasing surfactant concentration did not increase rate of cell death. Direct Solutol HS15 action is most likely therefore not driving this toxicity but instead only triggering it, suggesting pro-apoptotic mechanisms are the mediators.

In this regard, it can be noted that relatively low levels of toxicity are observed following 60 minutes (~ 10% drop in metabolic activity with 50 mM), and one would not typically associate this alone to substantial cell death inducing effects[4].

In fact, the cells exposed for longer exposures (60 minutes) brought about cell death at a slower rate than cells treated for short exposures (10 and 20 minutes).

Following a 60 minutes exposure plasma membrane permeability is apparent, unlike at the shorter exposures, and this may be hindering pro-apoptotic functions. A 20 minutes exposure brought about metabolic decline post exposure at an earlier time point than 10 minutes exposure. This is likely related to the lower metabolic activity experienced immediately following a 20 minutes exposure; values following a 10 minutes exposure have further to fall.

Furthermore, post-exposure experiments demonstrated that if cells are exposed to Solutol HS15 for 5 minutes, followed by removal of surfactant, metabolic activity remains high for almost 180 minutes. Previously, in the presence of persistent exposure, the metabolic burst subsides by 20 minutes. The initiation of pro-death signalling may therefore be related to abating this response.

Interestingly following an initial 5 minutes exposure ≥1 mM Solutol HS15 induces a concentration-dependent decrease in effector caspase activation when measured post-exposure. This decrease is relative to cells treated with the vehicle control. Thus, the treatment is actively reducing background levels of apoptosis. One possibility for this arising is the induction of an anti-apoptotic environment, inducing the presence of caspase inhibition. Such a response is exhibited by cells undergoing survival mechanisms[83], such as a survival response to heat shock[84,85].

Thus, the events occurring initially (0-20 minutes) can be divided into two distinct phases, an initial 'survival phase'

characterised by a metabolic burst and anti-apoptotic effects, and a subsequent 'death initiation phase'. Thus, the observed events are most likely associated with cellular stress responses.

5.4.3. Heat shock response

Undoubtedly one of the most remarkable results gathered throughout this work was the speed at which Solutol HS15 induces effects on Caco-2 cells; membrane permeabilising effects are not noted until ≥60 minutes, however preceding this, cells undergo rapid and transient mitochondrial-associated effects. These effects include mitochondrial membrane hyperpolarisation, oxidative stress, metabolic burst (increased NADH levels), as well as the activation of the apoptotic cascade. Because of the timeline that has been established, these responses cannot be attributed to membrane permeability or toxicity (observed later) but almost certainly associated with the initial fluidisation of this membrane, the first and primary effect of surfactants and Solutol HS15, which occurs almost immediately upon exposure. The connection of a stress response relating to membrane fluidity brings us thus to the prime suspect - the heat shock response (HSR).

The HSR is a highly conserved evolutionary mechanism that is initiated by physiological or environmental stressors such as heat, bacterial infections and toxins, and is vital for survival in stressful conditions[86]. The HSR was traditionally attributed to protein denaturation[87], however activation of this pathway occurs in various circumstances where no denaturation is noted[67]. The HSR was discovered in 1962[88], and since the early research on this response, knowledge on the plasma membrane has grown considerably, and it is now widely established that

cells sense and respond to stress signals *via* the induction of membrane-associated signalling pathways[89–91].

Membrane lipid phase structure is sensitive to temperature which confers the plasma membrane the ability to act as a 'membrane thermosensor'. The use of non-proteotoxic membrane fluidisers has demonstrated that alterations in membrane fluidity are the first events in the heat sensing pathway[67]. Fluidisers such as benzyl alcohol and hydroxylamine derivatives have demonstrated an ability to activate the heat shock pathway[72,92,93]. Induction of the HSR by these compounds is achieved when they exert a fluidising effect equivalent to that caused by heat shock, notably 42°C. It is therefore possible that Solutol HS15 is inducing the HSR in a similar manner to these other membrane fluidisers, and it is elements of this response that are observed initially.

The responses of the heat shock pathway are carried out by heat shock proteins (Hsps), which mediate a variety of cytoprotective functions, and may explain some of the unexpected effects observed after 5 minutes. Hsp17, for example, has been shown to stabilise heat shocked membranes by acting like an amphitropic protein, binding weakly and reversibly to membrane lipids[94]. This membrane protective mechanism may thus be interfering with cell endocytosis and explain the early decrease observed in FD4 internalisation (section 3.3.2). Moreover, to promote survival, other heat shock proteins have been shown to provide anti-apoptotic effects during the initial HSR; for example Hsp27 negatively regulates the activation of caspase-3 by interacting with cytochrome C[84,85]. The decrease in caspase-3/7 activation observed post-exposure following a 5 minute application of Solutol HS15 may thus represent cytoprotective actions of the

HSR prior to the activation of cell death (noted after 10 minute exposures).

Once the survival aspect of this response is over however, cells undergoing heat shock will engage in cell death mechanisms. As with other environmental stresses, heat shock induces mitochondrial-mediated (intrinsic) apoptosis. Heat shock has been observed to result in mitochondrial outer membrane permeabilisation (MOMP) and induce the activation of effector caspase-3[95]. Thus, this matches observation made here regarding Solutol HS15 inducing depolarisation of $\Delta\Psi_m$ and activation of effector caspases.

Another HSR-associated event observed during Solutol HS15 exposure is the induction of early $\Delta\Psi_m$ hyperpolarisation. In addition to HSP synthesis, Balogh *et al.,* (2005) observed similar extents of hyperpolarisation in both heat treatment and treatment with membrane fluidisers, and the authors suggested this event may serve as a key signal in the HSR[72]. Mitochondrial hyperpolarisation has also been demonstrated to represent an early event in intrinsic apoptosis[63,96]. The importance of this event in Solutol HS15 exposure was explored further, and disused below.

5.4.4. Inhibition of mitochondrial hyperpolarisation

Solutol HS15 induced mitochondrial hyperpolarisation was successfully inhibited with the use of the uncoupling agent FCCP, at a non-depolarising concentration. The use of FCCP in this manner has been reported by others and provides a useful pharmacological tool to investigate the nature and role of mitochondrial hyperpolarisation in signalling[62,63]. The exact

mechanism of FCCP inhibition of hyperpolarisation remains elusive but most likely stems from the compounds ability to act as a protonphore. At low concentrations, instead of uncoupling and depolarising the mitochondria potential, FCCP may act as a buffer, or 'overflow spillway', preventing the build-up of excessively high levels of protons in the mitochondrial interior.

Inhibition of mitochondrial hyperpolarisation resulted in inhibition of subsequent effector caspase activation, suggesting that this early event is vital in the apoptotic pathway activated in response to Solutol HS15 exposure. Hyperpolarisation is observed on 5 and 10 minutes exposures, however only 10 minutes generates post-exposure toxicity and apoptotic induction. Thus, it would appear that *'sustained'* hyperpolarisation is required for triggering consequent apoptosis. The association between the mitochondrial effects and apoptosis further indicates that Solutol HS15 exposure is inducing intrinsic apoptosis.

Inhibition of hyperpolarisation also resulted in delaying mitochondrial depolarisation; it is originally observed after approximately 60 minutes, however once hyperpolarisation is inhibited it is not present until 180 minutes. Thus, it is proposed that the depolarisation observed at 60 minutes is occurring in an apoptotic manner, as discussed in section 4.4. Once the outer membrane is permeabilised, pro-apoptotic proteins are released and the intrinsic route of apoptosis progresses (as discussed above in section 5.1). Interestingly, MOMP is often considered as the 'point of no return' in the apoptotic process[42,97–99], however, data gathered here demonstrates that this threshold is passed much early in this system and is associated with mitochondrial hyperpolarisation.

The mitochondrial depolarisation occurring at the later time point of 180 minutes is likely unassociated with apoptosis due to the absence of caspase activation observed with FCCP. It is more likely that this event is a consequence of the direct surfactant permeabilisation of the mitochondrial membranes. Moreover, Solutol HS15 induced nuclear membrane permeabilisation was unaffected by FCCP treatment, suggesting this process is occurring in a non-apoptotic fashion, and also as a result of direct surfactant permeabilisation. These observations indicate the presence of surfactant in intracellular organelle membranes later during exposure. This supports the earlier discussion in section 3.4, which outlines how Solutol HS15 directly permeabilises the nuclear membranes, and how it may gain entry intracellularly to do so.

Unexpectedly, when mitochondrial hyperpolarisation and effector caspase activation are inhibited, through use of FCCP, a significant reduction in LDH release is noted. This finding could imply that the apoptotic process is inciting plasma membrane damage on top of that directly resulting from surfactant-induced fluidisation. During apoptosis, cytoskeletal reorganisation is known to occur[100–102], as is insertion of phosphatidylserine into the outer leaflet of the plasma membrane[103–105], and more recent research demonstrates that outer leaflet of the plasma membrane in apoptotic cells becomes more disordered in state[106]. These pro-apoptotic, membrane-associated effects could be confounded by the already disordered (fluidised) plasma membrane exposed to Solutol HS15. It is reasonable therefore to suggest that the induction of these apoptotic mechanisms may be further damaging the already fragile plasma membrane.

The use of FCCP to inhibit mitochondrial hyperpolarisation had an interesting effect on MTS reduction (indicating NADH levels) and on ROS levels. In the absence of hyperpolarisation, both parameters remain excessively high for prolonged periods, suggesting several notions. Firstly, the lack of FCCP inhibition indicates that these features may lie upstream of apoptotic signalling, and associated with the 'survival phase' of the cell response and not induced by hyperpolarisation. Furthermore, their sustained induction suggests that once triggered *via* sustained hyperpolarisation, the initiation of the apoptotic cascade signals for the inhibition of this response. Finally, the association between NADH (MTS reduction) and ROS levels signifies that oxidative stress is likely related to the metabolic burst rather than the hyperpolarisation (as discussed in section 4.4).

5.5. Conclusions

Data from this chapter demonstrate that irreversible cell death is induced 5-10 minutes during exposure to Solutol HS15 solutions ≥1 mM. The mode of cell death is characterised by the fragmentation of nuclei and, activation of effector caspases in a manner-dependent on the presence of mitochondrial hyperpolarisation. Furthermore, activation of this death pathway is associated with inducing mitochondrial depolarisation at 60 minutes of exposure and, metabolic decline observed at 120 minutes. Together the results indicate that surfactant exposure is inducing a form of rapid mitochondrial-mediated apoptosis in Caco-2 cells, and it is suggested that this cell death mechanism may be activated by surfactant induced plasma membrane fluidisation.

5.6. References

1. Dimitrijevic, D., Shaw, A. J. & Florence, A. T. Effects of some non-ionic surfactants on transepithelial permeability in Caco-2 cells. *J. Pharm. Pharmacol.* **52,** 157–162 (2000).

2. Anderberg, E. K., Nyström, C. & Artursson, P. Epithelial transport of drugs in cell culture. VII: Effects of pharmaceutical surfactant excipients and bile acids on transepithelial permeability in monolayers of human intestinal epithelial (Caco- 2) cells. *J. Pharm. Sci.* **81,** 879–887 (1992).

3. Lin, H. *et al.* Enhancing effect of surfactants on fexofenadine??HCl transport across the human nasal epithelial cell monolayer. *Int. J. Pharm.* **330,** 23–31 (2007).

4. Kroemer, G. *et al.* Classification of cell death: recommendations of the Nomenclature Committee on Cell Death 2009. *Cell Death Differ* **16,** 3–11 (2009).

5. Petersen, S. B. *et al.* Evaluation of alkylmaltosides as intestinal permeation enhancers: Comparison between rat intestinal mucosal sheets and Caco-2 monolayers. *Eur. J. Pharm. Sci.* **47,** 701–712 (2012).

6. Vllasaliu, D. *et al.* Epithelial toxicity of alkylglycoside surfactants. *J. Pharm. Sci.* **102,** 114–125 (2013).

7. Arechabala, B., Coiffard, C., Rivalland, P., Coiffard, L. J. M. & De Roeck-Holtzhauer, Y. Comparison of cytotoxicity of various surfactants tested on normal human fibroblast cultures using the neutral red test, MTT assay and LDH release. *J. Appl. Toxicol.* **19,** 163–165 (1999).

8. Strober, W. Trypan Blue Exclusion Test of Cell Viability. *Curr. Protoc. Immunol.* **111,** A3.B. 1-A3.B.3. (2015).

9. Kepp, O., Galluzzi, L., Lipinski, M., Yuan, J. & Kroemer, G. Cell death assays for drug discovery. *Nat. Rev. Drug Discov.* **10,** 221–237 (2011).

10. J. F. R. KERR*, A. H. W. A. A. R. Currie. APOPTOSIS: A BASIC BIOLOGICAL PHENOMENON WITH WIDE- RANGING IMPLICATIONS IN TISSUE KINETICS. *J. Intern. Med.* **258,** 479–517 (1972).

11. Thompson, C. B. Apoptosis in the pathogenesis and treatment of disease. *Science* **267,** 1456–62 (1995).

12. Faouzi, S. *et al.* Anti-Fas Induces Hepatic Chemokines and Promotes Inflammation by an NF-κB-independent, Caspase-3-dependent Pathway. *J. Biol. Chem.* **276,** 49077–49082 (2001).

13. Green, D. R., Ferguson, T., Zitvogel, L. & Kroemer, G. Immunogenic and tolerogenic cell death. *Nat. Rev. Immunol.* **9,** 353–363 (2009).

14. Casares, N. *et al.* Caspase-dependent immunogenicity of doxorubicin-induced tumor cell death. *J. Exp. Med.* **202,** 1691–1701 (2005).

15. Krysko, D. V. *et al.* Immunogenic cell death and DAMPs in cancer

therapy. *Nat. Rev. Cancer* **12,** 860–875 (2012).

16. Trambas, C. M. & Griffiths, G. M. Delivering the kiss of death. *Nat. Immunol.* **4,** 399–403 (2003).

17. Fuchs, Y. & Steller, H. Live to die another way: modes of programmed cell death and the signals emanating from dying cells. *Nat. Rev. Mol. Cell Biol.* **16,** 329–344 (2015).

18. Fuchs, Y. & Steller, H. Programmed cell death in animal development and disease. *Cell* **147,** 742–758 (2011).

19. Berghe, T. Vanden, Linkermann, A., Jouan-Lanhouet, S., Walczak, H. & Vandenabeele, P. Regulated necrosis: the expanding network of non-apoptotic cell death pathways. *Nat. Rev. Mol. Cell Biol.* **15,** 135–147 (2014).

20. Maiuri, M. C., Zalckvar, E., Kimchi, A. & Kroemer, G. Self-eating and self-killing: crosstalk between autophagy and apoptosis. *Nat. Rev. Mol. Cell Biol.* **8,** 741–752 (2007).

21. Tsujimoto, Y., Finger, L. R., Yunis, J., Nowell, P. C. & Croce, C. M. Cloning of the chromosome breakpoint of neoplastic B cells with the t(14;18) chromosome translocation. *Science (80-.).* **226,** 1097–1099 (1984).

22. Cleary, M. L., Smith, S. D. & Sklar, J. Cloning and structural analysis of cDNAs for bcl-2 and a hybrid bcl-2/immunoglobulin transcript resulting from the t(14;18) translocation. *Cell* **47,** 19–28 (1986).

23. Youle, R. J. & Strasser, A. The BCL-2 protein family: opposing activities that mediate cell death. *Nat. Rev. Mol. Cell Biol.* **9,** 47–59 (2008).

24. Vaux, D. L., Weissman, I. L. & Kim, S. K. Prevention of programmed cell death in Caenorhabditis elegans by human bcl-2. *Science* **258,** 1955–7 (1992).

25. Yuan, J. & Kroemer, G. Alternative cell death mechanisms in development and beyond. *Genes and Development* **24,** 2592–2602 (2010).

26. Hengartner, M. O. The biochemistry of apoptosis. *Nature* **407,** 770–6 (2000).

27. Thornberry, N. A. Caspases: Enemies Within. *Science (80-.).* **281,** 1312–1316 (1998).

28. Liu, X. *et al.* The 40-kDa subunit of DNA fragmentation factor induces DNA fragmentation and chromatin condensation during apoptosis. *Proc. Natl. Acad. Sci. U. S. A.* **95,** 8461–8466 (1998).

29. Thornberry, N. A. *et al.* A Combinatorial Approach Defines Specificities of Members of the Caspase Family and Granzyme B : FUNCTIONAL RELATIONSHIPS ESTABLISHED FOR A Combinatorial Approach Defines Specificities of Members of the Caspase Family and Granzyme B. **272,** 17907–17911 (1997).

30. Micheau, O. & Tschopp, J. Induction of TNF receptor I-mediated apoptosis via two sequential signaling complexes. *Cell* **114,** 181–190

(2003).

31. Gaur, U. & Aggarwal, B. B. Regulation of proliferation, survival and apoptosis by members of the TNF superfamily. in *Biochemical Pharmacology* **66,** 1403–1408 (2003).

32. Wang, S. & El-Deiry, W. S. TRAIL and apoptosis induction by TNF-family death receptors. *Oncogene* **22,** 8628–8633 (2003).

33. LeBlanc, H. N. & Ashkenazi, A. Apo2L/TRAIL and its death and decoy receptors. *Cell Death Differ.* **10,** 66–75 (2003).

34. Scaffidi, C. *et al.* Two CD95 (APO-1/Fas) signaling pathways. *EMBO J.* **17,** 1675–1687 (1998).

35. Waring, P. & Müllbacher, A. Cell death induced by the Fas/Fas ligand pathway and its role in pathology. *Immunology and Cell Biology* **77,** 312–317 (1999).

36. Kischkel, F. C. *et al.* Cytotoxicity-dependent APO-1 (Fas/CD95)-associated proteins form a death-inducing signaling complex (DISC) with the receptor. *EMBO J.* **14,** 5579–88 (1995).

37. Rich, T., Allen, R. L. & Wyllie, a H. Defying death after DNA damage. *Nature* **407,** 777–783 (2000).

38. Sendoel, A. & Hengartner, M. O. Apoptotic Cell Death Under Hypoxia. *Physiology* **29,** 168–176 (2014).

39. Tricker, E. *et al.* Apoptosis induced by cytoskeletal disruption requires distinct domains of MEKK1. *PLoS One* **6,** (2011).

40. Gu, Z. T. *et al.* Heat stress induced apoptosis is triggered by transcription-independent p53, Ca2+ dyshomeostasis and the subsequent Bax mitochondrial translocation. *Sci. Rep.* **5,** 11497 (2015).

41. Saelens, X. *et al.* Toxic proteins released from mitochondria in cell death. *Oncogene* **23,** 2861–2874 (2004).

42. Green, D. R. & Kroemer, G. The pathophysiology of mitochondrial cell death. *Science* **305,** 626–629 (2004).

43. Decaudin, D., Marzo, I., Brenner, C. & Kroemer, G. Mitochondria in chemotherapy-induced apoptosis: A prospective novel target of cancer therapy (Review). *International Journal of Oncology* **12,** 141–152 (1998).

44. Chinnaiyan, A. M. The apoptosome: heart and soul of the cell death machine. *Neoplasia* **1,** 5–15 (1999).

45. Hill, M. M., Adrain, C., Duriez, P. J., Creagh, E. M. & Martin, S. J. Analysis of the composition, assembly kinetics and activity of native Apaf-1 apoptosomes. *EMBO J.* **23,** 2134–45 (2004).

46. Reubold, T. F., Wohlgemuth, S. & Eschenburg, S. Crystal structure of full-length Apaf-1: How the death signal is relayed in the mitochondrial pathway of apoptosis. *Structure* **19,** 1074–1083 (2011).

47. Golstein, P. & Kroemer, G. Cell death by necrosis: towards a molecular definition. *Trends in Biochemical Sciences* **32,** 37–43 (2007).

48. Festjens, N., Vanden Berghe, T. & Vandenabeele, P. Necrosis, a well-orchestrated form of cell demise: Signalling cascades, important mediators and concomitant immune response. *Biochimica et Biophysica Acta - Bioenergetics* **1757,** 1371–1387 (2006).

49. Leist, M., Single, B., Castoldi, A. F., Kühnle, S. & Nicotera, P. Intracellular adenosine triphosphate (ATP) concentration: a switch in the decision between apoptosis and necrosis. *J. Exp. Med.* **185,** 1481–6 (1997).

50. Rasola, A. & Bernardi, P. The mitochondrial permeability transition pore and its involvement in cell death and in disease pathogenesis. *Apoptosis* **12,** 815–833 (2007).

51. Enomoto, R. *et al.* Cationic surfactants induce apoptosis in normal and cancer cells. in *Annals of the New York Academy of Sciences* **1095,** 1–6 (2007).

52. Inácio, Â. S. *et al.* Mitochondrial dysfunction is the focus of quaternary ammonium surfactant toxicity to mammalian epithelial cells. *Antimicrob. Agents Chemother.* **57,** 2631–2639 (2013).

53. Perani, a *et al.* Interactions of surfactants with living cells. Induction of apoptosis by detergents containing a beta-lactam moiety. *Amino Acids* **21,** 185–194 (2001).

54. Eskandani, M., Hamishehkar, H. & Ezzati Nazhad Dolatabadi, J. Cyto/Genotoxicity study of polyoxyethylene (20) sorbitan monolaurate (tween 20). *DNA Cell Biol.* **32,** 498–503 (2013).

55. Yang, Y. W., Wu, C. A. & Morrow, W. J. W. Cell death induced by vaccine adjuvants containing surfactants. *Vaccine* **22,** 1524–1536 (2004).

56. Yamaguchi, J. Y. *et al.* Cremophor EL, a non-ionic surfactant, promotes Ca2+-dependent process of cell death in rat thymocytes. *Toxicology* **211,** 179–186 (2005).

57. Wallen CA, Higashikubo R, R. R. J. Comparison of the cell kill measured by the Hoechst-propidium iodide flow cytometric assay and the colony formation assay. *Cell Tissue Kinet.* **16,** 357–65 (1983).

58. Ivanova, S. *et al.* MAGUKs, scaffolding proteins at cell junctions, are substrates of different proteases during apoptosis. *Cell Death Dis.* **2,** e116 (2011).

59. Hoek, J. B., Cahill, A. & Pastorino, J. G. Alcohol and mitochondria: a dysfunctional relationship. *Gastroenterology* **122,** 2049–63 (2002).

60. Belmokhtar, C. A., Hillion, J. & Ségal-Bendirdjian, E. Staurosporine induces apoptosis through both caspase-dependent and caspase-independent mechanisms. *Oncogene* **20,** 3354–3362 (2001).

61. Ivanova, S. *et al.* MAGUKs, scaffolding proteins at cell junctions, are substrates of different proteases during apoptosis. *Cell Death Dis.* **2,** e116 (2011).

62. Stoetzer, O. J. *et al.* Modulation of apoptosis by mitochondrial uncouplers: Apoptosis-delaying features despite intrinsic cytotoxicity. *Biochem. Pharmacol.* **63,** 471–483 (2002).

63. Giovannini, C. *et al.* Mitochondria hyperpolarization is an early event in oxidized low-density lipoprotein-induced apoptosis in Caco-2 intestinal cells. *FEBS Lett.* **523,** 200–206 (2002).

64. Rege, B. D., Kao, J. P. Y. & Polli, J. E. Effects of nonionic surfactants on membrane transporters in Caco-2 cell monolayers. *Eur. J. Pharm. Sci.* **16,** 237–246 (2002).

65. Dynlacht, J. R. & Fox, M. H. Heat-induced changes in the membrane fluidity of Chinese hamster ovary cells measured by flow cytometry. *Radiat. Res.* **130,** 48–54 (1992).

66. Williamson, J. R., Shanahan, M. O. & Hochmuth, R. M. The influence of temperature on red cell deformability. *Blood* **46,** 611–24 (1975).

67. Vigh, L. *et al.* Plasma membranes as heat stress sensors: From lipid-controlled molecular switches to therapeutic applications. *Biochimica et Biophysica Acta - Biomembranes* **1838,** 1594–1618 (2014).

68. Richter, K., Haslbeck, M. & Buchner, J. The Heat Shock Response: Life on the Verge of Death. *Molecular Cell* **40,** 253–266 (2010).

69. Jolly, C. & Morimoto, R. I. Role of the heat shock response and molecular chaperones in oncogenesis and cell death. *J. Natl. Cancer Inst.* **92,** 1564–72 (2000).

70. Arya, R., Mallik, M. & Lakhotia, S. C. Heat shock genes - Integrating cell survival and death. *Journal of Biosciences* **32,** 595–610 (2007).

71. Pirkkala, L., Nykanen, P. & Sistonen, L. Roles of the heat shock transcription factors in regulation of the heat shock response and beyond. *FASEB J* **15,** 1118–1131 (2001).

72. Balogh, G. *et al.* The hyperfluidization of mammalian cell membranes acts as a signal to initiate the heat shock protein response. *FEBS J.* **272,** 6077–6086 (2005).

73. Malago, J. J. *et al.* Expression levels of heat shock proteins in enterocyte-like Caco-2 cells after exposure to Salmonella enteritidis. *Cell Stress Chaperones* **8,** 194–203 (2003).

74. Phanvijhitsiri, K., Musch, M. W., Ropeleski, M. J. & Chang, E. B. Heat induction of heat shock protein 25 requires cellular glutamine in intestinal epithelial cells. *Am. J. Physiol. Cell Physiol.* **291,** C290-9 (2006).

75. Majno, G. & Joris, I. Apoptosis, oncosis, and necrosis. An overview of cell death. *Am. J. Pathol.* **146,** 3–15 (1995).

76. Weerasinghe, P. & Buja, L. M. Oncosis: An important non-apoptotic mode of cell death. *Experimental and Molecular Pathology* **93,** 302–308 (2012).

77. Trump, B. F., Berezesky, I. K., Chang, S. H. & Phelps, P. C. The pathways of cell death: oncosis, apoptosis, and necrosis. *Toxicol. Pathol.* **25,** 82–88 (1997).

78. Finan, J. D. & Guilak, F. The effects of osmotic stress on the structure and function of the cell nucleus. *Journal of Cellular Biochemistry* **109,** 460–467 (2010).

79. Dahl, K. N., Kahn, S. M., Wilson, K. L. & Discher, D. E. The nuclear envelope lamina network has elasticity and a compressibility limit suggestive of a molecular shock absorber. *J. Cell Sci.* **117,** 4779–4786 (2004).

80. Bortner, C. D. & Cidlowski, J. A. A necessary role for cell shrinkage in apoptosis. *Biochem. Pharmacol.* **56,** 1549–1559 (1998).

81. Yue, T.-L. *et al.* Staurosporine-induced Apoptosis in Cardiomyocytes: A Potential Role of Caspase-3. *J Mol Cell Cardiol* **30,** 495–507 (1998).

82. Nakazono-Kusaba, A., Takahashi-Yanaga, F., Morimoto, S., Furue, M. & Sasaguri, T. Staurosporine-induced cleavage of??-smooth muscle actin during myofibroblast apoptosis. *J. Invest. Dermatol.* **119,** 1008–1013 (2002).

83. Portt, L., Norman, G., Clapp, C., Greenwood, M. & Greenwood, M. T. Anti-apoptosis and cell survival: A review. *Biochimica et Biophysica Acta - Molecular Cell Research* **1813,** 238–259 (2011).

84. Bruey, J. M. *et al.* Hsp27 negatively regulates cell death by interacting with cytochrome c. *Nat. Cell Biol.* **2,** 645–52 (2000).

85. Pandey, P. *et al.* Hsp27 functions as a negative regulator of cytochrome c-dependent activation of procaspase-3. *Oncogene* **19,** 1975–1981 (2000).

86. Akerfelt, M., Morimoto, R. I. & Sistonen, L. Heat shock factors: integrators of cell stress, development and lifespan. *Nat. Rev. Mol. Cell Biol.* **11,** 545–55 (2010).

87. Hightower, L. E. & White, F. P. Cellular responses to stress: Comparison of a family of 71–73-kilodalton proteins rapidly synthesized in rat tissue slices and canavanine-treated cells in culture. *J. Cell. Physiol.* **108,** 261–275 (1981).

88. Ritossa, F. A new puffing pattern induced by temperature shock and DNP in drosophila. *Experientia* **18,** 571–573 (1962).

89. Vigh, L., Maresca, B. & Harwood, J. L. Does the membrane's physical state control the expression of heat shock and other genes? *Trends Biochem. Sci.* **23,** 369–374 (1998).

90. Parton, R. G. & del Pozo, M. A. Caveolae as plasma membrane sensors, protectors and organizers. *Nat. Rev. Mol. Cell Biol.* **14,** 98–112 (2013).

91. Berchtold, D. *et al.* Plasma membrane stress induces relocalization of Slm proteins and activation of TORC2 to promote sphingolipid synthesis. TL - 14. *Nat. Cell Biol.* **14 VN-r,** 542–547 (2012).

92. Vígh, L. *et al.* Bimoclomol: a nontoxic, hydroxylamine derivative with stress protein-inducing activity and cytoprotective effects. *Nat. Med.* **3,** 1150–1154 (1997).

93. Török, Z. *et al.* Heat shock protein coinducers with no effect on protein

denaturation specifically modulate the membrane lipid phase. *Proc. Natl. Acad. Sci. U. S. A.* **100,** 3131–3136 (2003).

94. Török, Z. *et al.* Synechocystis HSP17 is an amphitropic protein that stabilizes heat-stressed membranes and binds denatured proteins for subsequent chaperone-mediated refolding. *Proc. Natl. Acad. Sci. U. S. A.* **98,** 3098–3103 (2001).

95. Mosser, D. D. *et al.* The chaperone function of hsp70 is required for protection against stress-induced apoptosis. *Mol. Cell. Biol.* **20,** 7146–59 (2000).

96. Perl, A., Gergely, P., Nagy, G., Koncz, A. & Banki, K. Mitochondrial hyperpolarization: A checkpoint of T-cell life, death and autoimmunity. *Trends in Immunology* **25,** 360–367 (2004).

97. Tait, S. W. G. & Green, D. R. Mitochondrial regulation of cell death. *Cold Spring Harb. Perspect. Biol.* **5,** a008706 (2013).

98. Chipuk, J. E., Bouchier-Hayes, L. & Green, D. R. Mitochondrial outer membrane permeabilization during apoptosis: the innocent bystander scenario. *Cell Death Differ.* **13,** 1396–1402 (2006).

99. Perfettini, J.-L., Roumier, T. & Kroemer, G. Mitochondrial fusion and fission in the control of apoptosis. *Trends Cell Biol.* **15,** 179–183 (2005).

100. Wang, Y., George, S. P., Srinivasan, K., Patnaik, S. & Khurana, S. Actin reorganization as the molecular basis for the regulation of apoptosis in gastrointestinal epithelial cells. *Cell Death Differ.* **19,** 1514–1524 (2012).

101. Bursch, W. *et al.* Autophagic and apoptotic types of programmed cell death exhibit different fates of cytoskeletal filaments. *J. Cell Sci.* **113,** 1189–1198 (2000).

102. Ndozangue-Touriguine, O., Hamelin, J. & Bréard, J. Cytoskeleton and apoptosis. *Biochem. Pharmacol.* **76,** 11–18 (2008).

103. Fadok, V. A. *et al.* Exposure of phosphatidylserine on the surface of apoptotic lymphocytes triggers specific recognition and removal by macrophages. *J. Immunol.* **148,** 2207–16 (1992).

104. Mariño, G. & Kroemer, G. Mechanisms of apoptotic phosphatidylserine exposure. *Cell Res.* **23,** 1247–1248 (2013).

105. Gardai, S. J. Recognition ligands on apoptotic cells: a perspective. *J. Leukoc. Biol.* **79,** 896–903 (2006).

106. Darwich, Z., Klymchenko, A. S., Kucherak, O. A., Richert, L. & Mély, Y. Detection of apoptosis through the lipid order of the outer plasma membrane leaflet. *Biochim. Biophys. Acta - Biomembr.* **1818,** 3048–3054 (2012).

6. Chapter Six – Functional epithelial culture models

Summary

The aim of this chapter was to investigate surfactant toxicity on Caco-2 intestinal epithelial cells that had been cultured using methods and techniques that may more accurately model the intestinal conditions found *in vivo.* To do so, (i) extracellular matrix coatings were used to mimic the basement membrane, (iii) fibroblast conditioned medium was employed to introduce paracrine factors, and (iii) cells were cultured on semi-permeable supports to promote the formation of a (mono)layer of differentiated, polarised epithelia.

Routine viability assays demonstrate that the introduction of these elements to culture conditions significantly influenced Caco-2 cellular responses to surfactant. Application of extracellular matrix coating to replicate the basement membrane decreased surfactant-induced metabolic and plasma membrane damage to the cells by approximately 3- and 10-fold, respectively, while culture in fibroblast conditioned medium decreased cell plasma membrane damage by approximately 50-fold, and Caco-2 culture as a differentiated monolayer reduced metabolic damage by approximately 20-fold following 240 minutes of exposure to Solutol HS15.

Thus, the decreased toxicity elicited in these cultures conditions suggests that surfactant toxicity to the intestinal epithelia may be reduced *in vivo* compared to that experienced by the routinely used Caco-2 model *in vitro*.

6.1. Introduction

The work performed thus far has illustrated the effects of the surfactant Solutol HS15 on Caco-2 intestinal epithelial cells.

The work in this chapter investigated the contribution that cell culture model (*i.e*. culture conditions) have on the cellular response to surfactant exposure. To this end, addition culture elements, aimed to create conditions more functionally relevant to *in vivo* settings were employed. The main functional elements were cell differentiation, presence of basement membrane and paracrine signalling.

The routine culture of the Caco-2 intestinal cell model for *in vitro* toxicity testing, as described in the previous chapters, is normally performed by culturing cells in a sub confluent manner on a flat plastic surface. While relatively simple and easy to maintain, this method of culturing does not replicate the main elements of epithelium in the *in vivo* environment. Therefore, the *in vitro*-*in vivo* correlation of data collected to predict a non-ionic surfactant's *in vivo* behaviour is not clear. Thus, this work investigates what effects cell culture conditions that, in a relatively simple and cost-effective manner, aim to replicate the main functional elements of *in vivo* epithelium have on the analysis of *in vitro* toxicity.

6.1.1. Rationale for improved in vitro toxicity testing

The pharmaceutical, healthcare and food industries would benefit from more predictive *in vitro* models for toxicity and efficacy testing, that aim will reduce and potentially replace the use of animal testing. The discovery and development of new pharmaceuticals is an expensive and time-consuming endeavour; new chemical entities can be dropped from development for many different reasons, however two major reasons are their toxicity and lack of efficacy[1]. In 2004, it was estimated that only 1 in every 10,000 compounds identified in the discovery phase reached the market[1]. The attrition rate for new chemical entities during pre-clinical and clinical stages is constantly increasing; between 1980-90 ~21.5% of drugs from phase I trials went on to be approved for marketing, however between 2006-15 this value is estimated at ~9.6%[2].

The most expensive phases of drug development are the pre-clinical and clinical phases. If toxicity can be better assessed and identified in the earlier phases, a toxic compound can be 'stopped' at a less expensive phase of development. To achieve this, drug discovery and development would benefit from a robust, relevant and cost-effective means of identifying safety and toxicity during the earlier development stages using *in vitro* models.

Safety studies in animals provide valuable information on a compound's toxicity; the ability to test how a *whole* system responds in unison has obvious advantages over testing *ex-vivo* or *in vitro*. That said however, the major limitations of *in vivo* toxicity testing include the need to use animals, cost and the different physiologies of animals and humans, which make predicting of human outcomes problematic. For example,

phenobarbital, a barbiturate that is on the World Health Organisation's list of Essential Medicines[3], induces liver enlargement and tumour development in rodents but not in humans[4], highlighting a false positive detection of toxicity due to species differences.

On the hand, the TGN1412 trial held in 2006 is an infamous example of a false negative. This monoclonal antibody treatment was shown to be safe and efficacious in various animal models, including on rhesus and cynomolgus monkeys[5,6]. The studies demonstrated that at a hundred times the intended human dose, no toxic reactions were observed. However despite all these indications the drug induced catastrophic systemic organ failure in patients during first in human clinical trials[7]. It is believed that a 4% difference in the homology between human and primate CD28 receptor amino acid sequence was responsible for the difference in primate and human responses[8].

Important for the work in this chapter is the fact that before testing in animals, *in vitro* studies that were conducted with TGN1412 failed to predict toxicity due to an inadequate model – the *in vitro* model chosen did not functional replicate the signalling elements responsible for the toxic response induced by TGN1412[9]. Thus, this demonstrates the importance of *in vitro* testing on an appropriate and relevant model.

Chemical safety assessment is an area that remains heavily reliant on the use of animals, despite growing efforts to reduce the number of animals or work towards their replacement[10].

This continued reliance predominantly arises from recognised limitations of *in vitro* models to accurately predict the effects of chemicals on whole, intact animals[11]. Difficultly in establishing

in vivo relevant models *in vitro*, means that, for example, cells isolated from a tissue and cultivated in the laboratory can often differ substantially in their attributes from the corresponding cell type in an organism[12,13]. Furthermore, the complex architecture and organisation of tissues is difficult to replicate *in vitro*, and consequently surfactants and other compounds are generally more toxic to *in vitro* cultures than the tissue they represent[14–17]. Ultimately, this difficulty in replicating *in vivo* conditions limits conventional *in vitro* toxicity testing as it bestows inaccuracies in extrapolating *in vivo* doses from *in vitro* studies[18].

Toxicity of the model non-ionic surfactant used in this work, Solutol HS15, was previously studied *in vivo*. In 2012 Illum et al. demonstrated that 7.5% (w/v) Solutol HS15 solution was effective at enhancing the bioavailability of nasally delivered human growth hormone in rodents in a non-toxic manner; a five day repeat dose toxicity on the nasal mucosa of rats saw no toxic effect on nasal tissue[19]. This dose (corresponding to ~80 mM) is considerably higher than that shown in this work, and in previous studies, to induce toxicity *in vitro*[20,21].

6.1.2. The Caco-2 model of intestinal epithelium

Caco-2 cells are derived from a human colon carcinoma, and have been employed for decades as a model for predicting compound absorption across the intestinal epithleium[22–25]. When cultured on a semi-permeable filter insert, Caco-2 cells differentiate to form polarised epithelial cell layers, generating a biochemical and physical barrier to the flux of ions and other molecules[26]. Caco-2 cells cultured in this manner have become

a well-established model for human intestinal epithelium to predict oral drug absorption[25,26].

However, toxicity testing on this cell line is routinely performed not on cells cultured as described above on semi-permeable membrane, but on cells cultured under 'standard' conditions – *i.e.* on flat plastic in a sub confluent manner – conditions that do not reflect those found *in vivo* (Figure 6.). The main reasons for this may include issues arising from the cost of the plastic-ware required to culture a polarised cell layer of Caco-2 cells, as well as the time required for the polarised layer to be established (typically around 3 weeks).

A situation hence arises where Caco-2 polarised cell layers are used to test, for instance, a permeability enhancer ability to increase oral bioavailability of a compound, but sub confluent cells cultured on flat plastic are used to assess it toxicity, and the two studies are taken together to judge safety and efficacy[27–29].

Differentiated Caco-2 cells in a polarised layer will express proteins not found in the undifferentiated counterparts grown on flat plastic, such as alkaline phosphatase[30], a marker for the formation of an apical brush border[31].

The intestinal epithelial brush boarder is a highly specialised apical membrane feature, that functions as a primary site of nutrient absorption and major physical barrier that, *in vivo*, restrict luminal microbe entry[32,33]. The brush boarder of a cell comprises thousands of microvilli that are tightly packed and protrude from the apical surface[33]. Microvilli are actin based cylindrical protrusions and form a cytoskeletal scaffold that are capable of supporting a large membrane surface area[34]. It is estimated that because of this arrangement, the brush boarder

can accommodate approximately 100-fold more membrane than a flat surface[35,36]. In addition to the obvious benefit with regard to housing transporters, membrane-bound enzymes and channels required for absorptive functions, studies demonstrate that microvilli can also generate vesicles[35]. This is believed to be achieved by myosin-1a motor proteins, which connect the core actin bundle to the plasma membrane[34,37], and can propel the microvilli membrane over the actin bundle, resulting in the shedding of membrane from the microvilli tips to form small unilamellar vesicle[38]. It is believed that this may confer intestinal epithelia the ability to condition the lumenal environment to hinder bacterial invasion[39,40].

As characteristic for enterocytes, differentiation of Caco-2 on semi-permeable membranes also results in the increased expression of plasma membrane transporters such as p-glycoprotein[41,42], and the excitatory amino acid transporter 1 [43]. Moreover, Anderle et al. studied the messenger RNA expression in undifferentiated and differentiated Caco-2 cells grown as a polarised layer and observed that differentiation increased the expression of genes encoding for cell adhesion proteins[44]. Indeed, a distinctive feature of polarised epithelial cell layer is their specialised cellular junctions (Figure 6.), which are regulators of monolayer permeability, and are involved in epithelial differentiation, maintaining the differentiated phenotype and supporting the cytoskeleton[45,46].

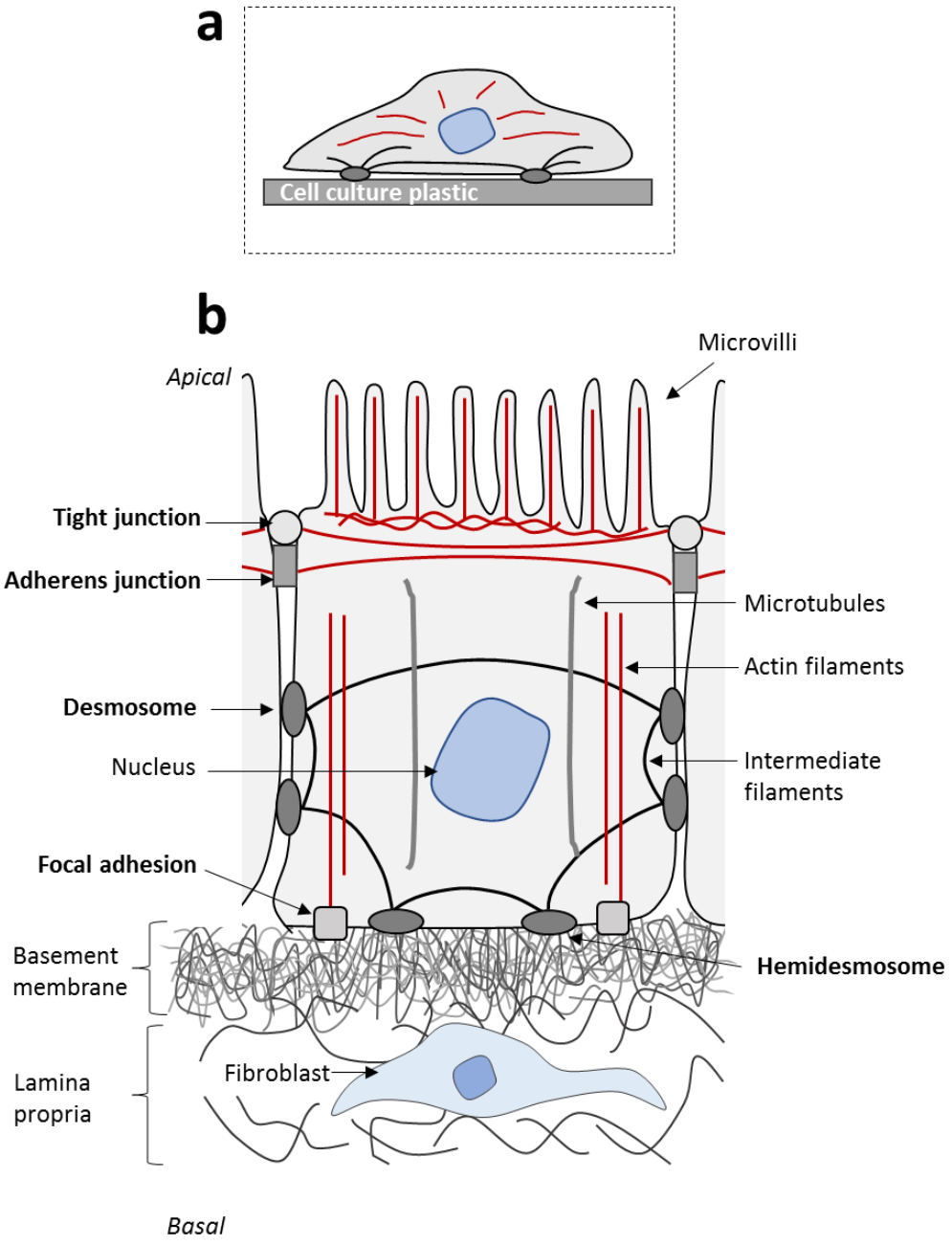

Figure 6.1. Schematic of Caco-2 cell culture environment. (a) Traditional culture for toxicity testing. Cells are grown on flat plastic, and grown in a subconfluent manner that does not promote junctional or cytoskeletal development. (b) Diagram representing intestinal epithelial condition *in vivo*. Cells grow and differentiate into polarised monolayer that promotes development of cell-cell junctional complexes. Furthermore, cells are adhered to a basement membrane structure formed from extracellular matrix material deposits, to which cell-matrix junctions attach. Cell are also supported biochemically by paracrine signalling from underlying fibroblasts in the lamina propria.

The cytoskeleton is formed from three main types of protein filaments: actin filaments, microtubules and intermediate filaments. These different cytoskeletal polymers are organised into networks that maintain cell shape and the integrity of intracellular compartments[47]. Tight junctions form the barrier that restricts the paracellular movement of water and solutes between epithelial cells, and thus across epithelial tissue layers[48,49]. A component of this junction bind, the zonula occludens 1 (ZO-1) protein, binds directly to actin and coordinates barrier fuinction[50,51]. Furthermore, underneath tight junctions in the basal direction, adherens complexes create junctions that interact with actin filaments through an interaction with a transmembrane protein component known as E-cadherin[52]. Desosomes are another cell-cell junctional complex that form connections between adjacent epithelia[53]. Desmosomes provide mechanical strength to intracellular connections through their attachments to intermediate filaments *via* desmoplakins[54,55]. Adherens junctions utilise their connections with the actomysin network, a complex of myosin and actin filaments associated with cellular movement and intracellular sorting, to remodel cell-cell interactions and confer dynamic and flexible adhesion during wound repair[56,57]. By contrasts, desmosomes, and their associated intermediate filaments, are described to function as 'molecular clamps' that reinforce intracellular junctions and provide robust anchor sites for intermediate filaments to maintain tissue architecture[54,58]. Thus, the cell-cell junctional complexes of differentiated epithelial play diverse and important roles in both cellular maintenance and adaption.

For the testing of compound toxicity on intestinal epithelia, Caco-2 cells are predominantly cultured directly on flat plastic

surfaces (Figure 6.a). However, this insufficiently reflects the *in vivo* environment in which the epithelial cells grow on a basement membrane that is composed of a variety of extracellular matrix (ECM) molecules (Figure 6.b). The basement membrane is mostly composed of different types of laminins, type IV collagen, sulphate proteoglycan and entactin[59–61]. *In vivo,* ECM molecules are secreted by both epithelial cells and underlying mesenchymal cells, such as fibroblasts, and create a framework that that promotes and maintains tissue integrity[62]. In addition to the structural role, ECM proteins are involved in control of epithelial proliferation, differentiation, gene expression, and adhesion[63,64]. Cells-ECM adhesion is facilitated by integrin transmembrane receptors at focal adhesions, and hemidesmosomes which subsequently link to actin and intermediate filament networks, respectively[65–67]. Thus, both cell-cell and cell-ECM adhesion systems are connected to the cytoskeleton, which facilitates cell polarisation. Indeed, cellular adhesion to the ECM contributes to apical-to-basal axis of epithelial polarity, *in vivo* and *in vitro*. The expression of laminin 1 *in vivo* coincides with the polarisation of kidney cells[68], and *in vitro*, addition of laminin promotes the formation of polarised epithelial cells in various cell lines, including mammary[69], salivary[70], and airway[71] cultures. Furthermore, Schreider et al. demonstrated that the functional polarisation of Caco-2 cells was promoted by seeding on ECM containing laminins and type IV collagen, which resulted in reinforcing the actin cytoskeleton and also E-cadherin functional complexes (i.e. adherens junctions)[46]; highlighting the molecular crosstalk between the two adhesion systems, cell-cell and cell-ECM.

ECM substrates have been mimicked *in vitro* by a variety of methods, including culturing cells on exogeneous ECM deposits[46,64,72], or on coatings of proteins that have been extracted from cell cultures or tissues, such as Matrigel coatings[69–71]. Additionally, *in vivo*-like substrates have also been replicated by bioengineered materials, such as hydrogels[73] and electrospun scaffolds[74]. Utilising biologically-derived material however, has the advantage of containing growth factors which confer an additional element of relevance for the *in vivo* condition[75–77].

In addition to biophysical support, epithelial cells *in vivo* are supported biochemically by paracrine signalling, provided by fibroblastic cells in the underlying lamina propria[78,79]. In addition to physical cues, provided by cell-cell and cell-ECM junctions, intestinal Caco-2 proliferation and differentiation has shown to be regulated and promoted by factors secreted by fibroblasts, such as keratinocyte growth factor (KGF), glucagon-like peptide-2 (GPLC-2), hepatocyte growth factor (HGF) and vascular endothelial growth factor (VEGF)[80–82].

Furthermore, paracrine signalling has also been demonstrated to play an important role in regulating epithelial repair[83]. Efficient repair mechanisms are crucial for preventing and limiting entry of noxious stimuli across potentially damaged intestinal epithelium[84]. For example, epidermal growth factor (EGF) is secreted by fibroblasts[85], and in addition to promoting growth and differentiation of intestinal epithelia[86], is reported to have a gastroprotective effect; preventing gastric ulceration induced by stress, aspirin, acid and ethanol[87–90]. Furthermore, pre-treatment of mouse ileal mucosal sheets, *ex vivo*, with EGF reduced the damage induced by luminally applied Triton X-100, as determined by measuring tissue resistance[91]. EGF has also

been shown to prevent damage induced by oxidative stress in Caco-2 cells[92]. Oxidative stress has been demonstrated to dissociate the tight junction proteins, ZO-1 and occludin, from the actin cytoskeleton in Caco-2 monolayers[93], and is thus associated with tight junction disruption and increasing paracellular permeability[93–95]. By binding to its transmembrane receptor in Caco-2, the EGF receptor, EGF is believed to activate the mitogen-activated protein kinase (MAPK) / extracellular-signal-regulated kinases (ERK) signalling pathways and prevent ROS induced tight junction disruption by stimulating ERK to interact with occudin[96,97]

Thus, through the use of fibroblast-conditioned media[81], co-cultures[80,82], and growth factor treatment[91,92,96,97], the importance of paracrine signalling on Caco-2 cells has been demonstrated.

The work in this chapter set out to replicate key functional elements observed in *in vivo* conditions using relatively simple, established techniques, in order to examine how surfactant toxicity may be influenced, and therefore gain *in vitro* data that may be more relevant and correlated better to *in vivo*. Caco-2 cells were cultured on semi-permeable filter inserts for 21 days to promote proliferation and differentiation into a tight monolayer of polarised cells. To replicate the ECM, Caco-2 cells were cultured in flat bottom plates that had been coated with Matrigel®, a commercially available basement membrane matrix, and to replicate paracrine signalling, cells were cultured in a medium from 3T3/NIH fibroblasts culture.

6.2. Methods

6.2.1. Replication of basement membrane

A basement membrane for epithelial culture was replicated by coating culture plates with Matrigel, a widely used commercial cell culture matrix[69–71,77,98]. Matrigel is a mixture of ECM proteins extracted from Englebreth-Holm-Swarm (EHS) tumours in mice[77,99]. It primarily consists of enactin, collagen IV and laminin and is used as a basement membrane preparation. As opposed to the thick layers of Matrigel used to investigate tumour cell migration[100], thin coatings of the mixture were applied for 2D culture of Caco-2 cells[101].

Matrigel (growth factor reduced) stock (10.2 mg/ml) was stored in 0.5 ml aliquots at -20°C and when needed thawed overnight at 4°C. All labware and medium that was used in the preparation of Matrigel coated plates was cooled to prevent premature gelling of the matrix. This involved storing pipette tips and universal tubes at -20°C for a few hours prior to use and placing the culture plates on ice. Once thawed, Matrigel was diluted in cold EMEM (without supplements) to the required concentrations (96, 480 and 960 µg/ml) and mixed by pipetting. 50 µl Matrigel:EMEM solutions of 96, 480 and 960 µg/ml were pipetted *per* well into 'standard' clear 96 well plates (well surface area = 0.32 cm^2) to achieve coatings of 15, 75 and 150 $\mu g/cm^2$, respectively, and incubated at room temperature for 2 hours in sterile conditions. Matrigel solution was then aspirated off the wells and Caco-2 cells (passage 30-40) seeded at a density of $1x10^4$ cells *per* well in complete EMEM for 48 hours (as described in section 2.2.4). Caco-2 cells cultured on Matrigel coated plates, were subjected to treatment

with 1% HEPES:HBSS, Solutol HS15 or 1% Triton X-100 solutions followed by assaying with the MTS and LDH release experiments (protocols described in sections 4.2.1.1 and 3.2.1, respectively).

6.2.2. Conservation of paracrine signalling

To investigate the influence of paracrine signalling on intestinal epithelial toxicity-induced by surfactant Solutol HS15, Caco-2 cells were cultured in medium conditioned by 3T3/NIH fibroblast cells (3T3-CM).

3T3/NIH cells (passages 15-20) were cultured in 75 cm^2 flasks in 15 ml complete EMEM until they were ~70% confluent. Culture medium was then collected and centrifuged at 200g for 5 minutes to pellet any cell debris. The supernatant was then syringe filtered, using a 0.2 µm filter, and kept. This medium was termed 3T3-CM and used immediately or stored at 4°C for a maximum of 3 days.

Caco-2 cells were routinely cultured in 15 ml 3T3-CM for at least four but no more than five passages to allow for any phenotype changes to occur. Once cells had surpassed this limit of being cultured in 3T3-CM for 5 passages they were discarded. Caco-2 cells (passage 35-45) were seeded into 96 well plates as described in section 2.2.4, with the exception of being seeded and culture in 3T3-CM instead of EMEM. 1% HEPES:HBSS, 1% Triton X-100 and Solutol HS15 were exposed to 3T3-CM cultured Caco-2 cells (as described in section 2.2.6), and the resulting effects on LDH release, nuclear membrane permeability and metabolic activity (MTS assay) were determined in the manners described in sections 3.2.1, 3.2.5 and 4.2.1.1, respectively.

6.2.3. Caco-2 differentiation using permeable inserts

Millicell-96 semi-permeable polycarbonate membrane cell culture insert plates, herein referred to as Millicell-96 inserts, are similar to the well-established Corning Transwell® filter membrane inserts[80,82,93,94,96,97,102]; they provide a culture setup with distinct apical and basolateral compartments separated by a microporous membrane. When cultured on the permeable membrane, epithelial cells are able to differentiate into a polarised monolayer. The Millicell-96 inserts have the advantage over the classical Transwell® filters of being available in a 96 well plate format, enabling a higher throughput more desirable for toxicity studies.

Prior to the addition of cells, Millicell-96 inserts were incubated with complete EMEM (75 µl and 250 µl on the apical and basolateral chambers, respectively) at 37ºC for approximately 20 minutes before being removed. This was performed to soften the membranes and coat them with FBS proteins to encourage cell attachment[103]. To prevent the formation of air bubbles underneath the permeable membranes media was added and removed to the setup in a specific manner; media was added first to the apical compartments and then basolateral; when removing media, it was first removed from the basolateral and then apical compartment.

Caco-2 cells (passages 30-50) were cultured to confluency in 75 cm^2 flasks and detached from the flasks using the method described in section 2.2.1. Cells were counted using a haemocytometer (section 2.2.4) and cell suspension of the appropriate concentration prepared. Caco-2 cells were seeded at a density of $1x10^5$ cells *per* cm^2; this was achieved by pipetting 75 µl of complete EMEM containing $1.1x10^4$ cells into

apical wells (surface area, 0.1 cm^2). 250 µl complete EMEM was then added to basolateral wells. Caco-2 cells were typically cultured on Millicell-96 inserts for 21 days prior to their use in experiments as confluent and polarised cell monolayers. Cell feeding began on the third day of culture, and continued thereafter every other day. The term 'polarised' is hereafter used to define fully differentiated cell layer cultured on semi-permeable membranes.

6.2.3.1. Measurement of TEER

Measurements of transepithelial electrical resistance (TEER) were made to assess growth of Caco-2 monolayers in Millicell-96 inserts. TEER is a convenient, non-invasive technique to study barrier integrity and evaluate the tightness of cellular tight junctions. TEER reflects ionic conductance across the epithelial layer and can be employed to measure basal levels of paracellular flux, study tight junction disruption and can indirectly assess toxicity[104,105].

TEER was measured using an Ohmmeter (EVOS, World Precision Instruments) and an electrode (STX100M, World Precision Instruments). The electrode was sterilised in 70% IMS for 20 minutes prior use, followed by sequentially washing in PBS and complete EMEM. The electrode was then air dried for 5 minutes to ensure no excess liquid would be transferred to the Millicell-96 inserts and receiver plate (potentially increasing apical volume and influencing data). The electrode was then inserted into the Millicell-96 insert setup; the shorter pin into the apical (insert) well medium and the longer pin into basolateral (receiver) well medium *via* an access hole.

For routine monitoring of monolayer growth, TEER was measured in culture medium. Due to the large number of wells present in Millicell-96 insert plates, TEER from only 20 wells was measured for routine assessment. TEER was measured from wells spread evenly across the plate, to obtain representative average values. Medium was replaced after TEER measurements had taken place to prevent damage to the cells caused by ion leakage from the electrode.

Routine TEER for growth assessment was measured every other day and this procedure was repeated for three successive Millicell-96 insert plates until the TEER profile was found to be reproducible; thereafter TEER was only measured on day 15 and 21 to verify monolayer growth and intactness. In addition, TEER from cell-free Millicell-96 insert wells (background resistance) was measured and subtracted from values gathered. TEER was expressed as Ωcm^2 to account for surface area of the semi-permeable membrane (0.11 cm^2) and enable standardisation and comparison to other semi-permeable filters.

Only polarised Caco-2 monolayers displaying TEER values ≥800 Ωcm^2, indicative of fully formed tight junctions, were assayed.

6.2.3.2. Assaying polarised Caco-2 cells

The effect of Solutol HS15 on differentiated, polarised Caco-2 layers was investigated by measuring TEER throughout exposure (5-240 minutes), followed by testing apical and basolateral compartments for released LDH, and then assessing the resulting metabolic activity of cells using the MTS assay.

Prior to the application of 1% HEPES:HBSS, Solutol HS15 or 1% Triton X-100 solution to cells, culture medium was removed and 1% HEPES:HBSS buffer was then added to both compartments (75 µl in the apical and 250 µl on the basolateral). Millicell-96 insert plates were then incubated at 37ºC with 5% CO_2 for 45 minutes to allow the cells to equilibrate in buffer, following which baseline TEER was measured in all wells. 1% HEPES:HBSS buffer was then removed from the basolateral and apical compartments, and 75 µl 1% HEPES:HBSS, 1% Triton X-100 or Solutol HS15 (0.01-50 mM) added to apical compartment and 250 µl 1% HEPES:HBSS added to the basolateral. TEER was then measured every 30 minutes until the desired exposure period had elapsed (60-240 minutes).

Following exposure 50 µl and 100 µl samples were taken from the apical and basolateral compartments, respectively, and transferred to fresh clear 96 well plates. 100 µl and 200 µl of LDH detection solution was then added to apical and basolateral samples, respectively. Section 3.2.1 described how this detection solution was prepared. Samples were incubated with LDH detection solutions for 25 minutes at room temperature followed by the detection of their absorbance at 492 nm. Results were processed into relative values as described in section 3.2.1. Figure 6.2 shows the apical release of LDH from Caco-2 cells following 1, 10 and 50% Triton X-100 solution, in

order to determine concentration required for total lysis in polarised cells.

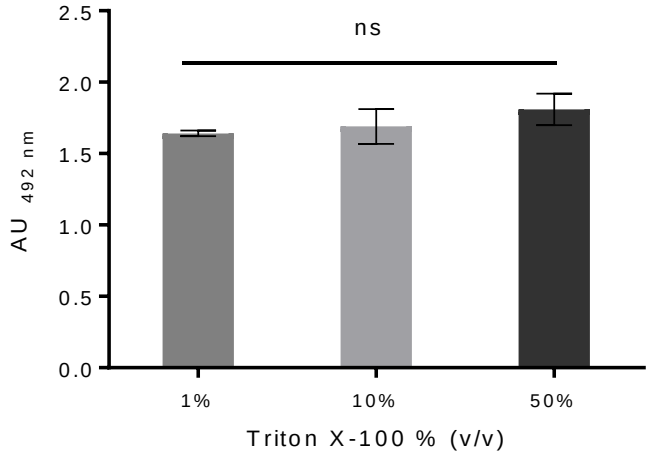

Figure 6.2. Apical LDH release signal induce by Triton X-100 concentrations from polarised Caco-2 monolayers. Solution absorbance was measured at 492nm following exposure to for 60 minutes. Data represents mean ± S.D from two experiments.

Once samples had been taken for LDH detection, Millicell-96 plate compartments (insert and receiver wells) were washed with PBS (twice) and 75 µl 17% (v/v) MTS:EMEM added to cells in the apical wells, and 250 µl EMEM added to the basolateral compartments. Millicell-96 insert plates were then incubated for 120 minutes at 37ºC with 5% CO_2, following which, apical filter plates were separated from basolateral plates, and absorption of the apical solution measured at 492 nm.

6.3. Results

6.3.1. Replication of basement membrane

6.3.1.1. Preliminary optimisation of Matrigel coating

To determine the most appropriate amount of Matrigel for coating on flat plastic well plates to culture Caco-2 cells, wells coated with 15, 75 and 150 μg/cm^2 Matrigel for 24 or 48 hours followed by analysis of cellular morphology and metabolic activity (Figure 6.3). Results demonstrate that Caco-2 cell growth was influenced by Matrigel coatings in a density-dependent manner.

After 24 hours of culture, cells grown on 15 μg/cm^2 Matrigel showed significantly increased metabolic activity (determined by MTS assay), which may indicate higher rate of proliferation than control cells not grown on Matrigel coatings (Figure 6.3b(i)). This may be supported by visual observation which shows a higher degree of surface coverage by cells Figure 6.3b(ii). Cellular metabolic activity remained unchanged in cells cultured on 75 μg/cm^2 Matrigel after 24 hours (Figure 6.3b(i)), and when imaged under the microscope, a more spherical morphology was observed than for the cells grown in control conditions (Figure 6.3a(i)). This morphological distinction was also observed after 24 hours for cells cultured on 150 μg/cm^2 Matrigel (Figure 6.3a(i), furthermore this group exhibited significantly lower levels of MTS reduction (Figure 6.3b(i)).

When studied after 48 hours of culture, Caco-2 cells seeded on 75 and 150 μg/cm^2 Matrigel demonstrated significantly lower MTS reduction levels than control cells (Figure 6.3b(ii)).

Moreover, both groups show lower cellular coverage of the growth surface than control cells, and appear to grow separate and in a spherical morphology (Figure 6.3b(i)). Cells cultured on 15 μg/cm^2, however, exhibited similar levels of MTS reduction to control cells (Figure 6.3b(ii)), and morphologies akin to Caco-2 cells cultured without Matrigel (Figure 6.3a(ii)).

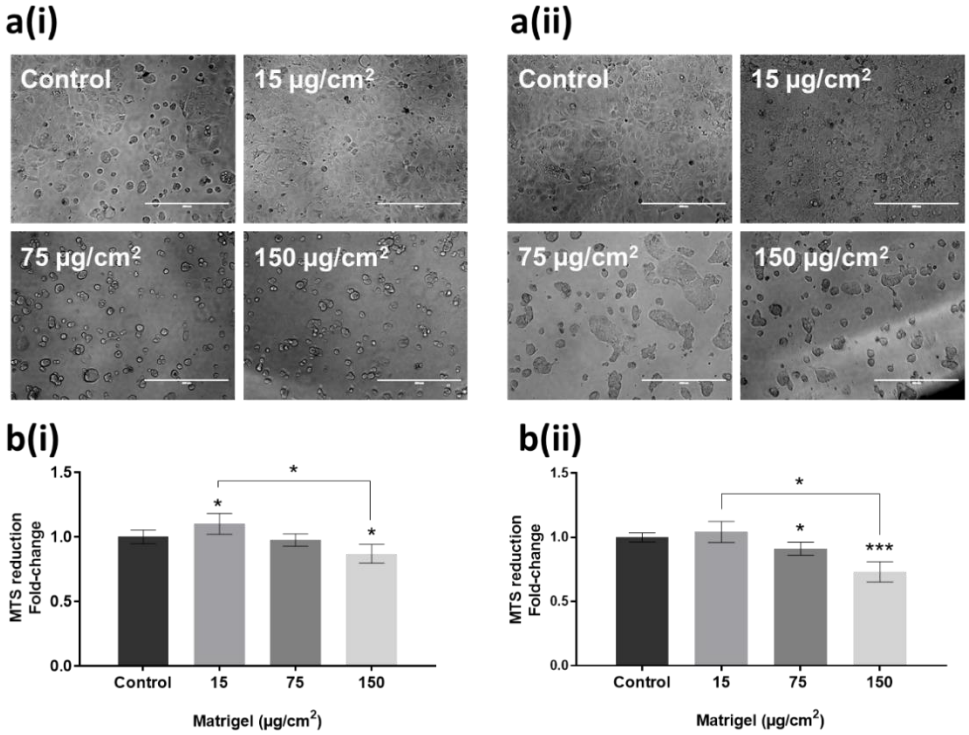

Figure 6.3. The effect of Matrigel coating density on Caco-2 (a) morphology and (b) proliferation after (i) 24 hour and (ii) 48 hours culture. Micrograph images (a) are taken on transmitted light filter on EVOS microscope, scale bar = 400 μm. Metabolic activity (b) was evaluated by measuring the reduction of the MTS salt. The control group represents Caco-2 cells grown in un-coated wells. MTS data presented as mean ± S.D and comes from triplicates from three independent experiments. Images shown are representative from three independent repeats. Statistical significance was determined using one-way ANOVA followed by Dunnett's multiple comparison post hoc test. *, $P < 0.05$; ***, $P < 0.001$.

Caco-2 cells cultured on 75 and 150 μg/cm^2 Matrigel coatings may have grown by developing spherical 3D structures, embedded in Matrigel, hence the spheroidal morphology

observed, as they may begin to form cysts[106–111]. Matrigel coatings were employed in the present study in attempt to replicate the basement membrane, rather than to promote the generation of 3D epithelial microtissues. Further testing was therefore performed on Caco-2 cells seeded on 15 μg/cm^2 Matrigel.

6.3.1.2. Effect on metabolic activity

Figure 6.4 illustrates that Caco-2 cells cultured on Matrigel coatings (15 μg/cm^2) were less susceptible to exposure to Solutol HS15 solutions, as indicated by their metabolic activity (MTS reduction).

Following exposures of 60, 120 and 180 minutes similar levels of metabolic damage are experienced by both the control and Matrigel cultured cells at all concentrations tested; however, after 60 minutes application of 50 mM Solutol HS15 solution, cells cultured on Matrigel displayed significantly higher levels of metabolic activity (Figure 6.4a,b, and c). Analysis of potency using LD_{50} calculations revealed that Solutol HS15 is significantly less toxic on Matrigel cultured cells following exposures ≥120 minutes relative to cells culture in control conditions (Figure 6.4e); following 120 and 180 minutes, cells cultured on Matrigel are approximately 2-fold more resistant to metabolic damage. After 240 minutes exposure cells seeded on Matrigel demonstrate significantly lower levels of metabolic damage following exposure to solutions of ≥0.1 mM Solutol HS15 (Figure 6.4d), and analysis showed a 3.3-fold reduction in metabolic damage after 240 minutes exposure (Figure 6.4e).

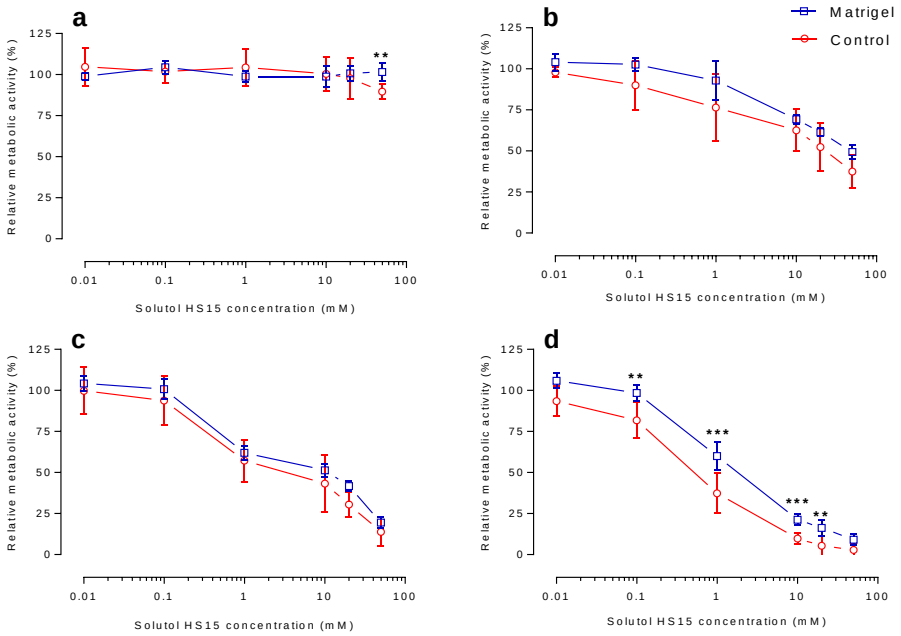

e

	LD_{50} (mean ± S.E) (mM)			
Exposure (min)	**60**	**120**	**180**	**240**
Control	> 50	21.9 ± 5.3	3.5 ± 0.7	0.56 ± 0.1
Matrigel	> 50	42.5 ± 5.3****	7.23 ± 1.1****	1.9 ± 0.2****

Figure 6.4. The effect of culturing Caco-2 cells on Matrigel on Solutol HS15 induced metabolic disruptions. Cells were exposed to treatment for (a) 60, (b) 120, (c) 180 and (d) 240 minutes, following 48 hours culture on 15 μg/cm^2 Matrigel. (e) Table of LD_{50} values. Metabolic activity was determined by reduction of MTS. The control group are cells grown in un-coated wells. Data presented as mean ± S.D and represents triplicates from three independent experiments. Statistical significance was determined using one-way ANOVA followed by Dunnett's multiple comparison post hoc test. *, P < 0.05; **, P < 0.01 ***, P < 0.001; P < 1x10^{-4}, ****

6.3.1.3. Effect on plasma membrane integrity

In addition to surfactant-induced metabolic damage, Matrigel cultured cells were significantly more resistant to plasma membrane damage resulting from 240 minutes of exposure to Solutol HS15 (Figure 6.5); however, no significant differences in LDH release were observed following 60, 120 or 180 minute exposures at all surfactant concentrations tested (Figure 6.5a,b,c and e).

However, cells seeded on Matrigel released significantly less LDH following 240 minutes exposure to solutions of ≥0.1 mM Solutol HS15 and LD_{50} values indicate a reduction in potency of approximately 10-fold (Figure 6.5d and e).

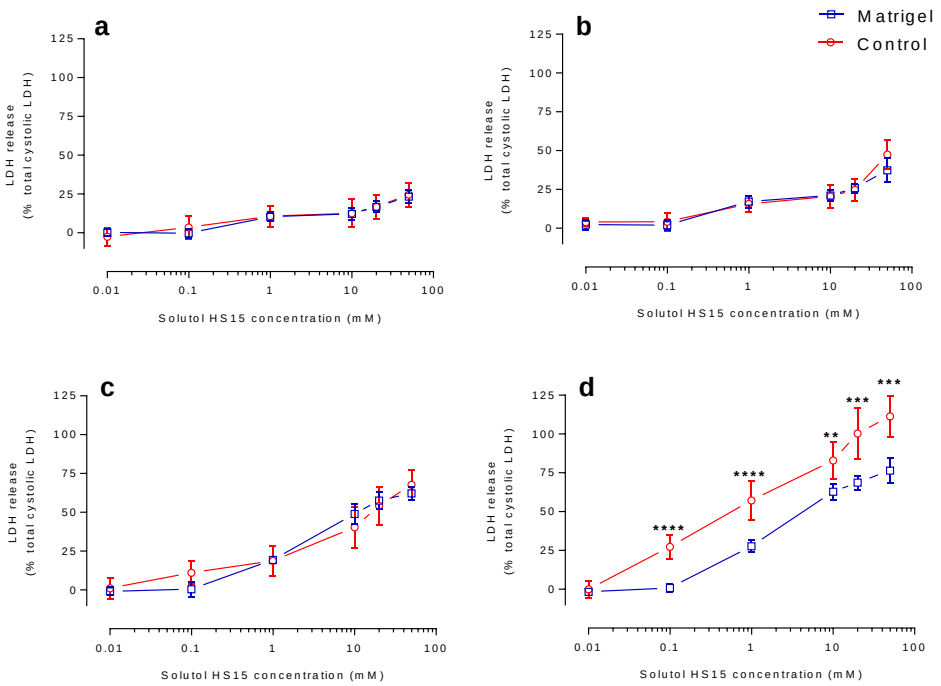

e

	LD_{50} (mean ± S.E) (mM)			
Exposure (min)	**60**	**120**	**180**	**240**
Control	> 50	> 50	15.6 ± 2.2	0.56 ± 0.1
Matrigel	> 50	> 50	13.7 ± 1.3	5.5 ± 0.5****

Figure 6.5. Plasma membrane damage induced by Caco-2 cells cultured on Matrigel in response to Solutol HS15 exposure. Cells were exposed to treatment for (a) 60, (b) 120, (c) 180 and (d) 240 minutes, following 48 hour culture on 15 μg/cm^2 Matrigel. (e) Table of LD_{50} values. Plasma membrane damage was assessed by observing cellular release of LDH. Results in the control group come from cells grown in un-coated wells. Data presented as mean ± S.D and represents triplicates from three independent experiments. Statistical significance was determined using one-way ANOVA followed by Dunnett's multiple comparison post hoc test. *, P < 0.05; **, P < 0.01 ***, P < 0.001; P < 1x10^{-4}, ****

6.3.2. Conservation of paracrine signalling with 3T3-CM

6.3.2.1. Effect on Caco-2 morphology and proliferation

Caco-2 cells cultured in medium conditioned by 3T3 cells (denoted as 3T3-CM) were observed to have significantly lower metabolic viability (MTS assay) than control cells (Figure 6.6). Following 24 hours, 3T3-CM cultured cells level of MTS reduction was approximately 0.9-fold that of the control, and after 48 hours approximately 0.7-fold the control level (Figure 6.6). 3T3-CM cultured cells displayed levels of confluency akin to the control cells and also appeared morphologically similar (Figure 6.6).

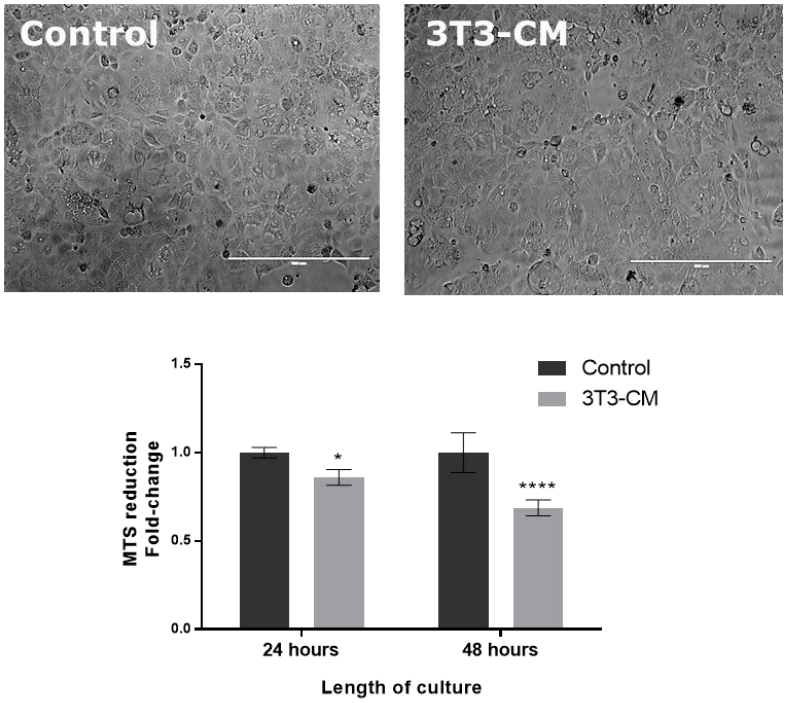

Figure 6.6. The effect of 3T3-condition media (3T3-CM) on Caco-2 morphology (top) and MTS reduction (below). Micrograph images are taken on transmitted light filter on EVOS microscope following 48 hours of culture, scale bar = 400 µm. The control group represents cells cultured in standard, complete EMEM, as opposed to 3T3-CM. MTS data presented as mean ± S.D and comes from triplicates from three independent experiments. Images shown are representative from three independent repeats. Statistical significance was determined using one-way ANOVA followed by Dunnett's multiple comparison post hoc test. *, $P<0.05$; $P<1x10^{-4}$, ****

6.3.2.2. Effect on Solutol HS15 induced loss of membrane integrity

The culture of Caco-2 cells in 3T3-CM did not significantly influence the amount of LDH release induced by exposure to Solutol HS15 solutions at all concentrations for 60 and 120 minutes (Figure 6.7a and b).

Exposing cells for 240 minutes to concentrations ≥0.1 mM revealed that Solutol HS15 elicited significantly lower LDH release from 3T3-CM cultured Caco-2 cells (Figure 6.7d); LD_{50} data show that Solutol HS15 is approximately 47-fold less potent at inducing LDH release from cells grown in 3T3-CM culture following 240 minutes exposure relative to control conditions (cell cultured in EMEM) (Figure 6.7e).

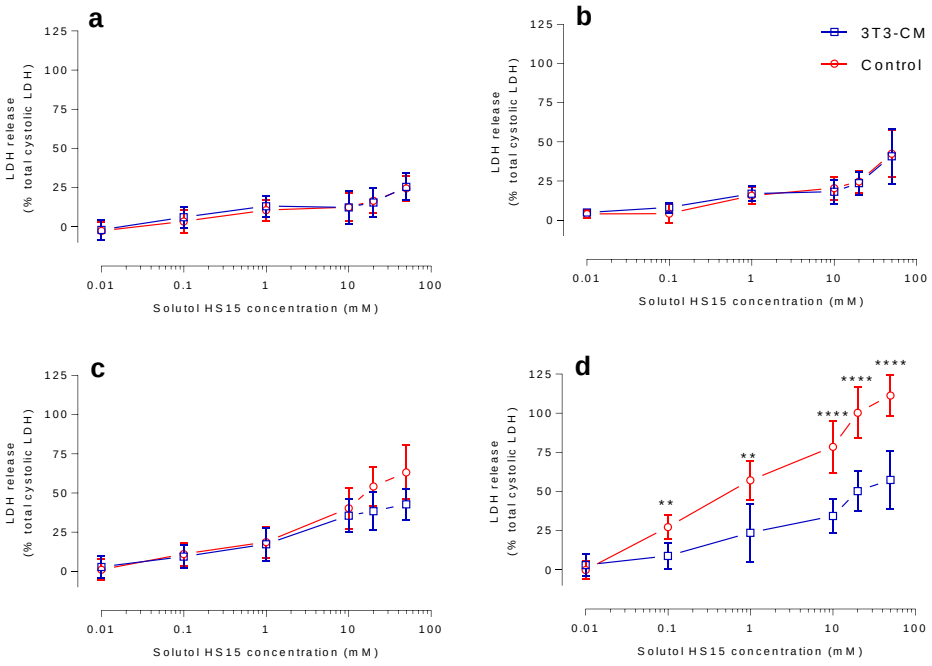

e

	LD_{50} (mean ± S.E) (mM)			
Exposure (min)	**60**	**120**	**180**	**240**
Control	> 50	> 50	15.6 ± 2.2	0.56 ± 0.1
Matrigel	> 50	> 50	> 50	26.3 ± 7.9****

Figure 6.7. Solutol HS15 induced LDH release on Caco-2 cells cultured in 3T3-CM. Cells were exposed to treatment for (a) 60, (b) 120, (c) 180 and (d) 240 minutes. (e) Table of LD_{50} values. Plasma membrane damage was assessed by the LDH release assay. Control group data comes from cells cultured in EMEM. Data presented as mean ± S.D and represents triplicates from three independent experiments. Statistical significance was determined using one-way ANOVA followed by Dunnett's multiple comparison post hoc test. *, $P < 0.05$; **, $P < 0.01$ ***, $P < 0.001$; $P < 1x10^{-4}$, ****

6.3.2.3. Effect on permeability of nuclear membranes

Data shown in Figure 6.8 depicts that exposure to the surfactant did not cause significant changes in nuclear membrane permeability of cell cultured in 3T3-CM, relative to cells cultured in control conditions at 60, 120, 180 and 240 minutes of Solutol HS15 exposure at all concentrations tested (Figure 6.8). Exposures ≤240 minutes induces normalised responses <50 %, thus potency (LD_{50}) could not be calculated.

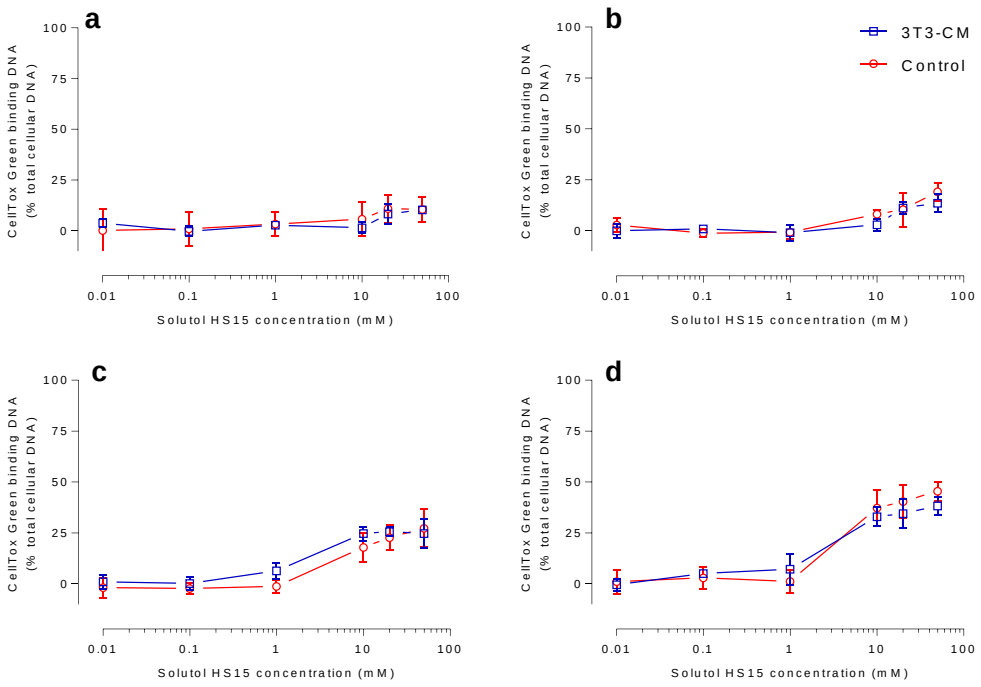

Figure 6.8. Permeabilisation of nuclear membranes induced by Solutol HS15 on 3T3-CM cultured Caco-2. Cells were exposed to treatment for (a) 60, (b) 120, (c) 180 and (d) 240 minutes. Nuclear membrane permeability determined by CellTox green assay. Control group data comes from cells cultured in EMEM. Data presented as mean ± S.D and represents triplicates from three independent experiments.

6.3.2.4. Effect on metabolic activity

The culture of Caco-2 cells in 3T3-CM resulted in significantly increased cellular susceptibility to the surfactant induced metabolic damage, as determined by the MTS assay (Figure 6.9). Exposure for 60 minutes of 3T3-CM culture cells to surfactant solutions of 20 and 50 mM resulted in significantly decreased metabolic activity, relative to control conditions (Figure 6.9a). After 120 and 180 minutes, 3T3-CM cultured cells have significantly diminished metabolic activities following exposure to solutions of ≥0.1 mM Solutol HS15, and exhibit LD_{50} values approximately 56- and 46-fold lower than control cells, respectively (Figure 6.9b, c and e).

Following 240 minutes exposure, it is estimated that cells cultured in 3T3-CM are approximately 8-fold more susceptible to Solutol HS15 induced metabolic decline, and significantly decreased values are observed at surfactants concentrations of 0.1 and 1 mM, however it is noted that application of Solutol HS15 solutions ≥10 mM elicit comparable responses in both culture groups; near to total loss of metabolic activity (<10% remaining) (Figure 6.9d and e).

The rate of metabolic decline in 3T3-CM cultured cells in response to Solutol HS15 did not appear linear. LD_{50} values demonstrate that the majority of the effect on metabolic activity occurs at 60-120 minutes (>125-fold increase in potency); an approximate 5-fold increase in potency occurs between 120 and 180 minutes of exposure, and an increase in potency of approximately 1.1-fold between 180 and 240 minutes (Figure 6.9e).

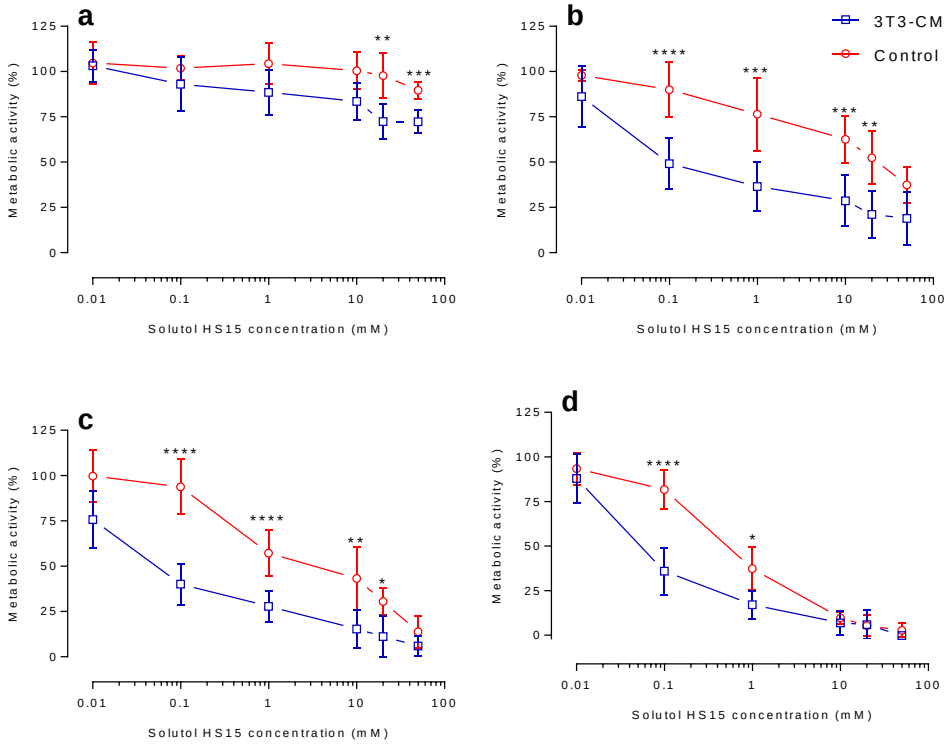

e

	LD_{50} (mean ± S.E) (mM)			
Exposure (min)	**60**	**120**	**180**	**240**
Control	> 50	21.9 ± 5.3	3.5 ± 0.7	0.56 ± 0.1
3T3-CM	> 50	0.39 ± 0.1****	0.08 ± 0.02****	0.07 ± 0.01****

Figure 6.9. The effect of 3T3-CM culture of Caco-2 cells on Solutol HS15 induced metabolic activities. Cells were exposed to treatment for (a) 60, (b) 120, (c) 180 and (d) 240 minutes. (e) Table of LD_{50} values. Metabolic activity was evaluated by measuring cellular reduction of MTS. Control group data is from cells cultured in EMEM. Data presented as mean ± S.D and represents triplicates from three independent experiments. Statistical significance was determined using one-way ANOVA followed by Dunnett's multiple comparison post hoc test. *, $P < 0.05$; **, $P < 0.01$ ***, $P < 0.001$; $P < 1x10^{-4}$, ****

6.3.3. Culture of Caco-2 cells in differentiated, polarised cell layer

6.3.3.1. TEER profile

TEER was measured to provide a reliable and non-invasive assessment of Caco-2 epithelial monolayer growth and the formation of tight junctions. Figure 6.10 shows the TEER profile of Caco-2 cells grown on semi-permeable Millicell-96 insert plates. Cells exhibited exponential increase in TEER values between approximately day 4 and 11, which the gradually plateaued between days 18 and 26 at a value of approximately 2000 Ωcm^2. TEER values began to decrease after culture ≥30 days on Millicell-96 inserts plates.

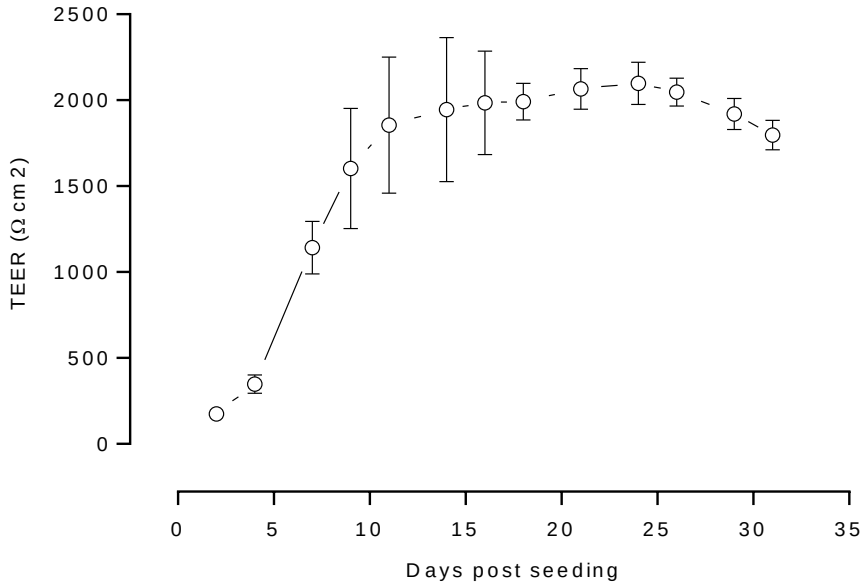

Figure 6.10. Caco-2 TEER development on Millicell-96 semi-permeable inserts. Data is presented as mean ± S.D of TEER values obtained from three separate experiments.

6.3.3.2. Solutol HS15 exposure effect on TEER

TEER profiles following exposure of cells cultured on Millicell-96 semi-permeable inserts to surfactant and shown in Figure 6.11. The profiles indicate concentration- and time-dependent TEER changes.

Polarised cells treated with 0.01 and 0.1 mM Solutol HS15 for ≤240 minutes remained at basal levels. Solutol HS15 did not affect TEER after 30 minutes, however following 60 minutes of exposure to ≥1 mM Solutol HS15 progressive decreases in TEER values were observed.

Calculation of LD_{50} values from TEER profiles (Figure 6.11c) demonstrate that the greatest effect on TEER occurs between 60 and 120 minutes of exposure (>40-fold increase in potency); between 120 and 180 minutes an increase in potency of approximately 2.5-fold was observed and between 180 and 240 minutes, and increase of approximately 1.1-fold.

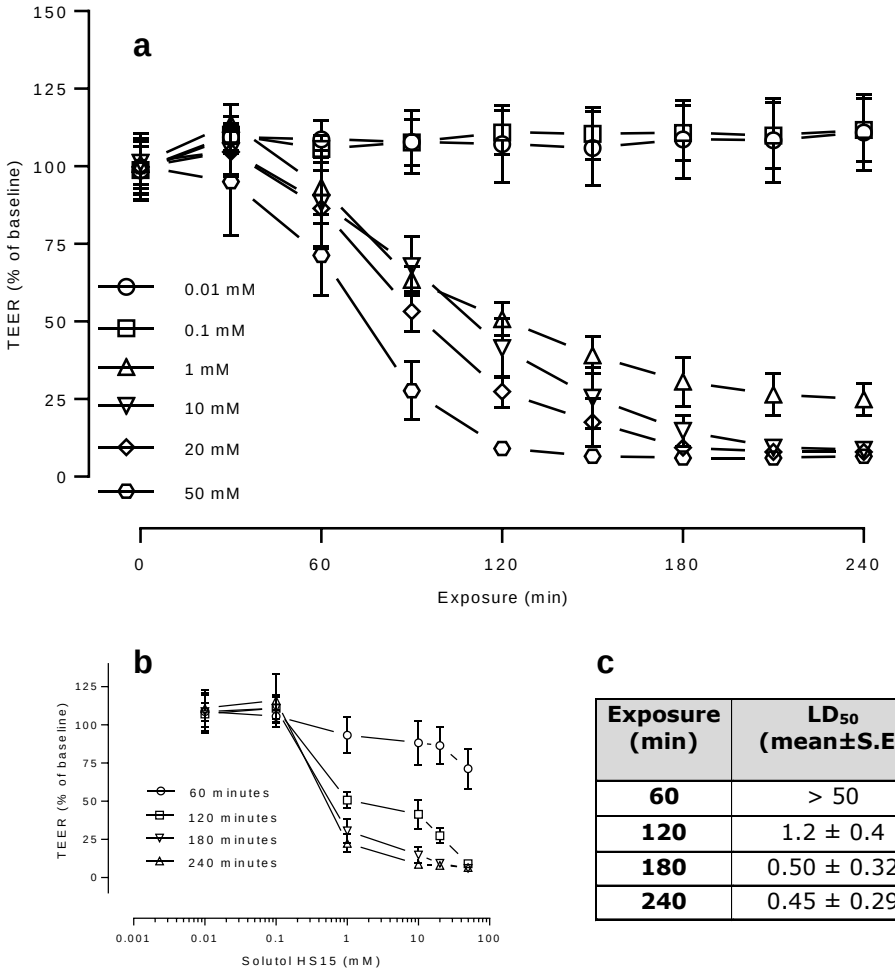

Exposure (min)	LD_{50} (mean±S.E)
60	> 50
120	1.2 ± 0.4
180	0.50 ± 0.32
240	0.45 ± 0.29

Figure 6.11. Effect of exposure to Solutol HS15 on TEER values in differentiated, polarised Caco-2 layers. TEER values plotted against (a) exposure time and (b) Solutol HS15 concentration. The latter enables calculation of (c) LD_{50} values of Solutol HS15 induced response. TEER values are shown as a percentage of the ΔTEER induced by the vehicle control (1% HEPES:HBSS). Values reported are mean ± S.D and come from three independent experiments performed in triplicate.

6.3.3.3. Solutol HS15 exposure induced metabolic activity in differentiated, polarised cell layer

The reduction of MTS by polarised Caco-2 cells in response to Solutol HS15 exposure, shown in Figure 6.12, was distinct from that exhibited by undifferentiated (control) cells; polarised cells were significantly more resistant to metabolic damage than control cells grown in control conditions on standard flat plastic well plates, observed at 60, 120, 180 and 240 minutes, and also did not demonstrate the 'metabolic burst' response following short exposures (5-10 minutes).

Exposing polarised cells for 5, 10, 20 and 60 minutes to Solutol HS15 solutions at concentrations ≥50 mM, did not induce any significant change from baseline levels of MTS reduction observed in polarised cells (Figure 6.12a, b, c and d). Exposures of 120, 180 and 240 minutes, resulted in a dose- and time-dependent decrease in metabolic activity with the application of solutions ≥10 mM; it should be noted that this is significantly different from undifferentiated control cells grown in standard plates, which respond to solutions of Solutol HS15 ≥1 mM (Figure 6.12e,f and g).

The calculation of LD_{50} values demonstrates that differentiated Caco-2 cells in a polarised layer show significantly higher resistance to the surfactant toxicity at increasing exposure time, compared to control cells as shown in Figure 6.12h; following exposures of 120, 180 and 240 minutes, differentiated Caco-2 layers display LD_{50} values approximately 1.7-, 7.9- and 21.7-fold higher than control cell values, respectively (Figure 6.12h).

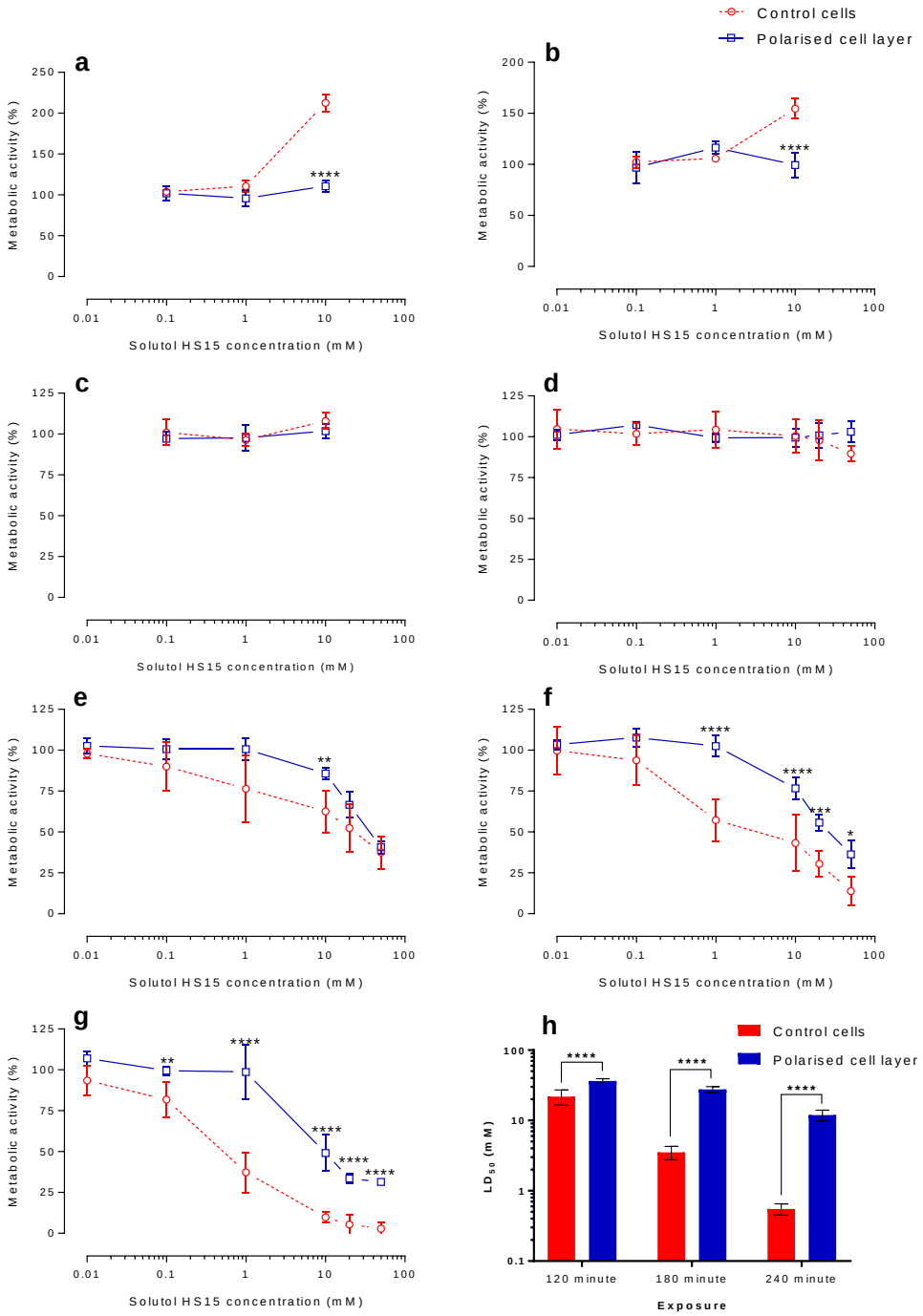

Figure 6.12. Effect of exposure to Solutol HS15 on metabolic viability of Caco-2 cells grown as polarised layer. Cells were exposed to for (a) 5, (b) 10, (c) 20, (d) 60, (e) 120, (f) 180 and (g) 240 minutes, following which metabolic activity was determined by measuring cellular reduction of MTS. (h) comparison of LD_{50} values. Data shown for the control group comes from undifferentiated, non-polarised cells grown on standard cell culture plastic, as opposed to Millicell inserts. Data presented as mean ± S.D and represents triplicates from three independent experiments. Statistical significance was determined using one-way ANOVA followed by Dunnett's multiple comparison post hoc test. *, $P < 0.05$; **, $P < 0.01$ ***, $P < 0.001$; $P < 1x10^{-4}$, ****

6.3.3.4. Plasma membrane damage in differentiated, polarised cell layer

The release of LDH from polarised Caco-2 cell layers (Figure 6.13) was measured on both the apical and basolateral sides of the culture, following apical application of Solutol HS15 exposure. Data expressed as LD_{50} values (Figure 6.13e) indicate significantly higher release of LDH, i.e. the surfactant effect on the cell membrane, on polarised cell layer relative to unpolarised control cells in response to the application of Solutol HS15 solutions; the apical release of LDH following an exposure of 120 minutes was >5.6-fold greater than control cells, and at 180 and 240 minutes exposure, approximately 3.1- and 1.4-fold greater, respectively.

Interestingly, apical release was detected at earlier time points of Solutol HS15 exposure for concentrations ≥ 10 mM, than basolateral release; apical LDH release was evident after exposures ≥60 minutes, however basolateral release only after ≥120 minutes (Figure 6.13b and c). The basolateral release of LDH was only observed following exposures to solutions ≥10 mM Solutol HS15.

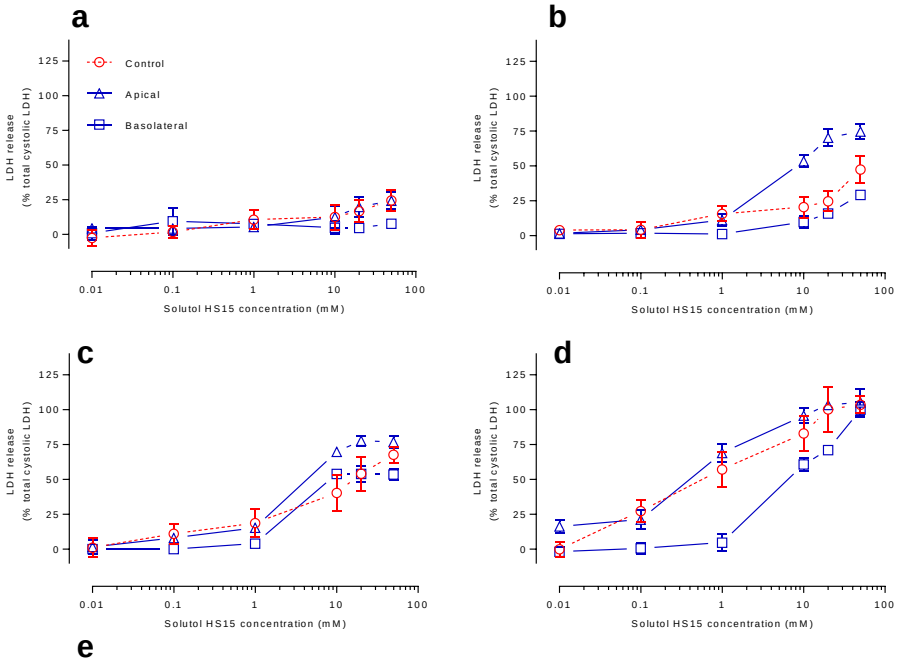

e

	LD_{50} (mean ± S.E) (mM)			
Exposure (min)	**60**	**120**	**180**	**240**
Control	> 50	> 50	15.6 ± 2.1	0.56 ± 0.1
Polarised Apical	> 50	8.9 ± 0.9	5.1 ± 0.7****	0.41 ± 0.1****
Polarised Basalateral	> 50	> 50	18.7 ± 3.8	8.2 ± 0.8

Figure 6.13. Solutol HS15 induced plasma membrane damage on polarised Caco-2 cells. Apical and basolateral LDH release was measured following surfactant exposures of (a) 60, (b) 120, (c) 180 and (d) 240 minutes. LDH release LD_{50} values displayed in (d). Data are displayed as mean ± S.D, and represent triplicates from three independent experiments. Control group data represents cells grown in standard cell culture plates. Statistical significance was determined using one-way ANOVA followed by Dunnett's multiple comparison post hoc test. *, $P < 0.05$; **, $P < 0.01$ ***, $P < 0.001$; $P < 1x10^{-4}$, ****

6.4. Discussion

Data obtained in this chapter from different analyses on the performance of each Caco-2 culture method are summarised in Figure 6.14.

Interestingly, data indicate that Caco-2 culture in NIH/3T3-cells condition medium (3T3-CM) was the most successful culture method to protect Caco-2 cells from surfactant induced LDH release, and thus plasma membrane damage; following 240 minutes exposure 3T3-CM cultured cells released approximately 4.7-fold less LDH in response to surfactant than Matrigel cultured cells, which was the next method to release the least (Figure 6.14b).

On the contrary, using 3T3-CM to culture Caco-2 cells resulted in significantly increasing the loss of metabolic activity in response to surfactant treatment (Figure 6.14a). Indeed, Caco-2 polarisation, which significantly increased apparent membrane damage, resulted in sustaining metabolic activity significantly more so than other culture methods, following exposure to surfactant.

Unexpectedly therefore, the culture condition which had the greatest effect at minimising surfactant induced metabolic damage, also induced the highest levels of membrane damage, and, the reciprocal was found; the culture condition to reduce LDH release most successfully also resulted in the highest metabolic damage in response to surfactant.

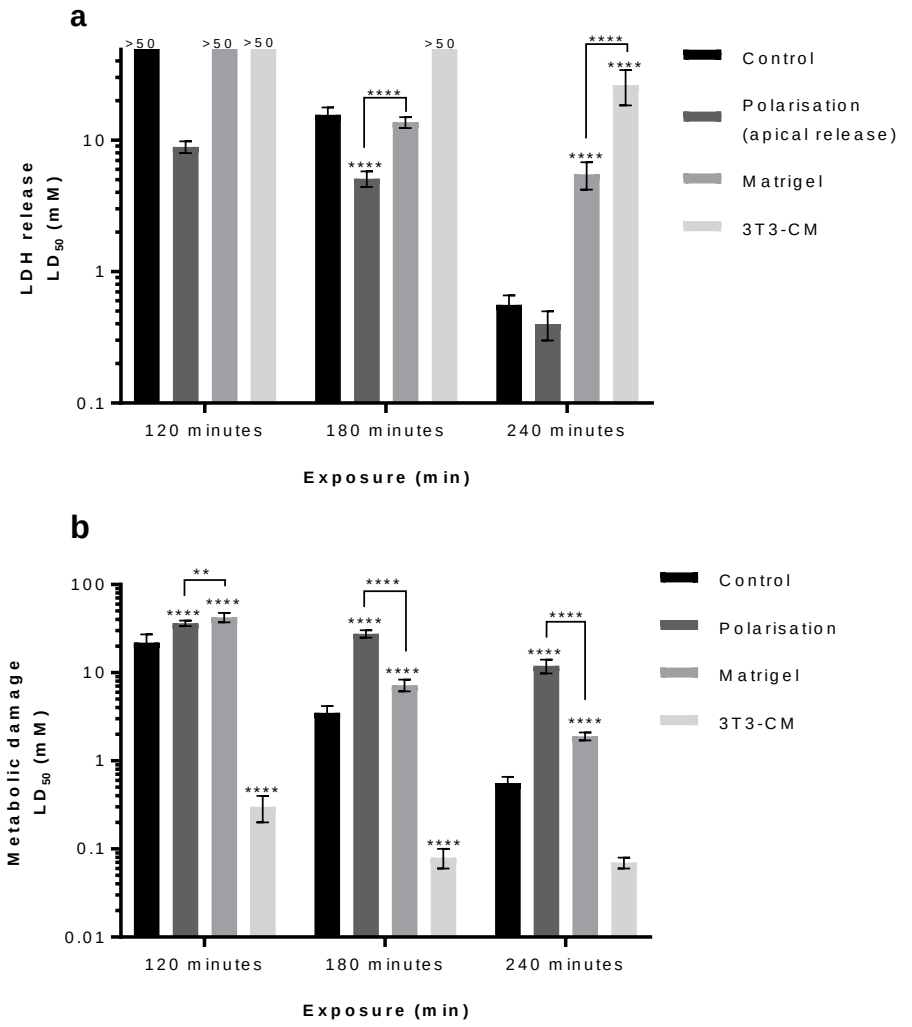

Figure 6.14. Comparison of culture methods on (a) LDH release assay LD_{50} values and (b) MTS reduction assay LD_{50} values. Data are presented as mean ± S.E.M. Statistical significance was determined using two-way ANOVA followed by Tukey's multiple comparison test. *, $P < 0.05$; **, $P < 0.01$ ***, $P < 0.001$; $P < 1x10^{-4}$, ****

6.4.1. The culture of Caco-2 cells as a polarised layer

Caco-2 cells cultured on Millicell-96 insert plates reached TEER values of approximately 2000 Ωcm^2 which are comparable with values reported in the literature, and indicate the formation of tight epithelial cell layer[112,113] (Figure 6.10). This validated the use of the Millicell-96 inserts plates which are not as well established or routinely used as 12 or 24 well Transwell inserts; the large number of semi-permeable filters provided on a Millicell-96 insert plate have the advantage over the Transwell systems because they allow for increased exposure parameters (compounds concentrations and exposure times) to be studied on a single plate, and thus enable a high throughput of cell assaying that benefits *in vitro* toxicity testing.

Figure 6.15 displays the results gathered on the time-dependence of cell response to exposure of 10 mM Solutol HS15 solution when cultured as polarised layer. It demonstrates the succession of effects occurring upon exposure. From calculated LT_{50} values (time required to induce 50% lethality), it appears that a decrease in cell layer barrier integrity, measured by TEER, precedes other effects on the layer, and this followed by loss in apical membrane integrity (apical LDH presence). Damage to the integrity of the basolateral membrane is subsequent to these effects, thus the decreased TEER values are likely due to increased paracellular permeability of ions, as opposed to transcellular permeability.

a

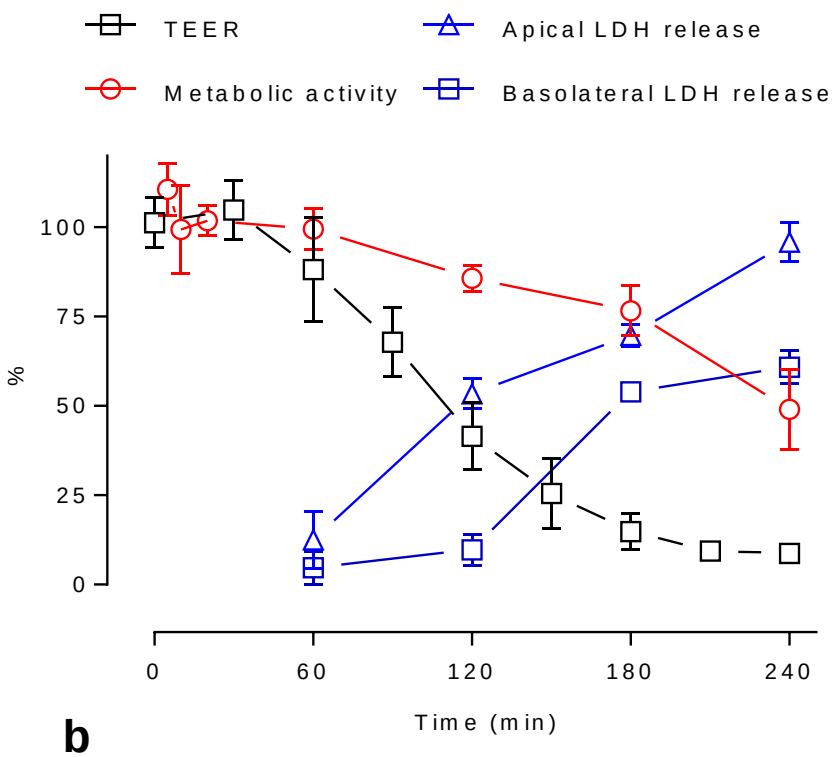

b

	LT_{50} (min)
TEER	110 ± 5.8
LDH_{AP}	115 ± 7.2
LDH_{BL}	175 ± 11.5
MTS	237 ± 10.1

Figure 6.15. Overview of polarised Caco-2 cells responses to 10 mM Solutol HS15 solution (a) versus time, accompanied by (b) calculated LT_{50} values. Y axis represents % LDH release, % metabolic activity and % of basal TEER. Data are presented as (a) mean ± S.D and (b) mean ± S.E.M. LT_{50}, Lethal time required for 50% response, calculated using GraphPad Prism software.

Perturbation to the apical membrane environment by incorporation of the surfactant molecule (see Chapter 3) (reflected by changes in Laurdan GP) may mediate/cause the loss of tight junction integrity; as discussed in section 6.1, tight

junctions are the most apical junctional complexes on the apical membrane and have transmembrane components, such as occluding and claudin proteins[114,115]. Thus, it is possible that surfactant incorporation may influence the function of these membrane embedded proteins.

Previous work from this laboratory, Shubber et al., demonstrated that, unlike the cationic polymer chitosan, Solutol HS15 induces an irreversible decreases in TEER values[21]. Chitosan is a classical permeability enhancer that has been shown to 'open' tight junctions reversibly by acting on the Protein Kinase C (PKC) and C-Jun NH_2-termal kinase (JNK) signalling pathways to induce disruptions in tight junctions protein function[116–118]. Thus, the irreversibility of Solutol HS15's effect on TEER values may be a result of it inducing this effect *via* the perturbation of the plasma membrane, and thus tight junction transmembrane function.

Following the application of surfactant on the apical side of cells, it is logical that they incorporate and damage apical membranes first. The release of LDH basolaterally, indicating perturbation of the basolateral membranes or loss of permeability barrier function of the cell layer, was observed later during surfactant exposure and, interestingly, coincided with time at which TEER values declined to <20% baseline (Figure 6.15).

Therefore, this could reflect the diffusion of apically released LDH to the basolateral compartment *via* a permeabilised cell layer (traversing paracellularly), and/or that the surfactant gains access to the basolateral membranes following the total loss of tight junction gating function.

It is unlikely that surfactant molecules would diffuse through the paracellular space free in solution as ions or small molecules

do[119]. Instead, surfactant molecules would be expected to incorporate in the lipid bilayer of the apical membrane (exposed to the applied surfactant), and thus, their movement to the basolateral side would be mediated *via* lateral diffusion along the continuity of the cell membrane lipid bilayer[120]. The restriction of the surfactant movement to the basolateral side may therefore not be mediated by the extracellular loops of claudin and occludin molecules which span the paracellular space, and functions as 'gates' to limit solute diffusion[51,114,115], but possibly the embedded transmembrane protein domains that function as a 'fence' to separate the apical and basolateral domains of the plasma membrane[121,122]. The plasma membrane is functionally divided into apical and basolateral domains that differ in both their lipid and integral protein compositions[123]. Thus, the 'fence' function of tight junctions prevents lateral diffusion of material in the plasma membrane[121–123]. In this manner, tight junctions may therefore be restricting the lateral diffusion of Solutol HS15 towards the basolateral side, and the abolishment of this function may thus require substantial loss of tight junction and apical membrane integrity.

Surprisingly, when measuring apical LDH release, polarised monolayers of Caco-2 cells were more susceptible to surfactant-induced LDH release than control cells, (Figure 6.13). The reasons for this are unclear; Figure 6.2 illustrates that the concentration of Triton X-100 solutions used (1% v/v) was sufficient to lyse polarised Caco-2 cells, and is supported by others[124,125], therefore, ruling out the possibility that data is normalised to incorrect levels of lysis (i.e. Triton X-100 induced lysis ≠ 100% cell lysis).

One possible explanation could be that there are differing levels of LDH expression in polarised Caco-2 cells exposed to Solutol HS15 compared to those treated with Triton X-100. The LDH enzyme is a ubiquitously expressed enzyme[126], hence its use as a marker for cytosolic contents, however, it is also a vital dehydrogenase in cellular metabolism, and catalyses the conversion of lactate to pyruvic acid during glycolysis[127]. Accordingly, the cellular enhancement of glycolysis has been reported to involve the upregulation of LDH[128], and this effect appears to be promoted by heat shock factor 1 (HSF1)[129], a major mediator of the heat shock response[130] – as discussed in section 5.4.3. Therefore, exposure to Solutol HS15 may result in the upregulation of the LDH enzyme in polarised cells, such that normalisation to Triton X-100 results in an overestimate of membrane damage. To overcome this, the normalisation to total lysis (100% LDH release) could have been achieved by lysing Solutol HS15 exposed cells with Triton X-100 after the treatment period, to obtain a more accurate estimate to total cellular LDH content.

However, results demonstrate that polarised Caco-2 cells do not express an increased reduction in MTS (Figure 6.12), and thus, may not undergo the possible enhancement of glycolysis expressed by unpolarised Caco-2 cells (as discussed in Chapter 4). Therefore, the likelihood of the upregulation of the LDH enzyme in response to Solutol HS15, suggested above, may be questioned.

An alternative explanation for the high levels of apical LDH release in polarised cells, may lie with the functionality of polarised epithelial apical membranes, and the expression of microvilli. As discussed in section 6.1, microvilli dramatically increase the surface area of the apical membrane[35,36], as a

consequence, this may increase the magnitude of surfactant incorporation and accumulation into the apical cell plasma membrane. Furthermore, Marzesco et al., observed that the depletion of membrane cholesterol, with methyl-β-cyclodextrin, enhanced the release of vesicles from Caco-2 microvilli[131], and Solutol HS15 has been observed to reduce airway epithelial membrane cholesterol[132]. Therefore, it may be possible that Solutol HS15 is promoting the enhanced formation of vesicles from microvilli, which consequently may be augmenting the perturbation of the apical membrane *via* the depletion of the membrane[133]. However, a more likely concept is that the larger surface area, mediated by microvilli, of the apical membrane enables greater membrane perturbation and thus LDH release.

It is noted however, that despite the levels of apical membrane perturbation, polarised cells appear to maintain their ability to reduce MTS, significantly more so than control cells (Figure 6.12). Taken together, this may suggest that perturbation to the apical membrane, in polarised cells, is less critical to the overall cell condition so long as cell-cell adhesion remains maintained.

An interesting observation made regarding the MTS assay was the absence of a metabolic burst following surfactant exposures of 5-10 minutes in the polarised cell layers relative to control cells cultured on standard flat plastic plates. This may indicate that polarised Caco-2 cells are not undergoing the survival response that is proposed to occur in unpolarised cells (as discussed previously in Chapters 2 and 6). Therefore, polarised cells may not be experiencing the heat shock response, in the same manner or magnitude as unpolarised cells.

Results from Chapter 5 suggest that the decreases in metabolic activity observed following surfactant exposure may have been mediated *via* the cellular induction of the apoptosis, possibly by the heat shock response. Thus, the perseveration of normal levels of metabolic activity that is observed in polarised Caco-2 cells (Figure 6.12 and Figure 6.15), may be a result of the absence of the heat shock response and the subsequent lack of activation of apoptosis and metabolic decline.

Hyperthermal stress (≥41°C) has been shown to increase the paracellular permeability of epithelial monolayers[137–139]. Dokladny et al., demonstrated that 41°C heat shock resulted in decreased TEER values and increased flux of the paracellular marker inulin, across Caco-2 cells monolayers[137,140]. The authors report that the gating function of tight junctions was restored *via* the upregulation of occuldin, in a manner dependent on heat shock protein (Hsp) expression[137]. Furthermore, they report that no significant increases in Caco-2 apoptosis, or necrosis, was observed in response to the heat treatment[141]. Increased paracellular permeability was also reported for MDCK kidney epithelial cell monolayers upon heat shock, and akin to Caco-2 cells, TEER was shown to be restored in a HSP expression dependent manner[138,139].

Therefore, the literature suggests that heat response does occur in the polarised cell layer, however the lack of response-induced apoptosis in monolayers suggests that even if surfactant was to induce this response, it may not result in the subsequent apoptosis-mediated metabolic decline, and thus higher levels of metabolic activity would be maintained.

There is a paucity of data concerning the membrane fluidity of epithelial cells in monolayers, therefore it is difficult to ascertain

if the heat shock response is triggered in a similar manner in these cells. The absence of surfactant-induced heat shock could be related to the apical membrane of polarised cells being more resistant to heart shock triggered *via* membrane fluidisation than in unpolarised cells. The microvilli of the apical membrane, for example, are well stabilised and supported by actin scaffolds[34]. Furthermore, the heat shock response is associated with lipid rafts[142,143], and the apical membrane is described as being enriched in sphingolipids[144], which as discussed in Chapter 3, are typically components of the more ordered membrane regions that rafts reside in[145]. Thus, the morphology and composition of polarised apical cell membranes could be altering the manner in which the heat shock response is regulated, relative to unpolarised cells. In polarised Caco-2 cell layers heat treatment was observed to decrease the expression of the ZO-1 protein[137], therefore, the induction of heat shock may rely on protein denaturation such as this, as a trigger, more so than membrane fluidisation in polarised cells[146–148].

Therefore, it would be of interest to investigate polarised cell membrane fluidity, as was conducted for unpolarised cells grown on standard flat plastic plates (section 3.3.4, Figure 3.8) in response to heat and surfactant treatment, to study the mechanism of heat shock response induction in epithelial monolayers.

6.4.2. The culture of Caco-2 cells in 3T3-conditioned medium

The proliferation of Caco-2 cells has been previously shown to increase in response to either direct co-culture with human

intestinal fibroblasts (CCD-18) or through use of conditioned medium derived from these fibroblasts[80,82]. However, work performed here with 3T3/NIH fibroblast conditioned medium (3T3-CM) resulted in the apparent decrease of Caco-2 metabolic viability, as determined by MTS reduction, possibly suggesting decreased proliferation (Figure 6.6). This discrepancy however, might be associated with the different methods used between the studies to evaluate proliferation; in our work, MTS reduction was used as an indication, however Göke et al. measured ^{3}H-thymidine incorporation[82] and Visco et al. employed an optical method based on the assessment of cell confluence[80].

Measuring levels of MTS reduction, determines the reduction environment of the cells, and is not necessarily an indicator of cell number, unlike ^{3}H-thymidine incorporation, which detects for the generation of new chromosomal DNA strands that occurs during mitotic cell division[149].

The production of bioenergetic molecules, through glycolytic pathways could be altered by, for example, the presence of enhanced EGF receptor signalling[150,151]. Thus, the employment of MTS reduction for the assessment of proliferation may not be suitable. Indeed, images of cell confluence in Figure 6.6 do not necessarily indicate a reduction in cell number, perhaps the opposite, however this assessment would require quantification for more accuracy, through means of nuclear staining for example[80]. The alterations in cellular growth and proliferation (Figure 6.6) may hint at possible modifications to the Caco-2 phenotype with 3T3-CM culture, however, without further investigation employing expression profiling techniques (such as expression microarrays)[44], this is difficult to conclude.

Upon exposure to surfactant, 3T3-CM culture cells demonstrated a more rapid and potent decrease in metabolic activity compared to control cells (Figure 6.9). However, this was also coupled with reduced LDH release (Figure 6.7), and no alterations in nuclear membrane permeability (Figure 6.8), suggesting that it may not necessarily be a direct influence of surfactant action on membranes, and perhaps, instead an enhancement of a cellular response. Growth factors have been shown to increase cell proneness to apoptosis[152,153], therefore increased surfactant-induced metabolic damage in 3T3-CM cultured cells, may be a consequence of a lower threshold for apoptotic sensitivity. The Noxa protein, for example, is a member of the bcl-2 family, and an established regulator of apoptotic sensitivity and is sensitive to the level of growth factor expression[154–156].

However, contrary to this hypothesis is work performed by Tseng et al., which demonstrated that 3T3-CM conferred anti-apoptotic activity to corneal epithelial cells treated with DNase I[157]. Therefore, the reasons for the enhanced metabolic damage in 3T3-CM cultured Caco-2 cells remains unclear, however, future work evaluating apoptosis in this condition, may prove useful.

There are no other reported studies employing 3T3/NIH cells in the culture of Caco-2 cells, however 3T3/NIH fibroblasts have been employed in co-cultured systems with human ocular epithelial cells[158], and with keratinocytes[159]; where they have been shown to increase epithelial proliferation and regeneration[158,159]. However, it has been suggested that 3T3/NIH act primarily by enhancing epithelial cell attachment through their production of hyaluronic acid (HA), an ECM component, rather than through paracrine singling[160–162].

Therefore, the reduction in LDH release following surfactant exposure in 3T3-CM cultured cells (Figure 6.7) may be associated with the increased presence of ECM components in the culture. NIH/3T3 fibroblast ECM secretions, such as HA, could be present in the collected 3T3-CM, these components might then deposit on the culture surface and provide Caco-2 cells with a substrate to adhere too – in manner similar to Matrigel coatings, that are discussed below.

6.4.3. Replicating ECM using Matrigel

The seeding of Caco-2 cells on culture plates coated with 15 μg/cm^2 Matrigel reduced surfactant-induced metabolic and membrane damage (Figure 6.4 and Figure 6.5, respectively).

The ECM components present in Matrigel may act as a basement membrane-like substrate and promote attachment to the plastic surface of the cell culture plate. Hemidesmosomes, for example, have been shown to form at sites of cell-Matrigel interaction in breast epithelial cells, *via* the association of Matrigel-deposited laminin-5 and cellular α6β4 integrin receptors[163]. Moreover, Matrigel coating was shown to increase the transcription and expression of β1 integrin subunit in mammary epithelial cells[164]. Therefore, by providing more ECM components, such as laminins and collagens[101], it is possible that Matrigel coatings are upregulating cell-ECM adhesion proteins and increasing the cell anchorage to culture plates[165].

As disused in section 6.1, cell-ECM junctions support the cytoskeleton, therefore the suggested upregulation of such junctions mediated by Matrigel coatings may have reinforced Caco-2 actin networks, in a similar manner to that observed by

Schreider et al. following their use of ECM comprised of laminins and collagen IV[46]. Actin filaments organise in a meshwork-like fashion on the cytoplasmic side of plasma membranes and appear to regulate lipid microenvironments and associate with lipid raft regions[166–170]. Moreover, the membrane lipid known as phosphatidylinositol 4,5-bisphosphate (PI(4,5)P2) connects to actin filaments and has shown to be enriched in L_o regions and co-localise with lipid rafts[171,172].

Therefore, the augmentation of the actin cytoskeleton *via* the increase in cell-ECM adhesion could in turn promote the increase in plasma membrane order. Lipid rafts and L_o regions are associated with being "detergent-resistant"[173,174], the promotion of the formation of these regions may therefore, reduce the incorporation and action of our surfactant, Solutol HS15, and thus potentially explain the reduced levels of membrane and metabolic damage observed in Caco-2 cells cultured on Matrigel coatings.

6.4.4. Future work

It would have been interesting to combine of all the culture elements studied so that surfactant could be tested on for example, a polarised Caco-2 monolayer that was seeded on ECM-based substrate on semi-permeable supports and culture with fibroblast conditioned medium, or in a co-culture with fibroblasts seeded basolaterally on the well bottom surface or basolateral side of the semi-permeable insert. However, in the present work this was never achieved due to time constraints. Similarly, investigating the effects of 3T3-CM and Matrigel culture on surfactant induced MTS reduction following 5-20

minutes exposure may have provided relevant information relating to the cellular responses and signalling.

In addition to the culture elements studied, it would have been of interest to replicate other factors, such as the intestinal mucus layer which has been suggested to increase protection against the medium fatty acid sodium caprate (C10) *in vivo*[175,176]. *In vivo* the gastro intestinal tract is covered in mucus[177,178]. In the colon the inner mucus layer is firmly attached to the epithelium and suggested to be 50-200 μm thick and considered an obstacle for compound access to epithelium[179,180]. To test the effect of the mucus on surfactant toxicity *in vitro* intestinal cell lines that are known to secrete mucus would have to be employed, such as HT29-MTX or the Caco-2 cell line sub-clone TC7[181,182].

6.5. Conclusions

Work presented in this chapter has demonstrated that replication of vital *in vivo* elements of epithelial tissue into *in vitro* culture reduces the toxic effect on exposure to the model surfactant Solutol HS15, on Caco-2 intestinal epithelial cells. Thus, these results may help to explain the discrepancies in surfactant doses observed between *in vitro* and *in vivo* toxicity[19], and also aid the development of Caco-2 models for future toxicity testing of surfactants and other compounds.

Results obtained appear to indicate that through replication of the basement membrane using a Matrigel layer, Caco-2 cells develop more *in vivo* relevant cell-ECM adhesion, which results in decreased surfactant-induced metabolic and membrane damage. The culture of Caco-2 cells in fibroblast conditioned medium had the greatest effect on limiting membrane damage in response to surfactant exposure. However, culture in fibroblast conditioned medium also appeared to increase the metabolic sensitivity to surfactant exposure, and it is proposed that this may be related to an increased proneness to induce apoptosis in the cells, however further work is required to confirm this. Finally, the culture of Caco-2 cells as polarised layers had a significant effect on reduction surfactant-induced metabolic damage.

Therefore, the methods used, in general, reduced surfactant toxicity and thus, may be a path towards collecting toxicity data that may correlate better to *in vivo* effects.

6.6. References

1. Kola, I. & Landis, J. Can the pharmaceutical industry reduce attrition rates? *Nat. Rev. Drug Discov.* **3,** 1–5 (2004).

2. Mullard, A. Parsing clinical success rates. *Nat. Rev. Drug Discov.* **15,** 447–447 (2016).

3. World Health Organization. WHO Model List of Essential Medicines - 19th List (April 2015). *Essent. Med.* 1–45 (2015). doi:10.1016/S1473-3099(14)70780-7

4. McKim, J. M. *et al.* Evaluation of octamethylcyclotetrasiloxane (D-4) as an inducer of rat hepatic microsomal cytochrome P450, UDP-glucuronosyltransferase, and epoxide hydrolase: A 28-day inhalation study. *Toxicol. Sci.* **41,** 29–41 (1998).

5. Cohen, A. & Kenter, M. Lessons from TGN1412 - Authors' reply. *Lancet* **368,** 1570 (2006).

6. Attarwala, H. TGN1412: From Discovery to Disaster. *J. Young Pharm.* **2,** 332–6 (2010).

7. Suntharalingam, G. *et al.* Cytokine storm in a phase 1 trial of the anti-CD28 monoclonal antibody TGN1412. *N.Engl.J.Med.* **355,** 1018–1028 (2006).

8. Firestone, R. TGN1412: scrutinizing preclinical trials of antibody-based medicines. *Nature* **441,** 282–282 (2006).

9. Hünig, T. The storm has cleared: lessons from the CD28 superagonist TGN1412 trial. *Nat. Rev. Immunol.* (2012). doi:10.1038/nri3192

10. Prescott, M. J. & Lidster, K. Improving quality of science through better animal welfare: the NC3Rs strategy. *Lab Anim. (NY).* **46,** 152–156 (2017).

11. Burden, N., Sewell, F. & Chapman, K. Testing Chemical Safety: What Is Needed to Ensure the Widespread Application of Non-animal Approaches? *PLoS Biol.* **13,** (2015).

12. Kauffman, A. L. *et al.* Alternative functional in vitro models of human intestinal epithelia. *Front. Pharmacol.* **4 JUL,** (2013).

13. Chen, P., Edelman, J. D. & Gharib, S. A. Comparative evaluation of miRNA expression between in vitro and in vivo airway epithelium demonstrates widespread differences. *Am. J. Pathol.* **183,** 1405–1410 (2013).

14. Chao, a C. *et al.* In vitro and in vivo evaluation of effects of sodium caprate on enteral peptide absorption and on mucosal morphology. *Int. J. Pharm.* **191,** 15–24 (1999).

15. Lewis, A. L., Jordan, F. & Illum, L. CriticalSorb(TM): Enabling systemic delivery of macromolecules via the nasal route. *Drug Deliv. Transl. Res.* **3,** 26–32 (2013).

16. Brunetti, J. *et al.* In vitro and in vivo efficacy, toxicity, bio-distribution and resistance selection of a novel antibacterial drug candidate. *Sci. Rep.* **6,** 26077 (2016).

17. Hayyan, M., Looi, C. Y., Hayyan, A., Wong, W. F. & Hashim, M. A. In Vitro and in Vivo toxicity profiling of ammonium-based deep eutectic solvents. *PLoS One* **10,** (2015).

18. Tice, R. R., Austin, C. P., Kavlock, R. J. & Bucher, J. R. Improving the human hazard characterization of chemicals: A Tox21 update. *Environmental Health Perspectives* **121,** 756–765 (2013).

19. Illum, L., Jordan, F. & Lewis, A. L. CriticalSorb: a novel efficient nasal delivery system for human growth hormone based on Solutol HS15. *J. Control. Release* **162,** 194–200 (2012).

20. Brayden, D. J., Bzik, V. a, Lewis, a L. & Illum, L. CriticalSorb™ promotes permeation of flux markers across isolated rat intestinal mucosae and Caco-2 monolayers. *Pharm. Res.* **29,** 2543–54 (2012).

21. Shubber, S. *et al.* Mechanism of Mucosal Permeability Enhancement of CriticalSorb® (Solutol® HS15) Investigated In Vitro in Cell Cultures. *Pharm. Res.* **32,** 516–527 (2014).

22. Pinto, M. *et al.* Enterocyte-like differentiation and polarization of the human colon carcinoma cell line Caco-2 in culture. *Biol. Cell* **47,** 323–330 (1983).

23. Hidalgo, I. J., Raub, T. J. & Borchardt, R. T. Characterization of the human colon carcinoma cell line (Caco-2) as a model system for intestinal epithelial permeability. *Gastroenterology* **96,** 736–49 (1989).

24. Artursson, P., Palm, K. & Luthman, K. Caco-2 monolayers in experimental and theoretical predictions of drug transport. *Adv. Drug Deliv. Rev.* **46,** 27–43 (2001).

25. Lennernas, H. Human intestinal permeability. *J Pharm Sci* **87,** 403–410 (1998).

26. Artursson, P. Epithelial transport of drugs in cell culture. I: A model for studying the passive diffusion of drugs over intestinal absorbtive (Caco-2) cells. *J. Pharm. Sci.* **79,** 476–482 (1990).

27. Gupta, V., Hwang, B. H., Doshi, N. & Mitragotri, S. A permeation enhancer for increasing transport of therapeutic macromolecules across the intestine. *J. Control. Release* **172,** 541–9 (2013).

28. Shah, R. B., Palamakula, A. & Khan, M. A. Cytotoxicity Evaluation of Enzyme Inhibitors and Absorption Enhancers in Caco-2 Cells for Oral Delivery of Salmon Calcitonin. *J. Pharm. Sci.* **93,** 1070–1082 (2004).

29. Vinogradov, S. V., Zeman, A. D., Batrakova, E. V. & Kabanov, A. V. Polyplex Nanogel formulations for drug delivery of cytotoxic nucleoside analogs. *J. Control. Release* **107,** 143–157 (2005).

30. Basson, M. D. & Hong, F. Regulation of human Caco-2 intestinal epithelial brush border enzyme activity by cyclic nucleotides. *Cancer Lett.* **99,** 155–160 (1996).

31. Stieger, B., Marxer, A. & Hauri, H. P. Isolation of brush-border membranes from rat and rabbit colonocytes: Is alkaline phosphatase a marker enzyme? *J. Membr. Biol.* **91,** 19–31 (1986).

32. Nougayrede, J. P., Fernandes, P. J. & Donnenberg, M. S. Adhesion of enteropathogenic Escherichia coli to host cells. *Cell Microbiol* **5,** 359–372 (2003).

33. Mooseker, M. S. ORGANIZATION, CHEMISTRY, AND ASSEMBLY OF THE CYTOSKELETAL APPARATUS OF THE INTESTINAL BRUSH BORDER. *Annu. Rev. Cell Biol.* 209–241 (1985).

34. Mooseker, M. S. & Tilney, L. G. Organization of an actin filament-membrane complex: Filament polarity and membrane attachment in the microvilli of intestinal epithelial cells. *J. Cell Biol.* **67,** 725–743 (1975).

35. McConnell, R. E. *et al.* The enterocyte microvillus is a vesicle-generating organelle. *J. Cell Biol.* **185,** 1285–1298 (2009).

36. BROWN, A. L. Microvilli of the human jejunal epithelial cell. *J. Cell Biol.* **12,** 623–627 (1962).

37. Mooseker, M. S. & Coleman, T. R. The 110-kD protein-calmodulin complex of the intestinal microvillus (brush border myosin I) is a mechanoenzyme. *J. Cell Biol.* **108,** 2395–2400 (1989).

38. McConnell, R. E. & Tyska, M. J. Myosin-1a powers the sliding of apical membrane along microvillar actin bundles. *J. Cell Biol.* **177,** 671–681 (2007).

39. Bates, J. M., Akerlund, J., Mittge, E. & Guillemin, K. Intestinal Alkaline Phosphatase Detoxifies Lipopolysaccharide and Prevents Inflammation in Zebrafish in Response to the Gut Microbiota. *Cell Host Microbe* **2,** 371–382 (2007).

40. Goldberg, R. F. *et al.* Intestinal alkaline phosphatase is a gut mucosal defense factor maintained by enteral nutrition. *Proc Natl Acad Sci U S A* **105,** 3551–3556 (2008).

41. Quaroni, A. & Hochman, J. Development of intestinal cell culture models for drug transport and metabolism studies. *Advanced Drug Delivery Reviews* **22,** 3–52 (1996).

42. Anderle, P. *et al.* P-glycoprotein (P-gp) mediated efflux in Caco-2 cell monolayers: The influence of culturing conditions and drug exposure on P-gp expression levels. *J. Pharm. Sci.* **87,** 757–762 (1998).

43. Mordrelle, A. *et al.* EAAT1 is involved in transport of L-glutamate during differentiation of the Caco-2 cell line. *Am J Physiol Gastrointest Liver Physiol* **279,** G366-73 (2000).

44. Anderle, P., Rakhmanova, V., Woodford, K., Zerangue, N. & Sadée, W. Messenger RNA expression of transporter and ion channel genes in undifferentiated and differentiated Caco-2 cells compared to human intestines. *Pharm. Res.* **20,** 3–15 (2003).

45. Braga, V. M., Del Maschio, A., Machesky, L. & Dejana, E. Regulation of cadherin function by Rho and Rac: modulation by junction

maturation and cellular context. *Mol. Biol. Cell* **10,** 9–22 (1999).

46. Schreider, C., Peignon, G., Thenet, S., Chambaz, J. & Pinçon-Raymond, M. Integrin-mediated functional polarization of Caco-2 cells through E-cadherin--actin complexes. *J. Cell Sci.* **115,** 543–552 (2002).

47. Fletcher, D. A. & Mullins, R. D. Cell mechanics and the cytoskeleton. *Nature* **463,** 485–492 (2010).

48. Shen, L., Weber, C. R., Raleigh, D. R., Yu, D. & Turner, J. R. Tight Junction Pore and Leak Pathways: A Dynamic Duo. *Annu. Rev. Physiol.* **73,** 283–309 (2011).

49. Gunzel, D. & Yu, A. S. L. Claudins and the Modulation of Tight Junction Permeability. *Physiol. Rev.* **93,** 525–569 (2013).

50. Fanning, A. S., Jameson, B. J., Jesaitis, L. A. & Anderson, J. M. The tight junction protein ZO-1 establishes a link between the transmembrane protein occludin and the actin cytoskeleton. *J. Biol. Chem.* **273,** 29745–29753 (1998).

51. Hartsock, A. & Nelson, W. J. Adherens and tight junctions: Structure, function and connections to the actin cytoskeleton. *Biochimica et Biophysica Acta - Biomembranes* **1778,** 660–669 (2008).

52. Gumbiner, B. M. Cell adhesion: The molecular basis of tissue architecture and morphogenesis. *Cell* **84,** 345–357 (1996).

53. Garrod, D. & Chidgey, M. Desmosome structure, composition and function. *Biochim. Biophys. Acta - Biomembr.* **1778,** 572–587 (2008).

54. Huber, O. Structure and function of desmosomal proteins and their role in development and disease. *Cellular and Molecular Life Sciences* **60,** 1872–1890 (2003).

55. Garrod, D. R., Merritt, A. J. & Nie, Z. Desmosomal cadherins. *Curr.Opin.Cell Biol.* **14,** 537–545 (2002).

56. Perez-Moreno, M., Jamora, C. & Fuchs, E. Sticky business: Orchestrating cellular signals at adherens junctions. *Cell* **112,** 535–548 (2003).

57. Tepass, U. Adherens junctions: New insight into assembly, modulation and function. *BioEssays* **24,** 690–695 (2002).

58. Kobielak, A. & Fuchs, E. Alpha-catenin: at the junction of intercellular adhesion and actin dynamics. *Nat. Rev. Mol. Cell Biol.* **5,** 614–625 (2004).

59. Sawada, N. *et al.* Extracellular matrix components influence DNA synthesis of rat hepatocytes in primary culture. *Exp Cell Res* **167,** 458–470 (1986).

60. Erickson, A. C. & Couchman, J. R. Still more complexity in mammalian basement membranes. *J. Histochem. Cytochem.* **48,** 1291–306 (2000).

61. Beaulieu, J.-F. *Extracellular Matrix Components and Integrins in Relationship to Human Intestinal Epithelial Cell Differentiation*.

Progress in Histochemistry and Cytochemistry **31,** (1997).

62. Simon-Assmann, P. & Kedinger, M. Heterotypic cellular cooperation in gut morphogenesis and differentiation. *Semin. Cell Biol.* **4,** 221–30 (1993).

63. Bissell, M. J., Hall, H. G. & Parry, G. How does the extracellular matrix direct gene expression? *J. Theor. Biol.* **99,** 31–68 (1982).

64. Le Beyec, J. *et al.* A complete epithelial organization of Caco-2 cells induces I-FABP and potentializes apolipoprotein gene expression. *Exp. Cell Res.* **236,** 311–320 (1997).

65. Boudreau, N. & Bissell, M. J. Extracellular matrix signaling: integration of form and function in normal and malignant cells. *Curr Opin Cell Biol* **10,** 640–646 (1998).

66. Chen, C. S., Alonso, J. L., Ostuni, E., Whitesides, G. M. & Ingber, D. E. Cell shape provides global control of focal adhesion assembly. *Biochem. Biophys. Res. Commun.* **307,** 355–361 (2003).

67. Borradori, L. & Sonnenberg, A. Structure and function of hemidesmosomes: More than simple adhesion complexes. *Journal of Investigative Dermatology* **112,** 411–418 (1999).

68. Klein, G., Ekblom, M., Fecker, L., Timpl, R. & Ekblom, P. Differential expression of laminin A and B chains during development of embryonic mouse organs. *Development* **110,** 823–37 (1990).

69. Li, M. L. *et al.* Influence of a reconstituted basement membrane and its components on casein gene expression and secretion in mouse mammary epithelial cells. *Proc. Natl. Acad. Sci. U. S. A.* **84,** 136–40 (1987).

70. Hoffman, M. P., Kibbey, M. C., Letterio, J. J. & Kleinman, H. K. Role of laminin-1 and TGF-beta 3 in acinar differentiation of a human submandibular gland cell line (HSG). *J. Cell Sci.* **109,** 2013–2021 (1996).

71. Matter, M. L. & Laurie, G. W. A novel laminin E8 cell adhesion site required for lung alveolar formation in vitro. *J. Cell Biol.* **124,** 1083–1090 (1994).

72. Vllasaliu, D., Falcone, F. H., Stolnik, S. & Garnett, M. Basement membrane influences intestinal epithelial cell growth and presents a barrier to the movement of macromolecules. *Exp. Cell Res.* **323,** 218–31 (2014).

73. Smithmyer, M. E., Sawicki, L. a. & Kloxin, A. M. Hydrogel scaffolds as in vitro models to study fibroblast activation in wound healing and disease. *Biomater. Sci.* **2,** 634 (2014).

74. Heydarkhan-Hagvall, S. *et al.* Three-dimensional electrospun ECM-based hybrid scaffolds for cardiovascular tissue engineering. *Biomaterials* **29,** 2907–2914 (2008).

75. Vukicevic, S. *et al.* Identification of multiple active growth factors in basement membrane matrigel suggests caution in interpretation of cellular activity related to extracellular matrix components. *Exp. Cell*

Res. **202,** 1–8 (1992).

76. McGuire, P. G. & Seeds, N. W. The interaction of plasminogen activator with a reconstituted basement membrane matrix and extracellular macromolecules produced by cultured epithelial cells. *J. Cell. Biochem.* **40,** 215–227 (1989).

77. Kleinman, H. K. & Martin, G. R. Matrigel: Basement membrane matrix with biological activity. *Semin. Cancer Biol.* **15,** 378–386 (2005).

78. WL., D. The structure of the colonic mucosa. The epithelium and subepithelial reticulohistiocytic complex. *Gastroenterology* **49,** 496–514 (1965).

79. Pascal, R. R., Kaye, G. I. & Lane, M.D, N. Colonic Pericryptal Fibroblast Sheath: Replication, Migration, and Cytodifferentiation of a Mesenchymal Cell System in Adult Tissue: I. Autoradiographic studies of normal rabbit colon. *Gastroenterology* **54,** 835–851 (1968).

80. Visco, V. *et al.* Human colon fibroblasts induce differentiation and proliferation of intestinal epithelial cells through the direct paracrine action of keratinocyte growth factor. *J. Cell. Physiol.* **220,** 204–13 (2009).

81. Bulut, K. *et al.* Glucagon like peptide-2 induces intestinal restitution through VEGF release from subepithelial myofibroblasts. *Eur. J. Pharmacol.* **578,** 279–85 (2008).

82. Göke, M., Kanai, M. & Podolsky, D. K. Intestinal fibroblasts regulate intestinal epithelial cell proliferation via hepatocyte growth factor. *Am. J. Physiol.* **274,** G809-18 (1998).

83. Powell, D. W., Adegboyega, P. A., Di Mari, J. F. & Mifflin, R. C. Epithelial cells and their neighbors I. Role of intestinal myofibroblasts in development, repair, and cancer. *Am. J. Physiol. Gastrointest. Liver Physiol.* **289,** G2–G7 (2005).

84. Macdonald, T. T. & Monteleone, G. Immunity, inflammation, and allergy in the gut. *Science* **307,** 1920–5 (2005).

85. Kurobe, M., Furukawa, S. & Hayashi, K. Synthesis and secretion of an epidermal growth factor (EGF) by human fibroblast cells in culture. *Biochem. Biophys. Res. Commun.* **131,** 1080–1085 (1985).

86. Carpenter, G. & Cohen, S. Epidermal growth factor. *J Biol Chem* **265,** 7709–7712 (1990).

87. Brzozowski, T., Majka, J., Garlicki, J., Drozdowicz, D. and Konturek, S. J. Role of polyamines and prostaglandins in gastroprotective action of epidermal growth factor against ethanol injury. *J. Clincal Gastroenterol.* **13,** s98-101 (1991).

88. Konturek, J. W., Brzozowski, T. & Konturek, S. J. Epidermal growth factor in protection, repair, and healing of gastroduodenal mucosa. *J. Clin. Gastroenterol.* **13 Suppl 1,** S88–S97 (1991).

89. Konturek, P. K., Brzozowski, T., Konturek, S. J. and Dembinski, A. Role of epidermal growth factor, prostaglandin, and sulfhydryls in stress-induced gastric lesions. *Gastroenterology* **99,** 1607–1615

(1990).

90. Tepperman, B. L., Vozzolo, B. L. and Soper, B. D. Effect of maternal sialoadenectomy on ontogenic response of rat gastric mucosa to luminal H+. *Am. J. Physiol.* **265,** 354–360 (1993).

91. Rao, R. & Porreca, F. Epidermal growth factor protects mouse ileal mucosa from Triton X-100-induced injury. *Eur. J. Pharmacol.* **303,** 209–212 (1996).

92. Rao, R., Baker, R. D. & Baker, S. S. Inhibition of oxidant-induced barrier disruption and protein tyrosine phosphorylation in Caco-2 cell monolayers by epidermal growth factor. *Biochem Pharmacol* **57,** 685–695 (1999).

93. Rao, R. K., Basuroy, S., Rao, V. U., Karnaky Jr, K. J. & Gupta, A. Tyrosine phosphorylation and dissociation of occludin-ZO-1 and E-cadherin-beta-catenin complexes from the cytoskeleton by oxidative stress. *Biochem. J.* **368,** 471–481 (2002).

94. Rao, R. K., Baker, R. D., Baker, S. S., Gupta, A. & Holycross, M. Oxidant-induced disruption of intestinal epithelial barrier function: role of protein tyrosine phosphorylation. *Am. J. Physiol.* **273,** G812-23 (1997).

95. Rao, R. K., Li, L., Baker, R. D., Baker, S. S. & Gupta, A. Glutathione oxidation and PTPase inhibition by hydrogen peroxide in Caco-2 cell monolayer. *Am. J. Physiol. Gastrointest. Liver Physiol.* **279,** G332-40 (2000).

96. Aggarwal, S., Suzuki, T., Taylor, W. L., Bhargava, A. & Rao, R. K. Contrasting effects of ERK on tight junction integrity in differentiated and under-differentiated Caco-2 cell monolayers. *Biochem. J.* **433,** 51–63 (2011).

97. Basuroy, S., Seth, A., Elias, B., Naren, A. P. & Rao, R. MAPK interacts with occludin and mediates EGF-induced prevention of tight junction disruption by hydrogen peroxide. *Biochem. J.* **393,** 69–77 (2006).

98. Gopal, P., Rehman, R. U., Chadha, K. S., Qiu, M. & Colella, R. Matrigel influences morphology and cathepsin B distribution of prostate cancer PC3 cells. *Oncol. Rep.* **16,** 313–320 (2006).

99. Kleinman, H. K. *et al.* Isolation and Characterization of Type IV Procollagen, Laminin, and Heparan Sulfate Proteoglycan from the EHS Sarcoma. *Biochemistry* **21,** 6188–6193 (1982).

100. Anguiano, M. *et al.* Characterization of three-dimensional cancer cell migration in mixed collagen-Matrigel scaffolds using microfluidics and image analysis. *PLoS One* **12,** (2017).

101. Hughes, C. S., Postovit, L. M. & Lajoie, G. A. Matrigel : A complex protein mixture required for optimal growth of cell culture. 1886–1890 (2010). doi:10.1002/pmic.200900758

102. Vllasaliu, D., Fowler, R., Garnett, M., Eaton, M. & Stolnik, S. Barrier characteristics of epithelial cultures modelling the airway and intestinal mucosa: a comparison. *Biochem. Biophys. Res. Commun.* **415,** 579–85 (2011).

103. Vllasaliu, D. In vitro investigation into strategies for mucosal delivery of proteins. (2010).

104. Narai, A., Arai, S. & Shimizu, M. Rapid decrease in transepithelial electrical resistance of human intestinal Caco-2 cell monolayers by cytotoxic membrane perturbents. *Toxicol. Vitr.* **11,** 347–354 (1997).

105. Velarde, G. *et al.* Use of transepithelial electrical resistance in the study of pentachlorophenol toxicity. in *Toxicology in Vitro* **13,** 723–727 (1999).

106. Elamin, E. *et al.* Effects of ethanol and acetaldehyde on tight junction integrity: In vitro study in a three dimensional intestinal epithelial cell culture model. *PLoS One* **7,** (2012).

107. Ivanov, A. I. *et al.* Myosin II regulates the shape of three-dimensional intestinal epithelial cysts. *J. Cell Sci.* **121,** 1803–1814 (2008).

108. Cerchiari, A. *et al.* Formation of spatially and geometrically controlled three-dimensional tissues in soft gels by sacrificial micromolding. *Tissue Eng. Part C. Methods* **21,** 541–7 (2015).

109. Reininger-Mack, A., Thielecke, H. & Robitzki, A. A. 3D-biohybrid systems: Applications in drug screening. *Trends in Biotechnology* **20,** 56–61 (2002).

110. Breslin, S. & O'Driscoll, L. Three-dimensional cell culture: The missing link in drug discovery. *Drug Discovery Today* **18,** 240–249 (2013).

111. Cerchiari, A. E. *et al.* Probing the luminal microenvironment of reconstituted epithelial microtissues. *Sci. Rep.* **6,** 33148 (2016).

112. Chirayath, M. V *et al.* Vitamin D increases tight-junction conductance and paracellular Ca2+ transport in Caco-2 cell cultures. *Am.J.Physiol* **274,** G389–G396 (1998).

113. Claude, P. Morphological factors influencing transepithelial permeability: A model for the resistance of the Zonula Occludens. *J. Membr. Biol.* **39,** 219–232 (1978).

114. Furuse, M. *et al.* Occludin: A novel integral membrane protein localizing at tight junctions. *J. Cell Biol.* **123,** 1777–1788 (1993).

115. Schneeberger, E. E. The tight junction: a multifunctional complex. *AJP Cell Physiol.* **286,** C1213–C1228 (2004).

116. Zhang, J., Zhu, X., Jin, Y., Shan, W. & Huang, Y. Mechanism study of cellular uptake and tight junction opening mediated by goblet cell-specific trimethyl chitosan nanoparticles. *Mol. Pharm.* **11,** 1520–1532 (2014).

117. Smith, J. M., Dornish, M. & Wood, E. J. Involvement of protein kinase C in chitosan glutamate-mediated tight junction disruption. *Biomaterials* **26,** 3269–3276 (2005).

118. Yeh, T. H. *et al.* Mechanism and consequence of chitosan-mediated reversible epithelial tight junction opening. *Biomaterials* **32,** 6164–6173 (2011).

119. Tang, V. W. & Goodenough, D. A. Paracellular ion channel at the tight

junction. *Biophys. J.* **84,** 1660–73 (2003).

120. Balogh, J., Olsson, U. & Pedersen, J. S. Dependence on Oil Chain Length of the Curvature Elastic Properties of Nonionic Surfactant Films : Emulsification Failure and Phase Equilibria. *J. Dispers. Sci. Technol.* **27,** 497–510 (2006).

121. Schneeberger, E. E. & Lynch, R. D. Structure, function, and regulation of cellular tight junctions. *Am J Physiol* **262,** L647-61 (1992).

122. Gumbiner, B. M. Breaking through the tight barrier. *J Cell Biol* **123,** 1631–1633 (1993).

123. Tsukita, S., Furuse, M. & Itoh, M. Multifunctional strands in tight junctions. *Nat. Rev. Mol. Cell Biol.* **2,** 285–293 (2001).

124. Hurley, B. P. *et al.* An experimental platform using human intestinal epithelial cell lines to differentiate between hazardous and non-hazardous proteins. *Food Chem. Toxicol.* **92,** 75–87 (2016).

125. Castiaux, V., Laloux, L., Schneider, Y.-J. & Mahillon, J. Screening of Cytotoxic B. cereus on Differentiated Caco-2 Cells and in Co-Culture with Mucus-Secreting (HT29-MTX) Cells. *Toxins (Basel).* **8,** 320 (2016).

126. GTEx Portal. LDHA gene expression. Available at: https://www.gtexportal.org. (Accessed: 14th September 2017)

127. Markert, C. L. Lactate dehydrogenase. Biochemistry and function of lactate dehydrogenase. *Cell Biochem. Funct.* **2,** 131–4 (1984).

128. Chang, C.-C. *et al.* Upregulation of lactate dehydrogenase a by 14-3-3ζ leads to increased glycolysis critical for breast cancer initiation and progression. *Oncotarget* **7,** 35270–83 (2016).

129. Zhao, Y. H. *et al.* Upregulation of lactate dehydrogenase A by ErbB2 through heat shock factor 1 promotes breast cancer cell glycolysis and growth. *Oncogene* **28,** 3689–701 (2009).

130. Sorger, P. K. Heat shock factor and the heat shock response. *Cell* **65,** 363–366 (1991).

131. Marzesco, A. M. *et al.* Release of extracellular membrane vesicles from microvilli of epithelial cells is enhanced by depleting membrane cholesterol. *FEBS Lett.* **583,** 897–902 (2009).

132. Shubber, S. The evaluation of Solutol HS15 as a mucosal absorption enhancer. (University of Nottingham, 2015).

133. Lucocq, J., Berger, E. & Hug, C. The pathway of Golgi cluster formation in okadaic acid-treated cells. *J. Struct. Biol.* **115,** 318–330 (1995).

134. Rege, B. D., Yu Lawrence, X., Hussain, A. S. & Polli, J. E. Effect of common excipients on Caco-2 transport of low-permeability drugs. *J. Pharm. Sci.* **90,** 1776–1786 (2001).

135. Koga, K., Ohyashiki, T., Murakami, M. & Kawashima, S. Modification of ceftibuten transport by the addition of non-ionic surfactants. *Eur. J. Pharm. Biopharm.* **49,** 17–25 (2000).

136. Nerurkar, M. M., Burton, P. S. & Borchardt, R. T. The use of surfactants to enhance the permeability of peptides through caco-2 cells by inhibition of an apically polarized efflux system. *Pharm. Res.* **13,** 528–534 (1996).

137. Dokladny, K., Moseley, P. L. & Ma, T. Y. Physiologically relevant increase in temperature causes an increase in intestinal epithelial tight junction permeability. *Am J Physiol Gastrointest Liver Physiol* **290,** G204-12 (2006).

138. Moseley, P. L., Gapen, C., Wallen, E. S., Walter, M. E. & Peterson, M. W. Thermal stress induces epithelial permeability. *Am. J. Physiol.* **267,** C425-34 (1994).

139. Dokladny, K., Wharton, W., Lobb, R., Ma, T. Y. & Moseley, P. L. Induction of physiological thermotolerance in MDCK monolayers: contribution of heat shock protein 70. *Cell Stress Chaperones* **11,** 268–275 (2006).

140. Ma, T. Y., Hollander, D., Erickson, R. A., Truong, H. & Krugliak, P. Is the small intestinal epithelium truly 'tight' to inulin permeation? *Am. J. Physiol. Gastrointest. Liver Physiol.* **260,** G669–G676 (1991).

141. Dokladny, K., Wharton, W., Lobb, R., Ma, T. Y. & Moseley, P. L. Induction of physiological thermotolerance in MDCK monolayers: contribution of heat shock protein 70. *Cell Stress Chaperones* **11,** 268–275 (2006).

142. Chen, S., Bawa, D., Besshoh, S., Gurd, J. W. & Brown, I. R. Association of heat shock proteins and neuronal membrane components with lipid rafts from the rat brain. *J. Neurosci. Res.* **81,** 522–529 (2005).

143. Nimmervoll, B. *et al.* Cell surface localised Hsp70 is a cancer specific regulator of clathrin-independent endocytosis. *FEBS Lett.* **589,** 2747–2753 (2015).

144. Van Meer, G., Simons, K. & Simons, K. The function of tight junctions in maintaining differences in lipid composition between the apical and the basolateral cell surface domains of MDCK cells. *EMBO J.* **5,** 1455–1464 (1986).

145. Hjort Ipsen, J., Karlström, G., Mourtisen, O. G., Wennerström, H. & Zuckermann, M. J. Phase equilibria in the phosphatidylcholine-cholesterol system. *BBA - Biomembr.* **905,** 162–172 (1987).

146. Pinto, M., Morange, M. & Bensaude, O. Denaturation of proteins during heat shock: In vivo recovery of solubility and activity of reporter enzymes. *J. Biol. Chem.* **266,** 13941–13946 (1991).

147. Török, Z. *et al.* Heat shock protein coinducers with no effect on protein denaturation specifically modulate the membrane lipid phase. *Proc. Natl. Acad. Sci. U. S. A.* **100,** 3131–3136 (2003).

148. Whitley, D., Goldberg, S. P. & Jordan, W. D. Heat shock proteins: A review of the molecular chaperones. *J. Vasc. Surg.* **29,** 748–751 (1999).

149. Goncharova, E. a, Goncharov, D. a & Krymskaya, V. P. Assays for in

vitro monitoring of human airway smooth muscle (ASM) and human pulmonary arterial vascular smooth muscle (VSM) cell migration. *Nat. Protoc.* **1,** 2933–2939 (2006).

150. Makinoshima, H. *et al.* Epidermal Growth Factor Receptor (EGFR) Signaling Regulates Global Metabolic Pathways in EGFR-mutated Lung Adenocarcinoma. *J. Biol. Chem.* **289,** 20813–20823 (2014).

151. Baulida, J., Onetti, R. & Bassols, A. Effects of epidermal growth factor on glycolysis in A431 cells. *Biochem. Biophys. Res. Commun.* **183,** 1216–23 (1992).

152. Vander Heiden, M. G. *et al.* Growth factors can influence cell growth and survival through effects on glucose metabolism. *Mol. Cell. Biol.* **21,** 5899–912 (2001).

153. Reddy, K. B. Epidermal growth factor induced apoptosis. *Apoptosis* **1,** 33–39 (1996).

154. Oda, E. Noxa, a BH3-Only Member of the Bcl-2 Family and Candidate Mediator of p53-Induced Apoptosis. *Science (80-.).* **288,** 1053–1058 (2000).

155. Brinkmann, K. & Kashkar, H. Targeting the mitochondrial apoptotic pathway: a preferred approach in hematologic malignancies? *Cell Death Dis.* **5,** e1098 (2014).

156. Ploner, C., Kofler, R. & Villunger, A. Noxa: at the tip of the balance between life and death. *Oncogene* **27,** S84–S92 (2008).

157. Tseng, S. C., Kruse, F. E., Merritt, J. & Li, D. Q. Comparison between serum-free and fibroblast-cocultured single-cell clonal culture systems: evidence showing that epithelial anti-apoptotic activity is present in 3T3 fibroblast-conditioned media. *Curr Eye Res* **15,** 973–984 (1996).

158. Kinoshita, S., Koizumi, N. & Nakamura, T. Transplantable cultivated mucosal epithelial sheet for ocular surface reconstruction. *Experimental Eye Research* **78,** 483–491 (2004).

159. Liu, J. Y. & Burg, G. An improved organ culture for regeneration of pure autologous keratinocytes from small split-thickness skin specimens. *Dermatology* **210,** 45–48 (2005).

160. Kitchen, J. R. & Cysyk, R. L. Synthesis and release of hyaluronic acid by Swiss 3T3 fibroblasts. *Biochem. J.* **309 (Pt 2,** 649–56 (1995).

161. Takano, H. *et al.* Restriction of Mast Cell Proliferation through Hyaluronan Synthesis by Co-cultured Fibroblasts. *Biol. Pharm. Bull.* **35,** 408–412 (2012).

162. Kenneth W. Adolph. in *Advanced Techniques in Chromosome Research* 413–432 (1991).

163. Stahl, S., Weitzman, S. & Jones, J. C. The role of laminin-5 and its receptors in mammary epithelial cell branching morphogenesis. *J. Cell Sci.* **110 (Pt 1,** 55–63 (1997).

164. Delcommenne, M. & Streuli, C. H. Control of integrin expression by extracellular matrix. *J. Biol. Chem.* **270,** 26794–26801 (1995).

165. Lu, W., McCallum, L. & Irvine, A. E. A rapid and sensitive method for measuring cell adhesion. *J. Cell Commun. Signal.* **3,** 147–149 (2009).

166. Lenne, P.-F. *et al.* Dynamic molecular confinement in the plasma membrane by microdomains and the cytoskeleton meshwork. *EMBO J.* **25,** 3245–3256 (2006).

167. Sadegh, S., Higgins, J. L., Mannion, P. C., Tamkun, M. M. & Krapf, D. Plasma membrane is compartmentalized by a self-similar cortical actin meshwork. *Phys. Rev. X* **7,** (2017).

168. Chichili, G. R., Cail, R. C. & Rodgers, W. Cytoskeletal modulation of lipid interactions regulates lck kinase activity. *J. Biol. Chem.* **287,** 24186–24194 (2012).

169. Nebl, T. *et al.* Proteomic analysis of a detergent-resistant membrane skeleton from neutrophil plasma membranes. *J. Biol. Chem.* **277,** 43399–43409 (2002).

170. von Haller, P. D., Donohoe, S., Goodlett, D. R., Aebersold, R. & Watts, J. D. Mass spectrometric characterization of proteins extracted from Jurkat T cell detergent-resistant membrane domains. *Proteomics* **1,** 1010–21 (2001).

171. Parmryd, I., Adler, J., Patel, R. & Magee, A. I. Imaging metabolism of phosphatidylinositol 4,5-bisphosphate in T-cell GM1-enriched domains containing Ras proteins. *Exp. Cell Res.* **285,** 27–38 (2003).

172. Hope, H. R. & Pike, L. J. Phosphoinositides and phosphoinositide-utilizing enzymes in detergent-insoluble lipid domains. *Mol. Biol. Cell* **7,** 843–51 (1996).

173. Lingwood, D. & Simons, K. Detergent resistance as a tool in membrane research. *Nat. Protoc.* **2,** 2159–2165 (2007).

174. Schuck, S., Honsho, M., Ekroos, K., Shevchenko, A. & Simons, K. Resistance of cell membranes to different detergents. *Proc. Natl. Acad. Sci. U. S. A.* **100,** 5795–5800 (2003).

175. Lindmark, T. *et al.* Mechanism of absorption enhancement in humans after rectal administration of ampicillin in suppositories containing sodium caprate. *Pharm. Res.* **14,** 930–935 (1997).

176. Tscheik, C., Blasig, I. E. & Winkler, L. Trends in drug delivery through tissue barriers containing tight junctions. *Tissue Barriers* **1,** e24565 (2013).

177. Hansson, G. C. & Johansson, M. E. V. The inner of the two Muc2 mucin-dependent mucus layers in colon is devoid of bacteria. *Gut Microbes* **1,** 51–54 (2010).

178. Atuma, C., Strugala, V., Allen, a & Holm, L. The adherent gastrointestinal mucus gel layer: thickness and physical state in vivo. *Am. J. Physiol. Gastrointest. Liver Physiol.* **280,** G922-9 (2001).

179. Hansson, G. C. Role of mucus layers in gut infection and inflammation. *Current Opinion in Microbiology* **15,** 57–62 (2012).

180. MacAdam, A. The effect of gastro-intestinal mucus on drug absorption. *Advanced Drug Delivery Reviews* **11,** 201–220 (1993).

181. Georgantzopoulou, A. *et al.* Effects of silver nanoparticles and ions on a co-culture model for the gastrointestinal epithelium. *Part. Fibre Toxicol.* **13,** 9 (2015).

182. Gagnon, M., Zihler Berner, A., Chervet, N., Chassard, C. & Lacroix, C. Comparison of the Caco-2, HT-29 and the mucus-secreting HT29-MTX intestinal cell models to investigate Salmonella adhesion and invasion. *J. Microbiol. Methods* **94,** 274–279 (2013).

7. Chapter Seven – General Discussion

Summary

This chapter will discuss the possible suggested mechanism of cellular toxicity for a model non-ionic surfactant, Solutol HS15, by linking together the results obtained throughout the work described in previous chapters. The discussion will include the assessment of surfactant effects on the plasma membrane integrity and consequent membrane permeability, together with data on mitochondrial responses and the determination of the possible mode of cell death. The discussion will also reflect on how cell culture conditions modulate surfactant cytotoxicity. Finally, avenues for future work are reviewed and the significance of the findings presented in this thesis are concluded.

7.1. Cellular responses to surfactant exposure

The proposed mechanism of action of Solutol HS15 and the cellular response of Caco-2 intestinal epithelial cells is illustrated in Figure 7.. It should be noted that in this work an important parameter in the experimental design was to assess the effects measured as a function of exposure time, rather than a single time point, which allows the effects analysed to be discussed in the context of time, as follows;

i. Initial, primary surfactant effect

Immediately upon application (within 0-1 minute), surfactant molecules incorporate into the plasma membrane, causing membrane fluidisation, as determined by the change in fluorescence profile of the Laurdan probe indicating the creation of a more hydrophilic environment (Figure 3.8). This initial effect does not appear to induce increased membrane permeability, as indicated from FITC-dextran (4kDa) internalisation (Figure 3.6), or the loss of plasma membrane barrier function, evaluated by assessing LDH release (Figure 3.5).

However, the initial level of membrane fluidisation induced by high surfactant concentration (10 mM) appears comparable to that of cells exposed to 42°C heat shock (Figure 5.15), and it is suggested that this magnitude, or similar, of fluidisation triggers a mitochondrial response (observed at the 5 minutes time point and discussed below).

Increased membrane permeability was manifested at >60 minutes of exposure to surfactant concentrations ≥1 mM, as evidenced by the influx *and* efflux of material (Figures 3.6 and

3.5, respectively), and loss of ion homeostasis (Figure 3.7; only 50 mM solutions studied). As previously suggested for other non-ionic surfactants[1–3], the increased permeability can be associated with surfactant mediated-fluidisation of the plasma membrane which, with Solutol HS15, appears bi-phasic in nature; characterised by an initial (0-1 minute) and secondary (>30-40 minutes) change in Laurdan polarisation, and it is this latter phase in alterations in membrane microenvironment that increased permeability can be attributed to.

Subsequently, at later exposure time points, surfactant molecules may be able to traverse intracellularly, *via* membrane recycling mechanisms and/or membrane perforations (i.e. pores or ruptures), and induce increased permeability and/or permeabilise intracellular organelle membranes, such as the nuclear membranes.

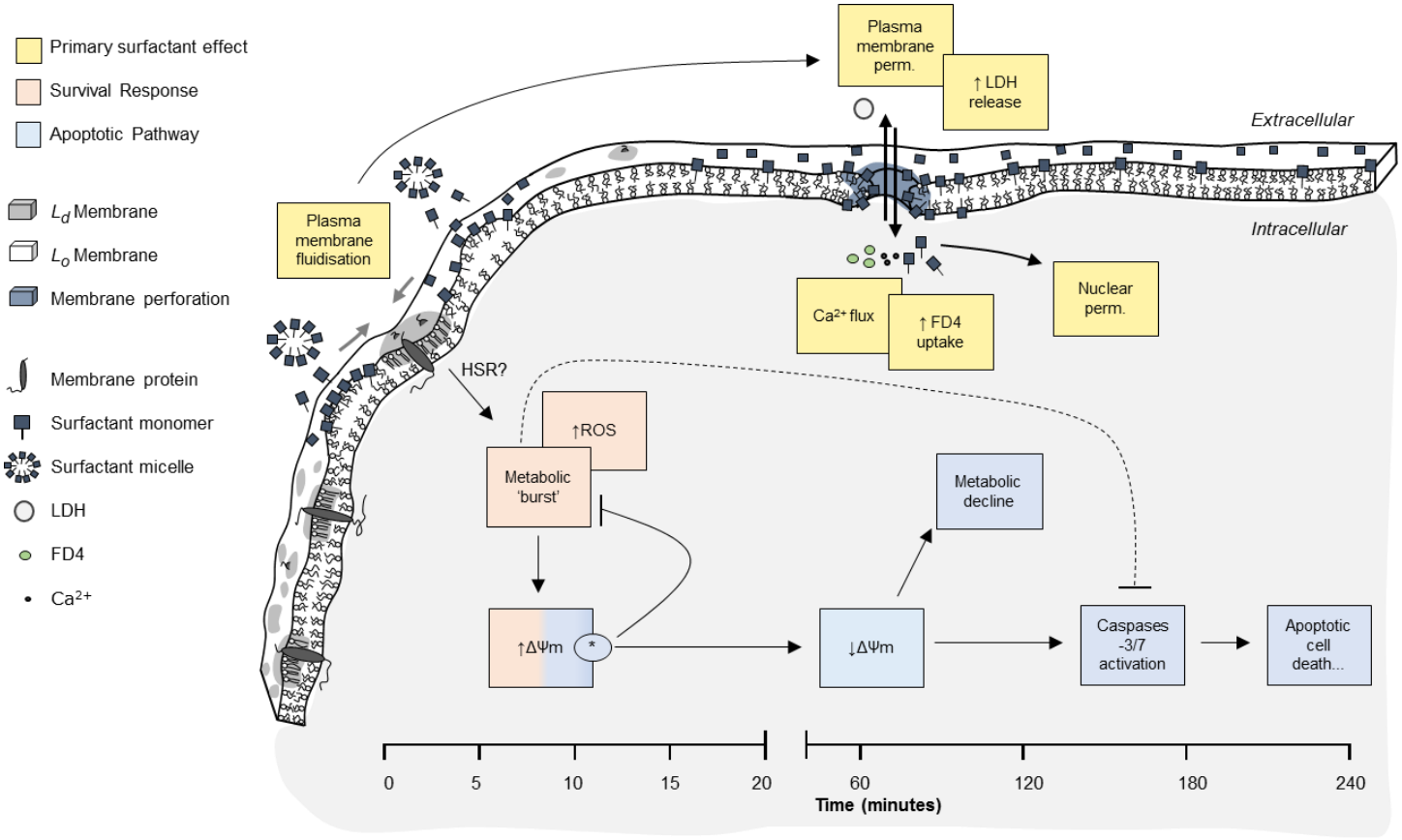

Figure 7.1. Suggested mechanism of toxicity of non-ionic surfactant on Caco-2 intestinal epithelial cells. Exposure to surfactant includes rapid fluidization of the cell plasma membrane which could incite a membrane-derived stress response, akin to the heat shock response, and is characterised by an early 'survival' phase (in red) and the subsequent initiation of a stress-induced mitochondrial-mediated apoptotic pathway (in blue). Occurring in parallel to these responses are the direct membrane effects of surfactant (in yellow) which, over time, progress from stress-inducing disruptions in membrane fluidity, to membrane perturbations associated with increased membrane permeability. LDH, lactose dehydrogenase; FD4, FITC-dextran (4kDa); ΔΨm, mitochondrial membrane potential; perm., permeabilisation.

ii Stress-induced survival response

The results gathered in this work indicated that the stress-induced survival response (illustrated in Figure 7.) is most likely triggered by the initial plasma membrane fluidisation[4–6] and appears be the link between membrane and mitochondrial effects (Figure 7.).

Surfactant molecule incorporation and plasma membrane fluidisation have been shown to induce the clustering of membrane raft regions[7]. This in turn alters the spatial coordination of membrane proteins involved in cellular thermal sensing, such as growth factor tyrosine kinase, similar to the effect of thermal stress on the membrane, and triggers the cellular heat shock response[8].

The metabolic burst observed at the 5 and 10 minutes time points (Figure 4.4) may be associated with the activation of survival pathways, providing energy for rapid cellular adaptation[9] to address the stress stimuli[10].

Inhibitions studies using FCCP suggest that a consequence of this metabolic burst may be oxidative stress and mitochondrial hyperpolarisation (Figures 5.12 and 5.11, respectively). The latter process has been established as an early step in mitochondrial-mediated apoptosis[11,12]. In the work carried out here, it appears that the induction of apoptosis *via* mitochondrial hyperpolarisation is a time-dependent process; the presence of hyperpolarised mitochondria alone does not trigger apoptosis (0-5 minutes), however its prolonged induction does (>5 minutes).

The metabolic burst of the survival response and the associated mitochondrial hyperpolarisation, may therefore be acting in manner akin to an 'internal timer' through which the survival phase triggers, and succumbs to, stress-induced death; i.e. if the cellular insult persists and/or is too severe to be addressed and corrected, the survival response is maintained, hyperpolarisation sustained and rapid death is activated mitochondrially.

iii. Stress-induced apoptotic cell death

Recovery experiments demonstrate that the trigger for apoptosis appears to occur between 5-10 minutes of surfactant exposure (Figure 5.7).

Activation of this apoptotic pathway is associated with inducing mitochondrial depolarisation following 60 minutes of exposure (Figure 5.9), metabolic decline after 120 minutes (Figure 5.11), the activation of effector caspases at 120-180 minutes (Figure 5.10), and at 240 minutes nuclear fragmentation (Figure 5.3).

Activation of the apoptotic pathway appears to inhibit the cell survival response, as suggested by the sustained metabolic burst that occurs in the absence of mitochondrial hyperpolarisation induced apoptosis (Figure 5.11); highlighting the crosstalk between these pathways and indicating a feed-back mechanism takes place (Figure 7.).

7.2. Cell death consequences

As discussed above, Solutol HS15 induced membrane fluidisation is possibly being sensed in a manner similar to thermal stress and thus triggers the heat shock response. Other non-ionic surfactants such as the alkylglycosides[1,2] and polysorbates[3], have been suggested to mediate their increases in drug permeability *via* the induction of membrane fluidisation. Therefore, the cell death mechanism described here may have relevance for other surfactants, and indeed other membrane fluidisers.

The activation of the heat shock response may protect the cell from early lysis and, in a similar manner, limit surfactant-induced increases in membrane permeability at early time points by upregulating proteins that function to stabilise the membrane[13–16]. Therefore, it may be proposed that increased plasma membrane permeability may only occur when response-induced membrane stabilisation has ceased and cell death mechanisms have been activated. Taken together, this suggests that the use of surfactants, which affect the plasma membrane for the enhancement of drug permeability, may be limited by the fact that their membrane permeability effects are intrinsically linked to cell death induced *via* alterations in membrane fluidity.

However, this apoptotic mechanism of death may confer protection to the cell population, or intestinal tissue as a whole, from surfactant-induced immunogenicity. The loss of barrier function induced by Solutol HS15 and the consequent loss, i.e. leakage of intracellular components, will likely promote immunogenic effects in the surrounding cells and tissue[17,18]. The induction of *rapid* mitochondrial-mediated apoptosis is

therefore advantageous; if the cell can package its contents into apoptotic bodies to be phagocytosed, before the necrotic-like cell lysis occurs, this may minimise the toxic potential of surfactant exposure.

Thus, on cells exposure to a non-ionic surfactant like Solutol HS15, there would appear to be a possibility for a non-immunogenic demise. Results show hallmarks of apoptosis; effector caspases are activated and there are signs of fragmented nuclei, indicating that the apoptotic pathway is likely occurring, however further study is required to confirm that pro-inflammatory 'danger signals' are not generated during this cell death[19,20]. That said however, it is now recognised that not all forms of apoptosis are non-immunogenic, therefore differentiating between necrotic and apoptotic outcomes based on immunogenicity may be limited[21–23].

Regarding immunogenicity, it would be important to assess if 'eat-me' signals are exposed and, how rapidly surfactant-treated cells are subsequently phagocytosed and cleared[24]. If, for example, rapid surfactant-induced apoptosis stimulates the swift phagocytosis of damaged cells, then perhaps cells might be cleared, before their plasma membranes become more permeable and loss of intracellular contents occurs. Indeed, intestinal epithelial cells have the highest turnover rate of any fixed-cell population[25,26], therefore, there is a high possibility for a fast rate of clearance *in vivo*[27,28]. The study of recognition ligands on apoptotic cells, such as 'find-me' and 'eat-me' signals, may provide more information as to the speed at which surfactant-damaged cells may be removed[29,30]. This avenue of research may provide further information as to the predicted toxicity of surfactants *in vivo*.

The work undertaken here has investigated the toxicity of Solutol HS15 alone (or with FCCP), however as discussed in Chapter 1, one application of non-ionic surfactants is as drug delivery vesicles / drug permeability enhancers. Therefore, the question arises if the toxicity of Solutol HS15 described here would be similar to Solutol HS15 dosed alongside drugs, and, for the most part, one believes it would. One exception however, would be if the co-administered drug(s) were to have membrane-associated effects, for example, the membrane permeabilising mechanism of aminoglycoside antibiotics. In these cases, it is possible that Solutol HS15 toxicity could be amplified.

7.3. Role of Surfactant concentration

It is observed that application of 0.1 mM Solutol HS15 solution generated membrane fluidisation, but not to the same level as a 10 mM solution or as heat shock (Figure 5.15). Therefore, the question is raised whether lower concentrations of surfactant are capable of inducing the heat shock response. Notably 1 mM Solutol HS15 did not induce a metabolic burst (Figure 4.4), however, it was associated with mitochondrial hyperpolarisation at 5-10 minutes of exposure and depolarisation at 60 minutes (Figure 4.6). Importantly, 1 mM of surfactant did induce activation of caspases (Figure 5.4), and was susceptible to FCCP inhibition of mitochondrial depolarisation, metabolic decline and caspase activation (Figures 5.9, 5.11 and 5.10, respectively).

It would therefore appear that 1 mM Solutol HS15 is indeed activating a mitochondrial-dependent cellular response that is responsible for cell death. This mechanism appears similar to

that induced by higher surfactant concentrations, however it is distinct in the fact that the initial metabolic burst is absent. The difference in cellular response may be associated with different thresholds of heat shock, namely mild (38-41°C) and severe (≥42°C) heat shock, which are reported to activate distinct heat shock proteins and pathways[31–35], however both can induce apoptosis[34,36,37]. Therefore, surfactant may be inducing different response pathways dependent on the surfactant concentration and the magnitude of membrane fluidisation elicited (Figures 3.8 and 5.15).

Additionally, of further note, is that 1 mM Solutol HS15 was the minimum concentration required to enhance the permeability of model drug (FITC-dextran, 4kDa) and also, to induce cell death. Therefore, it would appear that Solutol HS15 toxicity and efficacy (at enhancing drug permeability) are related.

Interestingly, effector caspase activation was not observed with 0.1 mM Solutol HS15 following exposures ≤240 minutes (Figure 5.4), however this concentration was observed to reduce plasma membrane fluidity (Figure 3.8), and induce mitochondrial hyperpolarisation (Figure 4.6). Application of this surfactant concentration was associated with cytotoxicity; inducing membrane damage after 180 minutes of exposure and metabolic decline at 240 minutes (Figures 3.5 and 4.4, respectively). Furthermore, mitochondrial depolarisation, but not metabolic decline, induced by 0.1 mM solutions of surfactant were responsive to FCCP inhibition (Figure 5.9 and 5.11). Therefore, it is established that all Solutol HS15 concentrations >CMC induce cellular effects. However, it is unclear if 0.1 mM induces apoptosis. It would be of interest, therefore, to increase exposure time to 12 or 24 hours and observe whether activation of apoptosis is induced with 0.1 mM

of surfactant, and relate apoptosis and the membrane-derived cellular response, to the presence of surfactant micelles.

7.4. In vitro - in vivo correlation

The majority of work that assessed cellular responses to surfactant exposure was performed on Caco-2 cells cultured in the standard manner for cytotoxicity testing (i.e. subconfluent manner on cell culture plastic), however it has been shown that differentiated Caco-2 cells express increased levels of genes encoding for membrane-associated transporters[38] and cytoskeletal elements[39]. Moreover, Caco-2 culture on extracellular matrix also increases cytoskeletal support[40], and paracrine signalling is associated with promoting Caco-2 proliferation, differentiation[41–43] and repair[44]. Accordingly, the final section of work studied cells cultured in manners which conserved elements of these *in vivo* features, and the results illustrate that surfactant toxicity was, in general, reduced by these methods. Moreover, as discussed in Chapter 1, non-ionic surfactants are typically subjected to hydrolysis in the gastrointestinal tract. Data specifically pertaining to the hydrolysis of Solutol HS15 is absent in the literature, however, it can be predicted that it also undergoes breakdown in a similar manner to previously studied surfactants (*e.g* polysorbates). Therefore, the concentration of Solutol HS15 in the intestinal tract may decrease relative to the orally administered amount. Thus, taken together, it can be predicted that Solutol HS15 will be less toxic *in vivo* than *in vitro*.

Interestingly, the surfactant did not induce the initial metabolic burst associated with short exposure to high concentrations (Figure 6.12), suggesting that differentiated Caco-2 cell

monolayers are less sensitive to stress generated by membrane fluidisation; it would therefore be worthwhile to increase the surfactant concentration and investigate this further. The additional cell membrane support conferred by cell-cell and cell-matrix junctions most likely increases resistance to surfactant toxicity, and paracrine signalling may bestow additional elements of cellular adaptation and repair, however, due to the non-specific nature of non-ionic surfactant effect[45,46], their mechanism of toxicity associated with membrane destabilisation and/or damage is most likely conserved.

7.5. Comparison with other surfactants

As mentioned in Chapter 1, the lack of standardisation with exposure times hinders comparison among surfactants of parameters such as LD_{50} values. However, general comparisons can be made to some studies presented in the literature.

Table 7.1. Solutol HS15 LD_{50} values (mM) obtained from different assays on Caco-2 cells. Values displayed are mean ± S.E. For reference Solutol HS15 CMC has been determined at 0.06-0.1 mM[47].

Assay	Exposure time (minutes)				Figure reference
	60	120	180	240	
JC-1 ($\Delta\Psi_m$)	3.73 ± 0.1	0.33 ± 0.1	0.12 ± 0.1	0.16 ± 0.1	4.6
MTS reduction	> 50	21.9 ± 5.3	3.5 ± 0.7	0.56 ± 0.1	4.4
LDH release	> 50	> 50	15.6 ± 2.2	0.56 ±0 .1	3.1

Similar to Solutol HS15 (Table 7.1), MTS and LDH release studies performed by Vllasaliu et al. on Calu-3 airway epithelia demonstrate that following 120 minutes of exposure, akylglycoside surfactants are more potent at reducing cellular metabolic activity than eliciting plasma membrane damage[2]. Considering that Solutol HS15-induced metabolic damage was significantly mediated by the induction of apoptosis (Figures 5.10 and 5.11), it is possible that exposure to akylglycoside surfactants also induces apoptosis, and that this is responsible for mediating their metabolic damage.

It appears Solutol HS15 is less toxic, following 120 minutes of exposure, than the akylglycoside surfactants. The least toxic of these surfactants reported by Vllasaliu et al., tetradecylmaltoside, is noted to present LD_{50} values approximately 8-fold higher than the surfactants CMC[2]. In comparison, following 120 minutes, the LD_{50} values for Solutol HS15 have been determined at >200-fold the CMC (Table 7.1) (taking into consideration only MTS and LDH results).

Lin et al. employed the MTT assay and determined that following 120 minutes of exposure on Caco-2 cells, polysorbate 80 presents an LD_{50} value ~ 600-fold greater than its CMC[48]. Furthermore, following 240 minutes of exposure in Caco-2 cells, Dimitrijevic et al. reported polysorbate 20 as having an LD_{50} value, determined by the MTT assay, >300-fold higher than the CMC[49]. Although these studies employed the MTT assay, as discussed in Chapter 4, the MTT and MTS assays are similar; they measure NADH-dependent reduction of a formazan salt, and others in the literature have reported comparable values between these assays[50]. Therefore, taken together these studies suggest that, based on metabolic activity measurements, polysorbates are less cytotoxic to Caco-2 cells

than Solutol HS15. Unfortunately, neither study[48,49] investigated LDH release or another cytotoxic parameter for further comparison.

7.6. Future work

To further develop the work performed here, several additional studies should be undertaken; (i) to confirm if the heat shock response is being induced by Solutol HS15, (ii) to investigate other non-ionic surfactants in the same exposure conditions with the same assays, and finally (iii) to research further into the cytotoxicity induced on epithelial monolayers.

Regarding (i), the expression of heat shock proteins (Hsps) following surfactant exposure should be assessed. Hsp70 would be a key protein to investigate, and its increased transcription and expression would indicate the high likelihood that the heat shock response is indeed occuring[51,52]; this work could be achieved by use of PCR and western blotting techniques, respectively.

Another important future step (ii), is to assess if other non-ionic surfactants, such as polysorbates and alkylglycosides, induce the same responses on Caco-2 cells as Solutol HS15. This could be approached with preliminary studies investigating high surfactant concentrations (>100-fold higher than surfactant CMCs), for short exposures 5-60 minutes, and assessing mitochondrial responses; the presence of metabolic bursts or hyperpolarised mitochondria would be a strong indicator that similar stress responses are unfolding.

(iii) Future work should also consider more detailed cytotoxicity testing on Caco-2 monolayers and/or the other techniques

outlined in Chapter 6. Studying effects on monolayers is perhaps more relevant for comparison than the other methods, considering permeability studies are performed on cell monolayers. As discussed, the possibility that Caco-2 monolayers are responding in a different manner to surfactant than undifferentiated cells, emphasises the need to confirm surfactant effects further in this model. Performing several of the assays on monolayers will be technically challenging; for instance, the high autofluorescence of the permeable membrane supports may confound fluorescence measurements. However, as suggested in Chapter 6, the quality of the data that can be gathered on monolayers outweighs any potential difficulties associated with culturing and differentiating epithelial cells in this manner.

In addition to studying surfactant effect on polarised epithelial monolayers, other complex models could be employed to obtain more relevant *in vitro* data. One such example could include a co-culture of Caco-2 cells with mucus secreted cells as discussed in section 6.4.4. Another culture model worthy of investigate would include the integration of immune cells, such as macrophages, with intestinal epithelial cells, similar to a system described by Al-Ghadban et al[53]; such a model would aid in the work described in section 7.2.

Regarding individual chapter work, addition techniques could be performed to further elucidate surfactant effect on intestinal epithelial cells. For example, Chapter 3 investigating membrane effects would benefit from the imaging of lateral segregation of lipid phases and this could be achieved by the use of L_o and L_d specific dyes and two photon microscopy[54]. Such data would support the Laurdan study performed here and also provide an

insight into the movement and localisation of membrane regions, such as lipid rafts, during surfactant exposure.

Chapter 4 studying metabolic effects could be furthered by investigating glucose and oxygen consumption rates[55]. Taken together, these techniques could be used to confirm if mitochondrial respiration is ceased following surfactant addition, and if a switch to a glycolytic pathway of bioenergetic synthesis is undertaken. Furthermore, in addition to the MTS and PrestoBlue reduction assays, NADH levels could be measured directly for a more accurate assessment of this redox system[56]. Similarly, metabolic activity could have been further investigating by measuring ATP levels, which in turn would aid in the understanding of mitochondrial function in response to surfactant[57].

Work in Chapter 5 could be enhanced by the investigation of initiator caspases. As discussed in section 5.1, the activation of specific initiator caspases is dependent upon the apoptotic pathway induced; caspases 8 and 10 are associated with extrinsic apoptosis and caspases 2 and 9 with intrinsic. Thus, by detecting for the presence of specific initiator caspases, through use of western blotting or PCR-based methods for example, one could make an accurate indication as to the apoptotic pathway activated[58]. Moreover, to further confirm the proposed apoptotic manner of cell death in response to Solutol HS15, one could employ a caspase inhibitor, such as Z-VAD-FMK[59]. Following such treatment, if the pro-death/apoptotic effects diminished (similar to the FCCP treatment performed in the current work), it would be possible to deduce apoptosis was indeed occurring as suggested.

7.7. Conclusions

The work carried out in this thesis has indicated that non-ionic surfactant cytotoxicity is indeed induced by membrane effects, however, it is the mitochondrial functions and their associated responses, that are consequently triggered, that in fact mediate the majority of observed cytotoxicity. This novel finding may change the manner in which surfactant toxicity is evaluated. It is thus highly encouraged for future surfactant studies to investigate effects at multiple time points, including short exposures (i.e. 5, 10 and 20 minutes) and, additionally, to study the reversibility of surfactant effects following 'recovery' periods. Surfactant toxicity could then be assessed on the propensity to induce cellular responses, and be compared accordingly.

7.8. References

1. Petersen, S. B. *et al.* Evaluation of alkylmaltosides as intestinal permeation enhancers: Comparison between rat intestinal mucosal sheets and Caco-2 monolayers. *Eur. J. Pharm. Sci.* **47,** 701–712 (2012).

2. Vllasaliu, D. *et al.* Epithelial toxicity of alkylglycoside surfactants. *J. Pharm. Sci.* **102,** 114–125 (2013).

3. Rege, B. D., Kao, J. P. Y. & Polli, J. E. Effects of nonionic surfactants on membrane transporters in Caco-2 cell monolayers. *Eur. J. Pharm. Sci.* **16,** 237–246 (2002).

4. Balogh, G. *et al.* The hyperfluidization of mammalian cell membranes acts as a signal to initiate the heat shock protein response. *FEBS J.* **272,** 6077–6086 (2005).

5. Balogh, G. *et al.* Heat stress causes spatially-distinct membrane re-modelling in K562 leukemia cells. *PLoS One* **6,** (2011).

6. Vigh, L. *et al.* Plasma membranes as heat stress sensors: From lipid-controlled molecular switches to therapeutic applications. *Biochimica et Biophysica Acta - Biomembranes* **1838,** 1594–1618 (2014).

7. Fine, M. *et al.* Massive endocytosis driven by lipidic forces originating in the outer plasmalemmal monolayer: a new approach to membrane recycling and lipid domains. *J. Gen. Physiol.* **137,** 137–154 (2011).

8. Vigh, L. *et al.* The significance of lipid composition for membrane activity: New concepts and ways of assessing function. *Progress in Lipid Research* **44,** 303–344 (2005).

9. Bolaños, J. P., Almeida, A. & Moncada, S. Glycolysis: a bioenergetic or a survival pathway? *Trends in Biochemical Sciences* **35,** 145–149 (2010).

10. Fulda, S., Gorman, A. M., Hori, O. & Samali, A. Cellular stress responses: Cell survival and cell death. *International Journal of Cell Biology* (2010). doi:10.1155/2010/214074

11. Sánchez-Alcázar, J., Ault, J., Khodjakov, A. & Schneider, E. Increased mitochondrial cytochrome c levels and mitochondrial hyperpolarization precede camptothecin-induced apoptosis in Jurkat cells. *Cell Death Differ.* **7,** 1090–1100 (2000).

12. Giovannini, C. *et al.* Mitochondria hyperpolarization is an early event in oxidized low-density lipoprotein-induced apoptosis in Caco-2 intestinal cells. *FEBS Lett.* **523,** 200–206 (2002).

13. Horváth, I., Multhoff, G., Sonnleitner, A. & Vígh, L. Membrane-associated stress proteins: More than simply chaperones. *Biochimica et Biophysica Acta - Biomembranes* **1778,** 1653–1664 (2008).

14. Torok, Z. *et al.* Evidence for a lipochaperonin: Association of active proteinfolding GroESL oligomers with lipids can stabilize membranes under heat shock conditions. *Proc. Natl. Acad. Sci.* **94,** 2192–2197 (1997).

15. Török, Z. *et al.* Synechocystis HSP17 is an amphitropic protein that stabilizes heat-stressed membranes and binds denatured proteins for subsequent chaperone-mediated refolding. *Proc. Natl. Acad. Sci. U. S. A.* **98,** 3098–3103 (2001).

16. Tsvetkova, N. M. *et al.* Small heat-shock proteins regulate membrane lipid polymorphism. *Proc Natl Acad Sci U S A* **99,** 13504–13509 (2002).

17. Thompson, C. B. Apoptosis in the pathogenesis and treatment of disease. *Science* **267,** 1456–62 (1995).

18. Green, D. R., Ferguson, T., Zitvogel, L. & Kroemer, G. Immunogenic and tolerogenic cell death. *Nat. Rev. Immunol.* **9,** 353–363 (2009).

19. Zitvogel, L., Kepp, O. & Kroemer, G. Decoding Cell Death Signals in Inflammation and Immunity. *Cell* **140,** 798–804 (2010).

20. Rock, K. L. & Kono, H. The inflammatory response to cell death. *Annu. Rev. Pathol.* **3,** 99–126 (2008).

21. Kroemer, G. *et al.* Classification of cell death: recommendations of the Nomenclature Committee on Cell Death 2009. *Cell Death Differ* **16,** 3–11 (2009).

22. Nagata, S. Apoptosis by death factor. *Cell* **88,** 355–365 (1997).

23. Faouzi, S. *et al.* Anti-Fas Induces Hepatic Chemokines and Promotes Inflammation by an NF-κB-independent, Caspase-3-dependent Pathway. *J. Biol. Chem.* **276,** 49077–49082 (2001).

24. Majno, G. & Joris, I. Apoptosis, oncosis, and necrosis. An overview of cell death. *Am. J. Pathol.* **146,** 3–15 (1995).

25. Gelberg, H. . in *Pathologic Basis of Veterinary Disease* (eds. McGavin, M. . & Zachary, J. .) 342–360 (Elsevier Mosby, 2007).

26. Potten, C. S. A comprehensive study of the radiobiological response of the murine (BDF1) small intestine. *International Journal of Radiation Biology* **58,** 925–973 (1990).

27. Nagata, S., Hanayama, R. & Kawane, K. Autoimmunity and the Clearance of Dead Cells. *Cell* **140,** 619–630 (2010).

28. Poon, I. K. H., Lucas, C. D., Rossi, A. G. & Ravichandran, K. S. Apoptotic cell clearance: basic biology and therapeutic potential. *Nat. Rev. Immunol.* **14,** 166–180 (2014).

29. Gardai, S. J. Recognition ligands on apoptotic cells: a perspective. *J. Leukoc. Biol.* **79,** 896–903 (2006).

30. Grimsley, C. & Ravichandran, K. S. Cues for apoptotic cell engulfment: Eat-me, don't eat-me and come-get-me signals. *Trends in Cell Biology* **13,** 648–656 (2003).

31. Tanabe, M., Nakai, A., Kawazoe, Y. & Nagata, K. Different thresholds in the responses of two heat shock transcription factors, HSF1 and HSF3. *J. Biol. Chem.* **272,** 15389–15395 (1997).

32. Demirovic, D., de Toda, I. M., Nizard, C. & Rattan, S. I. S. Differential

translocation of heat shock factor-1 after mild and severe stress to human skin fibroblasts undergoing aging in vitro. *J. Cell Commun. Signal.* **8,** 333–339 (2014).

33. Bettaieb, A. & Averill-Bates, D. A. Thermotolerance induced at a mild temperature of 40°C alleviates heat shock-induced ER stress and apoptosis in HeLa cells. *Biochim. Biophys. Acta - Mol. Cell Res.* **1853,** 52–62 (2015).

34. Adkins, I. *et al.* Severe, but not mild heat-shock treatment induces immunogenic cell death in cancer cells. *Oncoimmunology* **6,** (2017).

35. Toivola, D. M., Strnad, P., Habtezion, A. & Omary, M. B. Intermediate filaments take the heat as stress proteins. *Trends in Cell Biology* **20,** 79–91 (2010).

36. Harmon, B. V. *et al.* Cell death induced in a murine mastocytoma by 42-47°c heating in vitro: Evidence that the form of death changes from apoptosis to necrosis above a critical heat load. *Int. J. Radiat. Biol.* **58,** 845–858 (1990).

37. Lim, S. C. *et al.* Implication of PI3K-dependent HSP27 and p53 expression in mild heat shock-triggered switch of metabolic stress-induced necrosis to apoptosis in A549 cells. *Int. J. Oncol.* **36,** 387–393 (2010).

38. Anderle, P. *et al.* P-glycoprotein (P-gp) mediated efflux in Caco-2 cell monolayers: The influence of culturing conditions and drug exposure on P-gp expression levels. *J. Pharm. Sci.* **87,** 757–762 (1998).

39. Anderle, P., Rakhmanova, V., Woodford, K., Zerangue, N. & Sadée, W. Messenger RNA expression of transporter and ion channel genes in undifferentiated and differentiated Caco-2 cells compared to human intestines. *Pharm. Res.* **20,** 3–15 (2003).

40. Schreider, C., Peignon, G., Thenet, S., Chambaz, J. & Pinçon-Raymond, M. Integrin-mediated functional polarization of Caco-2 cells through E-cadherin--actin complexes. *J. Cell Sci.* **115,** 543–552 (2002).

41. Visco, V. *et al.* Human colon fibroblasts induce differentiation and proliferation of intestinal epithelial cells through the direct paracrine action of keratinocyte growth factor. *J. Cell. Physiol.* **220,** 204–13 (2009).

42. Bulut, K. *et al.* Glucagon like peptide-2 induces intestinal restitution through VEGF release from subepithelial myofibroblasts. *Eur. J. Pharmacol.* **578,** 279–85 (2008).

43. Göke, M., Kanai, M. & Podolsky, D. K. Intestinal fibroblasts regulate intestinal epithelial cell proliferation via hepatocyte growth factor. *Am. J. Physiol.* **274,** G809-18 (1998).

44. Powell, D. W., Adegboyega, P. A., Di Mari, J. F. & Mifflin, R. C. Epithelial cells and their neighbors I. Role of intestinal myofibroblasts in development, repair, and cancer. *Am. J. Physiol. Gastrointest. Liver Physiol.* **289,** G2–G7 (2005).

45. Inácio, Â. S. *et al.* In vitro surfactant structure-toxicity relationships:

Implications for surfactant use in sexually transmitted infection prophylaxis and contraception. *PLoS One* **6,** (2011).

46. Aranzazu Partearroyo, M., Ostolaza, H., Goni, F. M. & Barbera-Guillem, E. Surfactant-induced cell toxicity and cell lysis. A study using B16 melanoma cells. *Biochem. Pharmacol.* **40,** 1323–1328 (1990).

47. Shubber, S. *et al.* Mechanism of Mucosal Permeability Enhancement of CriticalSorb® (Solutol® HS15) Investigated In Vitro in Cell Cultures. *Pharm. Res.* **32,** 516–527 (2014).

48. Lin, H. *et al.* Enhancing effect of surfactants on fexofenadine??HCl transport across the human nasal epithelial cell monolayer. *Int. J. Pharm.* **330,** 23–31 (2007).

49. Dimitrijevic, D., Shaw, A. J. & Florence, A. T. Effects of some non-ionic surfactants on transepithelial permeability in Caco-2 cells. *J. Pharm. Pharmacol.* **52,** 157–162 (2000).

50. Wang, P., Henning, S. M. & Heber, D. Limitations of MTT and MTS-based assays for measurement of antiproliferative activity of green tea polyphenols. *PLoS One* **5,** (2010).

51. Mayer, M. P. & Bukau, B. Hsp70 chaperones: Cellular functions and molecular mechanism. *Cell. Mol. Life Sci.* **62,** 670–684 (2005).

52. Multhoff, G. Heat shock protein 70 (Hsp70): Membrane location, export and immunological relevance. *Methods* **43,** 229–237 (2007).

53. Al-Ghadban, S. *et al.* Cross-talk between intestinal epithelial cells anmd immune cells in inflammatory bowel disease. *Sci. Reports*. **6**, 29783 (2016).

54. Kaiser, H-J. *et al.* Order of lipid phases in model and plasma membranes. *PNAS*. **106**(39), 16645-16650 (2009).

55. Cook, C. *et al.,* Consuption of oxygen: a mitochondrial-generated progression signal of advanced cancer. *Cell Death & Disease*. **3**, e258 (2012).

56 Blacker, T., & Duchen, M. Investigating mitochondrial redox state using NADH and NADPH autofluorescence. *Free Radical Bio. and Med.* **100**, 54-65 (2016).

57 Taha, R. *et al.* Oxidative stress and mitochondrial function in the intestinal Caco-2/15 cell line. *PLOS ONE. **5***. (2017).

58 McIlwain, D. *et al.* Caspase functions in cell death and disease. *CSH perspectives.* **10**(4), (2013).

59 Chakrabarti, G. *et al.* Death pathways activated in caco-2 cells by clostridium perfringens enterotoxin. *Infect. & Immun.* **71**, 4260-4270 (2003).